Strip Tracking in Hot Strip Mills

Ben Carruthers-Watt

EngD Thesis
September 2011

Cardiff School of Engineering
Cardiff University

Summary

ID Number:	0303694	**Title:**	Mr
Surname:	Carruthers-Watt	**First names:**	Benjamin Nigel
School:	Engineering	**Degree:**	EngD
Thesis Title:	Strip tracking in hot strip mills		

In the finishing mill, steel strip is rolled from thick slabs through pairs of rollers housed in a continuous train of seven roll stands. As the strip is rolled, unwanted lateral movement, known as strip tracking, can cause the strip to collide with the edge of the mill.

Strip tracking control is currently a manual operation, relying on the skill of the operators. When tracking is observed, the stand tilt is adjusted asymmetrically, causing a camber in the strip, steering it towards the centreline. Tracking control can be automated if a reliable measurement of position is available.

A vision-based system was developed to measure strip position. Cooling water, steam, high temperatures and electrical noise create a hazardous environment for electronic equipment and hamper image analysis. Hardware was specified to protect all equipment against the environment. A novel image analysis method combining predictive elements, filtering and Bezier curve fitting was created to allow measurements to be made with large amounts of cooling water obscuring the strip edges. The measurement system was designed to integrate with the existing mill systems, using the OPC protocol for communication. The system was created as a development system with only two cameras included, but allowed for additional cameras to be easily added and automatically detected.

The results of the system showed that the image analysis techniques were effective, providing an estimated final resolution of 3.5mm/pixel, with measurements ±2mm within 60% confidence. Hardware performance provided good protection of the equipment against the environment but poor quality installation limited overall system performance.

A computer model was developed to simulate tracking behaviour in the mill with non-linear variations of strip properties across the strip. The model was not completed to a satisfactory standard capable of producing useful results but the theories described could be developed further.

Declaration

DECLARATION

This work has not previously been accepted in substance for any degree and is not concurrently submitted in candidature for any degree.

Signed …………………………………………… Date …………………………

STATEMENT 1

This thesis is being submitted in partial fulfilment of the requirements for the degree of EngD

Signed …………………………………………… Date …………………………

STATEMENT 2

This thesis is the result of my own independent work/investigation, except where otherwise stated.

Other sources are acknowledged by explicit references.

Signed …………………………………………… Date …………………………

STATEMENT 3

I hereby give consent for my thesis, if accepted, to be available for photocopying and for inter-library loan, and for the title and summary to be made available to outside organisations.

Signed …………………………………………… Date …………………………

Acknowledgement

Contents

List of Figures

List of Tables

List of Abbreviations

AGC: Automatic Gauge Control

BOS: Basic Oxygen Steelmaking

CCD: Charge Coupled Device

CMOS: Complimentary Metal Oxide Semiconductor

CONCAST: Continuous Casting

DS: Drive Side

fps: Frames per second

GigE: Gigabit Ethernet

HSM: Hot Strip Mill

LQR: Linear Quadratic Regulator

MAX: Measurement and Automation Explorer

OLE: Object Linking and Embedding

OPC: OLE for Process Control

OS: Operating System / Operator Side

px: Pixel

ROT: Run Out Table

ROI: Region Of Interest

RT: Real-Time

Literature Review Nomenclature

C : Roll gap

h : Strip thickness

h_I : Strip entry thickness

h_O : Strip exit thickness

K : mill modulus

L : Roll bite length

P : Rolling pressure

S : Constrained yield stress

x : Position along roll bite

Y : Yield stress

σ_y : Vertical shear stress

σ_x : Shear stress in rolling direction

μ : Coefficient of friction

Modelling Theories Nomenclature

Subscript indices:

i : Element number

n : Stand number

j : Sub-element number in point-by-point roll force calculation

The subscript indices i and n refer to specific elements and stands for each term. In some cases a term is used at stand and element level, e.g. $F_{(n)}$ refers to total roll force in stand n, whereas $F_{(n)(i)}$ refers to the portion of roll force at element i.

The subscript j is used only in the roll force calculation and refers to position along the roll bite at sub-element level in the point by point integration.

$A_{(n)(i)(j)}$: Area roll pressure is acting on (m^2)

$a_{(n)(i)}$: Roll bite length (m)

B : Total number of elements across strip width (-)

b : Strip width (m)

$C_{V(n)(i)}$: Strip speed constant ($m^2.s^{-1}$)

$D_{B((n+1)\_(n))}$: Bending force due to deflection from $n+1$ to n (N)

$D_{B((n)\_(n+1))}$: Bending force due to deflection from n to $n+1$ (N)

$D_{S((n+1)\_(n))}$: Slip force due to deflection from $n+1$ to n (N)

$D_{S((n)\_(n+1))}$: Slip force due to deflection from n to $n+1$ (N)

$D_{Sx(n)}$: Tangential shear slip force in x direction (N)

$D_{W(n)}$: Wedge force (N)

$D_{x(n)}$: Shear force in x direction (N)

$D_{y(n)}$: Shear force in y direction (N)

E : Youngs modulus (Pa)

$F_{(n)}$: Roll force (N)

$F_{0(n)}$: Setup roll force (N)

$F_{DS(n)}$: Roll force at DS screw (N)

$F_{OS(n)}$: Roll force at OS screw (N)

$h_{(n)(i)}$: Strip thickness (m)

$h_{DS(n)(i)}$: Strip thickness at DS side of element (m)

$h_{I(n)(i)}$: Strip entry thickness at stand entry (m)

$h_{N(n)(i)}$: Strip thickness at neutral point (m)

$h_{O(n)}$: Strip thickness at stand exit (m)

$h_{OS(n)(i)}$: Strip thickness at OS side of element (m)

$h_{Slope(n)(i)}$: Effective roll gap at element (m)

I: Second moment of area of strip (m^4)

J: Total number of sub-elements along roll bite (-)

$K_{(n)}$: Mill modulus (N.m^{-1})

$k_{T(n)(i)}$: Temperature effect coefficient (-)

L: Distance between stands (m)

$l_{(n)(i)}$: Length of element (m)

$l_{DS(n)}$: Length of strip between n and $n+1$ on DS side (m)

$l_{OS(n)}$: Length of strip between n and $n+1$ on OS side (m)

$l_{Slope(n)(i)}$: Gradient of effective slope of strip lengths at element (mm)

$M_{(n)}$: Moment acting on stand (N.m)

$M_{B((n+1)\_(n))}$: Bending moment due to deflection from $n+1$ to n (N.m)

$M_{B((n)\_(n+1))}$: Bending moment due to deflection from n to $n+1$ (N.m)

$M_{S((n+1)\_(n))}$: Slip moment due to deflection from $n+1$ to n (N.m)

$M_{S((n)\_(n+1))}$: Bending moment due to deflection from n to $n+1$ (N.m)

$N_{(n)}$: Location of neutral point (-)

$P_{(n)(i)(j)}$: Roll pressure (Pa)

$R_{(n)}$: Roll radius (m)

$R_{c(n)}$: Radius of camber of strip (m)

$R_{0(n)}$: Setup (nominal) roll radius (m)

$R_{\omega(n)(i)}$: Radius of angular rotation of the strip (m)

$S_{(n)}$: Average screw position (m)

$S_{0(n)}$: Setup screw position (m)

$S_{DS(n)}$: DS screw position (m)

$S_{OS(n)}$: OS Screw position (m)

$s_{1(n)}$: Entry tension (Pa)

$s_{2(n)}$: Exit tension (Pa)

$T_{(n)(i)}$: Strip temperature (°C)

T_m : Strip melting point (°C)

t : Current time step (s)

$V_{(n)(i)}$: Strip velocity (m.s^{-1})

$V_{D(n)}$: Lateral strip velocity due to lateral forces (m.s^{-1})

$V_{DS(n)}$: DS strip velocity (m.s^{-1})

$V_{I(n)(i)}$: Strip entry velocity (m.s^{-1})

$V_{N(n)(i)}$: Strip velocity at the neutral point (m.s^{-1})

$V_{OS(n)}$: OS strip velocity (m.s^{-1})

$V_{R(n)}$: Roll surface velocity (m.s^{-1})

$V_{t(n)(i)}$: Elemental tangential strip velocity (m.s^{-1})

$V_{tx(n)}$: Tangential slip velocity in x direction (m.s^{-1})

$V_{x(n)}$: Strip velocity in x direction (m.s^{-1})

$V_{y(n)}$: Strip velocity in y direction (m.s^{-1})

$V_{\alpha(n)}$: Lateral velocity due to entry angle (m.s^{-1})

W : Stand width (distance between screws) (m)

$x_{(n)(i)(j)}$: Distance along roll bite of sub element (m)

Y_o : Yield stress at 20°C (Pa)

$Y_{S(n)(i)}$: Constrained yield stress at elevated temperature (Pa)

$y_{(n)}$: Position of strip in stand (m)

$y_{c(n)}$: Position of strip due to camber (m)

$y_{V(n)}$: Position of strip due to lateral velocity (m)

$y_{\alpha(n)}$: position of strip due to exit angle (m)

$a_{(n)}$: Angle of strip in stand (rad)

$\alpha_{c(n)}$: Angle of strip in stand due to camber (rad)

$\alpha_{I(n)}$: Entry angle of strip (rad)

$\alpha_{O(n)}$: Exit angle of strip (rad)

$\alpha_{\omega(n)}$: Angle of strip due to rotational velocity (rad)

$\beta_{(n)}$: Wedge angle (rad)

$\theta_{(n)(i)(j)}$: Rolling angle at sub-element (rad)

$\theta_{c(n)}$: Angle of curvature in cambered strip (rad)

$\theta_{N(n)(i)}$: Neutral point angle (rad)

$\mu_{(n)}$: Coefficient of friction during rolling (-)

$\mu_{x(n)}$: x-component of coefficient of friction (-)

$\mu_{y(n)}$ y-component of coefficient of friction (-)

$\omega_{(n)}$: Angular velocity of strip (rad.s^{-1})

$\omega_{M(n)}$: Angular velocity due to bending moment (rad.s^{-1})

$\omega_{V(n)}$: Angular velocity due to differential strip speed (rad.s^{-1})

$\Delta y_{D(n)}$: Strip deflection (m)

$\Delta \alpha_{D(n)}$: Angular deflection (rad)

$\Delta \theta_{(n)(i)(j)}$: Difference in rolling angle at sub-element (rad)

$Y'_S, Y''_S, p_1, p_2, \xi, \eta, f$: Terms used in the Von Karman equation

$(F_{OS}-F_{DS})/F$

Measurement System Nomenclature

$B(t)$: Bezier curve function

G_{Max}: Max gradient limit

G_{Min}: Min gradient limit

G_{Norm}: Normalised gradient limit

i: Index of Bezier curve knot

j: Index of search line

$\mathbf{K}$: Edge detection kernel

L_x: Average x-position of line

L_y: Average y-position of line

$L_0[x, y]$: Line start point

$L_1[x, y]$: Line end point

m: Total number of search lines

n: Bezier curve order

t: Bezier curve parametric value

x: Position in lateral direction

y: Position in rolling direction

$\mathbf{P_i}$: Bezier curve knot

1 Introduction and Review of Literature

1.1 Steel production at Port Talbot integrated steelworks

Strip steel is used in a wide variety of applications, including car body panels, food cans, white goods, building cladding and roofing materials amongst many others. For these applications the steel must be a fraction of a millimetre thick and with a good dimensional accuracy to ensure high quality final products. Coils of steel are produced for the manufacturing industry by rolling in mills. The work behind this thesis was based around and aimed at one stage in the steel rolling process, the finishing train of a hot rolling mill.
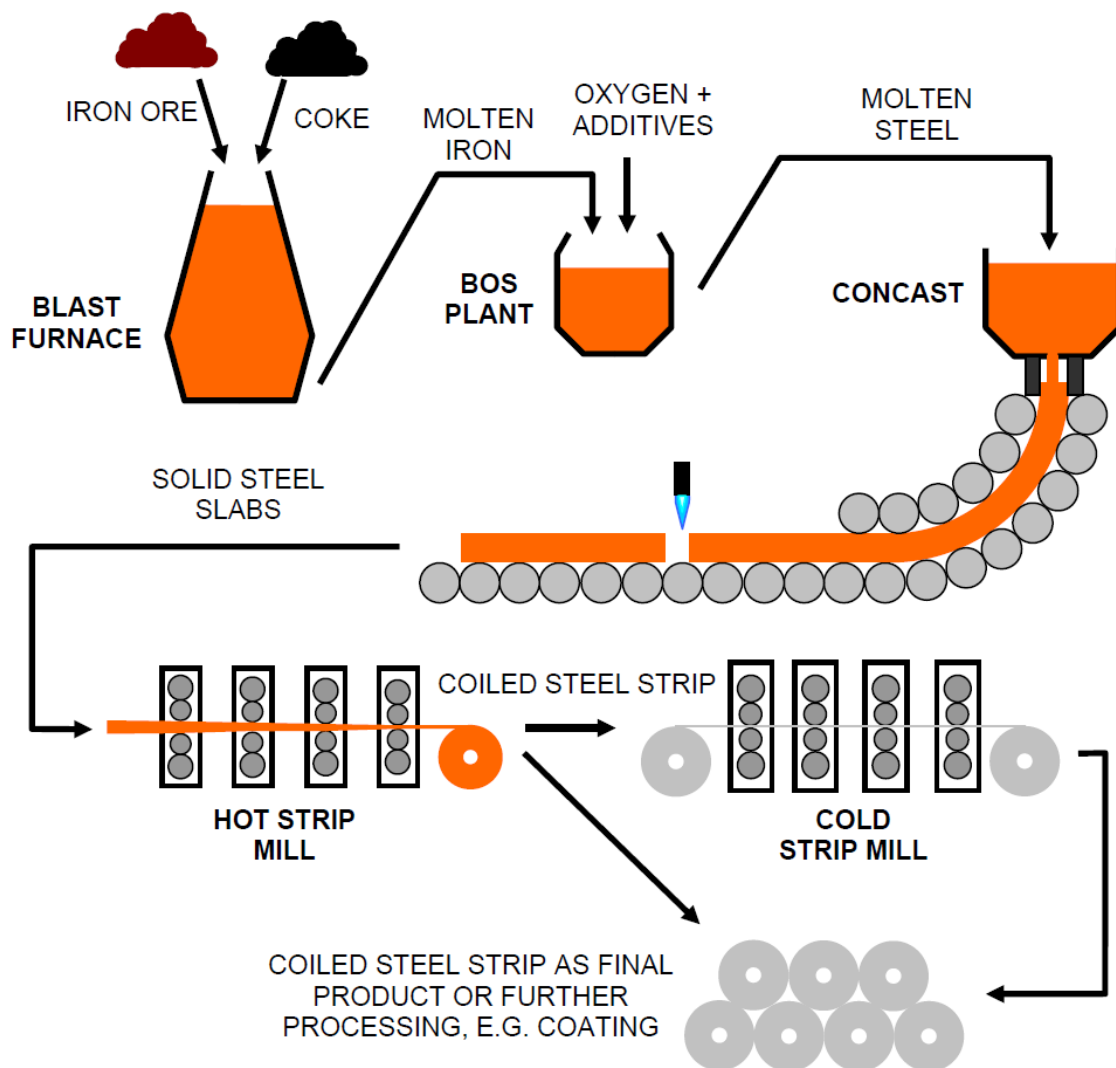
Figure 1.1: Steel Production

Figure 1.1 shows a simplified diagram of the steel production process [1]. The first stage is to reduce the iron ore to iron in a blast furnace. The molten iron is tapped out of the bottom of the furnace and transferred to the Basic Oxygen Steelmaking (BOS) plant. The molten iron is

poured into the BOS ladle, along with scrap steel for recycling. Oxygen is passed through the molten iron in the ladle, reacting with the carbon in the iron and removing it as carbon monoxide. At this point other alloying elements are added to the ladle to convert the material into a precise iron alloy known as steel..

The molten steel is transferred to the Continuous Caster (CONCAST) to be cast into slabs. At CONCAST, molten steel is held in a ladle and tapped between a pair of water-cooled dies which solidify the outer edge and create the rectangular slab shape, approximately 250mm thick. The solidifying steel is supported by rollers and transferred through a right angle onto a horizontal bed where slabs are cut to length. These steel slabs are now ready for rolling into strip.

The rolling process consists of two operations; hot rolling and cold rolling. Hot rolling reduces the steel slabs from CONCAST into coils of steel strip between about 2mm to 12mm thick. During rolling, the steel is deformed between pairs of rolls until the required thickness is achieved. Hot rolling is a two-stage process, roughing and finishing, and is discussed in more detail in section 1.2. The hot rolled steel coils can be used as a final product, or can be cold rolled to produce finer thicknesses and surface finish. Cold rolling is a very similar operation to hot rolling, except the steel is not pre-heated but performed 'cold'.

The final coiled products following hot and cold rolling can be used directly, or go on for a variety of further processing, for example coating by painting or galvanising.

1.2   Hot strip rolling

1.2.1 Overview of hot rolling process

The hot strip rolling process is the initial stage of reduction following CONCAST. A diagram showing an overview of the hot rolling process is shown in Figure 1.2. Steel slab enters the mill either directly from CONCAST or from the slab yards, having been in storage and cooled. The slabs are then heated in the re-heat furnaces up to a temperature of around 1200°C to reduce the yield stress and hence the force required for rolling [2]. The slab is then passed through scale breakers to remove surface oxidisation before entering the roughing mill.
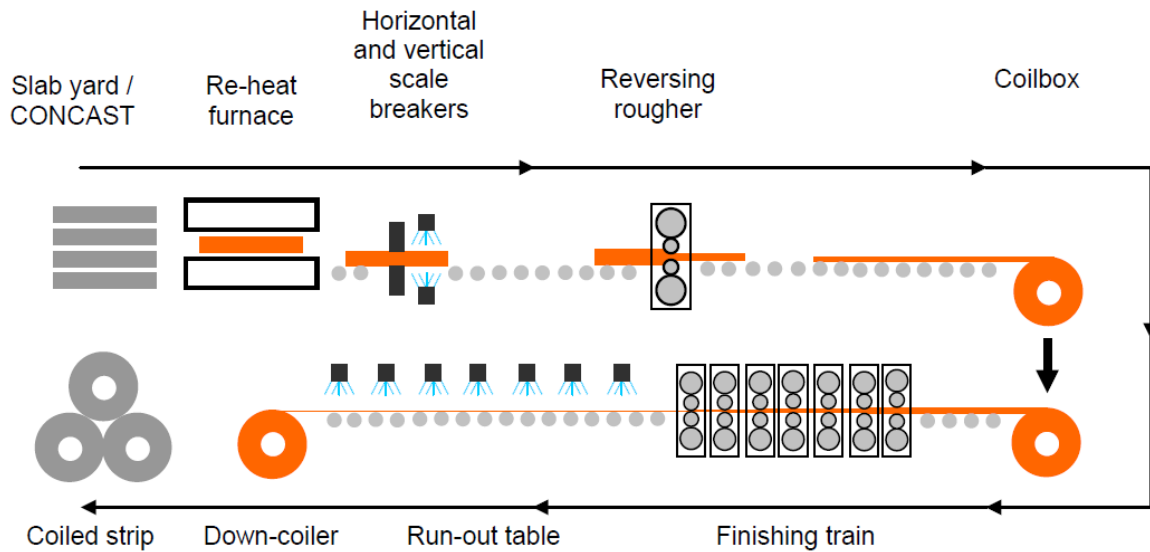
Figure 1.2: Hot strip mill

The reversing rougher is a single, high-power roll stand which reduces the slab down to about 40mm in a number of passes. The rougher is reversing because the strip passes back and forwards through the stand up to seven times, as opposed to a roughing train where the strip passes in one direction through a number of stands in series. After roughing, the strip undergoes further de-scaling. The strip is then coiled in an intermediate coil-box, which reduces the total required mill length as opposed to a straight-through mill.

The strip is uncoiled from the coil-box and the head and tail end are cropped to ensure they are square directly into the finishing train, which is explained in detail in section 1.2.2, where it undergoes final and more precise deformation before cold rolling. The finishing train in Port Talbot consists of 7 rolling stands and reduces the strip from the rougher to thicknesses of between about 2mm and 12mm. The strip is then cooled at a controlled rate on the run-out table (ROT) before being coiled in the down-coiler.

1.2.2 The finishing train

The finishing train of the hot strip mill in the Tata Port Talbot steelworks [1] consists of seven 4-high finishing stands, numbered F5 through to F11, F5 being the first finishing stand in the train. A diagram showing the layout of the finishing train is shown in Figure 1.3. Strip enters the first stand from the coil box, having been reduced in the rougher to between approximately 35mm and 42mm.
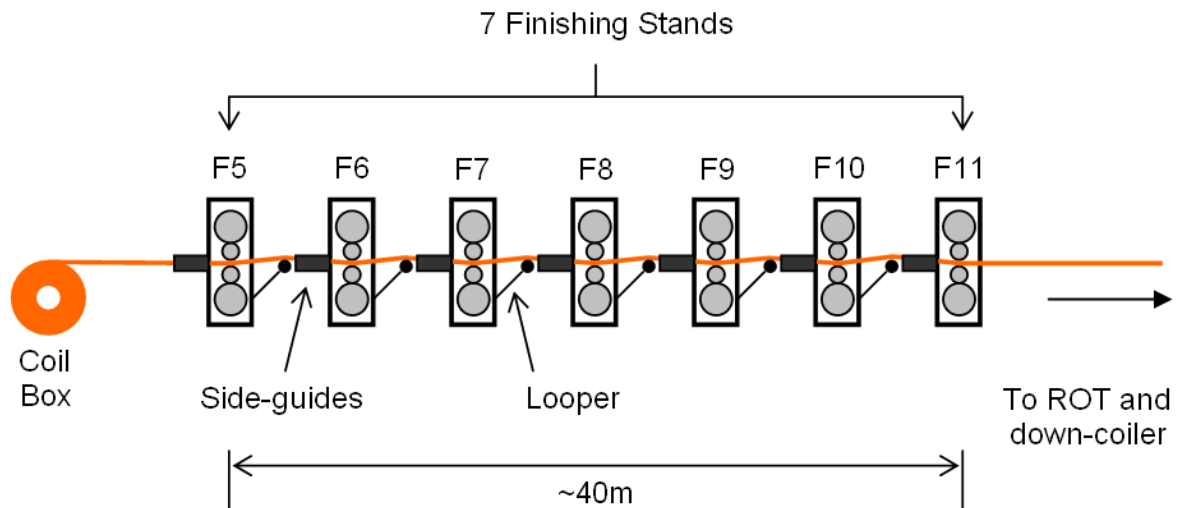
Figure 1.3: Finishing train

The finishing train is approximately 30m from end to end, each stand is about 5m high. Strip speed at the exit of the last stand is typically around 600m/min (~20mph).

The strip is guided into the stands using side-guides which keep the strip from running out of the side of the stand and are particularly useful during threading when the strip is first entering the stands. Between each stand is a looper roller which rises up beneath the strip to maintain strip tension.

In general, the first three stands are used for heavy duty reduction, and the final four stands have more refined control to ensure final product tolerances.

1.2.3 Roll stand structure

The roll stands, depicted in a simplified diagram in Figure 1.4, are known as "4-high" roll stands due there being 4 rolls in the stand [3]. The strip is driven through a narrow gap between the two work rolls, reducing it to the desired output thickness. The work roll radius is relatively small in order to increase the pressure acting on the strip, hence reducing the required roll force (the force deforming the strip). However, with a small radius, the work roll has a relatively low stiffness and hence is prone to bending under the high roll forces. To reduce work roll bending, a larger pair of rolls, the backup rolls, are above and below the work rolls increasing the stiffness. Work roll bending is further reduced by the work roll bending cylinders; hydraulic cylinders which push the edges of the work rolls apart, counteracting the bending of the rolls due to the roll force.

4
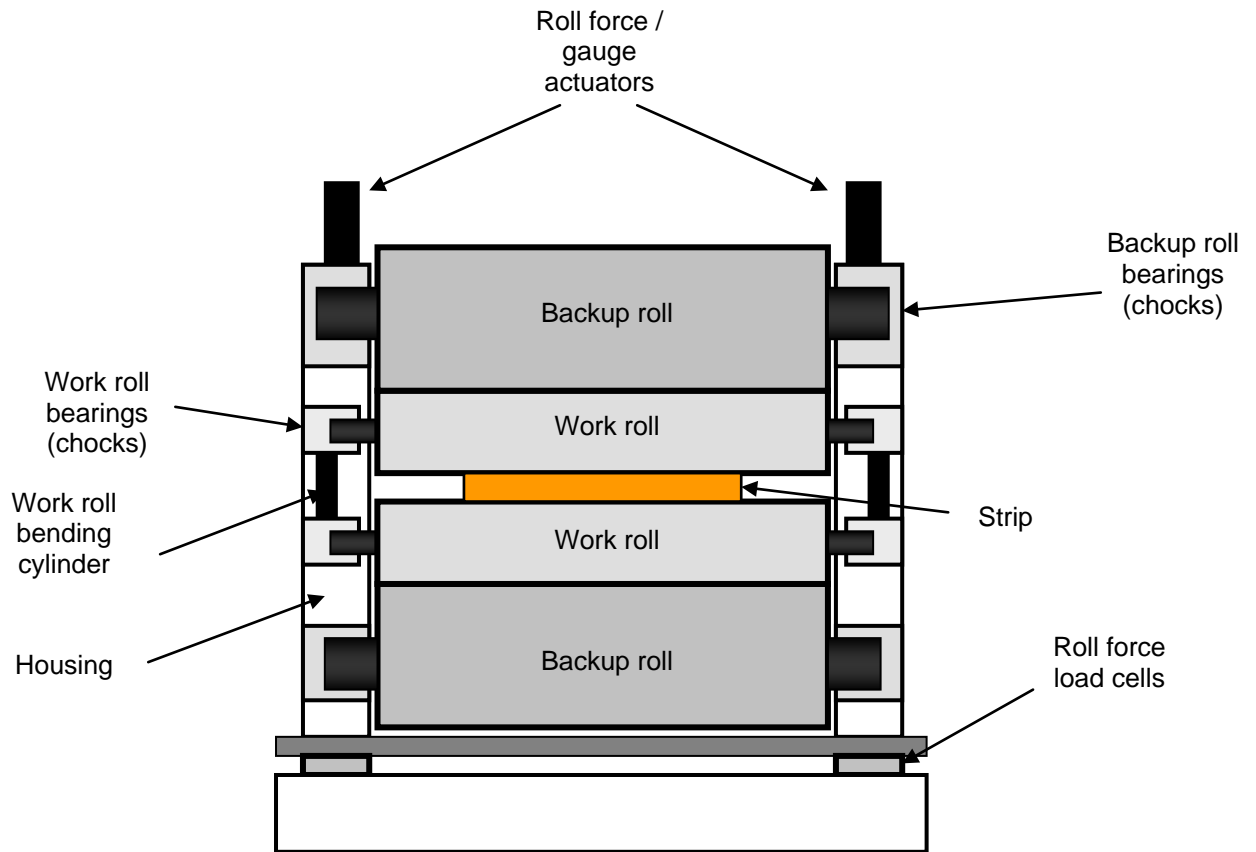
Figure 1.4: Typical 4-high roll stand

As a result of the high forces required to deform the strip, which are typically in the order of 2000 Tonnes, the entire mill frame will stretch significantly. The mill stretch is linear in the working force range and is expressed as a coefficient of elasticity known as the mill modulus. Typically the mill modulus will be approximately 500T/mm [4], i.e. the gap between the rolls will stretch 1mm for every 500 Tonnes of roll force.

The roll force occurs as a result of the strip being driven through a gap narrower than the thickness of the strip. The gauge is controlled by two actuators on top of each stand which are controlled by force feedback from a pair of load cells on the base of the stand. The gauge actuators can be driven independently from each other and act to change the gap between the work roll. On the first three stands where heavier and rougher reduction occurs these actuators are relatively slow moving mechanical screws and on the final stands the actuators are faster hydraulic capsules, providing finer control of final output gauge.

1.3 Strip tracking

Strip tracking is the unwanted lateral movement of the strip during rolling. There are a number of reasons that strip can track sideways, including camber, rotation and lateral forces [5].

Camber is induced in the strip due to any factor causing one side of the strip to be reduced more than the other side, resulting in a differential elongation along the strip length and hence inducing a curve (camber) in the strip. The most common causes of this are if either the strip has one edge thicker than the other entering a level roll gap, or if a level strip is entering a roll gap with the work rolls non-parallel. This is known as "wedge". These situations are depicted in Figure 1.5.
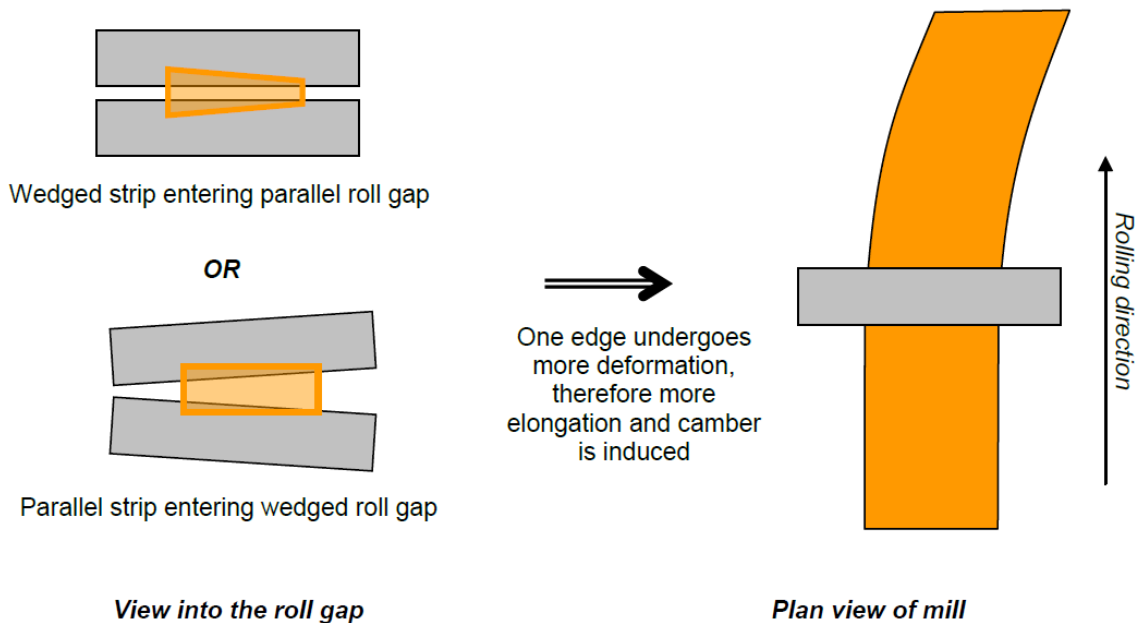
Figure 1.5: Formation of camber

The formation of camber occurs due the principle of mass conservation; the mass entering the roll bite must be equal to the mass that leaves the roll bite. Assuming a constant density across the strip, this translates to conservation of volume, and hence, assuming negligible lateral spread [6], elongation of a strip is proportional to its thickness reduction.

Strip rotation occurs in the roll gap when there is a differential speed across the roll gap. This can occur when the strip or roll gap is wedged and is a result of the principle of mass-flow conservation.

Lateral forces occur in the strip generally as a consequence of the strip being restrained between adjacent roll stands and when the strip is in a position it would not naturally be in if unrestrained. For example, if a strip was in the first two stands and a wedge was introduced into the first stand roll gap, a camber would hence be induced into the strip between stands 1 and 2. However, as the strip is restrained by stand 2, it cannot freely move to form the camber and hence a strain is induced in the strip causing a lateral force.

To control the strip when it is tracking sideways the wedge of the roll gap is adjusted, known as tilting the roll gap. The effect of this is identical to the causes of tracking – camber is formed, the strip rotates and lateral forces push the strip sideways, correcting the position of the strip. Tracking control is traditionally manually controlled by operators observing the rolling process from the pulpit. The operators have a side-on view of the finishing mill and look for indication of the strip tracking sideways, such as the formation of a wavy-edge in the strip, indicating the strip is undergoing more deformation on that edge. Tracking can be automatically controlled, but first the strip position must be measured in order to provide a control signal. Tracking control performed by the operator requires a lot of skill and experience because steering is performed on indications, not a direct knowledge of strip position. By introducing automatic control, the reliance on operator skill is reduced and more predictable strip tracking can be achieved. If full automatic control is not possible then any improvement to the information on strip position available to the operators will improve their ability to successfully control tracking.

Strip tracking is very important to the rolling process as it affects the stability of the entire mill. In the worst cases, a strip tracking sideways can collide with the mill and side-guides, folding an edge over, known as a pinch. When the strip pinches, the effective thickness approaching the roll gap is doubled, preventing it from entering successfully. Pinched strip can break off and can lodge in the stand and fall down onto subsequent strips. In these cases the strip will bunch up in the inter-stand space, known as a "cobble". because it cannot enter the roll bite. Pinches, cobbles and other less serious collisions can all cause damage to the mill, which requires downtime and loss of productivity to inspect and fix any problems.

Certain geometries of strip have a higher tendency to track sideways, and hence the process window is often limited by the pinch-risk of a given product. One factor which naturally affects tracking stability is roll crown; a convex roll gap profile is where the roll gap is slightly thicker in the centre than at the edges. The amount of crowing on a strip can typically be in the order of 1% of the strip thickness.
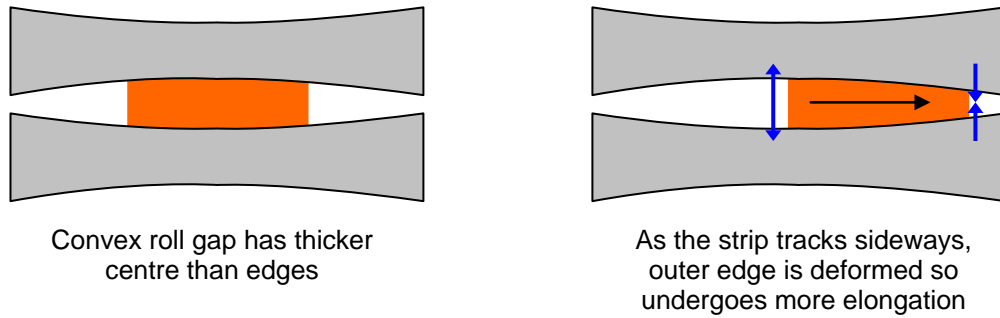
Figure 1.6 : Effect of convex roll gap crown

As Figure 1.6 shows, when a strip tracks off-centre in a convex crown roll gap, the edge on the side the strip is moving towards undergoes more deformation, and hence curves the strip back towards the centre with the same effect as tilting the roll gap. Conversely, a roll gap with a concave crown, with the centre thinner than the edges has the opposite effect on tracking stability. If the final product must be very flat then crowning must be minimal, hence forming a naturally more unstable strip than compared to a convex crown. Also, a harder material requires more roll force, and hence increased mill stretch and work roll flattening, counteracting the effect of crown. Wider strips are also prone to more roll flattening at the outer edges. By improving strip tracking control, the pinch risk of all products can be reduced and hence the process window can be extended into the more difficult geometries. This will enable the mill to roll wider, thinner, harder products which are increasingly in demand, especially in the automotive industry where it is desirable to use a minimal amount of material to reduce weight.

1.4   Automatic control in a rolling mill

Continual technological advancement in steel rolling is important to ensure that a steel plant remains competitive in the market by improving product quality and production rates. Historically, improvements in both the machines and the control methods used have been used to this end [7]. The utilisation of computer control systems in a modern steelworks is a fundamental tool in the development of steel rolling technology. A steel mill is a very large distributed control system [8] with a multitude of sensors and actuators and many different machines. The control system architecture is based on levels, where level 0 is the machine interface level comprising of actuators and sensors, level 1 is low level control, e.g. speeds, AGC (Automatic Gauge Control), looper tensions and level 2 is higher level control and coordination of individual areas, e.g. the finishing mill, roughing mill and furnaces, often involving computationally intense processes and model-based control.

The adoption of sophisticated computer control system and model based control methods has advanced the capabilities of modern steel rolling mills and most operations in the mill are automatically controlled [9]. However, with increasing control technology comes a demand for increasingly sophisticated sensing and measurement equipment and the nature of the environment has not changed. Cameras and other high-tech sensor devices are becoming common in the steel mill and the challenge of suitably protecting them is still a very real one. Computer control within the finishing includes cooling water, stand drive speeds, looper angle and AGC amongst others and the control methods are constantly under review [10]. However, the control of strip steering (tracking) still remains a manual operation in Tata steel mills and therefore is an area for development in order to keep the mills at the forefront of technology.

1.5   Strip tracking measurement and control

1.5.1   Strip tracking control

Automatic control of strip tracking has been considered on multiple occasions in both hot and cold strip mills and much work has been done in developing the control methods which can be used. In [11] the method of automatically controlling the strip position by adjusting the screw-down actuators was used, although details of the method of position measurement were lacking.

To provide an input for the strip tracking control system, differential forces (the difference in force across the stand) has been used [12]. Differential force as an input is a common theme in tracking control and even relatively modern control systems have specified it [13].

Developments in differential roll force based control were made and the concept of parallel mill modulus was used in [14] by adjusting the roll gap to compensate for the mill stretch caused by the strip off-centre.

In [15], roll forces in conjunction with roll gaps were used in an aluminium hot strip mill with a state feedback control system. The controller was tuned using plant parameters to ensure robust control.

Force feedback control was also used in [16], which used an LQR (Linear Quadratic Regulator) to regulate a state feedback control system in a simulated 6-high mill. This work was primarily focussed on tail-out and not full-body strip steering. Tail out is the part of the rolling process where the strip has left the subsequent stand so is no longer constrained

laterally, hence is more unstable. Also focussing on tail-out control was [17], but using VSS (Variable Structure System) control.

In [18], another force-based control system was presented. Here, it was identified that the dynamics of strip motion change when the strip tails of preceding stands and the coil box. A switched control system was adopted to take this into account.

A control strategy for the entire strip body was presented in [19] and [20], by same authors as [18], however this time using cameras to provide a feedback signal. This control system recognised that the product range in a hot rolling mill is highly variable and product families were identified, each with separate control parameters.

The control of strip tracking is a well studied area and many theories and methods for effecting this control have been developed. In order for any control system to function, a measurement of the parameter to be controlled is required.

1.5.2 Strip position measurement

The work presented to date has significantly focussed on the control of strip tracking and not the measurement method. In order to develop a successful control system, a robust method of measuring strip position is required.

The method of deriving a control signal representing strip position in [12] to [18] was by using the differential roll force, which varies as the strip moves laterally. However, in [18], [19] and [20], it was noted that the use of differential roll force measurements was difficult due to the complex relationships affecting the roll-force asymmetrically. Also, on a more practical level, it had been noted by engineers at the steelworks [4] that the load cells that measure roll-force can be unreliable and factors such as stiction in the roll stand can cause unpredictable behaviour.

Some work on strip tracking was done within Corus (now Tata) preceding the work undertaken for the EngD which is presented in this thesis. The most significant contributor to this prior work is de Roo and the core of his work is summarised in [5]. This report contains a summary of modelling work undertaken within RD&T in Corus and was used to guide further research and development in solving the problem of strip tracking, and hence strongly guided the direction of the work described in this thesis.

The core of the work by de Roo was the development and use of a strip tracking model to investigate the effects of asymmetrical screw position, the significance of crown and the sensitivity of width-thickness ratio on tracking. The model was also used to look into various different methods of controlling strip tracking. The main conclusions from the report were:

- Increased crown stabilises tracking movements
- Increased width to thickness ratio destabilises tracking movements
- Flattening between work roll and backup roll is the most significant cause of tracking instability at the high width to thickness ratios

The key point to summarise from these conclusions is that the wider, thinner flatter and harder products are inherently more laterally unstable during rolling due to the flattening between the work roll and backup roll.

The investigations into control methods gave the following conclusions:

- Differential force can be used to control tracking but it is critical that there is a reliable roll force measurement and a robust stand model to provide a relationship for strip position.
- An accurate measurement of roll gap at each side of the stand can provide a good control signal for strip tracking. This can be achieved by either direct measurement of the roll gap or by measurement of the distance between backup roll and work roll bearing chocks. The aim of this would be to account for the flattening between the work roll and backup roll which does not conform to the standard linear elastic mill modulus assumption. Note that it is thought that this measurement alone would not be completely suitable because it would not account for a wedged strip which is rolling straight in a wedged roll gap.
- Differential strip tensions can provide a useful indicator to tracking, but the roll gap measurement is still required. These tension measurements are available from the looper as standard in the IJmuiden mill, but not in Port Talbot or Llanwern.
- A direct measurement of strip position, for example by using cameras, would provide a suitable control means for tracking. This would be more powerful in combination with the accurate roll gap measurements because it was anticipated that a camera measurement would be fast enough to control the strip body but not the more unstable tail where the roll gap measurements would be necessary.

The conclusions from [5] reinforce the comments made in [18], [19] and [20] that differential roll-force measurements of tracking are possible in theory but would be reliant on a robust model of the plant and reliable measurements of force. It has already been noted that roll

force measurements are known to be unreliable and the load cells prone to failure and also any model based control would be plant specific and liable to change with maintenance and plant alterations. It is therefore thought that in order to create a robust and reliable strip tracking system, roll force measurements would not be the most suitable choice.

The best total measurement strategy is thought to be combining accurate roll gap (work roll flattening) measurements for high speed control with a direct measurement of position, such as with cameras for lower speed control and direct knowledge of position.

Further work by de Roo [21] suggested that a limited measurement system was also of use. If only a few stands had a camera providing a measurement of strip position for a control system, then strip position would be improved throughout the mill. The preferred location of the cameras would be beginning at the mill first stands in the mill. The principle behind this is that if the strip is controlled at the beginning of the mill it will tend to run more centrally for its length. Also, if the body of the strip is held reasonably in the centre then the strip tail swing will be less dramatic.

The direct measurement of strip position has been noted previously. In [22] a strip steering method was proposed using an unmanned "Detector" to provide the control signal for the steering process. Also in [23] as control method was presented using a "Sensor" of unknown type.

Measurements of strip tracking have been shown to be successful using cameras and offline analysis in [24]. These studies were undertaken to analyse the amount of strip movement happening in the mill, although the measurement was for offline analysis and not for online control

An invention was presented in [25], [26] and [27] for a steering control system, primarily for a Steckel mill (a reversing finishing mill). This system named cameras as the sensor of choice for the control signal, although no mention was given to the precise nature of the measurement system. Also, the work presented in [19] and [20] used cameras in a finishing mill to provide a control signal to the strip tracking control system. Again, no detail was given to the precise nature of the measurement system or the image analysis techniques used.

The work to date has shown that an effective strip tracking control system can be implemented by using cameras to provide the control signal. Using a vision system to measure strip position is not a novel idea, but the work that has been presented has only demonstrated the use of vision information in principle and not a robust and reliable measurement system. In an industrial control situation such as this, the practical implementation of a system is critical.

1.5.3 Vision based measurement systems

Vision in a steel mill

The direct measurement of strip position by a camera based vision system provides more complete information about the strip location and without the need of a complex model as would be required with an indirect method, such as differential force. However, cameras are sensitive electronic devices and can be damaged, particularly in an aggressive environment present in a steel rolling mill [9], therefore thought must be given for complete system design to ensure a vision system is robust and reliable.

Camera based measurement systems are frequently implemented successfully for a variety of applications in the steel mill. The offline analysis of strip tracking shown in [24] demonstrated successful measurement of strip position using a vision system, although this was not a permanent installation for control purposes.

In a roughing mill, cameras have been used to measure strip camber (curvature in the lateral plane) which is inherently related to strip tracking in the finishing mill. In [28], what was described as a "cheap solution" was implemented, using CCD cameras to view the bar in the rougher to measure the amount of camber. This system noted the brightness of the hot bar, meaning no artificial illumination was required. A few implementation problems were faced, most significantly being blurring of the images when the bar was moving at speed, which was most probably due to the low-cost cameras used.

A similar system was described in [29] in the Port Talbot hot strip mill, using offline measurements of camber to prove the principle of the measurement process. This system was later developed into a full online measurement system [30] (an internal Tata report describing the measurement system and success of initial measurement trials), and has demonstrated that online image analysis can be successful in a steelworks.

More closely related to the strip tracking problem is [31], which describes the implementation of a vision-based fuzzy logic controller to steer a Steckel mill. In this case a line-scan camera providing an analogue output was used as an input to the control system.

Also, as previously mentioned, [19] and [20] have noted use of vision based measurements for strip tracking control.

A vision application that is measuring longitudinal position rather than lateral position is described in [32]. This system was used to measure the location of the head of the strip in the roll bite during threading. The work presented in this paper concentrates on some of the difficulties in implementing a vision system in this environment. Many of the points raised in this work are applicable to other vision systems in a steel mill. Some of the main points include:

- Image acquisition must be robust and withstand the harsh environmental conditions.
- Transmission of data (images) must be tolerant to electrical noise present in the mill.
- Well founded image processing techniques should be used to ensure robust analysis
- The system must have access to plant control signals and system outputs must be accessible to the plant

The cameras used were enclosed within tough, water cooled enclosures which were IP67 rated to protect against the mill environment. Noise tolerant Gigabit Ethernet was used to transmit the images from the cameras to the analysis computer. This protocol was found to be advantageous because it allowed the use of standard networking components, bi-directional communication allowing online configuration and allowed multiple cameras to be connected. A large challenge to the image analysis process was steam and cooling water obscuring parts of the image, occasionally completely losing the position of the strip between frames. A predictive analysis method, along with other statistical techniques, was employed to ensure measurements could be achieved under the most difficult conditions.

Vision based measurement system have been proven to be successful in the steelworks as the above examples have demonstrated. However, at every stage care must be taken to ensure the entire measurement system, including hardware and software components, are suitable to the task in the challenging environment.

Image analysis

Image analysis [33] is the process of using an image to provide a measure or verification of a quantity. The term typically refers to the use of computers to automatically analyse an image acquired by a camera to extract relevant data for a process in order to provide a control signal. Information gained through image analysis can be of various types, including a quantitative description of the image in terms of brightness and colour intensities, verification of the presence or absence of a part, verification of correct manufacture of a product using simple measurements and determination of the position of an object in the image. In many applications, the result of an image analysis process, particularly in the parts-manufacturing industry, would be a simple Boolean result verifying if a part was OK or NOT OK. This could typically be the end result of a number of measurements of size, location and shape and ensuring these all conform to a set of known limits. In other cases, for example a measurement of position, a numerical answer would be required.

Many of the techniques used in image analysis processes rely on the fundamental method of edge detection. Edge detection is determining the location of a boundary between two distinct parts of an image, for example the edge of an object in view. The basic method of edge detection is to identify the location where image brightness rapidly changes, and therefore is most effective with a high contrast between the image and the object. Ideal conditions for an edge detection are with an opaque part on a backlit white surface of uniform brightness, resulting in the camera seeing a black silhouette of the object against a white background. Analysis of an image uses the numerical values of pixel brightness in the image. In a 8-bit Greyscale image, each pixel is represented by a single byte (8 bits) with an integer value between 0 (black) and 255 (white). An edge detection process would use a differentiation type method to analyse each pixel in the image to determine whether the brightness of neighbouring pixels is significantly changing, and that pixel would be determined as an edge. In most processes a kernel operator would be used; an array which is cross-multiplied by a region of pixels. Kernels can be used to perform an edge detection, apply a filter or transformation to the image, or a combination of both. Kernels can be applied in two dimensions, using data from neighbouring pixels both horizontally and vertically, or just a single dimension, using only horizontal or vertical neighbours. A 2 dimensional kernel could also be used to perform a one dimensional diagonal edge detection, but using appropriate components (kernel weightings) of horizontal and vertical pixels.

The fundamental method of strip position measurement would use an edge detection method to determine the location of the strip edges. In the rolling mill, the strip moves in a single

direction and only edges in one dimension are required. The steel strip is at high enough temperature to glow brightly, therefore providing a natural contrast, although this would not be as ideal as a black/white contrast from an opaque object against a lit background, therefore image analysis would be more difficult and require more advanced methods. The task is to measure a position, therefore a numerical output is required and not a Boolean output.

Vision technology and communications

Transmission of images from the cameras to the computer performing the analysis is critical to ensure the system has data to analyse. The steel mill is a large area and has a lot of electrical noise, therefore a protocol which can cover suitable distances and be noise tolerant is required. The vision system presented in [32] used a Camera Link compatible camera but GigE for transmission over long distances, with an adapter to convert from Camera Link to GigE. The reasons for using GigE were transmission distances and noise tolerance, as well as online configurability and ability to use standard Ethernet connection hardware.

A comparison of various camera interface technologies is shown in Table 1.1 [34]. In terms of speed, Camera Link can provide the fastest acquisition rates, however when transmitting these images for a distance using another protocol such as GigE, then the acquisition rate would be limited by the transmission rates of that protocol. The GigE Vision protocol allows the transmission over the largest distances and at high speed, and the number of cameras per interface is only limited by the available address space (unlimited on a practical scale). Note that GigE Vision is a specific vision protocol with a set structure of camera settings, and uses Gigabit Ethernet as a transmission medium and therefore differs from using GigE to transmit images from a camera with another protocol. The use of GigE Vision, as well as the advantages mentioned above, would minimise hardware requirements by not requiring a converter, e.g. from Camera Link to GigE, in order to transmit over long distances.

Table 1.1: Industrial vision communication protocols comparison [34]

	GigE Vision	IEEE 1394a	IEEE 1394b	Camera Link	Analog
Cable Length	100 meters	4.5 meters (up to 72 meters with repeaters)	4.5 meters (up to 72 meters with repeaters)	Up to 15 meters (depending on the bandwidth)	Up to 100 meters (depending on the video signal and quality loss)
Bandwidth	100 MBytes/s	32 MBytes/s	64 MBytes/s	255 Mbytes/s (base configuration) 680 Mbytes/s (full configuration)	-
Bit Rate	1000 Mb/s	400 Mb/s	800 Mb/s	>2000 Mb/s	-
Standards	GigE Vision Standard	IEEE1394 Trade Association DCAM Standard	IEEE1394 Trade Association DCAM Standard	AIA Camera Link Standard	Various standards for video signal timing. No standards for software or configuration.
Interface Board	Common gigabit Ethernet Board	Common IEEE 1394a Board	Common IEEE 1394b Board	Special frame grabber	Special frame grabber
Maximum Number of Cameras	Unlimited	16 (DCAM)	16 (DCAM)	2 (per frame grabber)	6 (depending on the frame grabber)
Plug & Play Ability	Yes	Yes	Yes	No	No
Cables	Industrial and consumer	Industrial and consumer	Industrial and consumer	Industrial	Industrial and consumer

The two major competing camera technologies available are CCD (Charge Coupled Device) and CMOS (Complementary Metal Oxide Semiconductor) [35]. The main difference between the two is that in a CCD the circuit board which digitises the image is separate to the image sensor, whereas in a CMOS device the circuit board is incorporated in the sensor.

The two technologies have some individual characteristics that make each more suitable for different applications.

The shuttering ability of CCD sensors allows image capture of moving objects to be possible without blurring, whereas the rolling shutter of a CMOS could cause some blurring. CCD sensors also have inherently better image quality and a better uniformity of image and are the sensor of choice in most machine vision systems. One area where CMOS sensors have an advantage for this application though is natural anti-blooming abilities. The high temperature, bright strip could cause blooming of the image, which would be detrimental to clear edge detection. If blooming is a problem then CMOS may be a more suitable choice.

1.6   Hot rolling and tracking modelling

An automatic control system can have the capability of performing actions on a machine with no user intervention. It is vital that a control strategy is robust, reliable and safe to prevent any potentially catastrophic or fatal occurrences as a result of an automatically controlled action. In the steel mill, this is of critical importance because the controlled item, the steel strip, can be up to 30 Tonnes in weight and at temperatures exceeding 1000°C.

In order to implement a safe control system, a number of measures can be taken. The system should be introduced in closely monitored gradual stages, enabling human intervention to prevent accidents before they occur and so confidence can be gained in the system. The use of computer modelling and simulation is also very useful. A system model can provide an environment to test out and develop control strategies without any risk of harm to people, machines or the production process.

Modelling can also be a very useful tool to improve the understanding of a problem. Strip tracking is a complex occurrence and many parameters can effect how the strip moves. By using a model, the significance and effect of these parameters can be investigated.

1.6.1   Steel rolling modelling

The process of steel rolling is a well studied field. The work by Ginzburg [36] provides an excellent resource, covering many aspects of steel rolling from multiple contributing sources. The main points of interest in the steel rolling model are output strip thickness and the roll force used to deform the strip to that thickness.

The output thickness of the strip is a combination of the unloaded size of the gap between the work rolls, and the amount the mill stretches and is expressed with equation (1). The mill stretch is assumed to be linear for the working region of the mill. The mill stretch is described by the value known as the mill modulus, and is generally in the order of 500mm/T [4][5][37][38].

$$h_O = C + \frac{P}{K}$$

(1)

Theories on the calculation of roll force typically are either derived from the fundamentals of plastic deformation in the roll gap or empirically derived equations. The derivation of roll force using the theories of plastic deformation is based around the diagram shown in Figure 1.7.
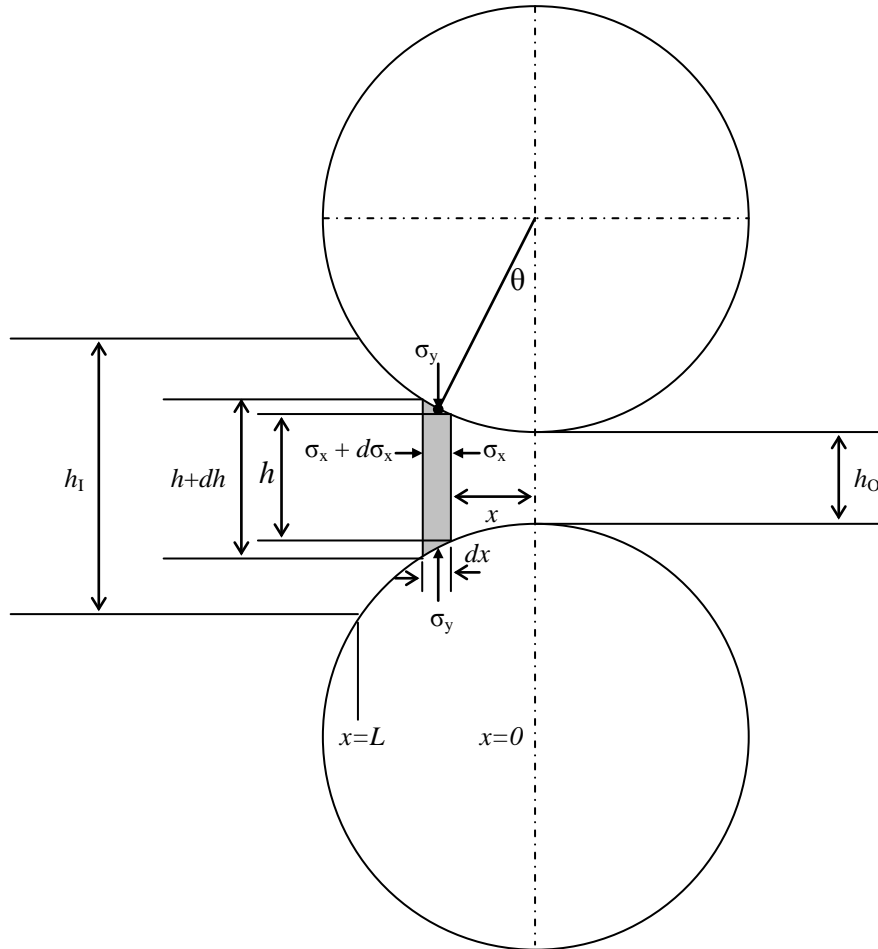
Figure 1.7: Deformation zone in rolling

The following assumptions are made for the analysis:

- There is no lateral spread
- There is no roll flattening
- Peripheral roll velocity is constant for the arc of contact
- No work hardening occurs
- The compression rate along the arc of contact does not have any effect on compression strength
- The vertical component of the friction force is negligible

Using the yield criterion expressed in (2) [36]

$$\sigma_y - \sigma_x = S = 1.15Y$$

(2)

The differential equation for rolling pressure along the roll bite is shown in (3) [36], given that the rolling pressure, P, equals the vertical shear stress, σ_y.

$$P\frac{dh}{dx} \mp 2\mu P = \frac{d\big(h(P-S)\big)}{dx}$$

<div align="right">(3)</div>

The solution to the differential equation depends on the assumptions made about the distribution of frictional force in the roll bite.

The advantage of a roll force calculation based on the plastic deformation differential equation is that it provides detail of the rolling pressure along the entire roll bite, as well as information such as the neutral point location (the point in the roll bite where there is no slip between the strip and the roll surface. However, these methods typically require a point-by-point calculation of the roll force so can be more computationally intense than an empirical equation. Empirical equations, on the other hand, are often suited only to the plant that they were derived on and can result in errors and inconsistencies in the roll force calculation. Observations by the author have noted that the point-by-point method has tended to result in values of roll force more accurately representing real plant data.

1.6.2 Strip tracking modelling

A strip being rolled is in contact with multiple locations of the mill, most significantly the roll stands, each of which will affect the movement.. These multiple points of contact mean that lateral strip movement in any roll stand is a combination of the conditions in that stand and the movement of the strip at all other roll stands. The strip is considered to be constrained laterally because of the effect of the neighbouring stands. A strip which was only being rolled in a single roll stand with no entry or exit tension is unconstrained.

In [6] a lateral strip model was put forward. The unconstrained movement of the strip was considered with the formation of camber, based on the theory of volume constancy. Volume constancy is the principle that the mass flow-rate (volume) entering the roll stand must equal the mass flow-rate of the strip leaving the stand. By assuming no lateral spread of material, this concept follows for asymmetrical variations in the roll gap and hence camber formation and asymmetrical strip velocities can be calculated.

The work also considered the case for a restrained strip by introducing a "camber change coefficient" which had a value between 0 and 1, depending on the amount of lateral constraint. The camber change coefficient was derived experimentally for a number of scenarios but an explicit method of calculation was not proposed.

<div align="right">20</div>

A method to account for the effect of neighbouring stands is to treat the strip as a bending beam element. This method has been used in a study involving a moving web [39], which is a very similar problem to strip tracking in a steel mill. This method was also adopted by Tarnopolskaya in [40],[41],[42] and [43], which describe various effects on strip tracking stability in a cold strip mill. Additionally, de Roo adopted the same approach in his model for strip tracking in the Corus steel mills [5],[44]. The aforementioned models all confirm that the assumption that the strip can be treated as a bending beam element is valid.

All of the above mentioned strip tracking models treat the strip as a single dimensional object, with a single value of asymmetry for the rolling parameters across the strip. Thus, they cannot account for a non-linear profile of factors such as temperature and wedge. The introduction of the ability to model variable profiles would further increase the knowledge of strip tracking behaviour.

1.7   Summary of literature

1.7.1 Measurement and control

Strip tracking is a well known problem in steel rolling. Numerous tracking control methods have been proposed. Historically, the feedback signal for a tracking control system has typically been the measurement of the difference in roll force at each side of the stand, known as the differential roll force. Using differential roll force can be difficult because a complex relationship exists between strip position and the differential force. More recently, tracking control systems using a direct measurement of strip position, typically with a vision system, have been proposed.

A steel mill is not the most suited environment for machine vision and analysis can be difficult compared to an ideal black silhouette on white background. Other factors such as steam and cooling water further impair analysis and more advanced image analysis methods can be required.

The physical environment of a steel mill is hostile and includes high temperatures, water, steam, oil and electrical noise. An electrical system must be suitably protected against all of these factors, using suitable physical protection for equipment and noise-tolerant data transmission mediums.

A complete system for strip position measurement must incorporate all the aspects considered above. In an industrial application, the design of the system as a whole, including hardware,

software and communication, is important to provide robust and reliable measurements. To the best of the authors knowledge, a complete system for online measurements of strip position in a finishing mill suitable for industrial control, has never been described.

1.7.2 Modelling

A computer model of the rolling process including lateral strip movements allows control strategies to be tested in a safe environment before implementation on the mill. Computer models also increase the understanding of the problem and can be used to direct further research and development efforts.

A strip tracking model can be considered as comprising of two component parts: a stand model and a strip model. The modelling of a rolling stand can be achieved using well founded theories and equations of plastic deformation of the strip and a linear elastic model of the stand. Strip tracking modelling is a relatively new field, but not completely novel. The movement and formation of strip in the stand can be modelled using the principle of volume constancy. The interactions of strip movement due to neighbouring stands can be modelled by treating the strip as a bending beam element.

Strip tracking models which have appeared in literature generally treat the strip with a linear profile of asymmetric parameters. Allowance for a variable (non-linear) profile of rolling parameters across the strip width could further enhance the understanding and causes of strip tracking dynamics.

1.8 Project aims

The work in this EngD project was centred in the finishing train of a hot strip mill and based on strip tracking. The general aim was to improve the knowledge on strip tracking and its causes and work towards fully automating strip tracking control.

The primary aim of this project was to develop a measurement system to enable the control of strip tracking. This measurement system can then be used as a basis of strip tracking control, either by manual control or in a fully automated system. The system and methods developed for strip tracking measurement were aimed at producing a solution to an industrial problem, therefore had to be robust.

Alongside the work on the measurement system, a secondary aim was working towards the creation of a computer simulation to model various rolling parameters and their effects on tracking. The computer model was designed to enable the determination of the significance of

various parameters on tracking stability. Being a secondary aim, the model was not designed to be an accurate representation of the entire mill, but to provide a tool to give relative results on the significance of the rolling parameters which could be used to support a targeted maintenance and improvement of the mill. The development of the computer model also provided a better understanding of the fundamentals of tracking behaviour and the problem of strip tracking control as a whole.

2 Strip tracking modelling theories

A computer model of the rolling process including lateral strip movements allows control strategies to be tested in a safe environment before implementation on the mill. Computer models also increase the understanding of the problem and can be used to direct further research and development efforts.

Strip tracking models which have appeared in literature [43],[44] generally treat the strip with a linear profile of asymmetric parameters. Allowance for a variable (non-linear) profile of rolling parameters across the strip width could further enhance the understanding and causes of strip tracking dynamics.

A strip tracking model was developed to allow the modelling of non-linear variable profiles of rolling parameters. This model was primarily designed to increase the understanding of strip tracking dynamics and to allow the determination of rolling parameters significant in increasing tracking instability. A potential further aim was to develop a control strategy for strip steering based on vision feedback control.

The development of this computer model was a secondary aim in this project as a whole, with the development of the strip tracking measurement system taking precedence. Therefore it was expected that the model would have limitations and the success of the project as a whole was not measured by the successful development of the computer model.

2.1 Overview

The principle idea behind the model was to allow the investigation into a variable profile across the strip width. This was achieved by splitting the strip into a series of discrete elements across the width and allowing each element to have different parameters. A further division into elements along the strip length was used to represent time steps in the model. Figure 2.1 is graphical representation of this idea, showing the strip split into elements with a hot patch about to enter the roll bite.
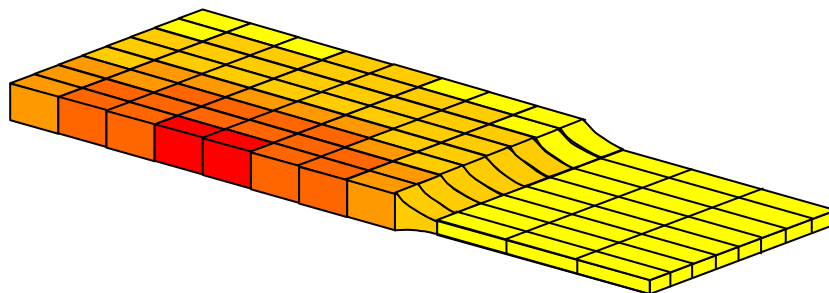
Figure 2.1: Representation of elemental model with hot patch entering roll bite

The model simulated a three stand rolling mill to include all three cases of lateral constraint in tracking:

- Stand 1: Constrained only at exit
- Stand 2: Constrained at exit and entry
- Stand 3: Constrained only at entry

Figure 2.2 and Figure 2.3 show the general layout of the model and the signs and conventions adopted throughout as follows:

- Three stands numbered $n = 1$ to 3 in rolling direction
- Elements across the strip $i = 1$ to B, numbered from OS to DS
- Lateral zero position is at roll centreline, positive movement is OS to DS
- Rotational zero position is parallel to rolling direction, positive rotation is clockwise viewed from above
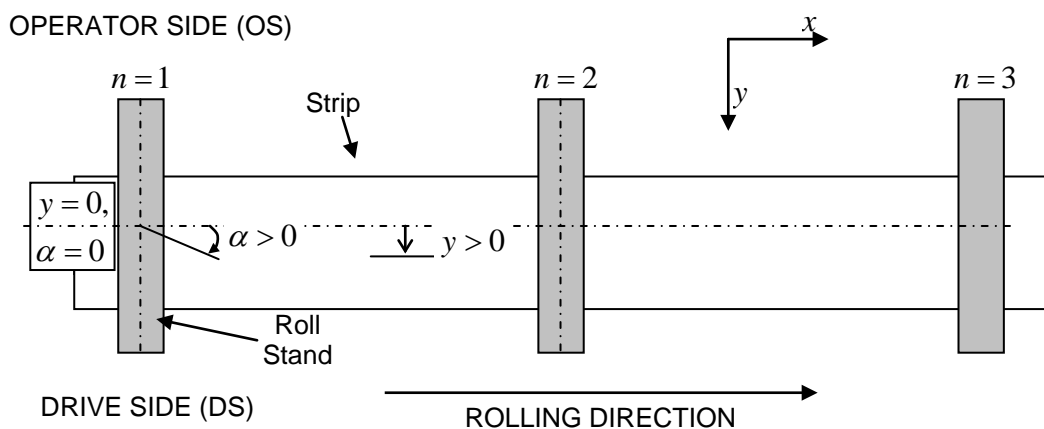
Figure 2.2: Plan view representation of model
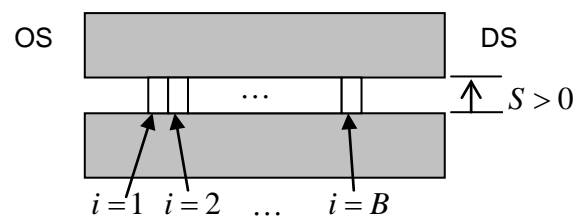
Figure 2.3: View into roll bite representation of model

2.2 Modelling theories

The strip tracking simulation was structured with two interlinked main component parts; the tracking model and the roll stand model. The tracking model component was used to calculate the strip motion and the roll stand model provided the necessary rolling process inputs, such as roll force, neutral point and deformation.

The strip model was developed based on existing theories of tracking and is based on the ideas of elongation and the formation of camber, and also treating the strip as a beam element with lateral forces and bending moments acting due to the lateral deflection of the strip [43] which causes a lateral velocity of the strip slipping across the roll bite [44].

The theories behind the roll stand model were based around well proven models of steel rolling [32], alongside a linear elastic model of the stand to handle mill stretch [4], [38].

2.3 Strip tracking model

The strip tracking component was used to model the lateral motion of the strip in the roll bite of each roll stand. The position of the strip in stand (n) is a combination of the position in the previous stand $(n-1)$, and the effects of the angle in the previous stand, camber induced by the previous stand and lateral and rotational speed in the current stand, as shown in equation (4).

$$y_{(n)} = y_{(n-1)} + y_{\alpha(n-1)} + y_{c(n-1)} + y_{V(n)}$$

(4)

Also, the strip entry angle in stand n is a combination of the exit angle in stand $(n-1)$, the effect of camber induced by stand $(n-1)$ and the rotational velocity in the current stand, shown in equation (5)

$$\alpha_{I(n)} = \alpha_{O(n-1)} + \alpha_{c(n-1)} + \alpha_{\omega(n)}$$

(5)

The exit angle of the strip was calculated as the entry angle multiplied by the OS-DS velocity ratio [44], as given by (6).

$$\alpha_{O(n)} = \alpha_{I(n)} \frac{V_{OS(n)}}{V_{DS(n)}}$$

(6)

The calculation of the component parts to equations (4) and (5) are discussed in the following sub-sections.

2.3.1 Position due to geometry and shape

Position from previous stand

The position of the strip in the previous stand has a direct influence on the position of the strip in the current stand; the component contributing the position in stand (n) from the position in stand $(n-1)$ is $y_{(n-1)}$, as shown in Figure 2.4.
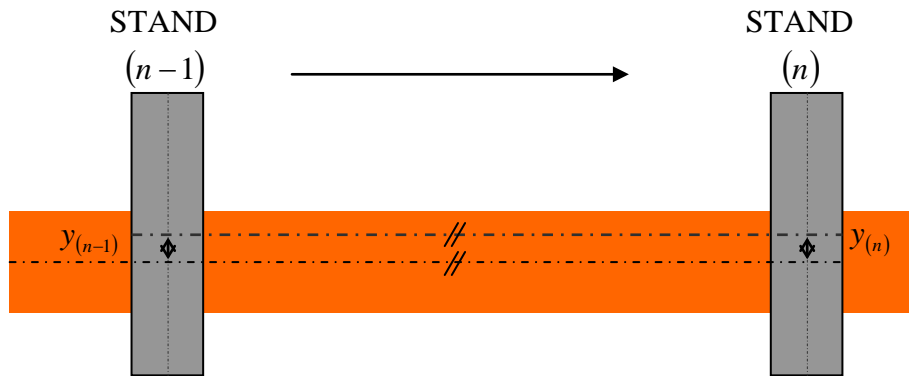
Figure 2.4: Position from previous stand

Angle from previous stand

The position in stand (n) due to an angular misalignment in stand $(n-1)$ is shown in equation (7) and Figure 2.5.
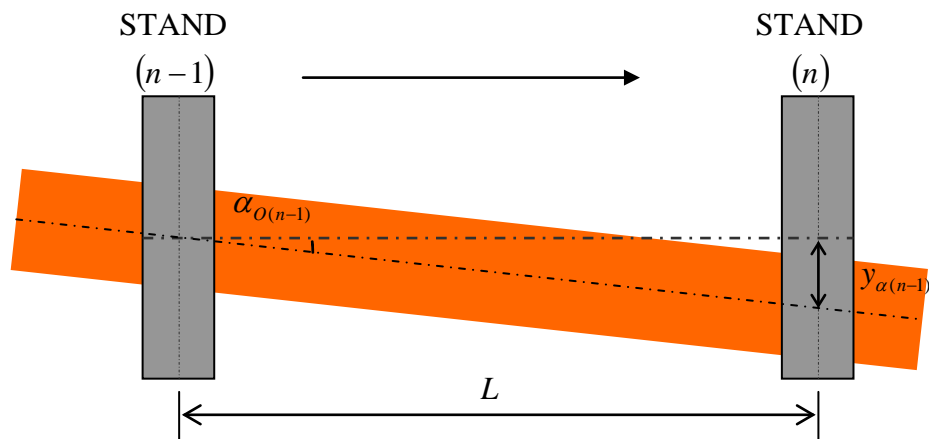
Figure 2.5: Position from angular misalignment in previous stand

$$y_{\alpha(n)} = L \cdot \tan\left(\alpha_{O(n-1)}\right)$$

$$(7)$$

The angular misalignment of the strip is a small angle (typically $\alpha_O \leq 0.5°$), therefore (7) was approximated by (8).

$$y_{\alpha(n)} = L \cdot \alpha_{O(n-1)}$$

<div align="right">(8)</div>

Position due to camber induced by previous stand

Strip camber is curvature of the strip in the rolling plane. Camber is induced in the strip by a difference in deformation across the strip, leading to a difference in elongation. This differential elongation manifests itself as a curvature in the strip, causing a lateral and angular offset in the next stand, as shown (exaggerated for clarity) in Figure 2.6.
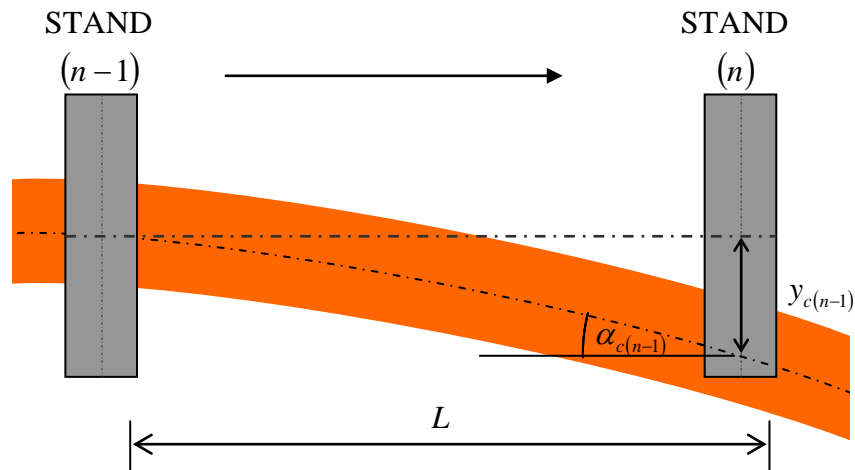
Figure 2.6: Strip camber

Figure 2.7 represents the geometry of a lateral deviation due to camber in the strip.
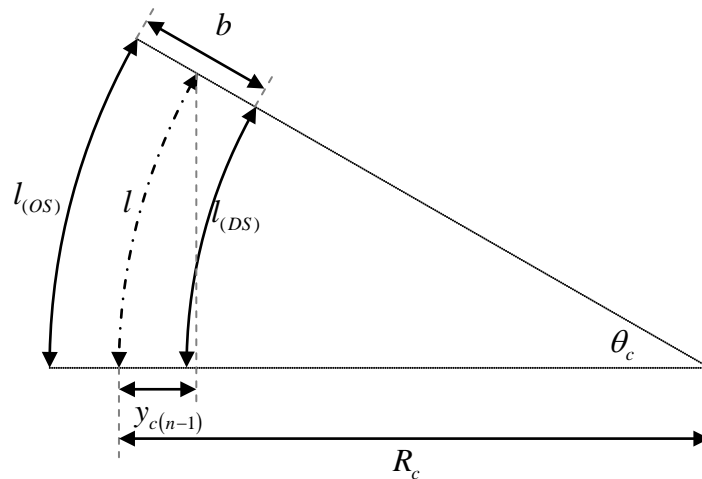
Figure 2.7: Offset due to camber

The length of the curved centreline of the strip between stands $(n-1)$ and (n) was given by equation (9)

$$l_{(n)} = R_{c(n)} \theta_{c(n)}$$

(9)

Therefore, the Operator Side (OS) and Drive Side (DS) lengths were found with equations (10) and (11) respectively.

$$\Rightarrow l_{OS(n)} = \left(R_{c(n)} + \frac{b}{2} \right) \theta_{c(n)}$$

(10)

$$\Rightarrow l_{DS(n)} = \left(R_{c(n)} - \frac{b}{2} \right) \theta_{c(n)}$$

(11)

By rearranging (10) and (11), the radius and angle of curvature were found with equations (12) and (13).

$$R_{c(n)} = \frac{b \left(l_{DS(n)} + l_{OS(n)} \right)}{2 \left(l_{OS(n)} - l_{DS(n)} \right)}$$

(12)

$$\theta_{c(n)} = \frac{2 l_{OS(n)}}{b \left(\dfrac{l_{DS(n)} + l_{OS(n)}}{l_{OS(n)} - l_{DS(n)}} + 1 \right)}$$

(13)

Hence the offset in stand (n) due to camber induced in stand $(n-1)$ was found with (14).

$$y_{c(n-1)} = R_{c(n)} \left(1 - \cos\left(\theta_{c(n)} \right) \right)$$

(14)

To calculate the effective OS and DS lengths of the strip edges, the elongation of the strip was separated into symmetrical and unsymmetrical components about the strip centre, and it was assumed that only the unsymmetrical component contributed to camber. A nominal strip length was calculated by taking an average of all elemental lengths across the width. Any elemental difference occurring symmetrically around the strip centreline would not contribute to camber. This principle is shown in Figure 2.8, which depicts the total elemental strip lengths in Figure 2.8(A), the unsymmetrical component was extracted and depicted by Figure 2.8(B), leaving the symmetrical component in Figure 2.8(C). The symmetrical component was not used in this model.
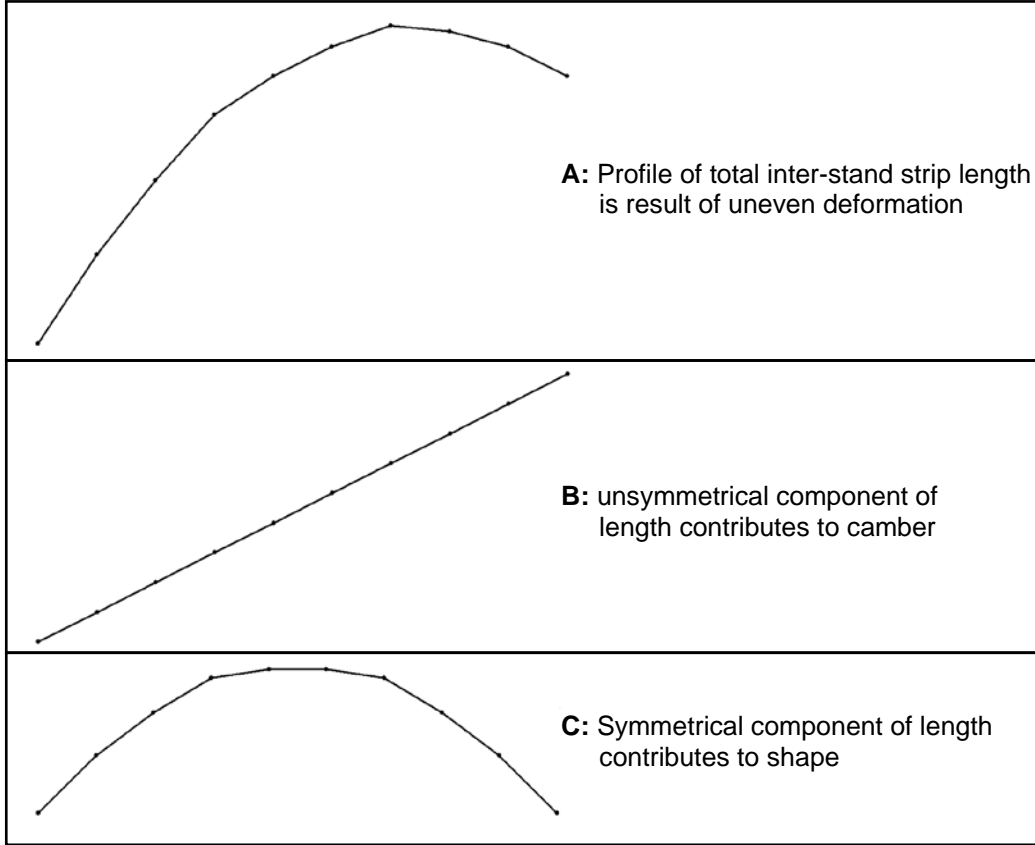
Figure 2.8: Components of strip length contributing to camber

First, the average strip length was calculated with (15), where B is the total number of elements across the strip width.

$$\overline{l_{(n)}} = \frac{\sum_{i=1}^{B} l_{(n)(i)}}{B}$$

(15)

The effective gradient of each elemental length was found with equation (16) by dividing the difference of each length and the average length by the distance that element is from the strip centre.

$$l_{Slope(n)(i)} = \frac{l_{(n)(i)} - \overline{l_{(n)}}}{i - \frac{B+1}{2}}$$

(16)

Hence the average gradient representing a linear average of the unsymmetrical elongation component was found with (17).

$$\overline{l_{Slope(n)}} = \frac{\sum_{i=0}^{B} l_{Slope(n)(i)}}{B}$$

(17)

The effective OS and DS lengths used in the calculation of camber were then found with equations (18) and (19) respectively.

$$l_{OS(n)} = \overline{l_{(n)}} + \frac{1-B}{2} \cdot \overline{l_{Slope(n)}}$$

(18)

$$l_{DS(n)} = \overline{l_{(n)}} + \frac{B-1}{2} \cdot \overline{l_{Slope(n)}}$$

(19)

2.3.2 Position due to lateral velocity

The strip position due to lateral velocity is the integral of the velocity over time, given by equation (20).

$$y_{V(n)} = \int_{t=0}^{T} V_{y(n)} \cdot dt$$

(20)

The lateral velocity was treated as a combination of a velocity component due to angular misalignment and a velocity component due to slip as a result of lateral forces acting on the strip. The total lateral velocity was hence given by (21)

$$V_{y(n)} = V_{\alpha(n)} + V_{D(n)}$$

(21)

2.3.3 Lateral velocity due to angular misalignment

A strip entering a roll bite at an angle will experience a driven lateral velocity as a result of the driving surface velocity of the roll and the angular input, as shown in Figure 2.9.
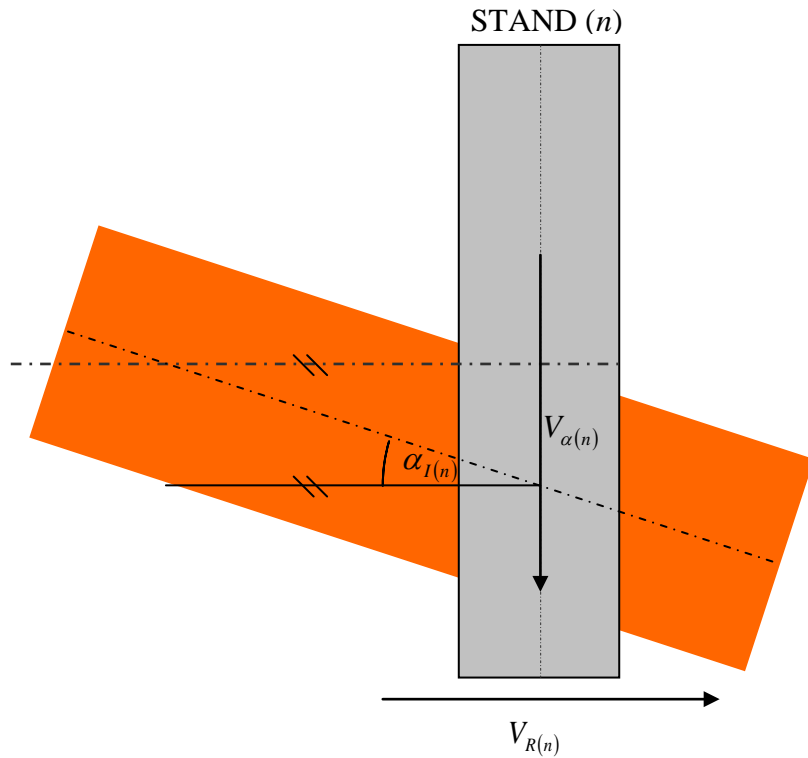
Figure 2.9: Lateral velocity due to angular input

The lateral velocity due to entry and was hence found using (22).

$$V_{\alpha(n)} = -V_{R(n)} \tan\left(\alpha_{I(n)}\right)$$

<div align="right">(22)</div>

Lateral velocity due to slip

A strip subject to a lateral force has a corresponding lateral velocity. The relationship between the lateral force and the velocity was found by vector analysis of the total shear forces acting on the strip [44]. The direction of the shear force acting on the surface of the strip in the roll bite is in the same direction as the relative velocity between the strip and the roll bite surface, depicted in Figure 2.10.
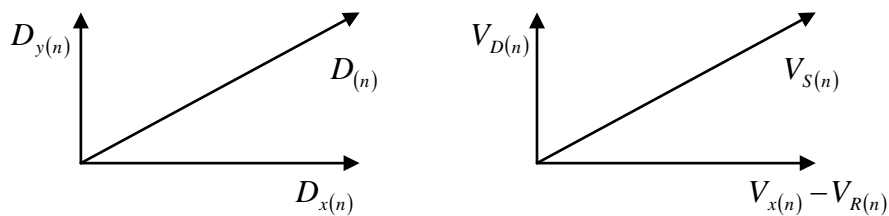
Figure 2.10: Vector analysis of shear force and slip velocity

The relative magnitudes of the force and velocity vectors is therefore given by equation (23)

$$\frac{V_{x(n)} - V_{R(n)}}{V_{D(n)}} = \frac{D_{x(n)}}{D_{y(n)}}$$

(23)

A coulomb friction model was assumed, i.e. equation (24) was used to define the relationship between shear forces and frictional forces.

$$D = \mu F$$

(24)

Hence (25) and (26) describe the relative component forces and coefficient of friction in the x and y directions.

$$D_{x(n)} = \mu_{x(n)} F_{(n)}$$

(25)

$$D_{y(n)} = \mu_{y(n)} F_{(n)}$$

(26)

The lateral slip velocity was hence derived in terms component coefficient of friction with (27).

$$V_{D(n)} = \frac{\mu_{y(n)}\left(V_{x(n)} - V_{R(n)}\right)}{\mu_{x(n)}}$$

(27)

The relationship between the component coefficients of friction was found using Pythagorean triangles in equation (28).

$$\mu_{(n)}^2 = \mu_{x(n)}^2 + \mu_{y(n)}^2$$

(28)

By using equations (25), (26) and (28), the component coefficients of friction were hence derived as in equations (29) and (30) in terms of total coefficient of friction and lateral force.

$$\mu_{y(n)} = \frac{D_{y(n)}}{F_{(n)}}$$

(29)

$$\mu_{x(n)} = \sqrt{\mu_{(n)}^2 - \left(\frac{D_{y(n)}}{F_{(n)}}\right)^2}$$

<div align="right">(30)</div>

The slip velocity in the x direction at the roll bite exit was evaluated by using the principle of conservation of mass and the result shown in (31). For reference, see the derivation of equation (45) in section 2.3.5.

$$V_{x(n)} - V_{R(n)} = \frac{2V_{R(n)} \cdot \left(R_{(n)} - \sqrt{R_{(n)}^2 - \left(N_{(n)} . a_{(n)}\right)^2}\right)}{h_{O(n)}}$$

<div align="right">(31)</div>

Equations (27),(29),(30) and (31) were combined to calculate the lateral velocity in the y direction due to a lateral force acting on the strip with equation (32)

$$V_{D(n)} = \frac{2V_{R(n)} . D_{y(n)} \cdot \left(R_{(n)} - \sqrt{R_{(n)}^2 - \left(N_{(n)} . a_{(n)}\right)^2}\right)}{F_{(n)} . h_{O(n)} \sqrt{\mu_{(n)}^2 - \left(\frac{D_{y(n)}}{F_{(n)}}\right)^2}}$$

<div align="right">(32)</div>

2.3.4 Angle due to geometry and shape

Angle from previous stand

As with the position in section 2.3.1, the exit angle of the strip in the previous stand has a direct influence on the entry angle of the strip in the current stand; the component contributing the entry angle in stand (n) from the exit angle in stand $(n-1)$ was $\alpha_{O(n-1)}$.

Angle due to camber induced by previous stand

The angular offset due to camber follows the same reasoning as described in 2.3.1. Figure 2.11 shows the geometry used in calculating the angular misalignment of a strip in stand (n) due to camber induced in stand $(n-1)$.
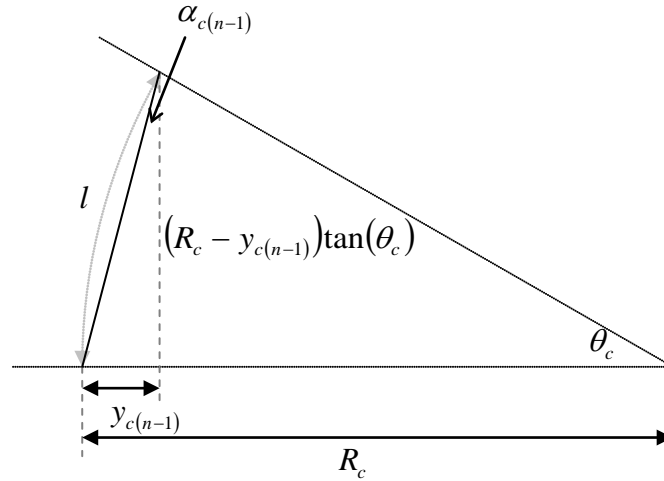
Figure 2.11: Angle due to camber

Hence equation (33) was used for the angular component due to camber.

$$\alpha_{c(n-1)} = \arctan\left(\frac{y_{c(n-1)}}{\left(R_c - y_{c(n-1)}\right)\tan(\theta_c)}\right)$$

(33)

2.3.5 Angle due to rotational velocity

The angular position of the strip due to rotational velocity is the integral of the rotational velocities over time, shown in equation (34)

$$\alpha_{\varpi(n)} = \int_{t=0}^{T}\omega_{(n)}.dt$$

(34)

As with the lateral velocity in section 2.3.2, the angular velocity was comprised of two components; the angular velocity due to a differential speed across the roll bite and an slip angular velocity due to bending moments in the strip. The total angular velocity was hence given by (35)

$$\omega_{(n)} = \omega_{V(n)} + \omega_{M(n)}$$

(35)

Angular velocity due to differential speed

A speed difference across the roll bite causes a rotational speed of the strip due to the effective tangential velocity of the strip [5]. By considering the centre of the strip at a entry of the roll bite, and the edges tangents of a circle of diameter equal to the strip width, the rotational velocity of the strip in the roll bite was defined by equation (36), using the

difference in entry velocity between the OS and DS edges as the tangential velocity. Note that the rotational velocity at the exit of the roll bite was assumed to be zero [43].

$$\omega_{V(n)} = \frac{2\left(V_{OS(n)} - V_{DS(n)}\right)}{b}$$

(36)

Considering the strip as a series of elements across the width, elemental tangential velocities were calculated for pairs of elements around the centreline, depicted in Figure 2.12.
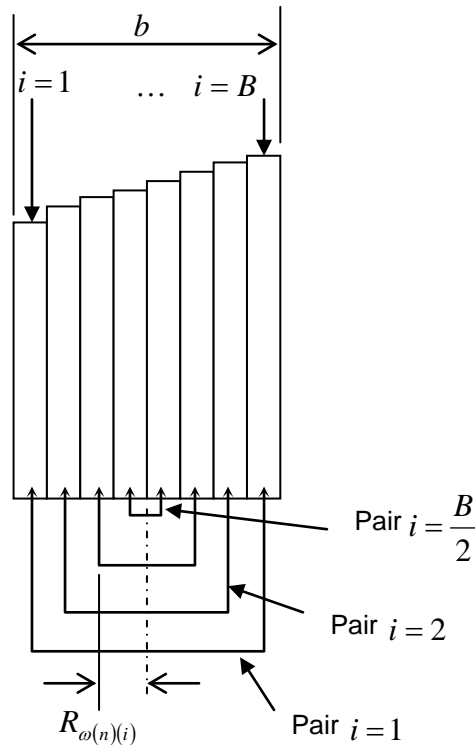
Figure 2.12: Elemental tangential velocities

The rotational velocity for element pair i was defined as equation (37).

$$\omega_{V(n)(i)} = \frac{V_{t(n)(i)}}{R_{\omega(n)(i)}}$$

(37)

The OS-DS elemental velocity was used as the elemental tangential velocity, given by equation (38).

$$V_{t(n)(i)} = V_{(n)(i)} - V_{(n)(B+1-i)}$$

(38)

The calculation of elemental rotational radius was defined as equation (39).

$$R_{\omega(n)(i)} = \frac{b}{2}\left(1 + \frac{2(1-i)}{B}\right)$$

(39)

The overall rotational velocity of the strip was defined as the average of the elemental rotational velocities in equation (40).

$$\omega_{V(n)} = \frac{2}{B}\sum_{i=1}^{\frac{B}{2}}\omega_{V(n)(i)}$$

(40)

To calculate the velocity of the strip at any point in the roll bite, the principle of mass-flow conservation was used. Mass flow conservation is the principle that the rate of flow of material is constant throughout the roll bite. Assuming no lateral spread, this was simplified to the product of thickness and velocity is constant, as in (41)

$$h'_{(n)(i)}V'_{(n)(i)} = C_{V(n)(i)}$$

(41)

Figure 2.13 shows a side view of the roll bite, with the strip moving left to right, depicting the geometry used in the calculation of strip velocity through the roll bite. Following equation (41), the thickness-velocity product of the strip at the roll bite is equal to that at the neutral point, expressed by equation (42).

$$h_{I(n)(i)}V_{I(n)(i)} = h_{N(n)(i)}V_{N(n)(i)}$$

(42)

The neutral point of the roll bite is the point where there is no slip between the strip and the roll, i.e. the strip velocity matches roll surface velocity, hence equation (43).

$$V_{N(n)(i)} = V_{R(n)(i)}$$

(43)

Equation (44) was used to calculate strip thickness at the neutral point, using the geometry in Figure 2.13

$$h_{N(n)(i)} = h_{O(n)(i)} + 2\left(R_{(n)(i)} - \sqrt{R_{(n)(i)}^2 - \left(N_{(n)(i)}a_{(n)(i)}\right)^2}\right)$$

(44)
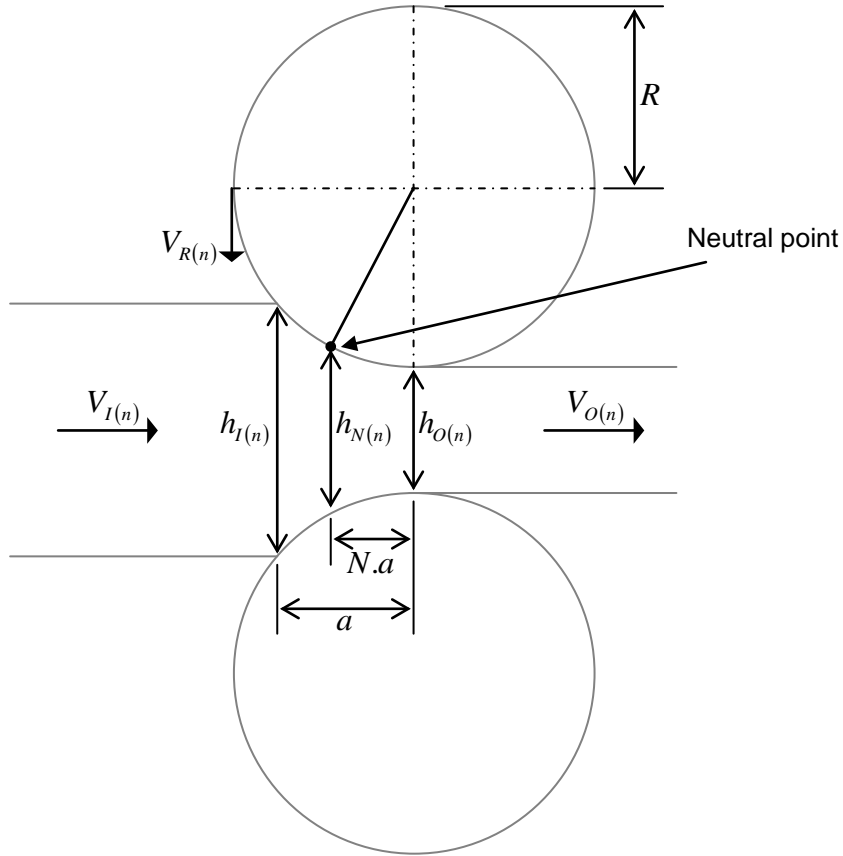
Figure 2.13: Side view of roll bite showing geometry for velocity calculation

Equations (42),(43) and (44)were combined to give equation (45), which was used to calculate strip entry velocity across the strip width.

$$V_{I(n)(i)} = \frac{h_{O(n)(i)} + 2\left(R_{(n)(i)} - \sqrt{R_{(n)(i)}^{2} - \left(N_{(n)(i)}a_{(n)(i)}\right)^{2}} \right)}{h_{I(n)(i)}} V_{R(n)(i)}$$

(45)

Angular velocity due to slip

Using the same reasoning as the lateral velocity due to slip, by considering the forces in the rolling direction, a similar relationship between slip velocity and force was derived. This was converted into a rotational velocity by considering tangential forces applied at the strip edges a result of a moment acting on the strip, as in Figure 2.14. The relationship between the moment and the tangential forces is given in equation (46).

$$M_{(n)} = D_{Sx(n)}b$$

(46)

38
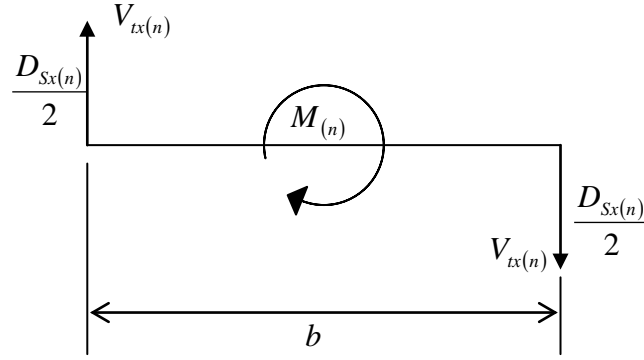
Figure 2.14: Tangential slip forces and moments acting on strip in roll bite

The equation used to calculate tangential slip velocity is shown in (47).

$$V_{tx(n)} = \frac{V_{y(n)}M_{(n)}}{bF_{(n)}\sqrt{\mu_{(n)}^2 - \left(\dfrac{M_{(n)}}{bF_{(n)}}\right)^2}}$$

(47)

The rotational slip velocity of the strip was calculated using equation (48).

$$\omega_{M(n)} = \frac{2V_{tx(n)}}{b}$$

(48)

2.3.6 Lateral forces and bending moments acting on the strip

The lateral forces acting on the strip were treated as a combination of two parts; a wedge force and a bending force [43],[44]. The wedge force is the component of the roll force acting in the lateral direction due to the roll bite being tilted (not level). The bending force is the reaction force of the strip having been deflected laterally.

Wedge force

Given a tilted roll bite as in Figure 2.15, then the component force acting in the lateral direction, the "wedge force", is given be equation (49).

39
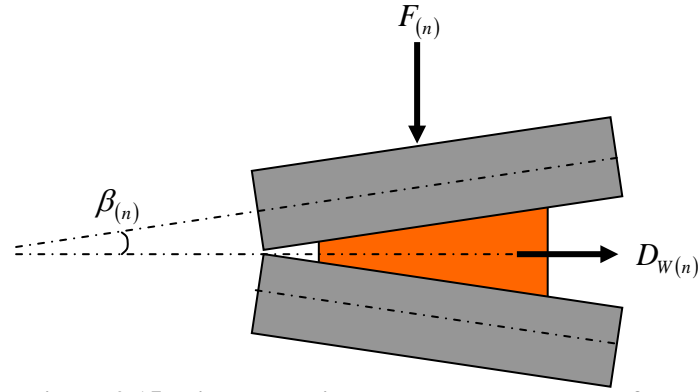
Figure 2.15: Tilted roll bite and component wedge force

$$D_{W(n)} = F_{(n)}.\tan\left(\beta_{(n)}\right)$$

(49)

Considering the strip as a set of discrete elements across the width, the wedge was calculated for each element individually then combined. Figure 2.16 shows a representation of three elements in the strip, and the elemental wedge of the central element is highlighted.
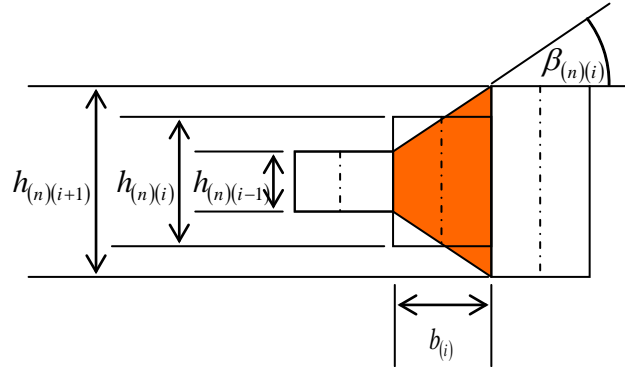
Figure 2.16: Elemental wedge

The total wedge force acting on the strip was calculated as the sum of the elemental wedge forces, as in (50).

$$D_{W(n)} = \sum_{i=1}^{B} D_{W(n)(i)}$$

(50)

Following equation (49), the elemental wedge forces were calculated by considering the portion of the total roll force acting on each element and the elemental wedge angle, as in Figure 2.16, calculated using equation (51).

$$D_{W(n)(i)} = F_{(n)(i)}\tan\left(\beta_{(n)(i)}\right)$$

(51)

Equation (52) was used to calculate the elemental wedge angle using the thicknesses from the adjacent elements.

$$\beta_{(n)(i)} = \arctan\left(\frac{h_{(n)(i+1)} - h_{(n)(i-1)}}{2b_{(i)}}\right)$$

(52)

The elemental width was defined as the total strip width divided by the number of elements across the width, as in (53).

$$b_{(i)} = \frac{b}{B}$$

(53)

The elemental wedge angles at the strip edges were approximated by assuming an elemental thickness beyond the strip extremities equal to the outer edge elemental thickness. Therefore the angles for $i = 1$ and $i = B$ were calculated using (54) and (55) respectively.

$$\beta_{(n)(1)} = \arctan\left(\frac{h_{(n)(2)} - h_{(n)(1)}}{2b_{(1)}}\right)$$

(54)

$$\beta_{(n)(B)} = \arctan\left(\frac{h_{(n)(B)} - h_{(n)(B-1)}}{2b_{(B)}}\right)$$

(55)

Hence, equation (56) was used to calculated total wedge force.

$$D_{W(n)} = \frac{1}{2b}\left(\sum_{i=2}^{B-1}\left[F_{(n)(i)}\left(h_{(n)(i+1)} - h_{(n)(i-1)}\right)\right] + F_{(n)(1)}\left(h_{(n)(2)} - h_{(n)(1)}\right) + F_{(n)(B)}\left(h_{(n)(B)} - h_{(n)(B-1)}\right)\right)$$

(56)

Bending forces and moments

The forces acting on the strip due to lateral deflection were calculated by treating the strip as a bending beam [41],[44]. Figure 2.17 shows a representation of the strip between stands (n) and $(n+1)$
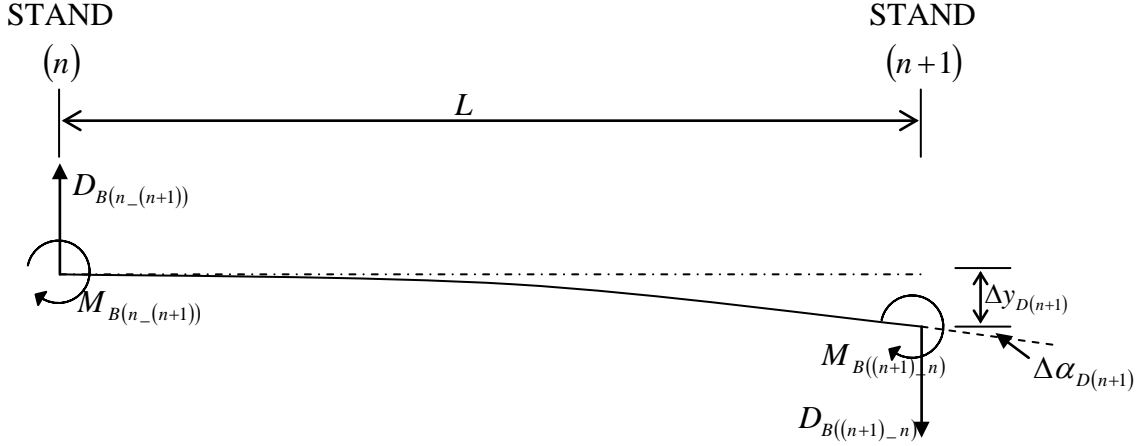
Figure 2.17: Bending forces acting on strip

The deflection of the strip in stand $(n+1)$ was considered to be the strained deflection, i.e. the difference between position in stand $(n+1)$ and stand (n), taking into account the factors due to the physical shape of the strip, such as camber and offset due to angle. Therefore, the deflection was defined with equation (57) and the angle of deflection in equation (58).

$$\Delta y_{D(n+1)} = y_{(n+1)} - y_{(n)} - y_{C(n)} - \alpha_{O(n)}.L$$

(57)

$$\Delta \alpha_{D(n+1)} = \alpha_{I(n+1)} - \alpha_{O(n)} - \alpha_{C(n)}$$

(58)

By analysis of Figure 2.17 using bending beam theory [56] the lateral and angular deflection were expressed in terms of bending forces and moments in equations (59) and (60).

$$\Delta y_{D(n+1)} = \frac{D_{B((n+1)\_(n))}L^3}{3EI} + \frac{M_{B((n+1)\_(n))}L^2}{2EI}$$

(59)

$$\Delta \alpha_{D(n+1)} = \frac{D_{B((n+1)\_(n))}L^2}{2EI} + \frac{M_{B((n+1)\_(n))}L}{EI}$$

(60)

Assuming the sum of all forces and moments is equal to zero, i.e. (61) and (62).

$$\sum D_B = 0$$

(61)

$$\sum M_B = 0$$

(62)

The bending forces, D_B, were defined as the forces bending the strip away from the centreline. The forces causing the strip to slip in the roll bite due to bending were the reactionary forces to the bending forces, the bending slip forces D_S. Hence equations (63) and (64) were used to define the bending slip forces.

$$D_{S((n+1)\_(n))} = -D_{B((n+1)\_(n))}$$

(63)

$$D_{S((n)\_(n+1))} = -D_{B((n)\_(n+1))}$$

(64)

As with the bending forces, the slip bending moments of the strip on the roll bite oppose the bending moments acting on the strip, hence equations (65) and (66) were used

$$M_{S((n+1)\_(n))} = -M_{B((n+1)\_(n))}$$

(65)

$$M_{S((n)\_(n+1))} = -M_{B((n)\_(n+1))}$$

(66)

By rearrangement and substitution of equations (57) to (64), the bending slip forces acting on the strip at stands (n) and $(n+1)$ due to the inter-stand deflection between those stands was defined using equations (67) and (68) respectively.

$$D_{S((n)\_(n+1))} = \left(y_{(n+1)} - y_{(n)} - y_{C(n)}\right)\frac{12EI}{L^3} - \left(\alpha_{I(n+1)} + \alpha_{O(n)} - \alpha_{C(n)}\right)\frac{6EI}{L^2}$$

(67)

$$D_{S((n+1)\_(n))} = \left(\alpha_{I(n+1)} + \alpha_{O(n)} - \alpha_{C(n)}\right)\frac{6EI}{L^2} - \left(y_{(n+1)} - y_{(n)} - y_{C(n)}\right)\frac{12EI}{L^3}$$

(68)

The total slip force acting on the strip in stand (n) was the sum of the bending slip forces in the previous and next inter-stand gaps and the wedge force in that stand, i.e. equation (69).

$$D_{y(n)} = D_{W(n)} + D_{S((n)\_(n+1))} + D_{S((n)\_(n-1))}$$

(69)

The total moment acting on the strip stand (n) was given as the sum of the bending moments from the adjacent inter-stand beams and the moments from the lever arms from the lateral forces acting in the adjacent stands, given in equation (70).

$$M_{(n)} = M_{S((n)\_(n-1))} + M_{S((n)\_(n+1))} + \left(D_{y(n+1)} - D_{y(n-1)}\right)L$$

(70)

2.4 Roll stand model

The roll stand model was used to calculate the rolling parameters at each stand for the tracking model. The parameters include roll force, output thickness and length, location of the neutral point, roll bite length and work roll surface velocity. The general principle behind the model was that the mill has two screw-down actuators which move the rolls apart. As the strip is driven through the narrow roll bite, it has a resistance to deformation, known as the roll force, which is measured at load cells at either edge of the mill. The large forces required during rolling cause the whole roll stand to stretch, which was considered to act as a spring with a linear coefficient of elasticity, known as the mill modulus [4], [5], [32]. The general roll stand model used in this simulation is shown in Figure 2.18.
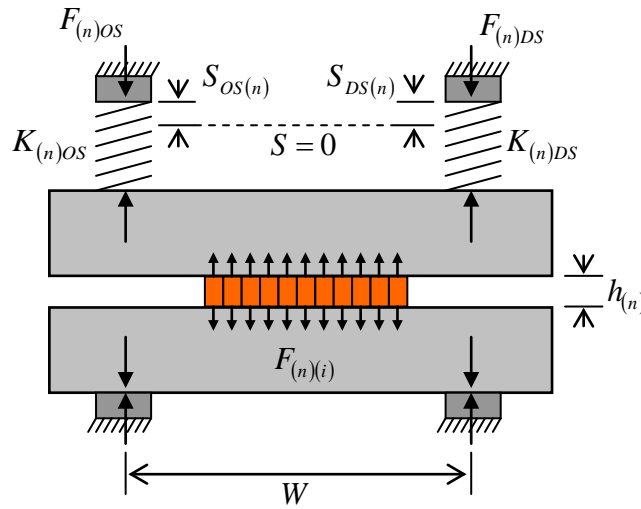
Figure 2.18: Roll force and deformation model

2.4.1 Roll force and deformation calculation process.

The effect of mill stretch causes the roll gap to widen when material is rolled, hence if the roll gap was set to be the desired output thickness of the strip, the mill would stretch and the output thickness would be larger than desired. To overcome this problem, the amount of mill stretch must be taken into account. This was achieved by using equation (71) to set the screw positions. This equation is of the same form as the AGC (automatic gauge control) equation used in a real steel mill [32].

$$S_{(n)} = h_{(n)} - \frac{F_{(n)}}{K_{(n)}}$$

(71)

However, the roll force required to deform a strip is highly dependent on the exit thickness, and from (71) it can be seen that the exit thickness is also dependent on the roll force. For known rolling conditions the roll force to achieve the required thickness can be calculated and the required screw position set from this force, but if there was a change to rolling conditions, then the roll force and exit thickness would not be able to be explicitly calculated. To solve the problem of interdependence of roll force and exit thickness, an iterative solution was derived, the process flow of which is shown in Figure 2.19.

The details behind the calculation of roll force are described in the following sub sections.
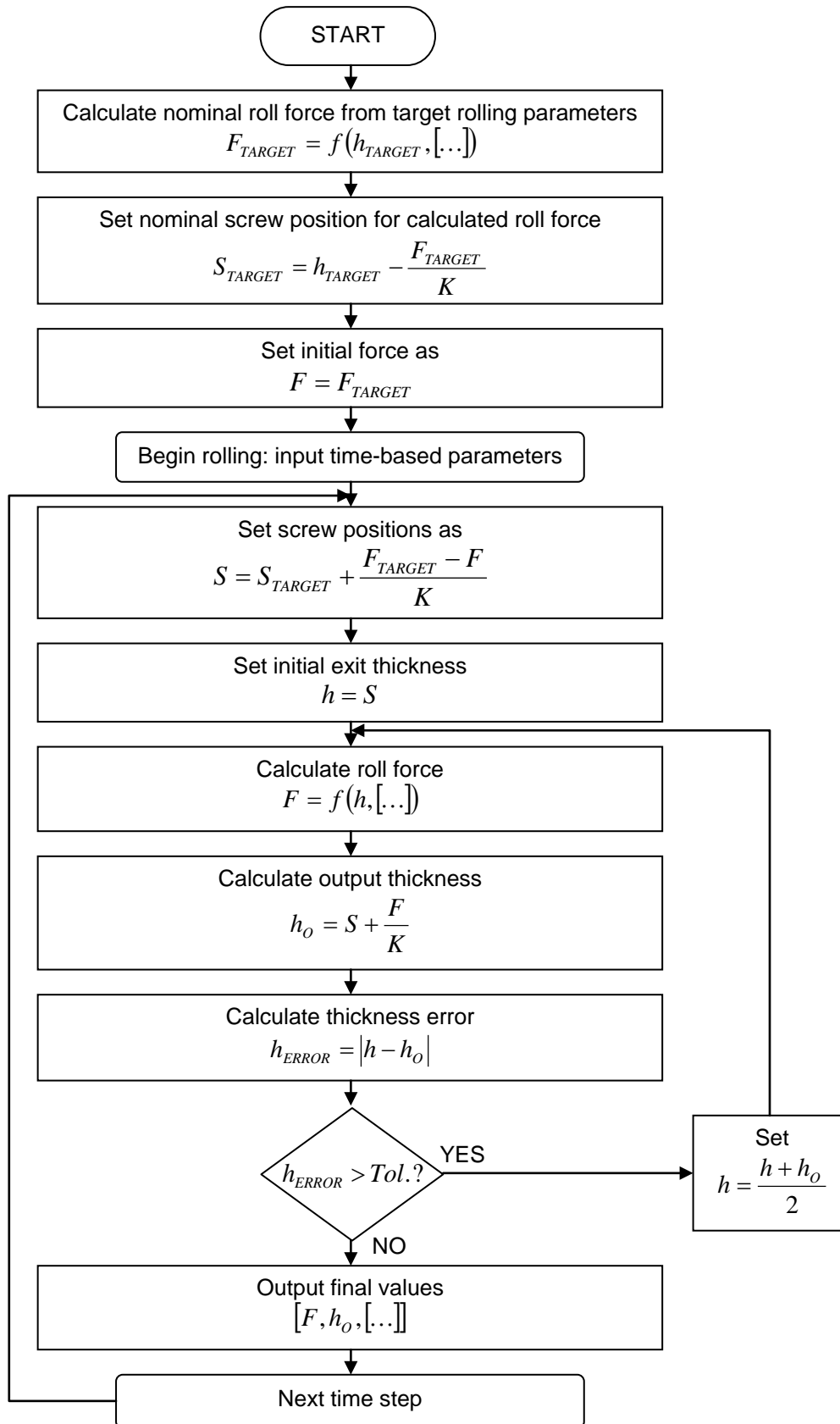
Figure 2.19: Calculation of roll force and output thickness

2.4.2 Calculation of roll force

To calculate roll force, a point by point integration of the VonKarman [32] method was used. Roll force was calculated as the product of pressure and area for a series of discrete points along the roll bite and summed for each elemental roll force. Figure 2.20 shows the geometry used in the calculation of the various parameters required.
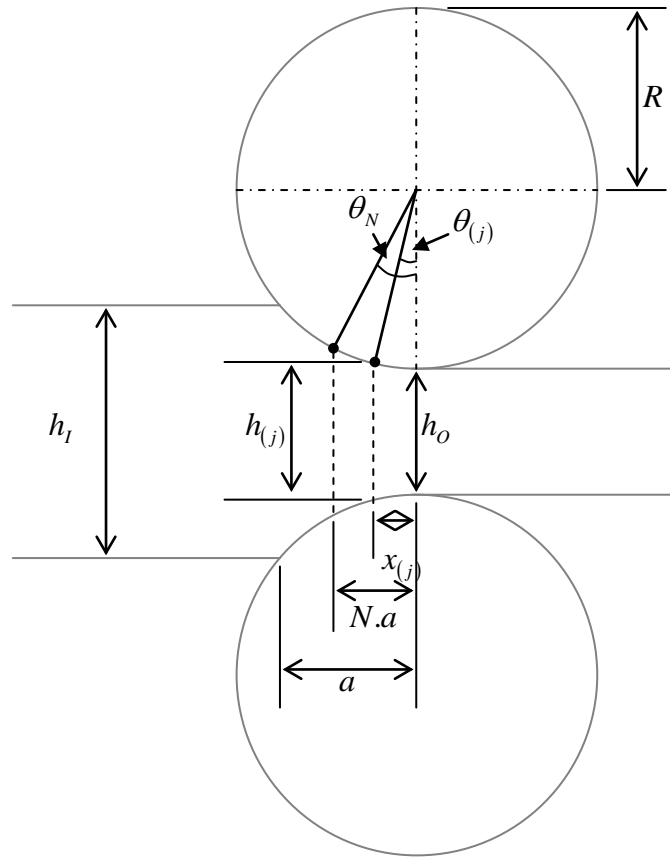
Figure 2.20: Geometry used in calculation of parameters for roll pressure

The rolling pressure at point j in element i of stand n was calculated using equation (72) for points between the entry plane and neutral point, and equation (73) for points between the neutral point and exit plane.

$$P_{(n)(i)(j)} = \frac{Y'_{S(n)(i)}}{\xi_{(n)(i)}} \left(\left(\frac{p_{1(n)(i)}}{Y'_{S(n)(i)}} \xi_{(n)(i)} - 1 \right) \left(\frac{h_{I(n)(i)}}{h_{(n)(i)(j)}} \right)^{\xi_{(n)(i)}} + 1 \right)$$

(72)

$$P_{(n)(i)(j)} = \frac{Y''_{S(n)(i)}}{\eta_{(n)(i)}} \left(\left(\frac{p_{2(n)(i)}}{Y''_{S(n)(i)}} \eta_{(n)(i)} - 1 \right) \left(\frac{h_{(n)(i)(j)}}{h_{O(n)(i)}} \right)^{\eta_{(n)(i)}} - 1 \right)$$

(73)

Equations (74) to (80) provide the terms for the VonKarman equations.

$$Y'_{S(n)(i)} = \frac{Y_{S(n)(i)}}{1 + \mu_{(n)(i)} \tan\left(\theta_{N(n)(i)}\right)}$$

(74)

$$Y''_{S(n)(i)} = \frac{Y_{S(n)(i)}}{1 - \mu_{(n)(i)} \tan\left(\theta_{N(n)(i)}\right)}$$

(75)

$$p_{1(n)(i)} = \frac{Y_{S(n)(i)} - s_{1(n)}}{1 + \mu_{(n)(i)} \tan\left(\theta_{N(n)(i)}\right)}$$

(76)

$$p_{2(n)(i)} \frac{Y_{S(n)(i)} - s_{2(n)}}{1 - \mu_{(n)(i)} \tan\left(\theta_{N(n)(i)}\right)}$$

(77)

$$\xi_{(n)(i)} = \frac{\tan\left(f_{(n)(i)} - \theta_{N(n)(i)}\right)}{\tan\left(\theta_{N(n)(i)}\right)} + 1$$

(78)

$$\eta_{(n)(i)} = \frac{\tan\left(f_{(n)(i)} + \theta_{N(n)(i)}\right)}{\tan\left(\theta_{N(n)(i)}\right)} - 1$$

(79)

$$f = \arctan\left(\mu_{(n)(i)}\right)$$

(80)

The total roll force for each element was calculated as the sum of the point roll pressures over discrete areas for the length of the roll bite, given by equation (81).

$$F_{(n)(i)} = \sum_{j=0}^{J} P_{(n)(i)(j)} . A_{(n)(i)(j)}$$

(81)

The discrete area was calculated using (82).

$$A_{(n)(i)(j)} = R_{(n)(i)} . \Delta\theta_{(n)(i)(j)}$$

(82)

The discrete change in rolling angle was given by (83).

$$\Delta\theta_{(n)(i)(j)} = \theta_{(n)(i)(j)} - \theta_{(n)(i)(j-1)}$$

(83)

48

The rolling angle was calculated using (84).

$$\theta_{(n)(i)(j)} = \arcsin\left(\frac{x_{(n)(i)(j)}}{R_{(n)(i)}}\right)$$

(84)

Equation (85) was used to calculate the distance from the exit of the roll bite.

$$x_{(n)(i)(j)} = \frac{j.a_{(n)(i)}}{J}$$

(85)

The total length of the roll bite was calculated using equation (86).

$$a_{(n)(i)} = \sqrt{R_{(n)(i)}^2 - \left(R_{(n)(i)} - \frac{h_{I(n)(i)} - h_{O(n)(i)}}{2}\right)^2}$$

(86)

The thickness of the strip at point j was calculated using (87)

$$h_{(n)(i)(j)} = h_{O(n)(i)} + 2\left(R_{(n)(i)} - \sqrt{R_{(n)(i)}^2 - x_{(n)(i)(j)}^2}\right)$$

(87)

To calculate the constrained yield stress, equation (88) was used [32], which includes the additional coefficient to calculate the yield stress at higher temperature.

$$Y_{S(n)(i)} = 1.15Y_o.k_{T(n)(i)}$$

(88)

The temperature coefficient modification to (88) was added using an adaptation of the Golovin-Tiagunov method for the calculation of resistance to deformation [32]. Equation (89) was used when $T_{(n)(i)} \geq T_m - 575$ and equation (90) was used when $T_{(n)(i)} < T_m - 575$.

$$k_{T(n)(i)} = \frac{T_m - T_{(n)(i)} - 75}{1500}$$

(89)

$$k_{T(n)(i)} = \left(\frac{T_m - T_{(n)(i)}}{1000}\right)^2$$

(90)

The coefficient of friction was given by (91) [32].

$$\mu_{(n)(i)} = 0.55\left(1.05 - 0.0005T_{(n)(i)}\right)$$

<div align="right">(91)</div>

The neutral point angle was given by (92).

$$\theta_{N(n)(i)} = \arcsin\left(\frac{N_{(n)(i)}a_{(n)(i)}}{R_{(n)(i)}}\right)$$

<div align="right">(92)</div>

The neutral point is the point which defines the position in the roll bite where the roll speed matches the strip speed. The location of the neutral point is the intersection point of (72) and (73) if both equations are calculated for the entire length of the roll bite. The roll pressure along the roll bite can also be given as the minimum of these two curves. Figure 2.21 is used to illustrate this, which is a graph showing calculated pressure along the roll-bite for a reduction from 4mm to 3mm with a work roll of radius 350mm. Note that distance is from the roll bite exit; the exit point is on the left of the graph, the entry on the right.
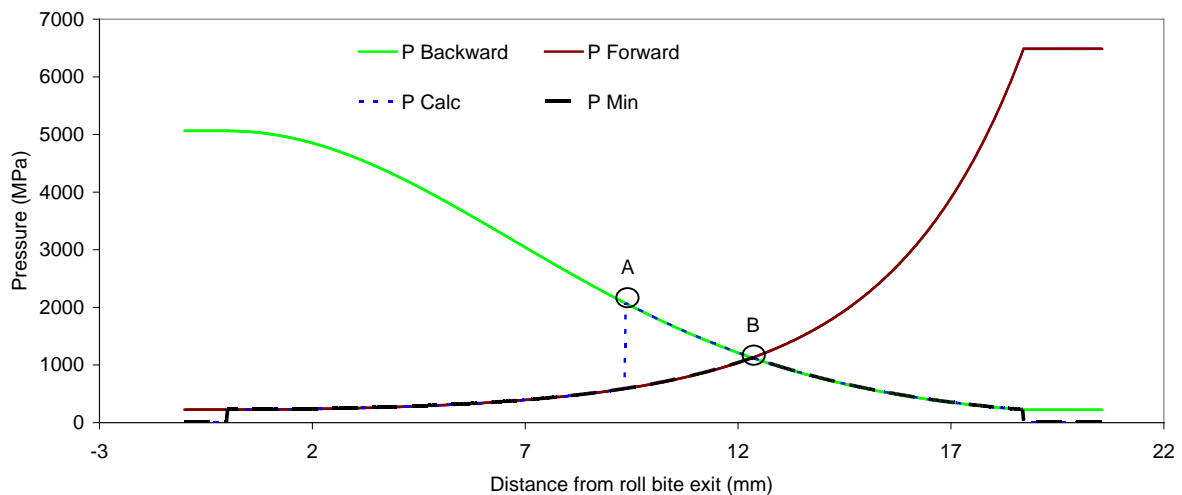
Figure 2.21: Neutral point location

The line "P Backward" was calculated using (72) and "P Forward" was calculated using (73). The line "P Calc is the output pressure using equation (73) before and (72) after an arbitrary neutral point of $N = 0.5$ and "P Min" is the result when the minimum of the two curves is used. Both "P Calc" and "P Min" have been set to zero for locations outside the roll bite. Points A and B represent two conflicting values of where the neutral point lies in this example – A was used to calculate the lines but B represents a calculated location of the neutral point given the same input parameters. To calculate a final value of N, an arbitrary neutral point of 0.5 was used then a new neutral point determined by the minimum of the

graphs (point B) was fed back into the roll force calculations, repeating the iteration until a stable answer was reached.

2.4.3 Calculation of screw positions

To control the gauge of the strip in the mill, the force-controlled AGC equation [4][32][44][10] was used. This equation adjusts the mill screw positions for any change in roll force, allowing for mill stretch and is shown in (93).

$$S_{(n)} = S_{0(n)} + \frac{F_{0(n)} - F_{(n)}}{K_{(n)}}$$

(93)

2.4.4 Calculation of output thickness

The output thickness of the strip was calculated by adding the effective roll gap thickness given the screw positions to the difference in nominal roll radius to actual roll radius, shown in (94). Note that the term $R_{(n)(i)}$ (elemental roll radius) as used in this model was not necessarily a true roll radius, but was used to set a final output profile of the strip which could account for factors such as roll bending and work roll expansion without explicit calculation of these factors.

$$h_{(n)(i)} = h_{Slope(n)(i)} + \left(R_{0(n)} - R_{(n)(i)}\right)$$

(94)

The effective roll gap given uneven screw positions was calculated using (95) by assuming a linear slope across the strip width.

$$h_{Slope(n)(i)} = h_{OS(n)(i)} + \frac{h_{DS(n)(i)} - h_{OS(n)(i)}}{B - 1}(i - 1)$$

(95)

Equations (96) and (97) were used to calculated the effective thicknesses at the edges of the strip on the OS and DS sides respectively.

$$h_{OS(n)} = \left(y - \frac{b}{2}\right)\frac{S_{DS(n)} - S_{OS(n)}}{W} + \frac{S_{OS(n)} + S_{DS(n)}}{2}$$

(96)

$$h_{DS(n)} = \left(y + \frac{b}{2}\right)\frac{S_{DS(n)} - S_{OS(n)}}{W} + \frac{S_{OS(n)} + S_{DS(n)}}{2}$$

(97)

The effective OS and DS screw positions given unsymmetrical mill stretch due to a differential force across the strip were calculated using (98) and (99).

$$S_{OS(n)} = S_{(n)} + \frac{F_{OS(n)}}{K_{(n)}}$$

(98)

$$S_{DS(n)} = S_{(n)} + \frac{F_{DS(n)}}{K_{(n)}}$$

(99)

2.4.5 Calculation of drive speeds

The roll speeds in the stands used in this model were simplified to create "perfect" roll speeds, i.e. matched for volume flow conservation throughout the model. The roll speed in the first stand was set to a nominal value and used as a reference for the calculation of roll speeds in the following stands. Equation (100)was used to calculate roll speeds in the second and third stands.

$$V_{R(n)} = V_{R(n-1)} \frac{\overline{h_{I(n)}}}{\overline{h_{O(n)}}}$$

(100)

2.4.6 Evaluation of computer model

The computer modelling work was not completed to a level where useful results could be gained. The work to this point is presented for reference purposes and to demonstrate and understanding of the dynamics of strip rolling and lateral movement. An implementation and evaluation of the model is given in Appendix B, where the limitations of the model are discussed. This evaluation identified large instabilities in the tracking component of the model, but the roll-stand component was shown to be reasonably well validated.

The model was considered as a secondary project aim, with the main focus being on the development of the strip tracking measurement system. Therefore, failings in the modelling work were not considered to be failings in the project as a whole.

3 Concept of Measurement System and Initial Trials

In Chapter 1, the relative merits of various options for strip tracking measurement were discussed and it was concluded that it is preferred to have a direct measurement of strip position for full strip tracking control. The preferred method was to use a camera for a direct, measurement in combination with an accurate roll gap measurement for faster and finer control [5].

The principle aim of this EngD project was the development of a vision system for the use in strip tracking control.

3.1 Vision based measurement

The principle idea behind a vision based measurement system was to use a camera to capture an image of the strip, analyse the image to find the location of the strip edges then calculate the centreline of the strip from the edge locations, as depicted in Figure 3.1, which shows a representation of a plan view of a strip. An imaginary camera view area is highlighted in grey The green and blue lines represent right and left edges of the strip respectively, as determined by some image analysis software. The result in this representation is the dashed white line, representing the strip centreline.

The strip edges could be detected using standard image analysis techniques and calculated with reference to the viewing window of the camera. The absolute centreline position would then be calculated by adding the offset between the camera centre and the mill centre.

In general, a camera would be mounted above the strip from the overhead gantry or other appropriate supporting structure viewing vertically downwards to the strip below. The images or video must then be made available for analysis. In a temporary system used for development purposes, they could be recorded locally or on a remote recording device and accessed at a later date for analysis. For an online system used for control, the images must be available to a dedicated computer system immediately in order for analysis to be undertaken in time to steer the strip.
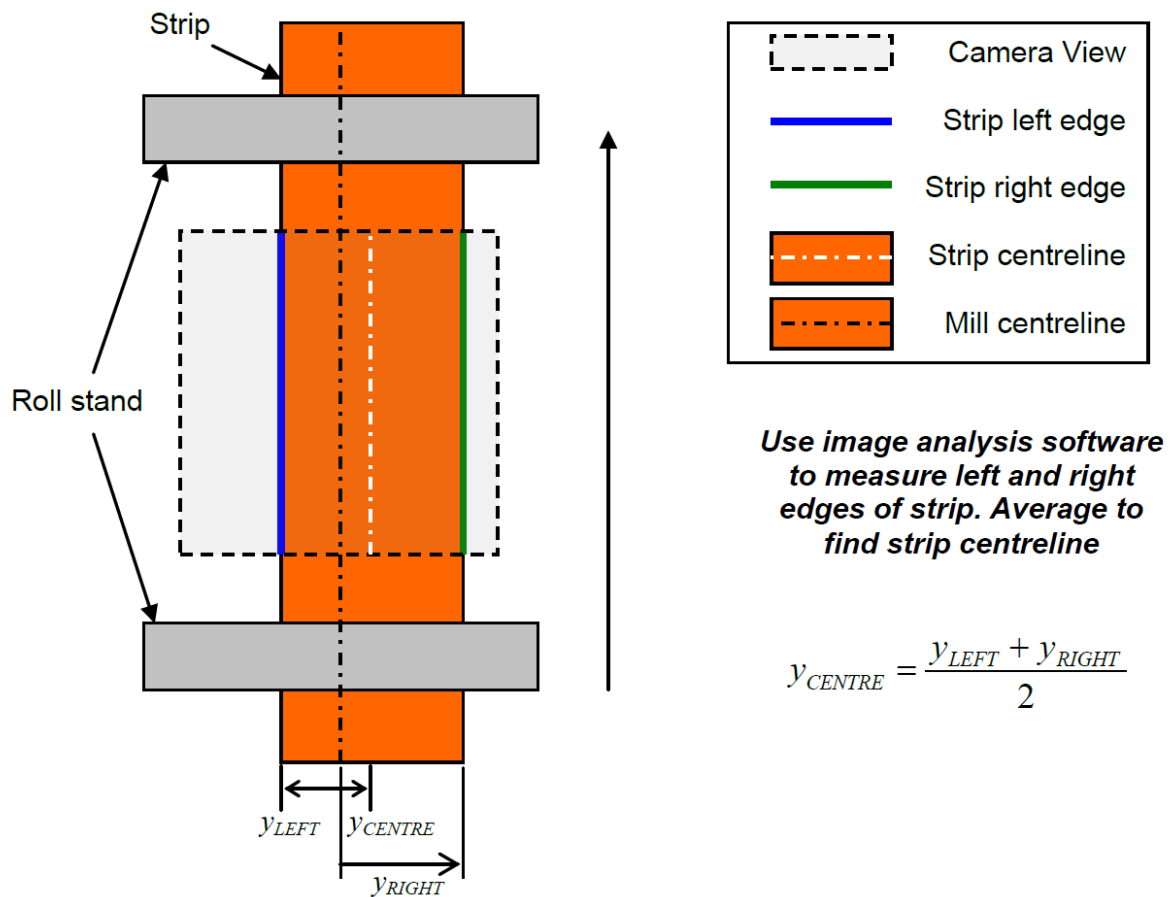
Figure 3.1 : Plan view of strip showing principle behind position measurement

3.2 Image analysis

Image analysis software identifies an edge when there is a change in pixel value (brightness) within specified limits. As the software evaluates numerical brightness, the colour depth must have a single value per pixel, hence the images are always analysed in greyscale, where pixel value relates directly to brightness, as opposed to full colour where the value is composed of three portions, one for each primary colour. The high temperature strip in hot rolling means that the strip glows brightly and is highly contrasted against the dimmer background. This allows for direct greyscale conversion, opposed to preferential favouring of one colour over another, as would be required if an edge is searched for between two colours at the same brightness.

Most edge detection tools have some common general settings that are required for successful operation of the tool [33]. The ROI (Region Of Interest) defines what section of the image is analysed. This is vital to be set up correctly because other objects in the image can be recognised as an edge if they are within the search window. The direction of search defines the scan direction of the tool, e.g. left-to-right / top-to-bottom. This is useful because

if an edge is more clearly defined on one side than the other the tool can determine the position more accurately. Finally, the threshold parameters of the tool define what is determined as an edge. This must be set so that any slight variations in brightness are not incorrectly determined to be an edge. Additionally, tools often have other configuration settings that can aid in correctly determining edge position.

To aid edge detection tools, filters can be applied to the images that highlight edge positions for clarity. There are many proven techniques for this but they largely rely on one general principle. The principle method is to analyse how much brightness is changing in a small search window (e.g. 5x5 pixels) and a filtered image is output with pixel brightness as a function of the change in brightness in the original image [33].

3.3 Measurement system design process

The development of the measurement system went through three stages. When the project began it was based in the Llanwern steel mill where the initial proof of concept took place. This initial study used relatively inexpensive temporary cameras on the sixth stand of the seven stand mill, bolted in place with minimal protection in order to perform a quick evaluation of the feasibility and whether developing a vision system further would be likely to succeed. For the first study, the camera was placed towards the end of the mill because simulations showed that there is more strip motion in the latter stands [5]. Shortly after the initial study in Llanwern, and when a full system proposal was near completion the hot strip mill was mothballed due to economic conditions. At this point the work was transferred to the Port Talbot steel plant. The work undertaken in Llanwern and the results to date were presented to the Port Talbot works to gain support for the continuation of the project and installation of the developed system at this plant. At this stage it was proposed that a similar study to the one in Llanwern be undertaken in the Port Talbot finishing mill. For this study the camera was on the first stand of the mill, following more recent research [21] suggesting that if cameras were on only a few stands then they should be placed at the beginning of the mill. This study also allowed any differences between the Llanwern mill and Port Talbot mill to be evaluated and highlight more unforeseen problems, such as an increased level in cooling water.

Following the Port Talbot feasibility study, the measurement system which had been designed was further refined with the results and findings from the new data, primarily a development of the image analysis method to cope with obscured images than seen in the

Llanwern trials due to cooling water. The system was then proposed as a cut-down version of a full installation with two cameras and room for expansion up to a full seven cameras. The proposed system was put online for evaluation and further development before potential investment in a full measurement system.

3.4 Llanwern vision trials

3.4.1 Introduction to initial investigation

For the Llanwern trials, a single camera was bolted to the rolling stand gantry, viewing vertically downwards to the strip below at the exit of the sixth roll stand, as shown in Figure 3.2. The temporary camera was a low-cost CCTV camera with a resolution of 358x252 pixels, which gave a resolution of 9.7mm/pixel at the strip. This is not sufficient resolution for a full control system [45] but was adequate for the initial proof of concept. Note that sub-pixel processing and linear interpolation of edges improves this resolution so position is measurable to a greater degree of accuracy. The camera recorded a total of 11 strips for analysis. In the images the strip was travelling from bottom to top.
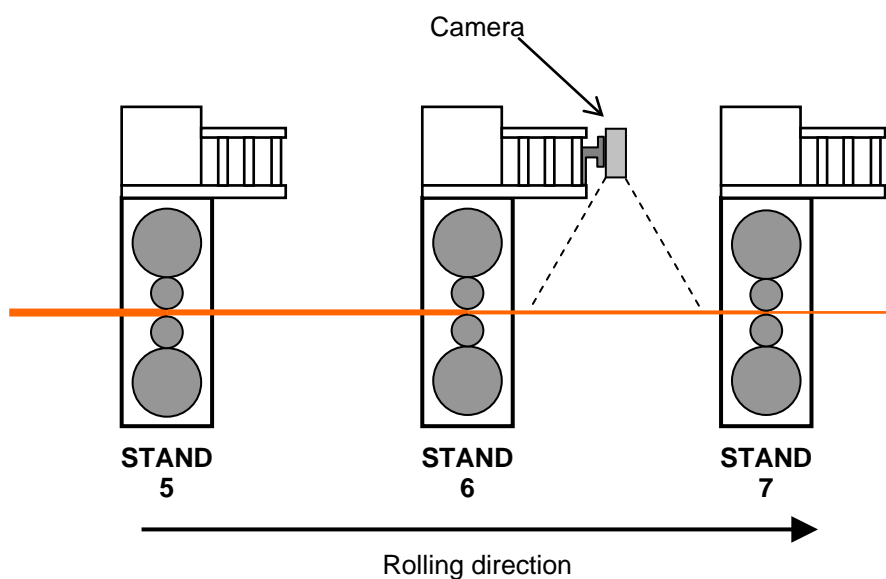
Figure 3.2 : Location of camera in Llanwern trials

3.4.2 Image analysis

Overview

To analyse the video, a sequence of images was extracted for all the strips recorded. Each image was analysed with a set of interest regions, looking for an edge in the image and recording the position when one is found. A piece of software was specially developed in

National Instruments LabVIEW to perform this analysis. The development and use of this software served the dual purpose of proving the ability of LabVIEW for this task and proving the ability to measure strip position by image analysis. The images were also analysed in the CV3000 control software from KEYENCE to provide a comparison with an off-the-shelf industrial system and a bespoke system.

Figure 3.3 shows an example of an image being analysed, showing search windows and directions. Windows 1 and 2 found strip edges, windows 3 – 6 observed side guide position and were used to monitor camera vibration and provide a reference to the mill centre.
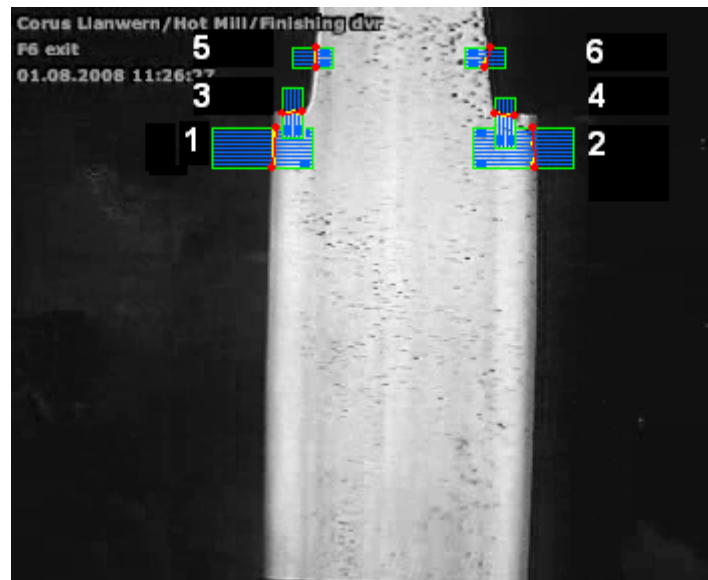
Figure 3.3 : Example edge detection windows

KEYENCE analysis

The CV3000 industrial vision system from KEYENCE [46] was considered as a potential system for strip tracking measurement. The system is controlled by freely available software which has the capability to analyse off-line images in order to evaluate a proposed system and develop a measurement strategy. This also provided a proven piece of industrial vision software with which to compare self-developed software. The CV3000 software can run in simulation mode, which emulates a connected CV-3000 controller on a PC, allowing settings to be checked off-line. Simulation mode hence facilitated using the software to analyse the images from a separate camera. However, the images imported into the software must be representative of those captured by a set camera, in this case a 512x480 pixel colour camera. This limitation meant that the images had to be resized to use with the software. As the

available images were not the same aspect ratio as required by the software, they were proportionally stretched then cropped to minimise distortion.

The primary aim of analysis with the KEYENCE software was to evaluate and provide a benchmark with a piece of industrial software. As the software is limited by the requirement for the images to be in the specified format, compounded with the fact that the user interface is purely keyboard-based and not always straightforward, only limited work was performed using this software. It was these limitations that drove the creation of the software in LabVIEW, to provide greater flexibility and ease of use.

The images were analysed in the KEYENCE software using plain greyscale images only, with no extra filtering, as this was found to be sufficient. The images were analysed with an edge detection tool for left and right strip edges for comparison with the developed LabVIEW software.

LabVIEW analysis

As mentioned above, the KEYENCE software did not provide all the flexibility and ease of use required, so a bespoke software solution was developed using National Instruments LabVIEW. This also provided a proving ground for potentially developing a piece of software for use in an integrated measurement and control system. Some of the benefits of this developed software over the KEYENCE software are detailed below.

The interface in the developed software was created to be simpler and more intuitive to the user, allowing faster configuration of the software tools. This also allowed comparison of different filter and edge detection types to be performed easily. The tools used can handle any image format so additional image manipulation was not required. The output format of the final file (comma separated variable (csv) listing edge positions) included a reference to individual analysed images and window titles for ease of understanding without knowledge of the configuration settings. The ability to save and edit window settings allowed the same analysis to be run on all image sets very quickly. Using the KEYENCE software, all image sets would have required conforming to strict naming conventions and be moved to specific folders individually. In contrast, the developed software would be pointed at any folder and all images within it analysed, only requiring that all images in a set be in a single folder. One of the most advantageous things is that any required extra functionality could be added

relatively easily if desired, and the techniques used could be directly applied to a full industrial application.

The software operated in a sequential manner, analysing one image set at a time. Initially a reference image was chosen. The location of this image determined the folder that was analysed by the software. The number of measurement windows was selected, then using the reference image, each window configured. The edge detection tool used in the software allowed detection of either a horizontal or vertical edge in a given direction. Additionally, a filter could be applied to the image to aid the tool. Filters available [33] were a set of standard filter methods (differentiation, gradient, Prewitt, Roberts, Sigma and Sobel) or a Canny edge filter. The standard filters refine the image by outputting each pixel in the search matrix as a function of the brightness variation, whereas the Canny filter outputs an image with only one pixel per edge. This is illustrated in Figure 3.4, which shows a Sobel filter and a Canny filter applied to the same reference image. All five standard filter types output very similar images, varying in brightness of output edge only.

| Raw image | Sobel Filter | Canny Filter |
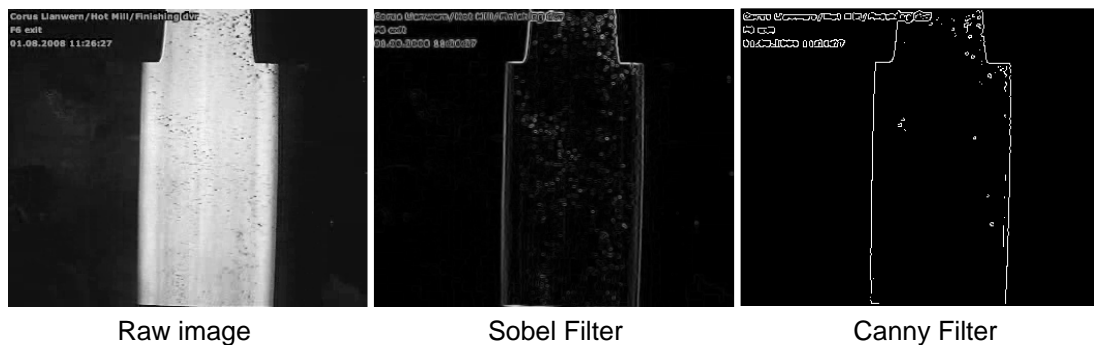
Figure 3.4: Comparison of filters

After window parameters were set, the software ran through every file in that folder, applying the defined windows and outputting x and y coordinates representing a line for every edge found. The files were analysed in alphabetical/numerical order so they had to be named in sequence to ensure the output data was in the correct order. When all images were processed, the line coordinates were converted to a single value for each edge by taking an average of the two points and outputting the average x value for vertical edges (equation (101)) and the average y value for horizontal edges (equation (102). See Figure 3.5 for reference.)

$$L_x = \frac{L_0[x] + L_1[x]}{2}$$

(101)

$$L_y = \frac{L_0[y] + L_1[y]}{2}$$

$$(102)$$
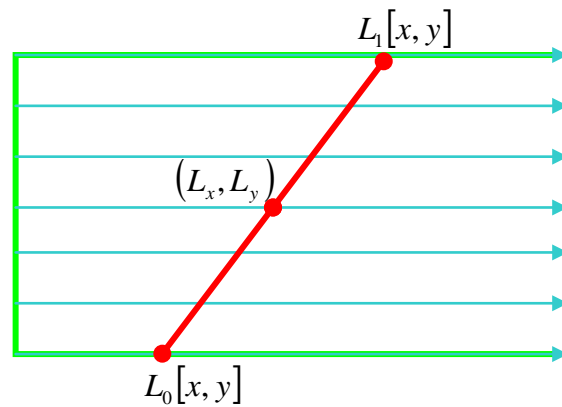
Figure 3.5: Calculation of line centre-point

These values were then put into a table with titles and a reference to the original image inserted, which could be saved as a csv file. The window settings could also be saved for use later with another image set.

3.4.3 Results

Limitations

Because the camera resolution was low, image quality was not ideal. This presented two main problems; one was that the measurements were approaching the limit of pixel resolution. Whilst sub-pixel processing and point-to-point interpolation of lines increased the resolution by some amount, the accuracy of results was not ideal. The other effect of low resolution was that edges could sometimes appear blurry and difficult to determine their exact position, adding a degree of uncertainty. Whilst these factors certainly limited detail that conclusions could be drawn, the results have shown that sufficient information could be extracted from the data retrieved.

Data analysis

The csv files from the software were loaded into Microsoft Excel for analysis. The files contained edge values as absolute positions from an origin in the bottom left corner of the image. The data was normalised by subtracting the mean from each data point so the data set is centred on zero, allowing easier comparison of left and right edges. Figure 3.6 shows a graph of deviation from the data set mean, representing a single coil measured with the LabVIEW software and no image filter applied. Note that this data set had additional

conditioning, ensuring any zero values (indicating no edge found) in the original data set were ignored. This ensured the data remained sensible. The image resolution was calculated from the known coil width of 1294mm and the average measured width of 133.65 pixels, giving a resolution of 9.7mm/pixel, allowing the position measurements to be converted from absolute pixel values to millimetres.
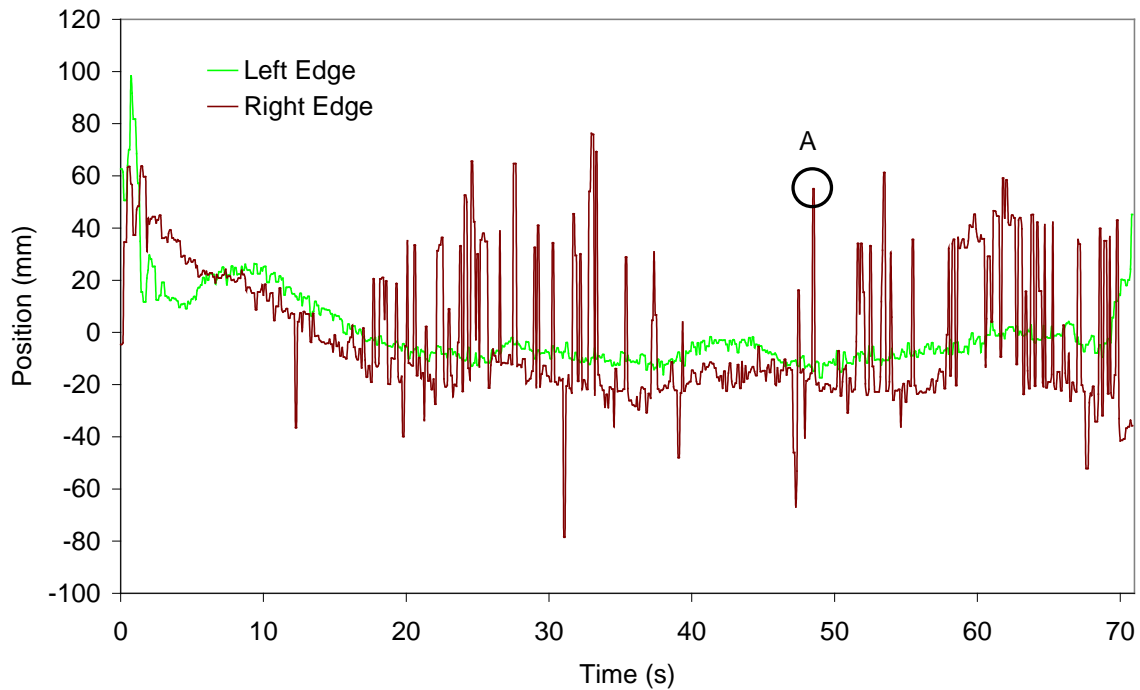
Figure 3.6 : Unfiltered deviation from mean position for left and right edges

The plots on the graph show the left and right edges of the strip as measured by the image analysis software. One thing to notice immediately is the noisy profile of the plots. The smallest spikes (high frequency, approximately 5-10mm, present in all plots) are due vibration of the camera position. This vibration could be the camera itself vibrating on its mounting, or could be the entire mill vibrating. This vibration does cause a problem, but applying a low-pass filter helps to show a trend through the data with more clarity. Figure 3.7 shows the application of a simple first-order filter of the form $y_{F(t)} = \alpha.y_{(t)} + (1-\alpha).y_{F(t-1)}$. In this case a value of 0.1 was chosen for α as this was found to be suitable. The operation of this filter was to allow a weighted proportion of previous data to be included in the next data point; by giving a previous data point a higher weighting (lower α), sudden spikes in the data could be filtered out. However, a large spike can affect the data more adversely by imposing itself on future data points in the same way. A lower value of α could be chosen to

combat large spikes but resulting in an overall loss of results amplitude. A higher order filter could potentially provide filtering for the high frequency noise than the simple first order filter presented here.
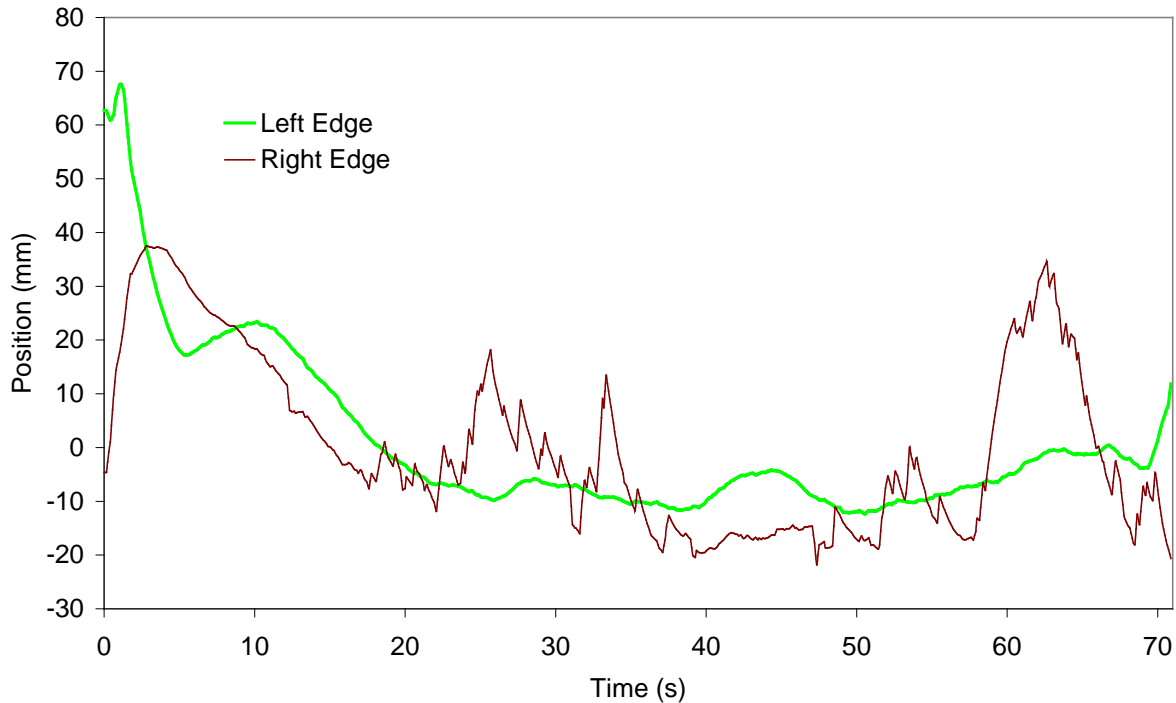
Figure 3.7: Filtered deviation from mean for left and right edges (α=0.1)

Effect of surface contamination

In Figure 3.7 the general trend of motion can be seen clearly from the trace of the left strip edge. However in Figure 3.6 and Figure 3.7 it can clearly be seen that the right edge of the strip is subject to very large spikes, greater then those attributed to vibration. These large spikes are consistent throughout the data for all measured strips; in many cases a lot worse than in the data presented here. The apparent reason for these large anomalies is surface water washing over the top of the strip. The water appears as a darkened area, when this was close to the strip edge, the edge itself was obscured causing an incorrect determination of the position and the large spikes in the data. Figure 3.8 shows the same image with and without a Canny filter applied. The water on the right edge has upset the image filter and edge detection tool as highlighted. This image corresponds to point A in Figure 3.6.

| A: Raw image | B: Filtered image |
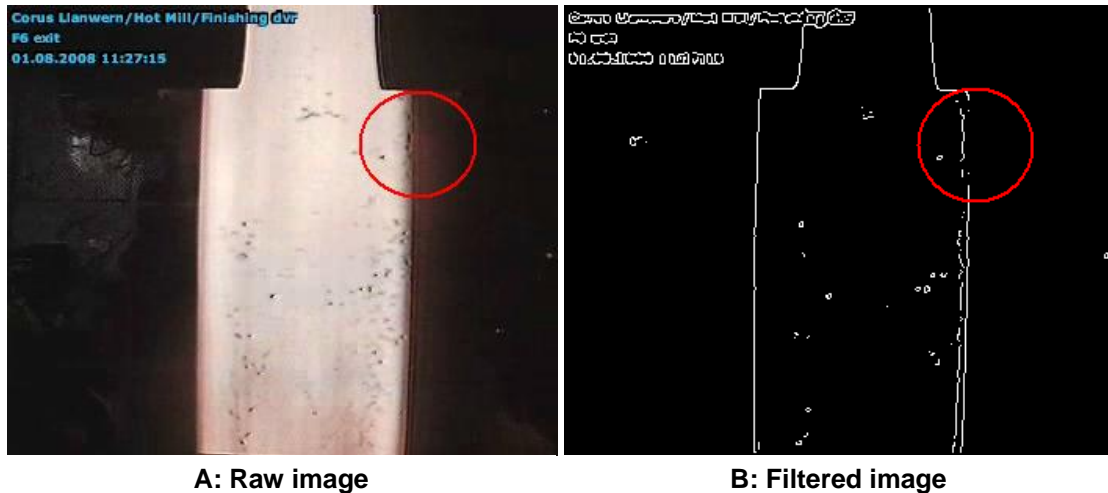
Figure 3.8: Plain image and image with canny filter applied showing effect of scale on edge detection

As an effort to reduce the effect of surface water on the right edge of the strip, a comparison was made of three different filters applied to the image to aid edge detection. Figure 3.9 to Figure 3.12 show the result of no filter, a Canny filter and a Sobel filter applied to the same data set, displayed as both raw deviation data and with a low-pass filter with $\alpha = 0.05$ applied.

Figure 3.9 and Figure 3.10 show data for the left edge of the strip. In these plots there is a clear correlation between all three data series, and a trend is clear in both filtered and unfiltered data. Conversely, for the right edge of the strip in Figure 3.11 and Figure 3.12, there are the characteristic spikes in the data. A trend can be seen in the data, but it is largely obscured by the noise. The correlation between the three traces is poor and as such, very little trust can be put into the measurements.
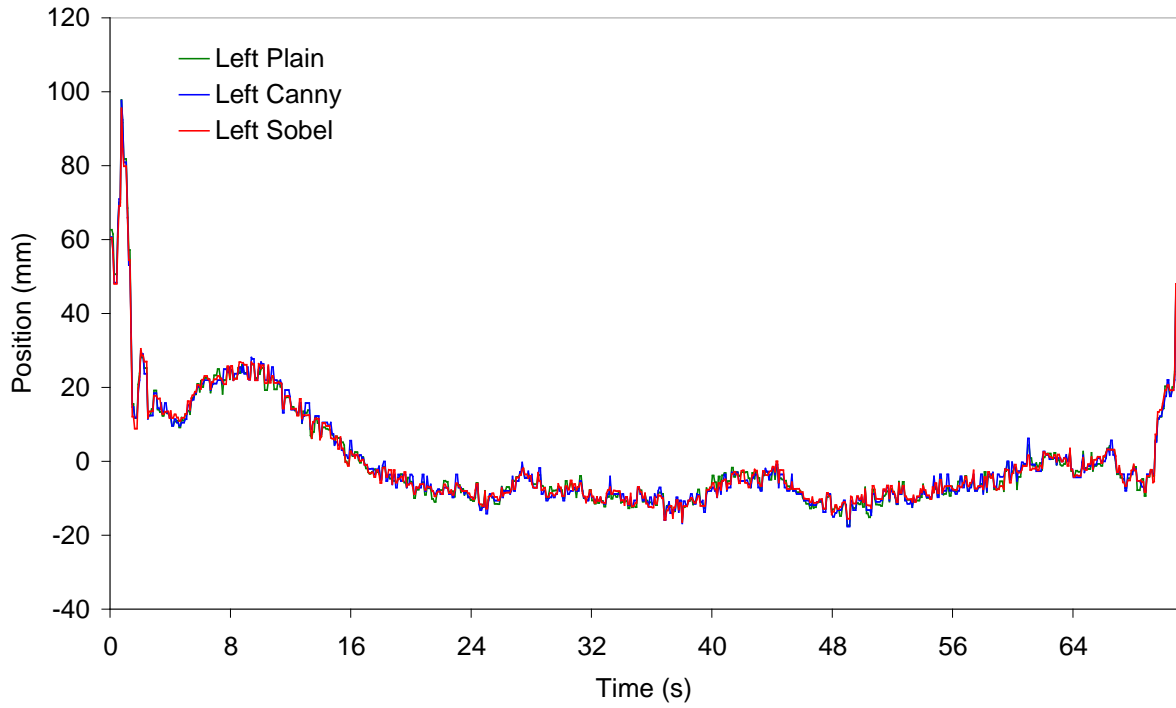
Figure 3.9: Comparison of image filters, left edge, raw deviation data
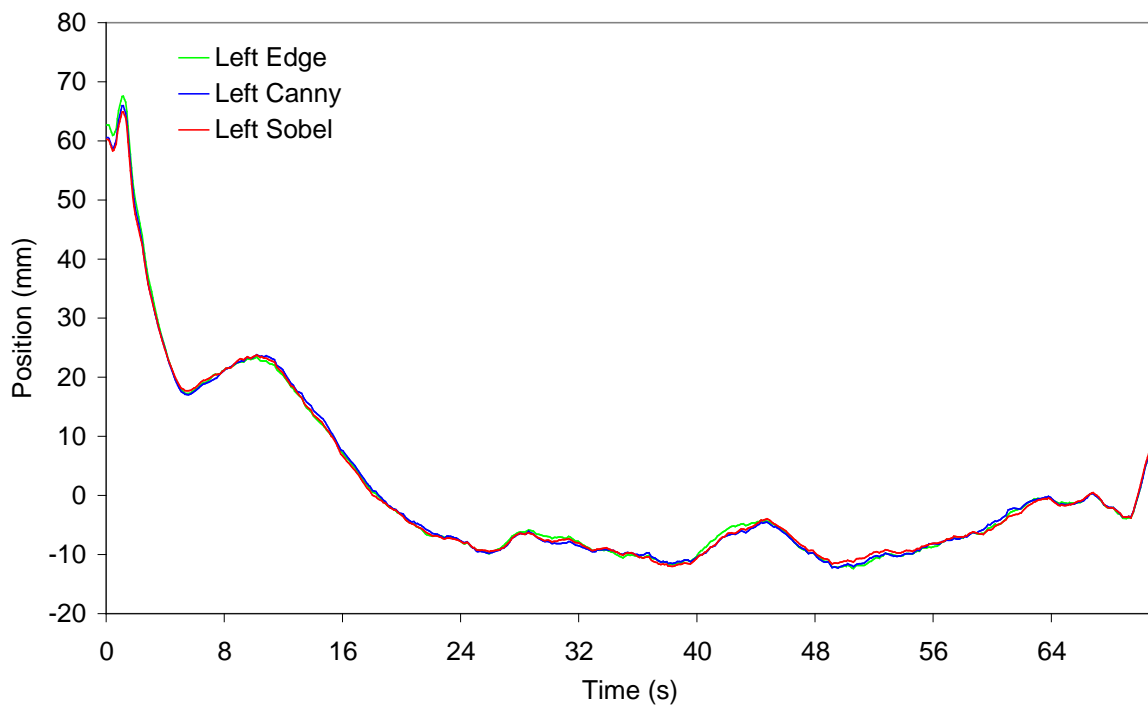
Figure 3.10: Comparison of image filters, left edge, low pass filter applied (α = 0.05)
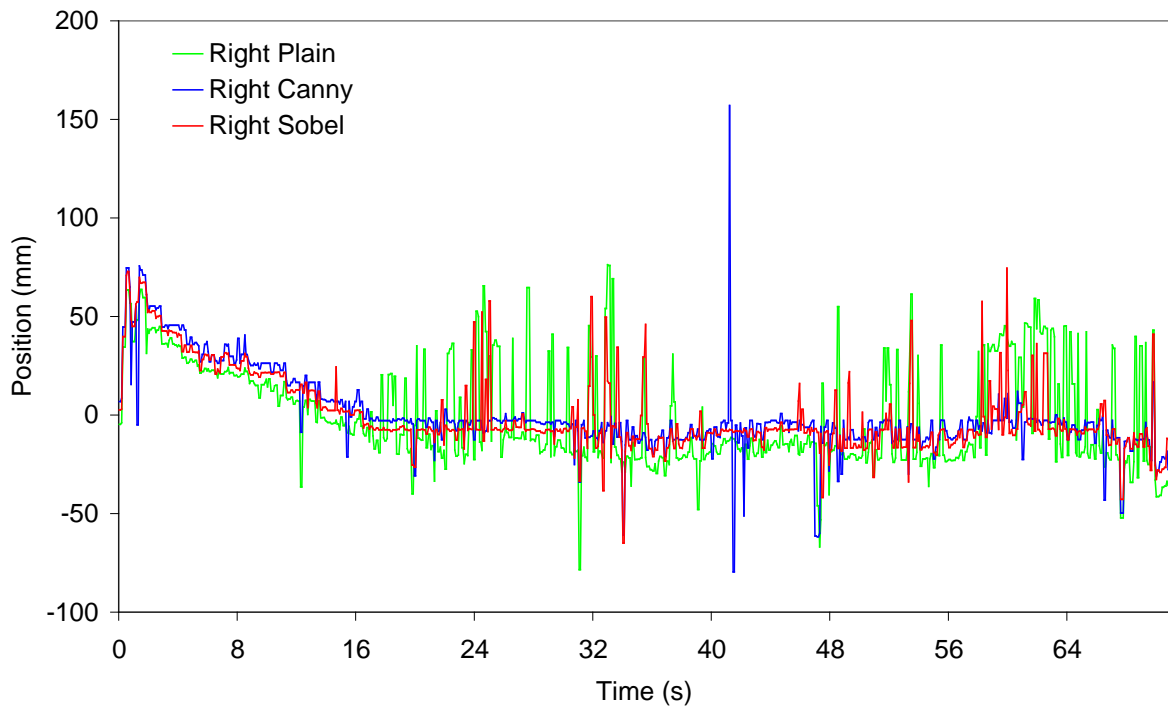
Figure 3.11: Comparison of image filters, right edge, raw deviation data
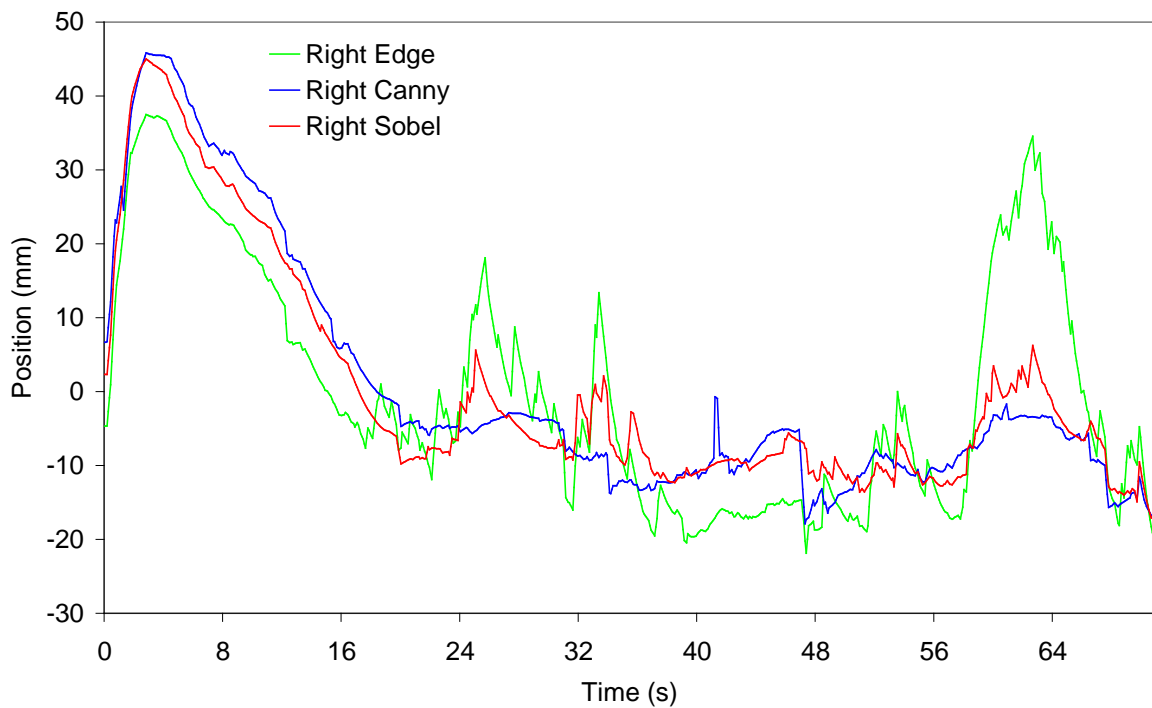
Figure 3.12: Comparison of image filters, right edge, low pass filter applied (α = 0.05)

The appearance of water on the strip is a major problem and one that had to be solved before vision data could be used in a control application. One possible method that could reduce this effect was to fix the camera exposure so the water cannot be seen on the surface. Figure 3.13 shows the image taken as the strip was entering the mill. The camera used for this study automatically adjusted for brightness and this image was taken in a transitional phase. As such, the image quality is quite poor but there are no visible dark patches.

Figure 3.13: Head end of strip at very high brightness

Comparison of image filters

In the above it was mentioned that different edge filters were applied as an attempt to reduce the effects of scale in the image. The results of that were not conclusive but did highlight the difference of quality between right and left edges. A more in-depth discussion of the different image filters is presented here.

At first appearance, the Canny filter may seem like the best choice because of the clarity of the edges extracted by the filter, providing a very easy target for the edge detection tool. However, this is not always a good thing. As a single line of pixels determines each edge, the edge detection tool must fully rely on the filter's determination of edge position, limiting the effectiveness of sub-pixel processing. Additionally, as seen in Figure 3.8, if the filter misinterprets the position of the edge, image data is lost, preventing the edge detection tool from finding the correct edge.

Whilst the Sobel filter does not produce edge clarity as fine as the Canny filter, there is not as much loss of image data, allowing the edge tool to interpret the edge in its own way.

However, sometimes the Sobel tool does not produce a clear enough edge for the edge detection tool to identify and it is possible for the edge to be lost altogether. This is possible to overcome by setting edge detection settings correctly, but the reliance on correct configuration is much greater.

By using no filter at all, no image data is lost and finding edges is entirely up to the edge detection tool. With the high contrast of the images analysed in this application, this does not present much of a problem and there is a very high chance of an edge being detected. By increasing image brightness, the contrast of the strip from the surroundings increases further and makes this a more viable option.

Taking a single set of data as an example, with a Canny filter applied, 57 zeros, representing no edge found, were reported, the Sobel 5 and no filter 3. The majority of the missing edges were on the right side of the strip; 52 of the 57 in the case of the Canny filter. This shows that a clear edge filter such as the Canny filter is not always the best choice, particularly in an environment such as this where image quality can be very variable. One thing to note about these results is that they could be slightly misleading. With a reading of 0, it is clear that no edge was found and measures can easily be taken to fill in or ignore the missing data. If an anomalous edge was found in its place, it is very difficult to identify that reading as anomalous.

Another comparison is the time taken in each for each of these filters to process the image. This was performed by processing the same set of images with identical window settings on a standard desktop PC, only changing the edge filter applied in each case, measuring and recording the average execution time for each image. The average times for the Sobel filter and no filter were very similar at around 15ms per image; the plain image tended to report a slightly faster time by around 1ms. In contrast, the time per image with the Canny filter applied was over 200ms – a significant difference. These times would be reduced in an industrial situation with a dedicated specialised computer, but the indications are that applying a Canny could result in a measurement time too slow for the required control system. A target value for measurement is under 20ms, with the aim being to reduce the time under 10ms. [4]

Comparison of LabVIEW developed software and KEYENCE software

A comparison between the KEYENCE software and the LabVIEW-developed software was performed by configuring window sets in both pieces of software as similarly as possible and running the same image set through both.

Figure 3.14 shows a graph of deviations from mean for an image set analysed in both pieces of software. There is a clear correlation between both methods, especially on the left strip edge. Unfortunately the troublesome right edge has caused large spikes in both analyses. This is highlighted in Figure 3.15, which shows the differences between both analyses. Here, the differences in the left edge measurements are largely insignificant, whereas the differences between the right edge measurements are very large; reinforcing the fact that surface-water noise is unpredictable as well as large.
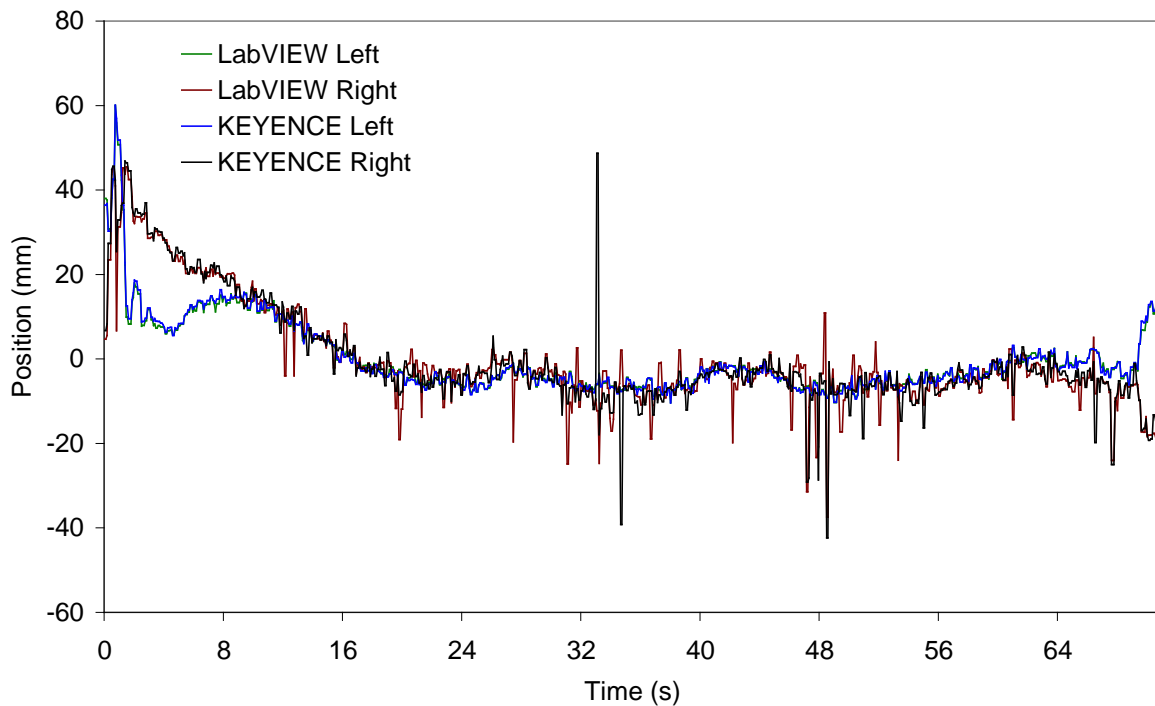
Figure 3.14: Deviation from mean data for images analysed in both LabVIEW-developed software and KEYENCE CV-3000 control software
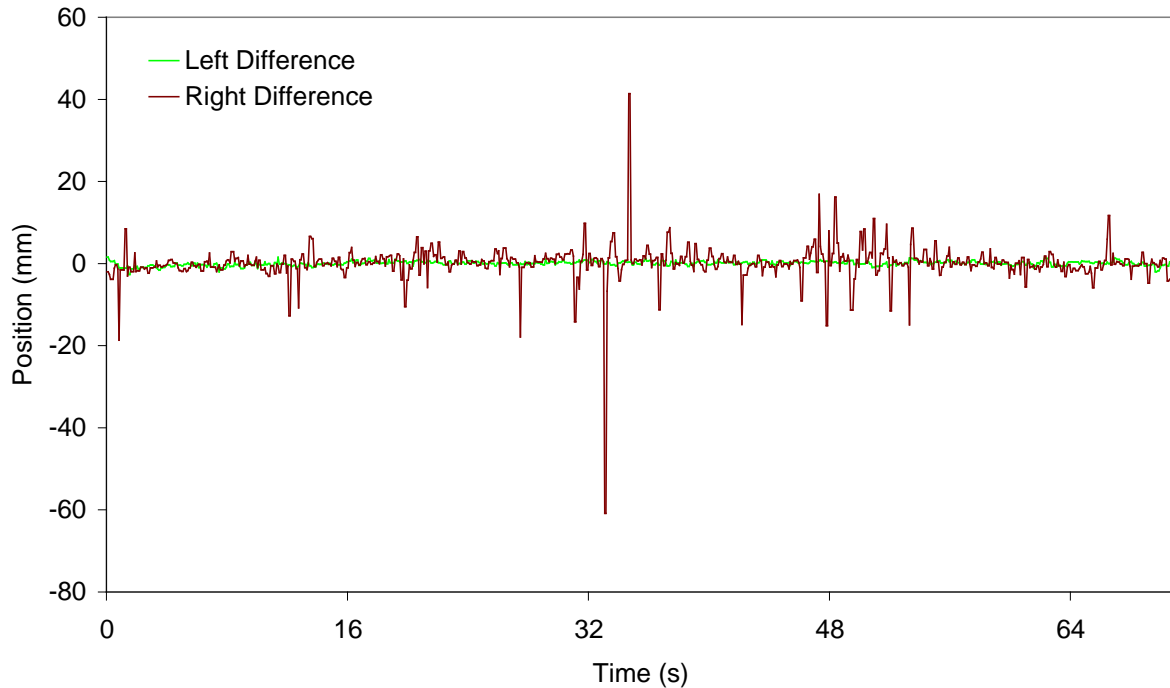
Figure 3.15: Difference between KEYENCE and LabVIEW analyses

On the whole, the similarity between the two analyses was encouraging and supported the idea for development of a bespoke piece of software for measurement and control in LabVIEW.

Secure fixing of the camera

It is important that the point the camera is viewing is constant throughout the measurement and control. If the camera moves, this could be falsely interpreted as strip motion, which would cause incorrect correction signals to be generated by a control system. Figure 3.16 shows data from a subsequent coil to the previous graphs, filtered with $\alpha = 0.05$. This graph also has additional plots for position of the side-guides as a static reference to position. The images from this strip showed large amounts of disruption, distorting many images. The cause of this disruption was thought to have occurred around point X marked on the graph. At this point, two things happen. One is that the data becomes highly disrupted, marking the distorted images. The other interesting occurrence is the sudden drop in value of all x-position (lateral direction) measurements in the data (strip edges and guide edges). This suggests that the camera was knocked off-centre by a jolt on the mill. This drop is only visible because the data is centred on an average value and not a fixed point. This highlights the fact that it is very important to know where the camera is pointing at all times to achieve

69

accurate measurements of position. In an industrial implementation, the camera must be secured in such a way that it is guaranteed not to move, or reference points in the image should be used to generate a robust coordinate system.
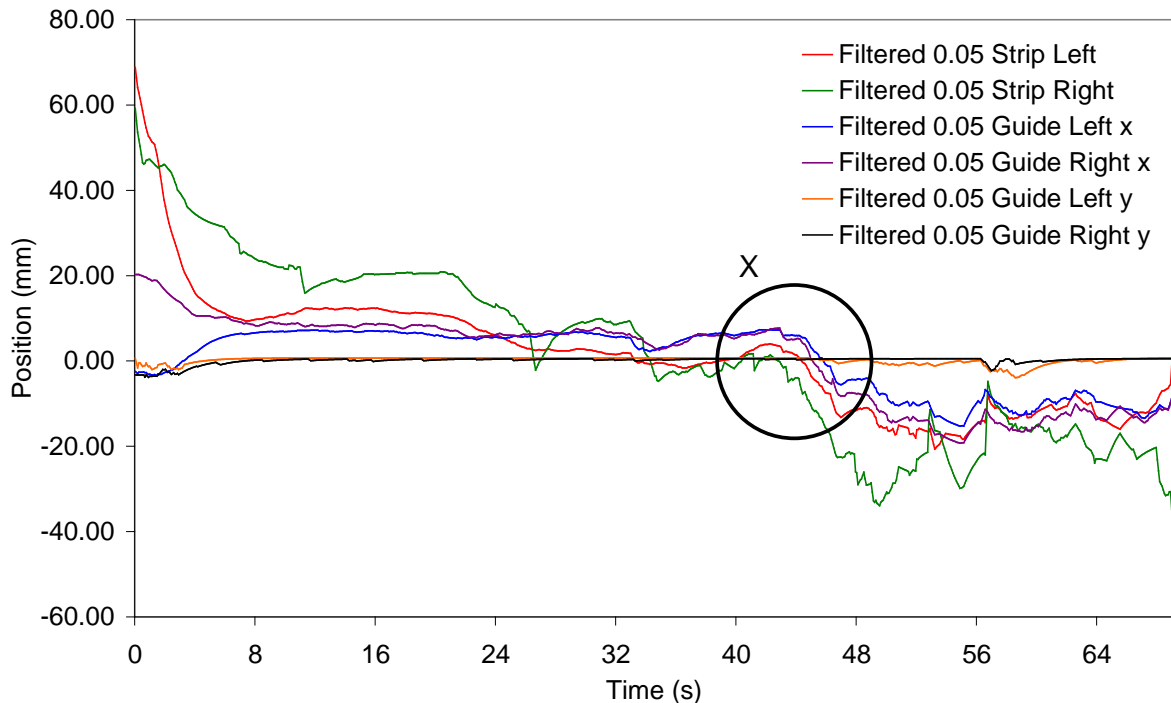
Figure 3.16: Filtered deviation data with camera disturbance

3.4.4 Findings from initial camera feasibility study

Although the data has been shown to have some flaws and limitations, some conclusions can still be drawn.

Two methods of analysing the images were tested; a highly flexible bespoke system and a robust industry proven (but less flexible) system. Both produced very similar results, supporting the argument for developing a bespoke piece of software for measurement and control.

It is possible to see trends in the data. These trends show that position can be measured but are distorted by vibration noise. Application of a low-pass filter can help remove some of the vibration noise but at the cost of signal amplitude and an effect on the signal dynamics.

Water present on the surface of the strip, significantly the right edge severely adversely affects the quality of the measurements. Methods to remove the effect of water could be

numerical, by applying a logical analysis to identify when surface water is present, or could be in the measurement itself, such as increasing the exposure time of the camera so dark patches are not visible.

Various methods of filtering the image itself to improve the effectiveness of the edge detection tool were demonstrated. It was thought that in this case these would not be required because of the already highly contrasted image presenting a good target for an edge detection tool.

Physical disruption of the camera and vibration disturbed measurement quality. This has highlighted the fact that all equipment must be protected from the harsh environment to ensure consistently reliable measurements.

Overall the results from this study show that vision is a possible method to measure strip-tracking position. This supported further work in this area to develop an on-line measurement system.

3.5 Port Talbot vision trials

3.5.1 Overview

Following the work undertaken in the Llanwern steelworks, economic problems and the mothballing of the Llanwern hot strip mill necessitated moving the project to the Port Talbot hot strip mill. As part of the agreement for the project to continue at Port Talbot, the trials undertaken at Llanwern were repeated to determine any differences between the Llanwern and Port Talbot mills before investment was put into a full vision system.

Before the Port Talbot trials, new information was found [21] regarding the placement of cameras. This research suggested that for a system with cameras on only a few stands, the optimal place to position the cameras would be at the beginning of the mill in order to improve the tracking at the input, therefore the trial camera in Port Talbot was placed on the first stand. This was the opposite of the Llanwern trials where thinking at that time was that cameras should be placed in the latter stands where tracking was more unstable.

As with the Llanwern trials, a low-cost temporary camera was placed on the roll stand viewing vertically downwards. The images were saved remotely and analysed offline.

3.5.2 Findings and evaluation

During an initial visual evaluation of the acquired images, one difference between the Llanwern and Port Talbot trials was the amount of cooling water visible on the strip. Figure 3.17 shows typical images from the Llanwern trial (A) and the Port Talbot trial (B). These images are presented here in colour for clarity but would be converted to greyscale for in-software analysis.

| A: Image from Llanwern trials | B: Image from Port Talbot trials |

Figure 3.17 : Comparitive images from Llanwern and Port Talbot trials

Whilst there was some variation with the amount of cooling water during the rolling process for any given strip, the images shown in Figure 3.17 are typical of the normal level of water for each data set.

The water levels in the Port Talbot image are very high, obscuring the strip edges and providing a very difficult task for the image analysis software, in contrast to the Llanwern trials where a relatively simple set up produced reasonable results with only a few problems from one strip edge. The highly obscured images from Port Talbot proved impossible to accurately analyse with the same methods used for the Llanwern analysis. However, despite the difficult images, the strip edges are visible through the water. With this in mind it was decided to continue the development of the vision measurement system, but first a new method of analysing the images would be required in order to provide reliable measurements of strip position.

3.6 Findings from early vision trials

Sections 3.4 and 3.5 describe the initial proof of concept trials undertaken at the Llanwern and Port Talbot steelworks. The aim of these trials was to determine whether using a vision system to measure strip tracking position would be possible and to highlight and potential

problems and to solve these before investing in a full system. The main findings from these trials are detailed below.

The first trial in Llanwern showed some good results with a relatively simple image analysis method. A bespoke piece of software was compared with an industrial piece of software with comparable results, supporting the development of a bespoke system to increase the flexibility and potential. A few issues were found with cooling water presenting as dark patches on the strip edge, but this was seen to be a minor problem and a simple solution expected. From this point, the continued development of a vision system was supported.

The second trial in Port Talbot was not as successful as the Llanwern trial, highlighting a larger problem with cooling water than originally thought. At this point the continuation of the system development was entirely dependent on developing an image analysis method which would successfully determine the strip edge despite the amount of cooling water.

4 Development of Image Analysis Method

For the Llanwern study as described in Chapter 3, a piece of image analysis software was developed in National Instruments LabVIEW in order to measure the position of the strip in the recorded images. This software was relatively simple and used the standard straight edge detection tools available in the LabVIEW Vision and Automation toolkit. This software was found to be adequate for the initial study, but was not suitable for analysing the images recorded for the secondary study undertaken in the Port Talbot mill.

The images used in the initial study and for the development of the original image analysis software from the Llanwern mill were from the end last stand in the mill and there was seen to be very little cooling water. The study in the Port Talbot mill was done using the camera placed at the beginning of the mill where more cooling water was seen. When the images from the study in Port Talbot were used in this study, the levels of cooling water obscuring the strip were found to be too great and the development of the image analysis software was seen to be required in order to maintain robust measurements of the strip position. A typical image from the Port Talbot trials is shown in Figure 4.1.
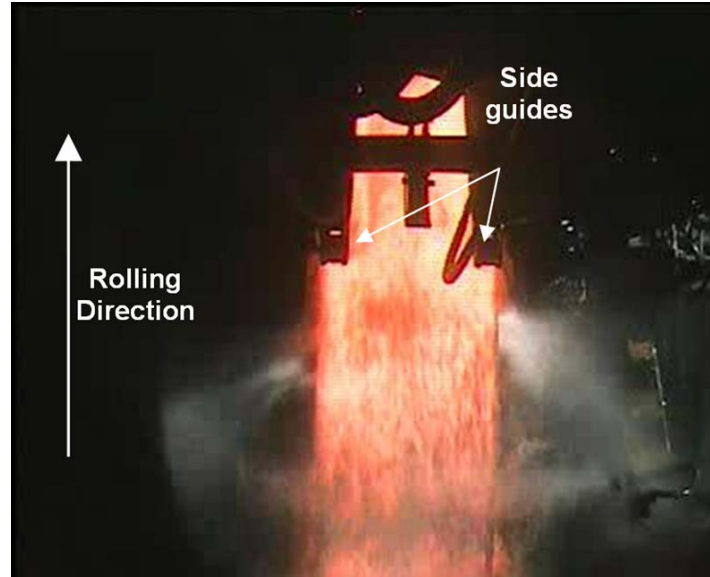
Figure 4.1: Image from Port Talbot showing large amount of cooling water

Following work by O'Leary [32], a method using spline fitting to the strip edges was developed and is described in the following sections. The work in this chapters was presented at ICMA 2010 and published in [47].

4.1 Overview of development

The aim of the measurement software is to determine the location of the strip centreline as far towards the rolls as possible, ideally at the point of the roll bite [45], although this is impossible in practice. In the image shown in Figure 4.1 the rolls are towards the bottom edge of the image. The problem with measurement was occurring because the concentration of water is highest at the point where measurement is desirable because of the cooling header spraying at the exit of the roll stand. It was thought that by using the entire visible section of strip to determine the edge position, and then fitting a line to this, the position at the required point could be derived despite the cooling water.

A first attempt was made trying to fit a straight line at the clearer top edge of the image, then interpolating this towards the bottom edge and picking an edge from a number identified. This method was flawed because the strip does not necessarily have a straight edge in the image; the looper, which rises up and down maintaining the strip tension, causes a curvature to be seen in the strip due to perspective. Additionally, picking the "correct" edge proved to be impossible because it was a case of choosing one from ten possibilities, some of which were very similar. It soon became apparent that pursuing this method would not yield good results so development was ceased and a different method was created.

As the strip edge appears curved, it was seen that the best option was to fit a curve to the strip. Additionally, the idea of choosing the correct edge from a selection was rejected, instead the entire strip edge was analysed and poor points ignored. The curvature of the edge is a simple curve, generally with a single apex such as a quadratic. To improve the quality of fit, a cubic function was chosen which could better follow the edge of the strip if it did not fit a perfect quadratic. The curve chosen for the job was a cubic Bezier curve. The resulting method is described in section 4.2, and a flow chart depicting an overview in Figure 4.2.

Acquire Image — Image loaded from file (offline) or Image captured by camera (online)

Scan for Edges — Region of Interest (ROI) set. Image scanned in horizontal lines. Pixel intensities extracted and edge positions determined

Identify acceptable edges — Edges compared to expected positions from previous measurements and accepted or rejected

Fit cubic curve — Cubic curves fitted for both strip edges for all acceptable edge points

Adjust for tolerances — Curve adjusted to fit within acceptable tolerances and bounds

Calculate central curve — Centreline curve found as average of two edge curves

Output results — Results output to data logger and measurement fed back to next cycle for edge point rejection step

Figure 4.2 : Image analysis process flowchart

4.2 Methodology

4.2.1 Edge detection

An edge is defined as a part of an image where pixel brightness changes significantly. In mathematical terms, for a greyscale U8 (unsigned 8-bit) image, each pixel is represented as a single byte; a number from 0 to 255 where 0 is black and 255 is white. Therefore, an edge can be defined as the maximum change in value between adjacent pixels, or the maximum gradient. The task for the edge detection component of the software was to identify significant edges along the search line. For example, consider the section of a strip image shown in Figure 4.3. The search line is the thick green line in the centre of the rectangular search area.
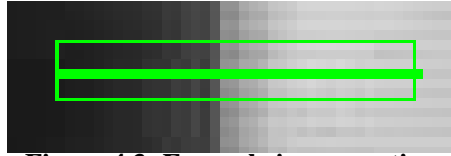
Figure 4.3: Example image section

By displaying the pixel intensities along this search line as a graph, the edge can be seen where the pixel values rapidly rise from dark to light, shown in Figure 4.4. The edge lies within the marked area at the point where the gradient is greatest.
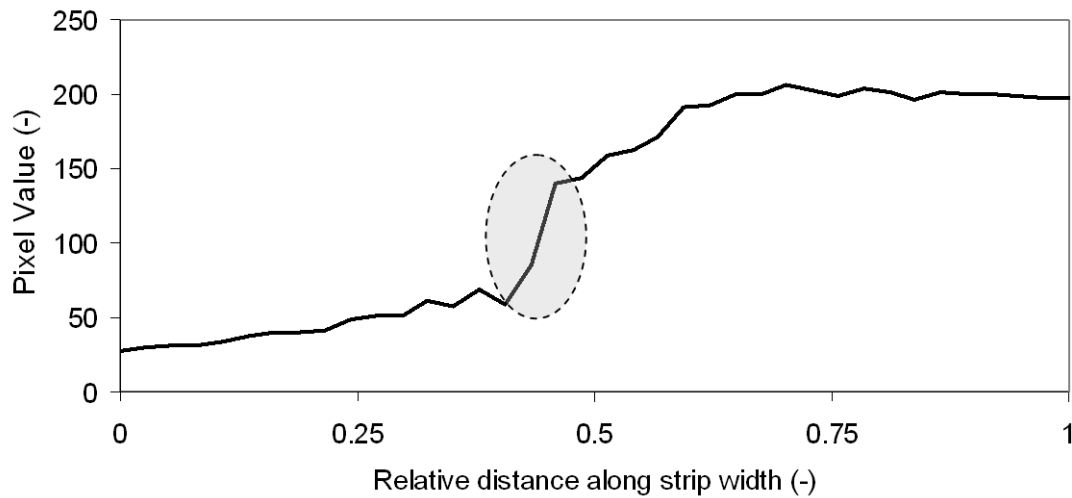
Figure 4.4: Pixel values along search line

To find the gradient of the pixel values, the data must be differentiated to determine the rate of change between pixels. In an image that has a tendency to be noisy such as this, then taking the gradient value across a range of pixels helps to filter out the noise. A "kernel" [33] is used to apply the calculation across a number of pixels. For example, the pixel values of the above line are shown in Table 4.1 and an example kernel in Table 4.2.

Table 4.1 : Pixel values in example line

Pixel Values																																				
27	30	31	31	34	37	40	40	41	49	51	51	61	58	69	59	85	140	144	159	162	171	191	193	200	200	206	202	199	204	201	196	201	200	200	199	198	197

Table 4.2: Example gradient kernel

Kernel								
1	1	2	2	0	-2	-2	-1	-1

To find the gradient of the dark-shaded cell, a section of pixel values the width of the kernel, centred on the target pixel, was extracted, which is marked by light shading. Kernel values

were then cross-multiplied with corresponding pixel values and the result summed to find the gradient at that point. Note that absolute kernel values are symmetrical about the centre value of zero, and positive on one side, negative on the other. The values of the kernel apply different weightings to cells dependent on their proximity to the target pixel. In this example, the pixels adjacent to the target pixel and one step away have a larger weighting than the outer two pixel pairs. The kernel can be fine-tuned to suit the need of the situation and the size expanded to offer a greater amount of filtering to the pixel values. The application of the kernel is demonstrated in Table 4.3.

Table 4.3: Application of kernel to calculate pixel gradient

Pixel Values	41	49	51	51	61	58	69	59	85	
Kernel	1	1	2	2	0	-2	-2	-1	-1	Sum (Gradient)
Multiple	41	49	102	102	0	-116	-138	-59	-85	**-104**

This was applied to the entire section of pixel values and is shown in Table 4.4. Note that because the kernel had to extract a number of cells around the target pixel, this limited the number of pixels for which a gradient can be calculated. The cells marked in grey have a default value of zero assigned to them to maintain a constant data set size. This was important when identifying the location of the edge in relation to the image. It was therefore important to ensure the search area extends sufficiently outside the range the edge is expected in.

Table 4.4: Pixel Gradients

Pixel Gradients																																					
0	0	0	0	-54	-59	-58	-63	-81	-84	-91	-85	-104	-157	-232	-387	-514	-524	-426	-338	-286	-242	-223	-163	-112	-71	-23	2	9	13	20	10	0	6	0	0	0	0

When viewed graphically, the pixel gradients show the position of the edge as the turning point on the graph shown in Figure 4.5.
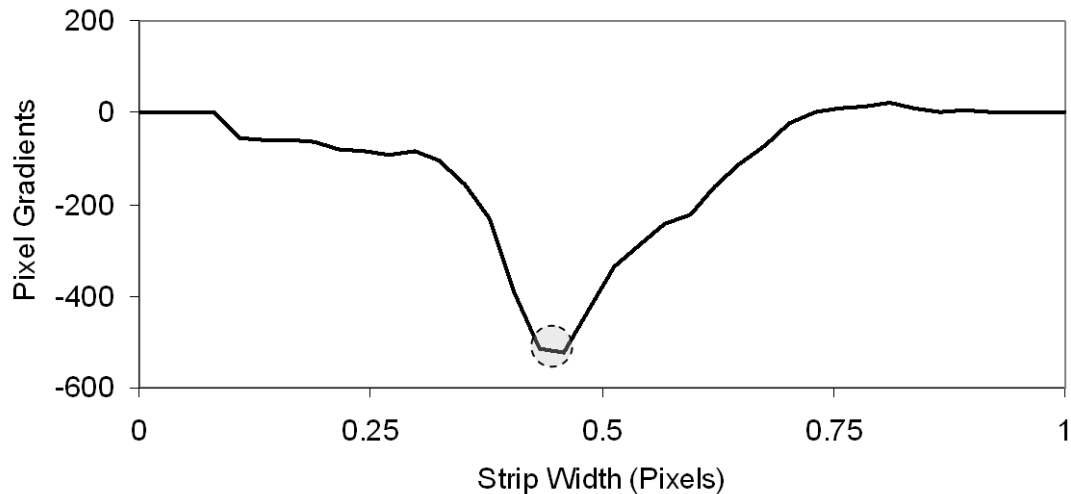
Figure 4.5: Pixel gradient values

This turning point is identified by the point this graph has a gradient of zero. This was found by differentiating this data and the result shown in Table 4.5.

Table 4.5: Differential of pixel gradients

Gradient of "Pixel Value Gradients" Graph																																	
0	0	0	0	-54	-5	1	-5	-18	-3	-7	6	-19	-53	-75	-155	-127	-10	98	88	52	44	19	60	51	41	48	25	7	4	7	-10	-10	6	-6	0	0	0

Note that as this was using discrete values, the zero point did not necessarily occur at a pixel site. To determine edge location, the points where the data crosses between negative and positive were determined to contain the zero value and linear interpolation performed to find the zero-crossing point. For displaying the results on the image, the pixel location was rounded to the nearest integer to best approximate the edge location. By following this process, the cells marked in grey in Table 4.5 were identified as "edges". In software, the location of these edges were identified in the image by adding the x-offset of the search line to the cell index of the pixels identified as edges, hence the need to maintain constant data set lengths throughout the process.

Working up to this point in reference to the example image, edges are shown as red dots in Figure 4.6.
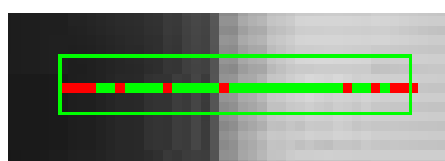
Figure 4.6: Example image section showing all edges found

The process to this point has identified a large number of edges, including the main strip edge. This was due to small variations in pixel values along the search line. To isolate the noisy edges from the true strip edge (highlighted darker grey in Table 4.5) a simple threshold was applied to the pixel gradients, rejecting any edge whose pixel gradient does not have an absolute magnitude greater than, for example, 150. After applying the threshold, the true edge was identified and the result shown in Figure 4.7.
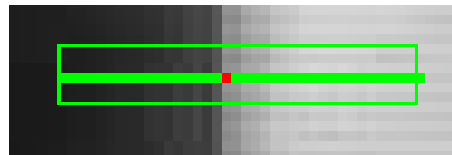
Figure 4.7: Correct identification of strip edge

4.2.2 Identification of acceptable edges

The example given in section 4.2.1 is a very "clean" section of image. The nature of this application means there were very noisy images and many false edges are identified. The thresholding process described above could only account for the worst of the false edges and other noise had to be additionally removed. Figure 4.8 shows an example image that has undergone the aforementioned edge detection, with a threshold value of 150 and the kernel shown in Table 4.2, scanning every second line in the image. Whilst a significant portion of "edges" have been filtered out, there are still groups of edges seen from steam and spray in the image.
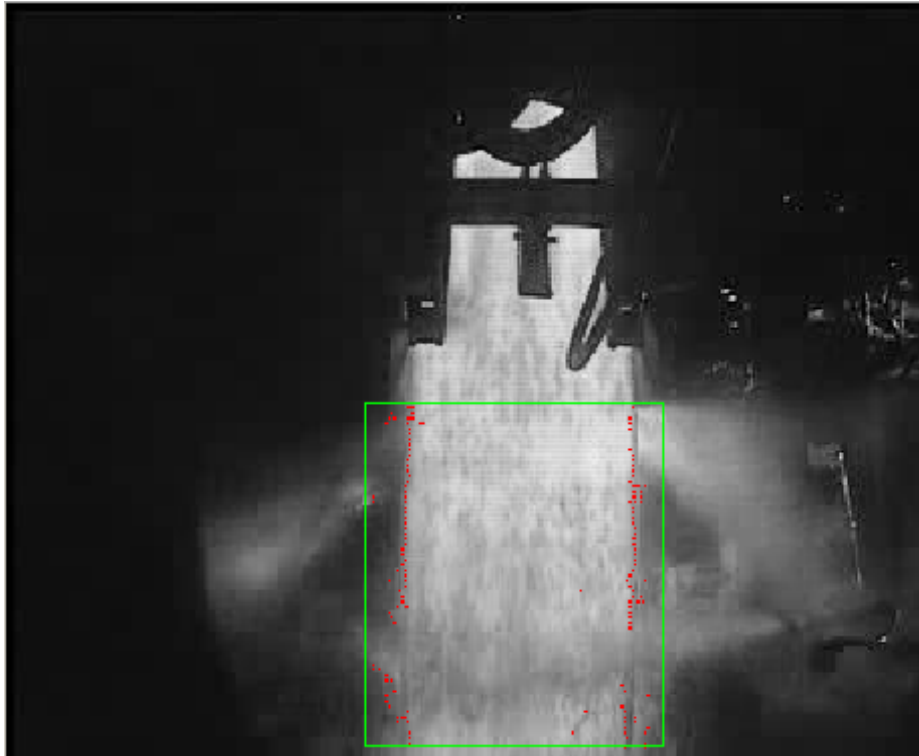
Figure 4.8: Example of multiple edge detection in strip image

These unwanted edges were ignored by using past information about the strip edge location. Using the fitted curve from the previous image, the expected edge position could be calculated for each search line. A threshold of 3 pixels was applied to the data and any points outside that range rejected. In some cases, multiple edges were identified with the tolerances on one search line. In these cases the average pixel position for the group was taken. By allowing two sets of acceptable regions, representing both edges of the strip, two distinct groups of pixels were identified to which curves were fitted. The result of this process can be seen in Figure 4.9. In this example, the group of pixels on the left edge are marked in yellow and the group on the right marked in blue. The red pixels show the rejected edges.
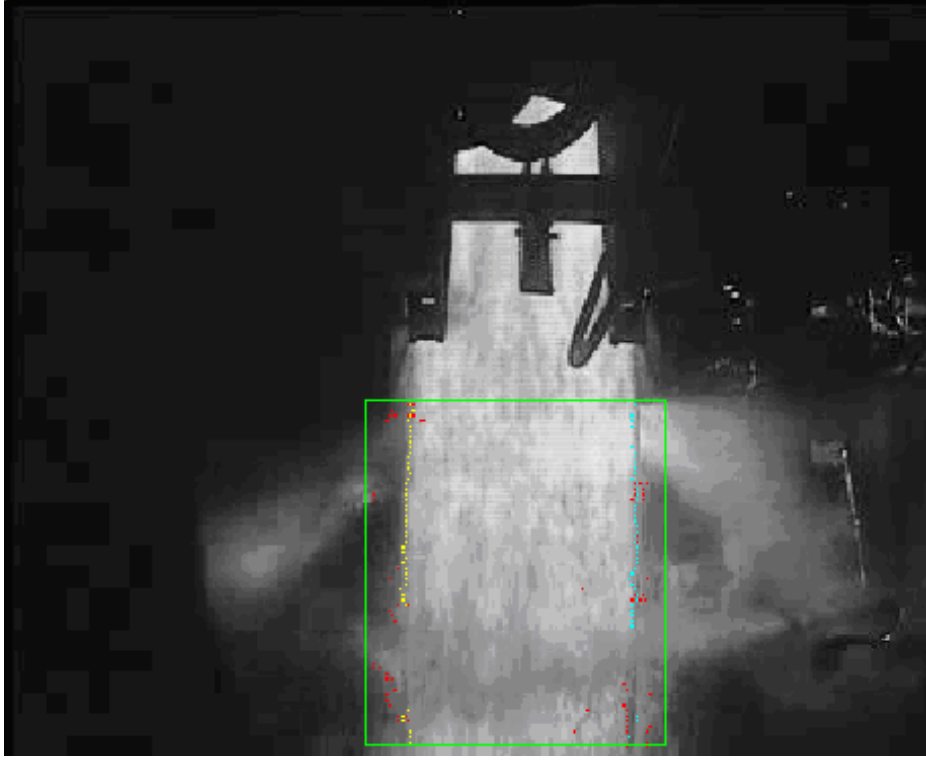
Figure 4.9: Two sets of valid edges identified in example image

4.2.3 Curve fitting

With the image processed now to a point where the edges were grouped into sets representing the two edges of the strip, a curve could be fitted to the data to find the location of the complete edge.

A Bezier curve [48] of order n can be defined by equation (103) and the binomial coefficient is given in (104).

$$B(t) = \sum_{i=0}^{n} \binom{n}{i} (1-t)^{n-i} t^i \mathbf{P_i} \quad , \quad t \in [0,1]$$

(103)

$$\binom{n}{i} = \frac{n!}{i!(n-i)!}$$

(104)

Therefore, a cubic Bezier curve (order $n = 3$) is defined by equation (105)

$$B(t) = (1-t)^3 \mathbf{P_0} + 3(1-t)^2 t \mathbf{P_1} + 3(1-t)t^2 \mathbf{P_2} + t^3 \mathbf{P_3}$$

(105)

The knots, $\mathbf{P}_0$ to $\mathbf{P}_3$ are points defining the curve and can be of any dimension, as long as they are all the same dimension. In this case the requirement is to fit a curve to known points in 2-dimensional space, therefore points $\mathbf{P_i} = \mathbf{P_i}[x, y]$. An example of a cubic Bezier curve is shown in Figure 4.10. Note only knots $\mathbf{P}_0$ and $\mathbf{P}_n$ lie on the curve as endpoints. The other knots define the magnitude and direction of curvature.
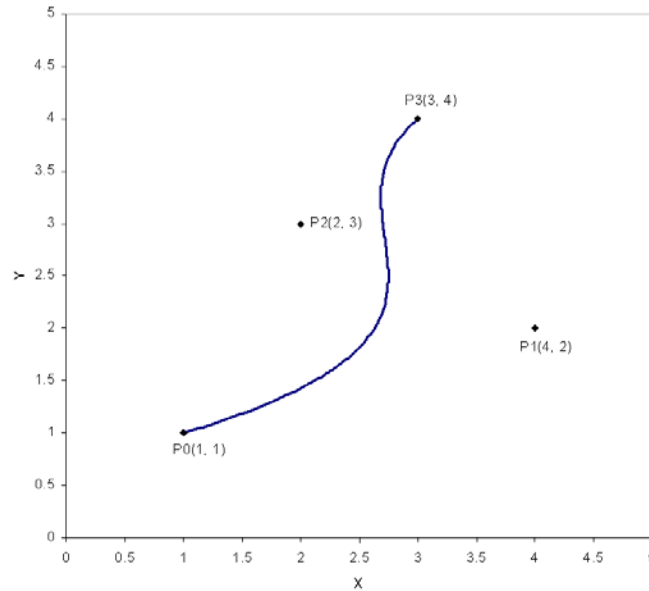
Figure 4.10: Example of cubic Bezier curve

The images were scanned in series of even steps down the y-axis, a total of m steps, i.e. m data points of $y_j = y_0, y_1, \ldots y_m$. Therefore, all the values of $\mathbf{P_i}[y]$ are defined by a uniform spread, calculated using equation (106).

$$\mathbf{P_i}[y] = y_0 + i\frac{y_m - y_0}{n} \quad , \quad i = 0,1\ldots n$$

(106)

The task here is to find values for $\mathbf{P_i}[x]$, using the least squares method.

The points along the curve are valid for $0 \leq t \leq 1$, however the data points from the image analysis process are defined by the y-values of the search line. Therefore each point must be mapped to a value defined by equation (107).

$$t_j = \frac{y_j - y_0}{y_m - y_0}$$

(107)

83

The least squares method [49] minimises an error function defined as the square of the error between the curve and the data as in equation (108), therefore the error function R^2 was defined by equation (109).

$$R^2 = \sum_{j=0}^{m} \left[x_j - B(t_j) \right]^2$$

(108)

$$R^2 = \sum_{j=0}^{m} \left[x_j - \left((1-t_j)^3 \mathbf{P_0}[x] + 3(1-t_j)^2 t_j \mathbf{P_1}[x] + 3(1-t_j)t_j^2 \mathbf{P_2}[x] + t_j^3 \mathbf{P_3}[x] \right) \right]^2$$

(109)

The method looks for the minimum change in error for a change in $\mathbf{P_i}[x]$, therefore a point defined by equation (110).

$$\frac{\partial(R^2)}{\partial \mathbf{P_i}[x]} = 0$$

(110)

The partial derivatives of R^2 with respect to $\mathbf{P_i}$ were hence found as equations (111) to (114).

$$\frac{\partial(R^2)}{\partial \mathbf{P_0}[x]} = -2\sum_{j=0}^{m} \left[\left(x_j - \left((1-t_j)^3 \mathbf{P_0}[x] + 3(1-t_j)^2 t_j \mathbf{P_1}[x] + 3(1-t_j)t_j^2 \mathbf{P_2}[x] + t_j^3 \mathbf{P_3}[x] \right) \right)(1-t_j)^3 \right] = 0$$

(111)

$$\frac{\partial(R^2)}{\partial \mathbf{P_1}[x]} = -2\sum_{j=0}^{m} \left[\left(x_j - \left((1-t_j)^3 \mathbf{P_0}[x] + 3(1-t_j)^2 t_j \mathbf{P_1}[x] + 3(1-t_j)t_j^2 \mathbf{P_2}[x] + t_j^3 \mathbf{P_3}[x] \right) \right)3(1-t_j)^2 t_j \right] = 0$$

(112)

$$\frac{\partial(R^2)}{\partial \mathbf{P_2}[x]} = -2\sum_{j=0}^{m} \left[\left(x_j - \left((1-t_j)^3 \mathbf{P_0}[x] + 3(1-t_j)^2 t_j \mathbf{P_1}[x] + 3(1-t_j)t_j^2 \mathbf{P_2}[x] + t_j^3 \mathbf{P_3}[x] \right) \right)3(1-t_j)t_j^2 \right] = 0$$

(113)

$$\frac{\partial(R^2)}{\partial \mathbf{P_3}[x]} = -2\sum_{j=0}^{m} \left[\left(x_j - \left((1-t_j)^3 \mathbf{P_0}[x] + 3(1-t_j)^2 t_j \mathbf{P_1}[x] + 3(1-t_j)t_j^2 \mathbf{P_2}[x] + t_j^3 \mathbf{P_3}[x] \right) \right)t_j^3 \right] = 0$$

(114)

Equations (111) to (114) were represented with a set of matrices, resulting in equation (115).

$$
\begin{bmatrix}
\sum\limits_{j=0}^{m}(1-t_j)^6 & \sum\limits_{j=0}^{m}3(1-t_j)^5 t_j & \sum\limits_{j=0}^{m}3(1-t_j)^4 t_j^2 & \sum\limits_{j=0}^{m}(1-t_j)^3 t_j^3 \\
\sum\limits_{j=0}^{m}3(1-t_j)^5 t_j & \sum\limits_{j=0}^{m}9(1-t_j)^4 t_j^2 & \sum\limits_{j=0}^{m}9(1-t_j)^3 t_j^3 & \sum\limits_{j=0}^{m}3(1-t_j)^2 t_j^4 \\
\sum\limits_{j=0}^{m}3(1-t_j)^4 t_j^2 & \sum\limits_{j=0}^{m}9(1-t_j)^3 t_j^3 & \sum\limits_{j=0}^{m}9(1-t_j)^2 t_j^4 & \sum\limits_{j=0}^{m}3(1-t_j)t_j^5 \\
\sum\limits_{j=0}^{m}(1-t_j)^3 t_j^3 & \sum\limits_{j=0}^{m}3(1-t_j)^2 t_j^4 & \sum\limits_{j=0}^{m}3(1-t_j)t_j^5 & \sum\limits_{j=0}^{m}t_j^6
\end{bmatrix}
\times
\begin{bmatrix}
\mathbf{P_0}[x] \\
\mathbf{P_1}[x] \\
\mathbf{P_2}[x] \\
\mathbf{P_3}[x]
\end{bmatrix}
=
\begin{bmatrix}
\sum\limits_{j=0}^{m}(1-t_j)^3 x_j \\
\sum\limits_{j=0}^{m}3(1-t_j)^2 t_j x_j \\
\sum\limits_{j=0}^{m}3(1-t_j)t_j^2 x_j \\
\sum\limits_{j=0}^{m}t_j^3 x_j
\end{bmatrix}
$$

$$
\equiv \quad \begin{bmatrix} \mathbf{T} \end{bmatrix} \quad \times \quad \begin{bmatrix} \mathbf{P} \end{bmatrix} \quad = \quad \begin{bmatrix} \mathbf{X} \end{bmatrix}
$$

(115)

Therefore, values of $\mathbf{P_i}[x]$ were found by evaluating equation (115) as equation (116).

$$\mathbf{P} = \mathbf{T}^{-1} \times \mathbf{X}$$

(116)

Applying this method to the point sets shown in Figure 4.9, the edge of the strip could be clearly identified, as shown in Figure 4.11.
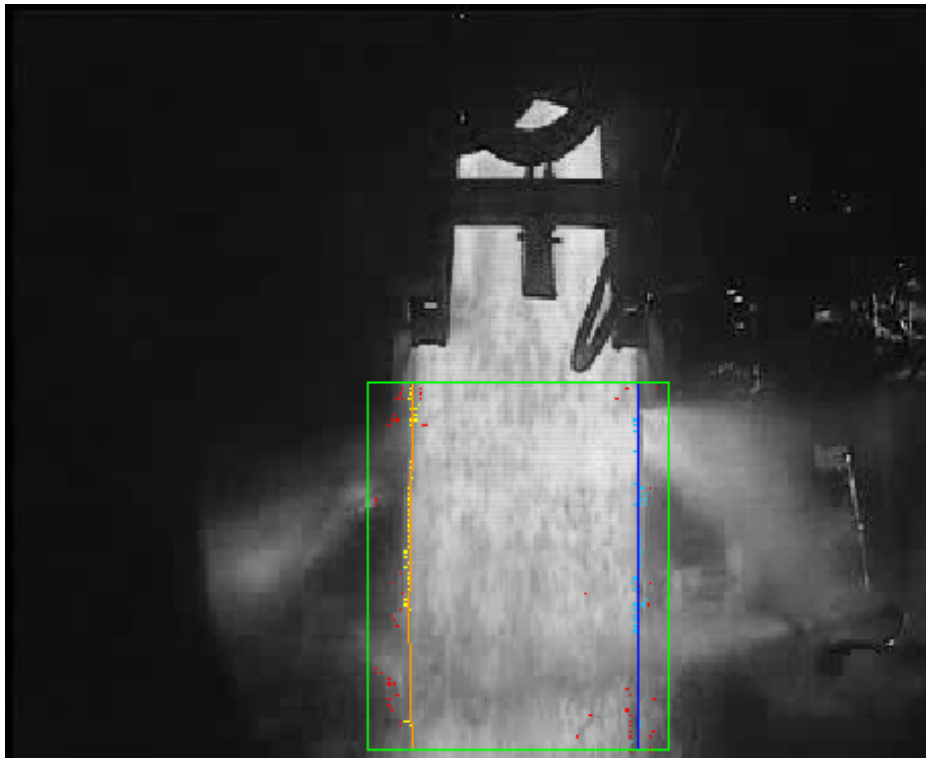
Figure 4.11: Image with strip edges identified

The resulting edges shown in Figure 4.11 were defined by the knots given in

Knot	Left [y]	Right [y]
P_0	320.1	498.0
P_1	314.3	498.1
P_2	319.7	498.7
P_3	319.8	498.0

The knots were then averaged to find a Bezier curve defining the centre-line of the strip, show in Figure 4.12.
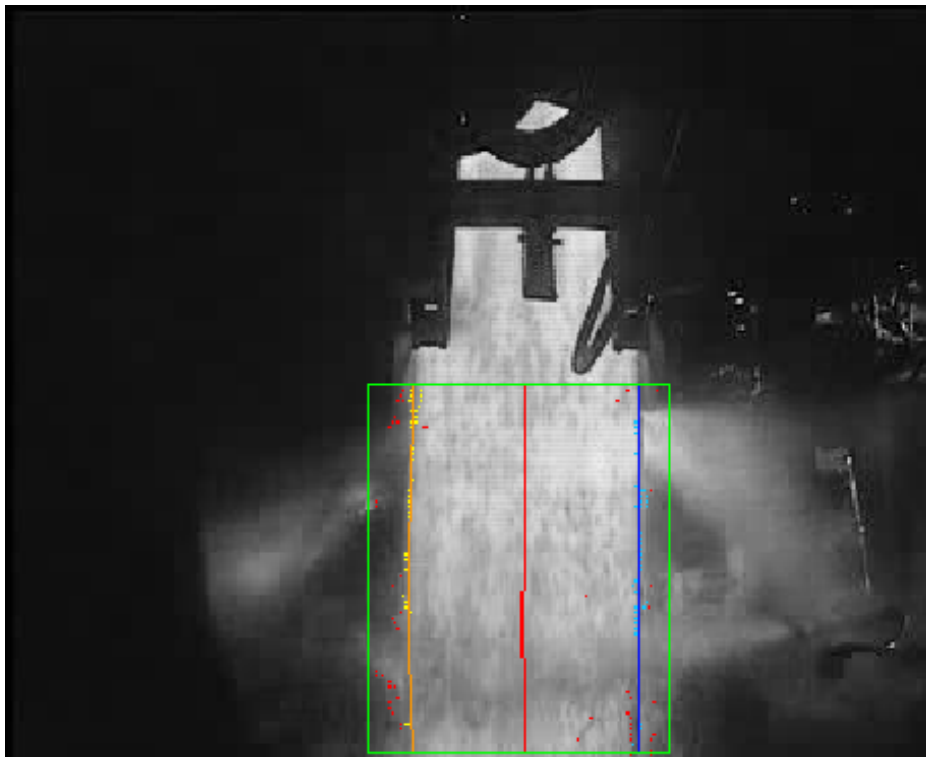
Figure 4.12: Image with strip edges and centreline identified

4.2.4 Tolerances and boundaries

The processed images presented in section 4.2.3 were subjected to a degree of limitation on the placing of points and curves. The "Acceptable Point" tolerance of a few pixels has already been discussed in section 4.2.2 but further limitation was applied to the curve location to enhance the correct edge identification.

The first condition is a boundary condition, limiting the overall placement of the curve. The strip runs between guides and the camera was in a fixed location, therefore the edge would always lie within a given section of the image. The expected location of the edge was set in software and a wide boundary given, in this case 10 pixels each side, limiting the position of

the curve. This boundary condition prevented the curve "running away" if there were consistently bad edges detected.

The second condition imposed on the curve effectively limited the "straightness" of the curve. This limited the location of the knots depending on the average of all calculated knot positions. The limit was applied separately for endpoint knots and mid-section knots. The endpoint knots were limited to a given number of pixels each side of the average, the mid-section knots were limited to double this value each side. The difference was applied because the mid-section knots lie further out than the curve itself. In this example the limit was set to 2 (4 for mid-section) pixels either side. This limit was applied to prevent anomalous edges pulling a section of curve outwards away from the strip edge, and then further affecting the acceptable region for subsequent images.

The application of these limits dramatically improved the reliability and robustness of the analysis.

4.3 Evaluation following Port Talbot initial trials

The methods used to measure the strip edge position all contributed to the success of the software and worked together for optimal results.

By measuring the position down the entire length of the strip, as much data as possible could be found about the shape and position of the strip in the mill. Utilising existing knowledge on the position of the strip as an edge-rejection method allowed filtering of the data points which could then be used to fit a cubic Bezier curve, interpolating the missing positions. The least-squares method used to fit the curve was a straightforward matrix multiplication, requiring no iterative process, optimising processing time.

The use of tolerances and limits was the key to the successful operation of this software and hence there was a requirement to set these to reasonable values for the application.

The first tolerance that was used is the Acceptable Point tolerance, defining how far an edge on a given search line could be from that in the previous image. This limit was designed to filter the random edge noise from small amounts of spray that appeared in the measurement area. If this value was set too low then any strip movement will not be detected, however too high and steam around the strip would be considered to be the edge.

The Curve Bound tolerance limited the space in which the curve could be determined to be. This allowed a reasonable working space but prevented the edge to be determined to be too far from the expected position. This bounding proved to be very effective in the case of total

loss of strip image, such as in between strips passing through the mill. This limitation allowed the strip to recover very quickly from these situations and resume measurement very quickly. The bounding size did not have a big impact on the general operation of the software, but if it was set too low then the strip could move out of the working area of the curve. Likewise, the expected position had to be a reasonable average strip position to ensure even bounding on both edges of the strip. If this value was set too high then it allowed the curve to wander too far from the expected position and the software could not recover after losing strip images. The straightness tolerance has proven to be the most effective method in maintaining good measurements and ignoring steam and spray. This applied a limitation on the curviness of the curve, preventing patches of stream and spray pulling sections too far from the correct line. If the value was too low then the curve was limited to a straight line, but too high and steam and spray begun to be interpreted as strip edge.

To evaluate the effectiveness of the software before development of the complete system, a set of images from the initial Port Talbot trials were analysed by the software to determine the centreline point at the bottom of the ROI. These were compared to centreline positions determined manually. The absolute errors between observer measurements and software measurements were calculated and the distribution plot shown in Figure 4.13. The accuracy of manual measurements was estimated to be 0.5-1px.
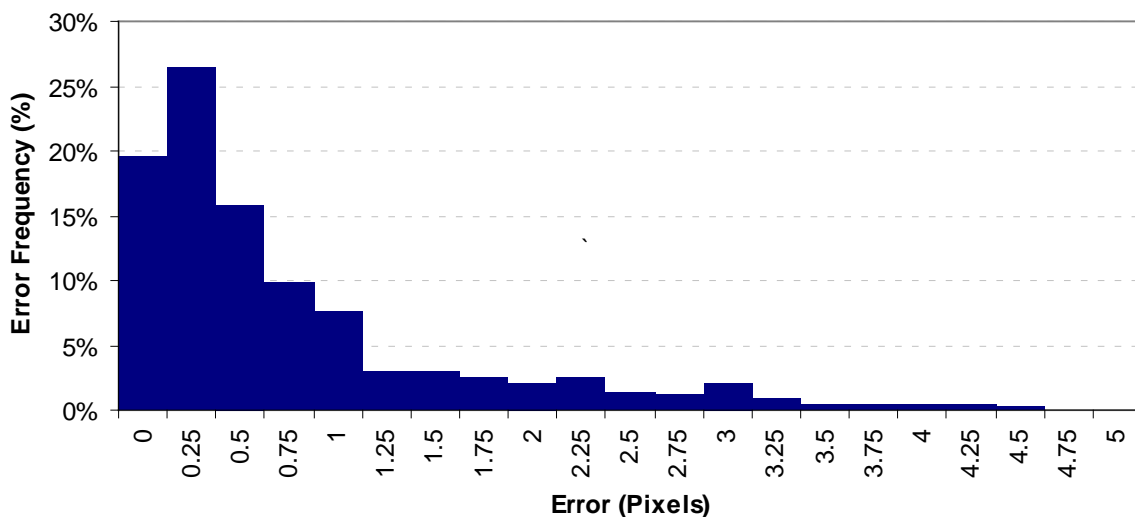
Figure 4.13: Distribution of Measurement Errors

The pixel resolution for the images used in this study was estimated at 13mm/px, the resolution for the complete measurement system was initially designed to approximately 3mm/px.

The results from this study have shown that for 90% of the results, measurements were determined to be within 2px accurate. 80% of the results were better than 1px and 60% better than 0.5px.

In the worst-case situations, errors of 3-4px were seen. These occurred in extremely obscured images and in very few cases with only 5% of errors over 3px.

The magnitude of these errors was thought to be increased by limiting factors of the camera used. The images were slightly out of focus, which proved very detrimental to edge detection. Additionally, if an infrared filter were used, edge clarification is likely by reducing blooming and pixel bleeding in the camera. From this data it was anticipated that using a higher quality camera that is in focus and equipped with an IR filter would shift the error distribution towards smaller errors. In addition to this, because the worst errors occurred very infrequently, application of simple data filtering could aid in reducing the magnitude of these errors.

5 Original Measurement System Design

5.1 Introduction

Following the work in Chapters 3 and 4 on trialling and developing methods, a design for an online measurement system could be formulated. The overall design scheme was to use cameras mounted to view the strip from above, as in the trials in Chapter 3, and running the analysis method that was developed in Chapter 4, to provide online measurements of strip position.

The initial requirement was for a scaled down proof of concept system with the ability for future expansion if required at a later date therefore was designed as a two camera system. The findings from [21] suggested that the two cameras were placed on the first two stands.

5.1.1 Requirements

The system design was subject to the following requirements:

- Capable of running the analysis software created in LabVIEW
- Robust
    - Tolerant to electrical noise from the mill
    - Suitably protected from hazards
    - Stable computer system
- Measurement speed faster than 20ms
- Total accuracy of <2mm (Note: final accuracy is potentially higher than camera resolution due to interpolation of position)
- Integration with mill logging system
    - Port Talbot: OPC (Ethernet connection)
    - Llanwern: analogue voltages
- Ability to expand to full seven stands

5.1.2 Concept overview and initial design choices

At the core of the system and key to the design requirements was that the system be based around the image analysis method and software created using National Instruments LabVIEW. The controlling computer system also had to be stable and robust. To achieve this, it was decided that the best option was to use a dedicated computer for this task, and that using a National Instruments PXI industrial computer would provide ease of development, support and flexibility.

The second initial design choice was to use the Gigabit Ethernet Vision (GigE Vision) protocol for transmission of images from the cameras to the computer. This choice was made because GigE Vision offers 100m transmission at high speeds [34], exceeding the transmission capabilities of the alternatives and allowing the use of standard network components. Higher transmission distances are also possible using other technologies such as fibre optics instead of Ethernet cable

A schematic of the initial design is shown in Figure 5.1 with more detailed descriptions of the various components in the following sub-sections.
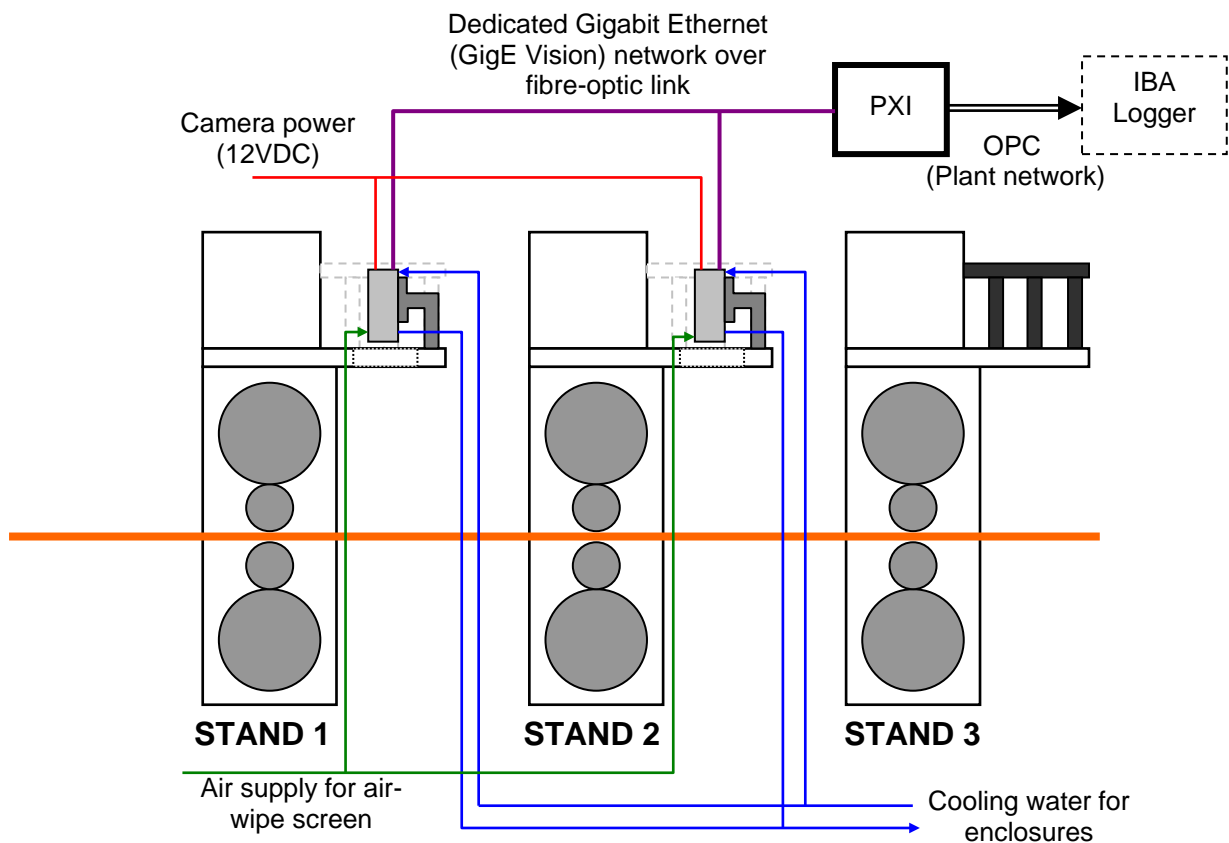
Figure 5.1: Measurement Sytem Configuration

5.2   Hardware design

The diagram in Figure 5.1 shows the general system configuration and components. At the core of the system was a National Instruments PXI-8110 Quad Core industrial computer, equipped with additional GigE and analogue output cards. The two cameras were connected through the GigE card on a dedicated network. The analogue output card was provided because the original specification came from the Llanwern mill where analogue inputs to the mill computers were preferred, however these were unused in the installation in Port Talbot as Ethernet was preferred. This computer had the following tasks:

- Control cameras
- Analyse images
- Send measurement results to external system
- Provide user interface
- Log images and results locally

The PXI was located in a computer room with a controlled environment, protecting it from the hazardous environment of the mill. The computer was also connected to the central plant network via Ethernet for communication of the measurements to the plant data logger (the IBA). The system was designed as a dual Operating System (OS) Hypervisor configuration, running LabVIEW Real Time (RT) to perform the analysis on three processor cores, and Windows XP on the remaining core to handle communication with the plant and provide a user interface. The Hypervisor configuration was designed to provide a high speed robust system by performing all the analysis on the dedicated RT section. A Real Time OS, as opposed to a standard OS such as Windows XP, is designed to be a very low-level implementation with minimal interrupts from other processes, such as user input devices (mice, keyboards, etc) and other programs, such as anti-virus protection. As such the repeatability of speed of execution is very high, providing a stable and reliable environment for measurements. However, the minimal nature of the RT OS means there is no functional user interface. In order to provide an interface, variables can be passed to the RT OS across a network. Hence a user interface can be created on a separate device, running a graphical user-oriented OS such as Windows or Linux and connected across the network to affect settings changes and transfer other data from the program running in the RT OS. In this case the "network" was in the form of a virtual Ethernet connection between the instance of Windows XP running on a single core of the machine and the RT OS running on the other three cores, managed by the Hypervisor. A user interface was deployed on the XP side of the PXI, hence providing a single box solution with a user interface and RT operation. A low-level process was also created on the XP side to manage communication of OPC variables with the IBA logger in the plant, discussed in more detail in section 5.3. A discussion of the software on the XP and RT sides is in section 5.4.
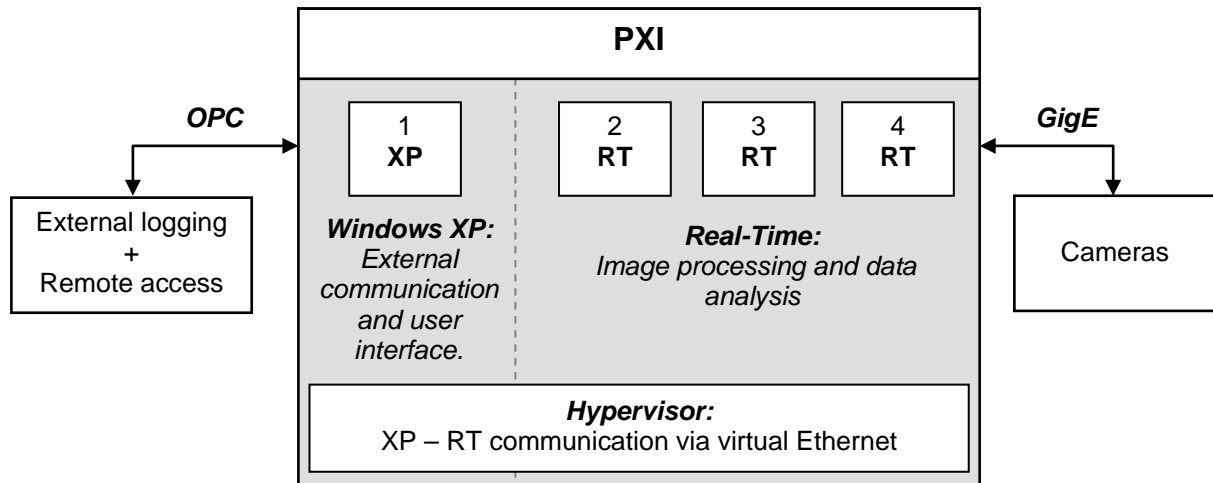
Figure 5.2 : PXI Configuration

The cameras chosen for the measurement task were Basler Scout scA780-54gm [50]. These cameras are 782x582 pixels (px) and monochrome, with a maximum frame rate at full resolution of 54 frames per second (fps), and frame rate would increase with decreased resolution. Each camera was fitted with a 12mm lens to achieve a suitable viewing area, and an infrared filter to minimise pixel bleeding and protect the cameras from the heat emitted from the strip. Measurement resolution was estimated at approximately 3mm/px at the design stage. The Basler Scout was seen as the best choice of camera for meeting the requirements of using the GigE Vision protocol, being supported by the LabVIEW vision toolkit, speed of acquisition and the lowest cost at the time of design, given the alternatives.

The location for the cameras above the strip was subject to very difficult conditions for electronic devices, including water sprays and high temperature. To protect the cameras from the hazards, they were situated in VideoTec NXW enclosures (Figure 5.3) [51].

Figure 5.3: VideoTec NXW Camera Enclosure

The enclosures were IP66 rated, protecting against high pressure water jets, and double skinned to allow circulation of cooling water. They were also equipped with an air-barrier,

designed to prevent the build up of debris on the viewing window. The enclosure windows were specified as Vycor glass for added thermal protection.

The bracket inside the enclosure for mounting the camera on was not directly compatible with the cameras, therefore an adapting bracket was required, and the design shown in Figure 5.4. This bracket also had the task of raising the level of the camera within the enclosure so the lens sat centrally in the viewing window. This bracket attached to the rail mounting inside the enclosure using two M8 bolts, and attached to the camera using four M3 bolts. A small piece of rubber padding was also put between the camera and the bracket to help dampen vibration.
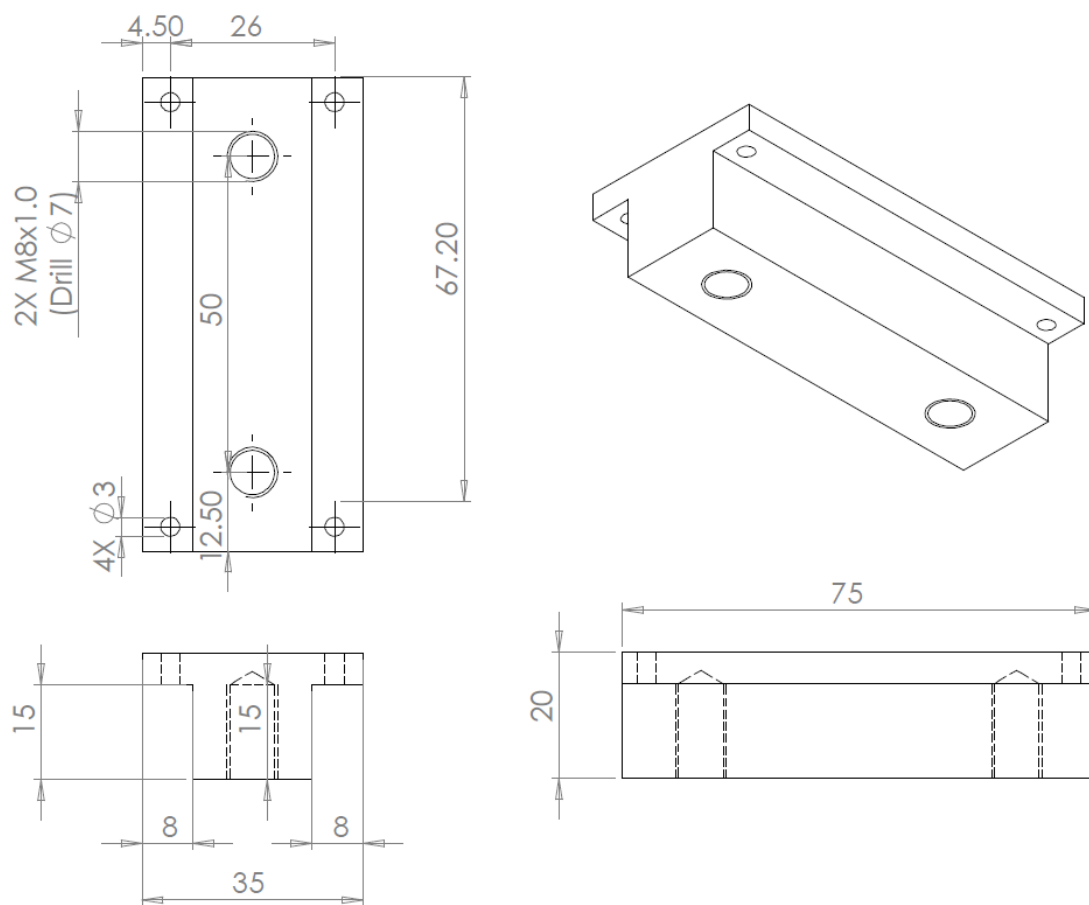
Figure 5.4 : Mounting bracket for camera in enclosure

The enclosures were attached to the gantries overhanging the mill on the first two stands, placed above cutaways previously used for other studies, shown in Figure 5.5. This image was from the first stand on the mill, from this view the strip travelled right to left. Also visible in this image is the looper roller and cooling headers for that stand. The enclosure

shown in this image sat just below the level of the gantry and was used for the preliminary studies.

Figure 5.5: Hatch and pre-existing mounting bracket

The existing enclosure provided minimal protection and was only used for the dispensable early trial cameras as a quick solution. A new bracket was fabricated for the new enclosures, sitting just above the level of the gantry and providing more adequate protection. Figure 5.6 shows a new enclosure in place, attached with the fabricated mounting bracket.

Figure 5.6 : Installed camera enclosure

Each enclosure was supplied with water for the cooling sleeve and air for window cleaning. Additionally connections for the cameras entered through the rear of the enclosure. These connections were a 12VDC power supply and the GigE network connection, both locally

terminated at the mill stand adjacent to the enclosures. The camera network used a fibre-optic link between the stands and the PXI in the computer room to minimise noise.

5.3   Communication and mill integration

To transmit the data from the measurement system to the mill computers for logging and to make the results available for other tasks, such as control, the preferred method was to use OPC (OLE (Object Linking and Embedding) for Process Control) [52]. OPC provides a standardised method to allow transfer of data between devices across a network, utilising connections already in place. In LabVIEW, publishing OPC variables is relatively simple; any Network Variable is automatically published as OPC data. This was achieved in practice by writing a simple program to access the data transferred from the RT side of the PXI and publish it on the main network with suitable names. Figure 5.7 shows the flow of data from the cameras acquiring images to the results being logged at the mill computers.

When this project was based in Llanwern in the initial stages, the requirement for mill integration was analogue outputs. The provision for these was made by including an analogue output card, but this was unused in this implementation.
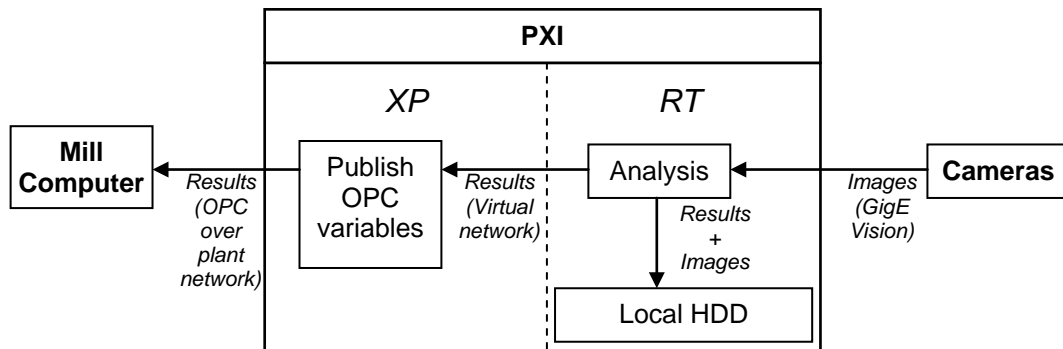
Figure 5.7 : Measurement system data flow

5.3.1   System costs

An approximate breakdown of system costs is shown in Table 5.1

Table 5.1: Approximate system costs

Item	Quant	Cost each	Total
CAMERAS			
Camera (inc. optics)	2	£1000	£2000
Enclosure	2	£1300	£2600
COMPUTER SYSTEM			
NI-PXI	1	8000	£8000
		TOTAL	**£12600**

Note that the system costs have been approximated. Computer cost includes analogue output card which was designed for use in Llanwern but not included in this implementation. Costs could be reduced by using a different hardware platform.

Costs do not include cabling and installation.

5.4   Software

The software running on the PXI was comprised of three distinct components:

- Image analysis, running in RT
- OPC data management, running in XP
- User interface, running in XP

The interactions between the software components are shown in Figure 5.8 and a more detailed discussion of each in the following sub-sections. The measurement and communication components were set to automatically start when the PXI was booted up, therefore measurement and transmission of results would begin with no user input required.
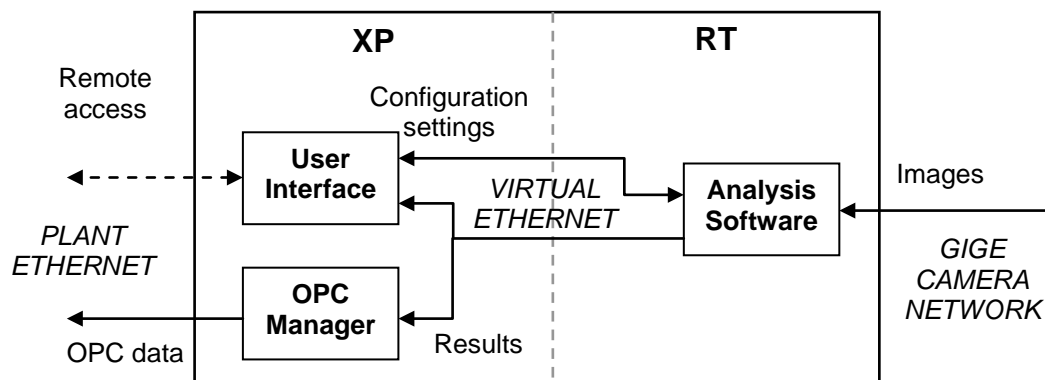
Figure 5.8 : Software components and communication

5.4.1   Real-Time measurement software

The software in the RT OS performed all the image analysis tasks and managed the cameras on the system forming the main functional part of the entire measurement system. The precise details of the image analysis method have been previously described in Chapter 4. The following provides a description of the software structure and general operation.

The design of the software was a state-machine architecture; the program progressed from one state to the next depending on the current and next desired operation. This architecture was chosen because it creates comprehensible and easy to follow program flow, and also easily facilitates jumping to an out of sequence mode (e.g. entering configuration mode) which can prove useful in an application such as this. A flowchart depicting program flow

between states is shown in Figure 5.9 with detailed explanations of each state below. In the flowchart, the rectangular boxes represent actual program states, the diamond boxes are decisions (either externally sourced interrupts or the result of a state) and the round-cornered boxes represent start-up and shut-down processes, whilst not being true states in themselves.
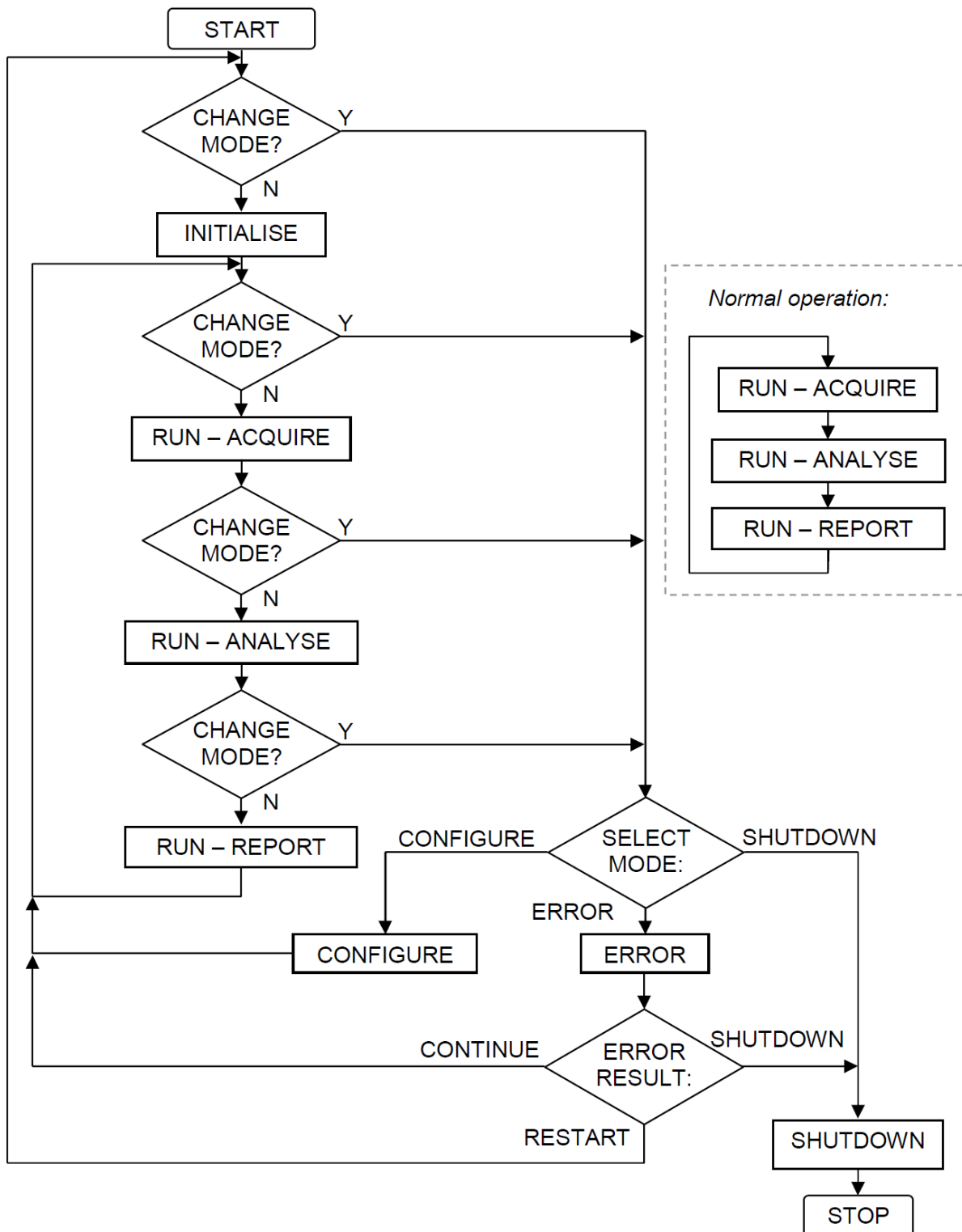
Figure 5.9: Image analysis program flowchart

The "Start" process initiated a small time delay before the program began, loaded start-up parameters into a few of core variables and initiated the text logging, which was used to save a record of program operation during the running cycle, including any errors that were encountered. The starting time delay was used to work around an issue found within the NI RT OS and allowed time for all OS components to load, specifically it was found that the variable manager loaded after the program started so would cause a crash when the software tried to write to a variable which was not yet loaded into memory by the OS. The program was set as a start-up executable so the analysis program started when the RT OS loaded.

The "Stop" process simply sent a final value of "Stopped" to the text log and terminated the program.

In between each state change, the program checked to see if anything had occurred which would require an out-of-sequence state change, this is represented by the "Change Mode?" decision and could be one of the following:

- Configuration request from the user interface to allow configuration of software parameters – "Configure"
- Error occurred during running - "Error"
- Request to shutdown program (from the user interface or result of an error) – "Shutdown"

The main program states and their functions are detailed in the following paragraphs.

Initialise

This state set the program up ready for running. First, a scan of the local system would be performed to determine the number and identity of connected cameras. This step allowed new cameras to be easily added, and could compensate for cameras which were missing from the system. If no cameras were found, the program would retry for one minute before timing out and shutting down.

When the connected cameras had been evaluated the program would determine whether each connected camera has previously been configured by checking whether there was an existing configuration file saved to the hard drive. If a camera had a configuration file then this file was loaded and the settings used to configure the camera. If no file existed then default settings were loaded into the camera and a new file created for that camera. The configuration settings set up two aspects of the acquisition: camera aspects such as size of captured image and exposure time, and analysis aspects, covering all analysis parameters. These are listed in Table 5.2. For more detailed explanations of the analysis parameters, see Chapter 4.

It was very unlikely that the default settings would be correct for good tracking measurement so new cameras added to the system had to be correctly configured; this is explained in more detail in section 5.4.3. All the cameras were set into continuous acquisition mode; that is they were constantly acquiring images and the software would grab the latest one available from the camera. The alternative was to use single grab mode, only taking images when required but the execution time would have been slower because the grab command has to be sent to each camera individually. Once all cameras had been initialised, memory references for images were created to allocate space for captured images. The program would then enter Acquire mode.

Table 5.2: Configurable camera and analysis parameters

CAMERA PARAMETERS		
Height		Specifies physical size and position of image captured by camera in pixels. By using a smaller image, all aspects of analysis (capture time, transfer rate and analysis time) could be improved
Width		
OffsetX		
OffestY		
ExposureTimeAbs		Camera exposure, used to adjust for brightness of strip to ensure clear image
NB: Additional MAX and MIN settings for these are also used, but not configurable. These are used to define the limits of parameter adjustment in the user interface and are obtained by querying an xml file within the camera.		
ANALYSIS PARAMETERS		
Kernel		Used to set filtering and differential rate on edge detection
Step Size		Defines increments of scan lines in pixels
Gradient Limits	Max	Sets limits of which points to ignore ("weak" edges) when performing initial edge detection step
	Min	
ROI	Top	Sets size and position of analysis area in pixels. This differs from camera settings because there is no change to the physical image size
	Left	
	Height	
	Width	
Previous Edge Tolerance		Maximum shift of point location between time-steps
Estimated Edge Position		Initial estimation of edge location
Bounds Tolerance		Maximum edge can possibly be from initial guess
Straightness Tolerance		Defines how straight the Bezier curves defining the edges must be

Run – Acquire

This state acquired the images. For every camera connected to the system the latest image was downloaded into the pre-allocated memory reference. These images were then used in the Analyse mode.

Run – Analyse

The Analyse mode was the central and most functional part of the software, performing the analysis detailed in Chapter 4 on each most recent camera image. This state used predefined parameters (set in the configuration file and shown in Table 5.2) to fit the Bezier curves to each strip edge then find the average of them to find the strip centreline. The results of this process were then sent to the Report mode.

Run – Report

Following analysis, the results were processed in the Report mode. This state performed the final position calculation, based on the centreline Bezier position and the mill centre datum position before outputting in the results to network-published variables on the virtual Ethernet link which could be read by a program running on the Windows XP section of the PXI. If the option had been selected, the images taken by the cameras were also saved to the local hard drive in this state, allowing off-line analysis at a later date. This state also handled the saving of numerical results to a local log file if the option was enabled. The program would then loop round to the beginning of the Run sequence, back to Acquire to start the process again.

The following states were only entered in certain circumstances, and were not used in general running of the software.

Configure

This state was used to configure the cameras and analysis parameters to ensure correct software operation. This state would be only be initiated when a request from the user interface was submitted, containing a number representing the camera to be initiated and a logical value to request configuration mode. This request is explained in more detail in section 5.4.3.

The configuration states operated in close coordination with a configuration window on the Windows XP side of the PXI. The core of the programming in this state was functionally identical to the analysis state, with some extra features to facilitate the configuration. The main difference between the two was a graphical representation of the analysis on the image, e.g. overlaying points and curves to show the results of each analysis step, allowing fine tuning of the parameters from the user interface. The lack of graphical interface combined with the need for a visual display from the cameras provided a challenge to enable this to be possible.

The camera network was isolated from the virtual Ethernet link so the RT OS could be the only OS to maintain control of the cameras; any settings changes had to be made through the RT OS and any images were handled by the RT OS.

A method was required to allow the user interface on the Windows OS to communicate with the cameras to view the images and change the settings. The first attempt at a solution made use of a remote front panel; a front panel hosted by the inbuilt web server in the RT OS that could be accessed through a web browser or from another local front panel. This method meant that all data handling was performed directly through the RT OS so any settings changes were made directly in camera. When operational this method proved very effective and provided an easy and fast method for a user on the Windows OS to configure the camera and acquisition parameters. Unfortunately, during the testing phases a problem was found where this method proved to be unstable, occasionally causing a total system crash and loss of connectivity to the RT OS. The precise cause of this problem was unknown but thought to be a limitation of the front panel in the National Instruments software.

To work around the limitation of the front panels, another method was found. Instead of hosting the front panel and connecting to it remotely, the display of the images was performed in a local front panel on the Windows OS with the analysis still performed on the RT OS. In this solution, first the latest settings were obtained from a network variable, then the program would operate in one of two modes, depending if analysis settings or camera settings were being changed. For analysis settings, the analysis was performed, overlaying all requested results (all edge points, used edge points, edge and central Bezier curves) on the captured image. The image, including overlays, was then flattened to a string and sent as a network variable, along with the numerical results of the analysis, on the virtual Ethernet link. If there were any camera settings changes (field of view or exposure time) then the camera had to first be un-configured from continuous acquisition mode, then changes could be made, then the camera was re-configured. Again, an image was acquired and transferred as a string in a network variable. The images had to be flattened to a string before they could be passed as a network variable because the "Image" data type is simply a pointer to a memory location containing the image, and would be meaningless on another computer.

The PXI would remain in Configure mode until a request to exit and continue with normal running was sent from the user interface. At this point the new settings were saved to the local configuration file then the program would return to state Run – Acquire.

Error

The Error state was initiated whenever a software error occurred and was used to manage any errors which occurred in an effort to maintain program operation. These errors were generated automatically within LabVIEW for numerous different causes. This state was programmed to handle specific errors so had to be kept updated with new software revisions if any unforeseen errors occur. The state was therefore only capable of handling a few error cases in the initial version, and other aspects of the software had been written in a way so that no errors should occur. There were three possible responses to an occurring error, these were:

- Continue. If the error was not deemed to be significant or could be handled very easily then it was cleared to prevent any further interruptions and the normal program operation was resumed in the state Run – Acquire

- Restart. If an error had caused a problem which could be overcome by making settings changes and re-initialising the cameras then the program was restarted.

- Shutdown. If an error could not be adequately handled the system was shut down. Typically this would only ever be used for unforeseen errors and errors that occurred due to a terminal failure.

Two specific error cases had been programmed in this initial version:

- Code -10743603032. Camera properties had been set out of permissible range. In this case the settings were coerced to the nearest permissible limits and the system would continue. Programming had been put in place which meant this error should not be able to occur but the ability to handle it remained to maintain a robust program.

- Code -1074360308. Camera had been removed from the system, typically a hardware failure either in the network itself or the camera had broken. The error was cleared and the system restarted in the Initialise state. This forced the system to enumerate the cameras again and the continue running with the remaining cameras. If no cameras remained on the system then this would be found in the Initialise state and the system would time-out and shut down.

All other errors would cause the system to shut down, but first the error was recorded in the text log which would allow analysis of the cause of the error so the program could be improved to both prevent and handle the error if it occurred again.

Shutdown

The Shutdown state was the final state which ran before terminating the software. This state could be called as a result of an error or a user request from the front panel. Following a shutdown, the RT OS had to be restarted in order for the analysis software to restart. This state cleared the memory references to all images, freeing up the memory locations for other uses and terminated the active camera sessions, before ending the program.

5.4.2 OPC manager

The OPC manager was the simplest of the programs on the PXI, the code is shown in Figure 5.10. The manager loaded all results data from the network variables on the virtual Ethernet then organised the relevant data into new variables which were published as OPC data on the external network.
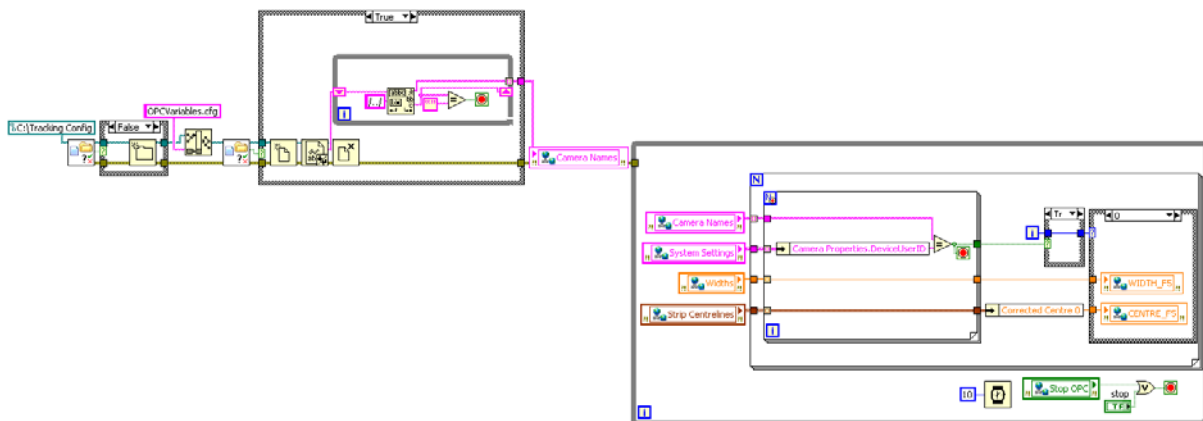
Figure 5.10 : OPC Manager LabVIEW code

This program was the only point of communication for results so had to always be running for data to reach external systems. To achieve this, the executable was set as a service to automatically load as soon Windows XP loaded (it did not require a user to login) and ran in the background with no visible user interface. To set a program up as a service, the Windows Server 2003 Resource Kit Tools were required, and instructions found in [53].

The program operated by assigning a set of variables to each connected camera, which were then transmitted on the network. Variables were allocated for up to seven cameras so additions could easily be managed. For programming simplification, the variables were assigned to cameras named "Scout1" through to "Scout7", in numerical order of roll stands so it was vital that new cameras were correctly named when added to the system. Cameras could be named in the NI Measurement and Automation Explorer (MAX) from the Windows XP desktop.

5.4.3 Windows XP user interface

Main interface

The user interface provided the only method of interacting with the analysis program running in the RT OS. The interface could be used to observe current results and control events in the RT OS, such as saving of images and log files, initiating configuration mode and accessing the ftp server on the RT OS to download images and log files. The interface could either be accessed directly on the PXI in the computer room of the mill, or more commonly would be accessed using the Windows Remote Desktop utility or Remotely Anywhere client from any PC connected to the plant network.

When running, interactions with the user controls were performed in an event-based manner. This means that program functions were only called when the value of the control changes, and allowed a simplified single event instead of individually polling each control manually for a change in value. This structure also very easily facilitated the addition of new functionality if required. The general indicators on the interface screen were updated every program loop by obtaining the values from the network variables. The user interface had four viewing modes: Standard, Camera Detail, Results Detail and Other. They were navigated by a simple tab interface at the top of the screen. Adjacent to the tabs was a current mode indicator, showing the current state of the analysis program. The tabs and mode indicator are shown in Figure 5.11, which is a screenshot of the front panel, displaying the standard interface display.
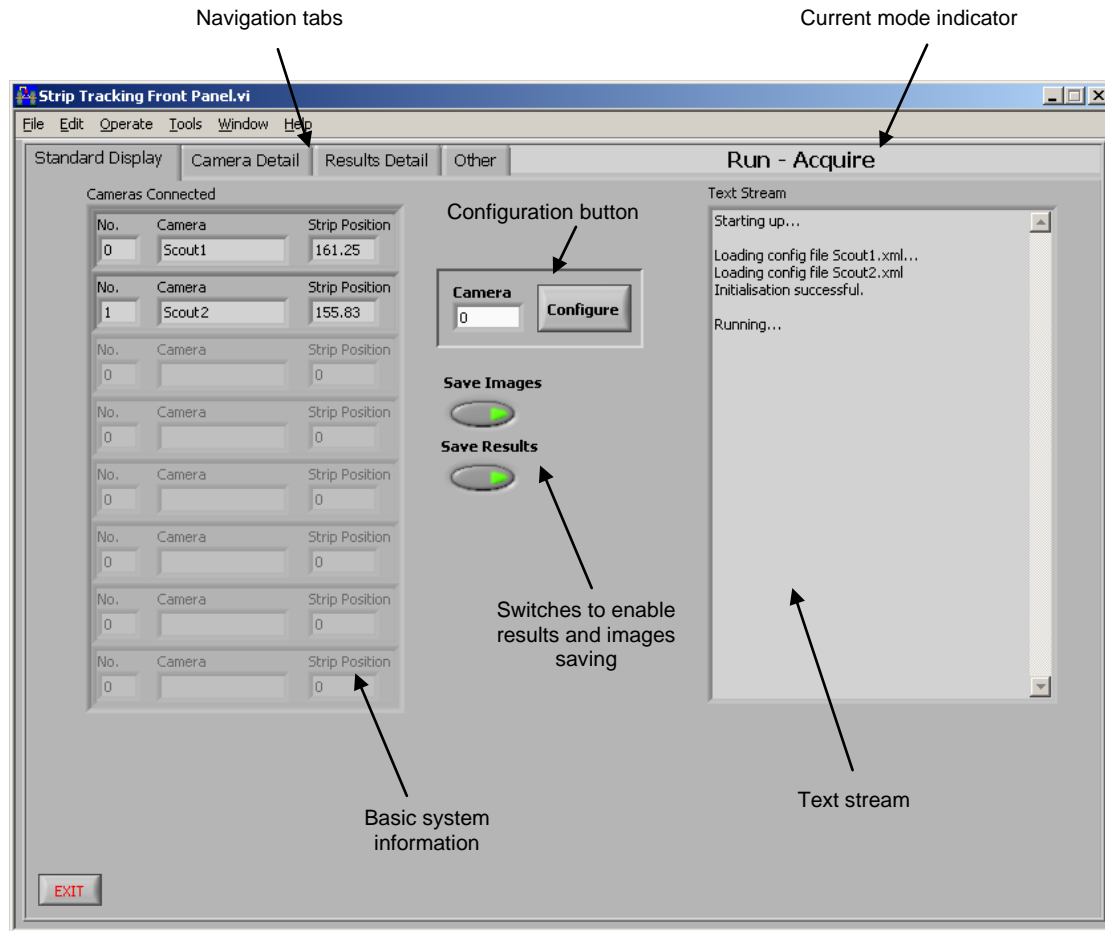
Figure 5.11: User interface: Standard Display

This standard display presented some very basic information on the current operation of the analysis program. The basic system information listed all connected cameras and the current reported centreline position. Two illuminated switches enabled the options to save the recorded camera images and the analysis results. These were not enabled by default to minimise disk usage during long-term running. When pressed, a value of TRUE was set to corresponding network variable which was used in the analysis program. The text stream provided some detailed information on program progress. This could give useful insight into any problems which occurred, showing errors and other information but was not as reliable as the text logs which were saved to the RT OS hard drive every time a session was initiated. This unreliability was due to the method used in accessing updated text information, which could cause new information to be overwritten to the general stream before it had been read by the user interface. The configuration button was used to initiate configuration mode for the index number of the camera specified (the "Cameras connected" panel could be used to find the correct number). When pressed, a value of TRUE was sent to a network variable, which would then be read by the analysis program to interrupt general program running. This occurs

in the "Change Mode?" decision box in Figure 5.9. Additionally, a separate configuration sub-program was launched, opening the Configuration front panel.

Figure 5.12 shows the Camera Detail view and Figure 5.13 shows the Results Detail view. These views provided more detailed information than the standard display. The camera view detailed all the analysis settings for each camera and provided more information about the camera settings. The Results view provided more information from the analysis results, with figures for the centreline Bezier curve lateral positions, and also a width measurement. The numbers reported in the Results view were all logged when data logging was enabled from the standard view.
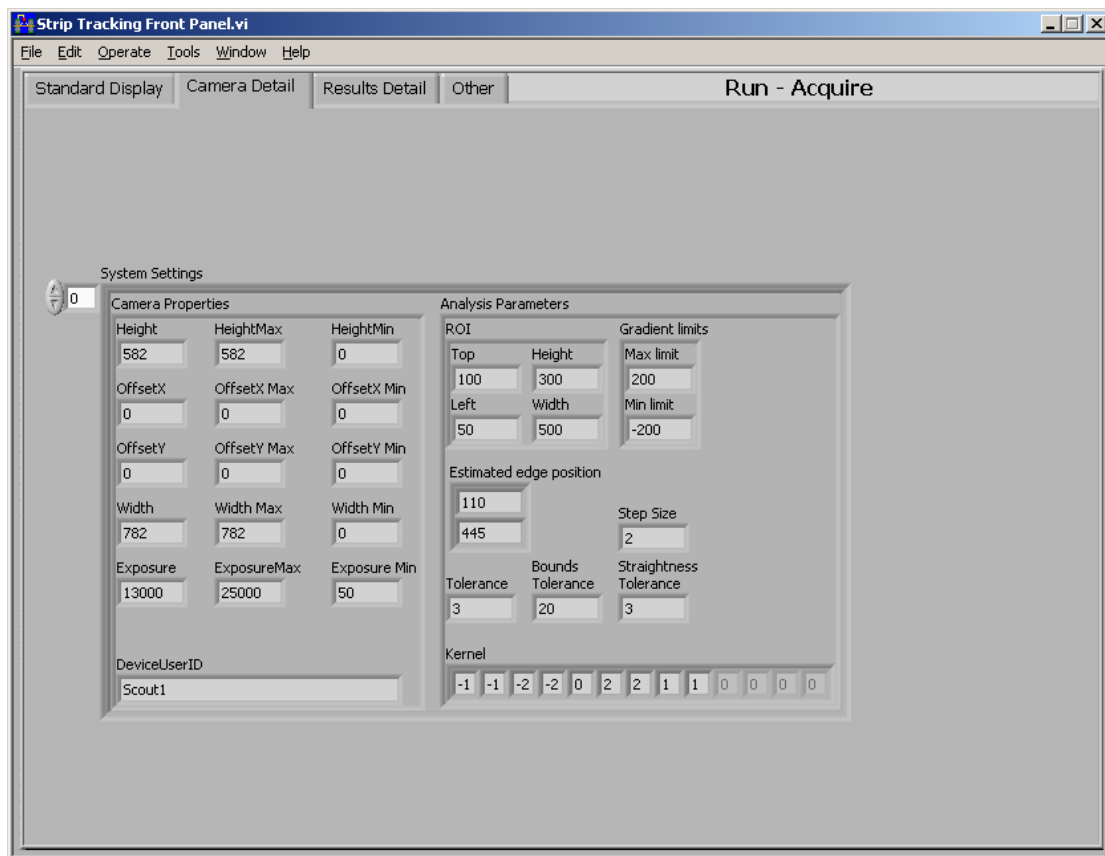
Figure 5.12: User interface: Camera Detail
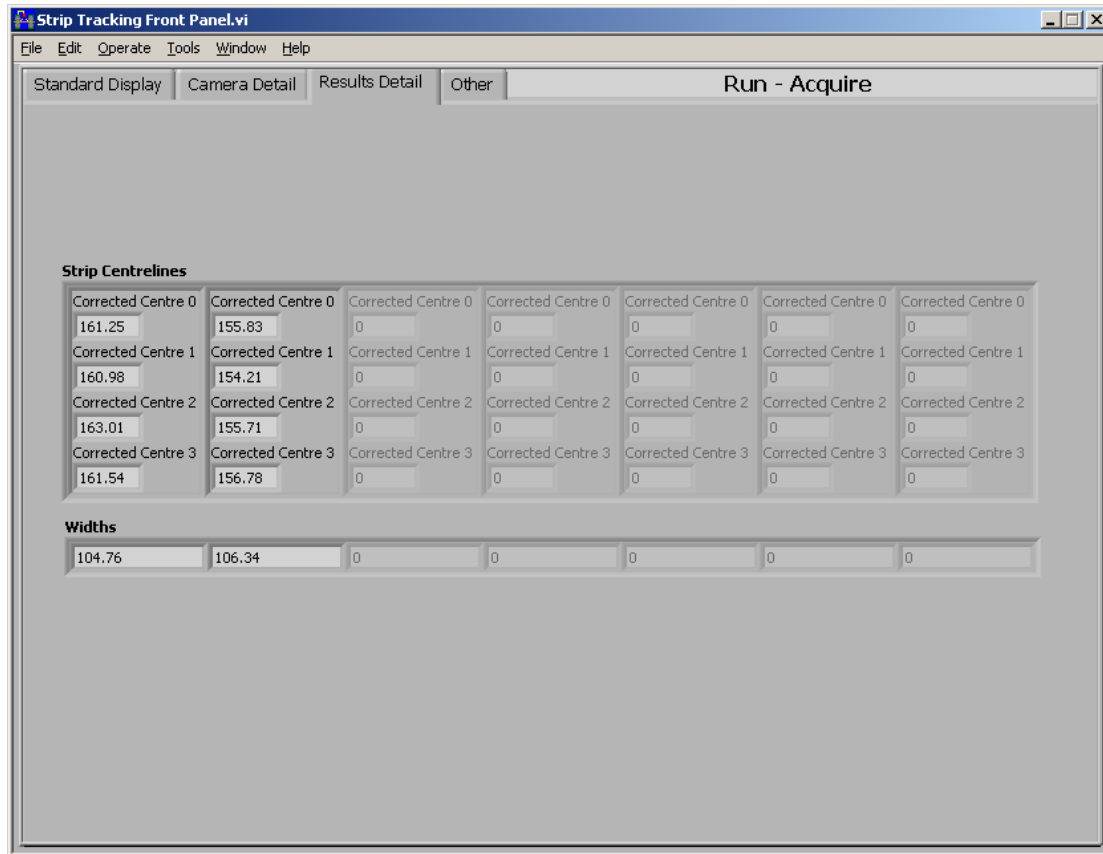
Figure 5.13: User interface: Results Detail

The final view, "Other" is shown in Figure 5.14. This view provided access to other program controls and information not seen in the standard display. The PXI information gave more detailed information about the RT side of the PXI, including network settings and the system state. The execution time indicator showed the time taken for each analysis cycle; the time between measurements, in milliseconds. The error report panel was used to show errors in the interface program (errors in the analysis program were seen in the text stream in the standard view). With the program control buttons the user could force certain occurrences to the various programs. Clear Text Stream and Clear Errors would clear information within the XP program. The Reset Edges button was used to force a reset of edge position estimation to the original values. The two STOP buttons could be used to shut down the analysis program and the OPC manager respectively. These programs had no user interface themselves, so these buttons were the only way to terminate them if desired but they would need to be manually restarted. The Reboot button forced a restart of the RT OS (it would not affect Windows) and was an effective method to restart the analysis program if it had been stopped. The FTP server in the RT OS was used as a direct access to the partitioned hard drive. During operation, log files, images and results files were saved to the hard drive if requested; log

files were automatically saved with every session, results and images were only saved if enabled from the Standard view. The FTP Server access button provided a convenient shortcut to the folders containing these items, although the ftp server could also be accessed directly from any web browser or file explorer window using the IP address.
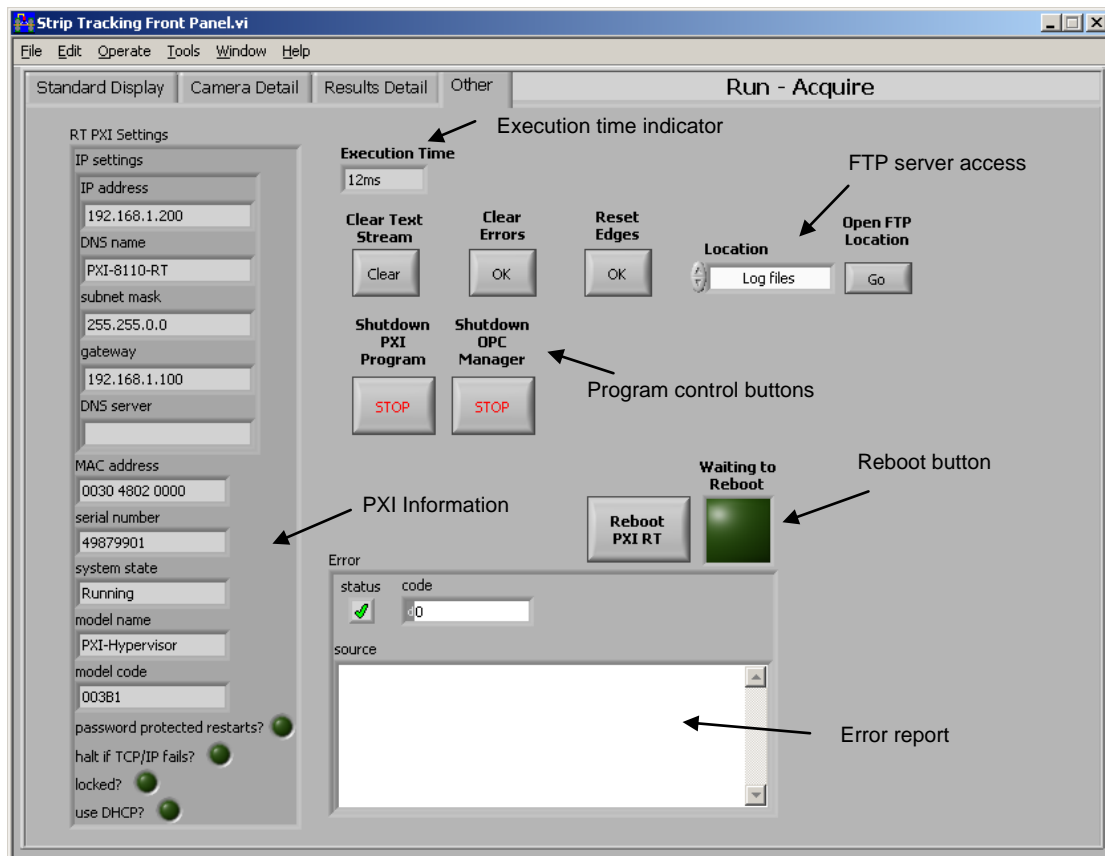
Figure 5.14: User Interface: Other

Configuration interface

When in the Standard view, pressing the Configure button would enter configuration mode in the RT analysis program, and launch the configuration sub-program from XP. Figure 5.15 and Figure 5.16 show the two views of the configuration screen for changing Analysis and Camera settings respectively. As with the main user interface these views were navigable using tabs at the top of the screen. A difference between the main interface and the configuration screen is that these tabs were functional, as opposed to purely aesthetic; changing tabs programmatically changed the running mode in the software and not just the viewable screen. Alongside the tab control was another small analysis program mode indicator, allowing the user to confirm the analysis program had correctly entered configuration mode. If the program had failed to enter configuration mode then the configuration interface had to be closed and re-opened with the main interface button.

Configuration mode would end when the EXIT button was pressed, but would not end if the configuration screen was closed using another method. To the left of the tab control panel was a display of the most recent image.

When the program was initially called from the user interface, maximum, minimum and current parameter values were loaded into the controls, providing an indication of current settings and limiting data entry to be within allowable ranges. This prevented any errors occurring due to specifying values outside allowable limits. After initialisation the program would continue to run until stopped using the exit button. During running the program loaded the most recent image as a string from the network variable, unflatten the data to an image and display it on the screen. Any parameter changes were then sent to the analysis program, which would act on them as required and continue to acquire and send images using the updated settings.
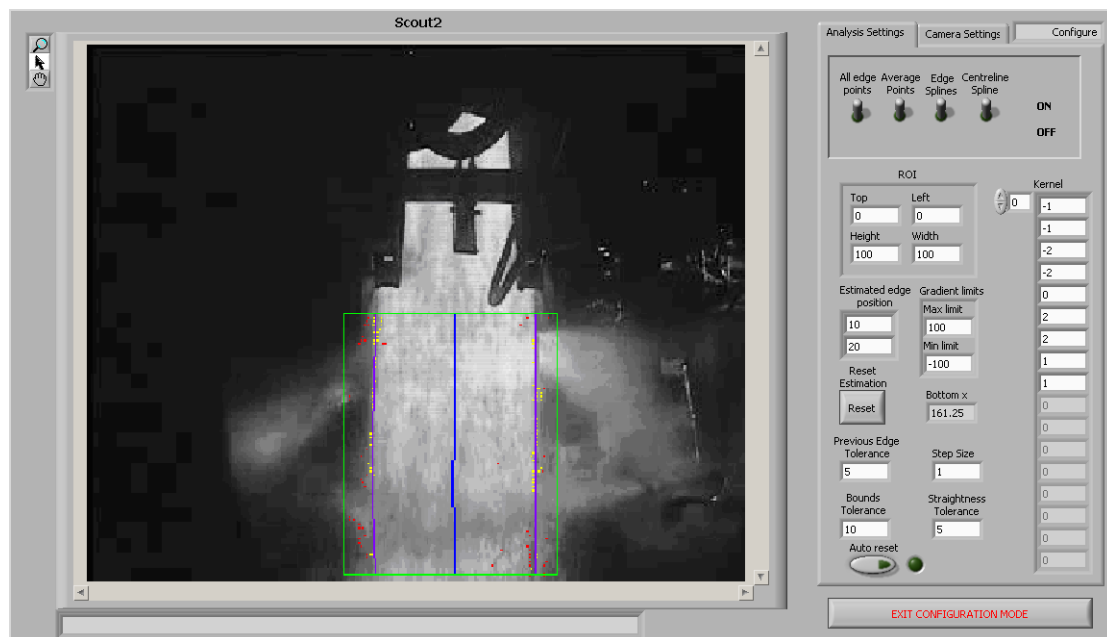
Figure 5.15: Configuration: Analysis Settings

The Analysis view was used to change parameters relating to the image analysis method, detailed in Table 5.2. These were changed using the numeric entry boxes and updated automatically. Additional to these parameters was a reading of the current centre position ("Bottom x") for verification, and a "Reset" button used to reset the edges after changing the estimated position. Additionally, there was an "Auto Reset" illuminated switch which mimicked the main analysis software recovery-reset feature. This reset feature identified when an edge it found was not reasonable and would reset the edge position used for the next predictive estimate to the specified value. This was used when the strip was lost from view,

for example in the inter-strip period or if an obstruction totally obscured the strip. At the top of the analysis panel were toggle switches to change which results overlays were displayed on the current image. These were:

- All Edge Points: Displayed all identified "edges" within the ROI as red dots
- Average Points: Highlighted in yellow those edge points which had been identified as acceptable (within the limits specified by the previous edge location and the previous edge tolerance) which were then used in the analysis
- Edge Splines: Displayed the calculated Bezier curves defining the strip edges in purple.
- Centreline Spline: Displayed resulting average centreline Bezier curve in blue

Additional to these options, the ROI was always displayed when in the Analysis Settings view as a green rectangle. These overlaid results provided the only method of feedback when setting up the system. They were an invaluable tool enabling the user to watch the analysis process as it happened to ensure that operation was as desired

The Camera Settings view was used to change camera parameters (the captured image size and the exposure time), allowing optimisation of acquisition time and image quality.

Figure 5.16: Configure: Camera Settings

6 Evaluation and Improvement of Original Design

6.1 Introduction

The measurement system described in Chapter 5 was installed on the mill in Port Talbot and left to run for four months before undergoing a critical evaluation of its performance and to highlight any modifications and improvements required. This evaluation found problems with both the hardware and software parts of the system. The process of this evaluation and the resulting improvements are detailed in the following sub-sections.

6.2 Equipment suitability

One of the key points to the choice of system components was their suitability to the task. In particular, how the equipment would survive in the harsh environment present in the hot mill. The equipment had to be able to survive and be reliable if the system was to be effective over a long period of time.

6.2.1 Cameras and enclosures

The cameras and enclosures were exposed to the most aggressive environment of all the system components, located where there is exposure to both high temperature and large amounts of water. The survival of the cameras was varied.

The camera mounted on the second stand was very quickly found to have been destroyed, shown in Figure 6.1. This occurred due to water leaking into the back of the enclosure past the cable glands. Although the enclosure has an IP66 rating, the design of the glands was such that the cable had to be an exact fit in order to be sufficiently water tight, and this was not the case. The result of this was the enclosure filling with water and the camera was damaged beyond repair.

Figure 6.1 : Destroyed camera from Stand 2

In contrast to the survival of the camera on Stand 2, the camera on Stand 1 lasted well and showed no signs of damage. This is thought to be due to extra waterproofing being made on the Stand 1 enclosure at the time of installation.

Regarding the operation of the enclosures, the fact that the Stand 1 camera lasted suggested that, with adequate extra waterproofing around the cable entry points, the enclosures were suitable for protecting the cameras from damage, including thermal damage from the heat of the strip. The other functional task of the enclosures was to maintain a clear view for the cameras to see the strip through, using the air barrier to prevent the build up of debris. It was noticed in some of the acquired images that steam was appearing on the window, causing some blurring of the images. Additionally, when inspected during a maintenance stop, the view screen of the enclosure was found to have significant debris build up on the outside. This could potentially cause a major problem if the camera view was prevented from seeing the strip and suggested the air-barrier was not working as well as initially expected.

6.2.2 Computer

The PXI unit was housed in a computer room with an environment which was not likely to present a hazard. This meant the survival of the computer was not expected to be a major concern. Instead, the suitability issue was whether the computer was performing as expected.

With only a single camera running for the duration of the initial trial the computer was only evaluated in a limited capacity. During the initial setup and installation phase of the system, some problems were found which caused difficulties in the system configuration. These problems were mostly due to unexpected bugs thought to be within the NI system components and due to the nature of the Hypervisor system. Some of the problems encountered with the behaviour of the Hypervisor system existed because it was new technology so had not been completely refined. These problems were typically with communication across the virtual Ethernet link between Windows XP and the RT OS. Often a loss of communication would require a total system re-start, and the problems with the core computer system made diagnosis and correction of issues with the measurement system difficult or nearly impossible at times. Once the system was in place and running, however, it has shown to be stable in operation and act as designed. The conclusion was made that in principle the computer system could perform the task as designed but due to the instability and unreliability during configuration it was decided to convert the system to a purely Windows XP configuration. This configuration could be used to fully evaluate the system and

also evaluate whether the Hypervisor configuration provided a faster analysis or if an XP system was also suitable.

6.2.3 Networking

The network (specifically the dedicated GigE network) section of the system was used to transmit the images from the cameras to the PXI. Any network problems would prevent the system acquiring images and stop it from functioning.

Upon initial configuration of the system once it was fully installed, a network problem became immediately apparent. Errors were found within the analysis software saying that a connection could not be made to the cameras due to the data packet size. The packet size refers to the amount of data transmitted in each frame across the network. It was found that the specified packet size, suitable for GigE transmission, was too large and the camera only functioned correctly once the packet size was reduced to standard Fast-Ethernet (100MBps) size. This behaviour suggested that some point of the network was not suitable for GigE transmission. The cause of this was thought to be the auto-negotiation of the network components. This would have to be rectified manually to ensure every network switch was configured for GigE transmission.

Another problem found was the camera on Stand 1 would periodically lose connection to the PXI. It was thought that this was a network-related problem, i.e. the camera occasionally lost connection to the network. This was an intermittent problem which would rectify itself in a short period of time but could cause the system to time-out whilst looking for the camera. It was also possible that this problem was caused by an intermittent power supply and was not a network issue. To work around this, it was decided that the time-out period of the system while looking for cameras be increased or removed completely, but the fundamental issue would also require resolution.

One final minor issue identified was the length of the connecting cable from the camera to the junction box. This cable was too short and therefore tight. It was thought that this contributed to the camera connection dropping out.

6.3 Quality of acquired images

The quality of the images acquired by the cameras was very important in the ability of the software to analyse the data. Figure 6.2 shows a range of images taken from the camera mounted on Stand 1 and show the problems found with the images.

	A Head of strip, no cooling water. Image is very bright. Blurring of strip image is due to steam on enclosure window.
	B Cooling water begins. Image is darker. Image still slightly blurred because of steam.
	C Significant amount of cooling water. Image is very dark. Blurring effect is less because of reduced brightness.
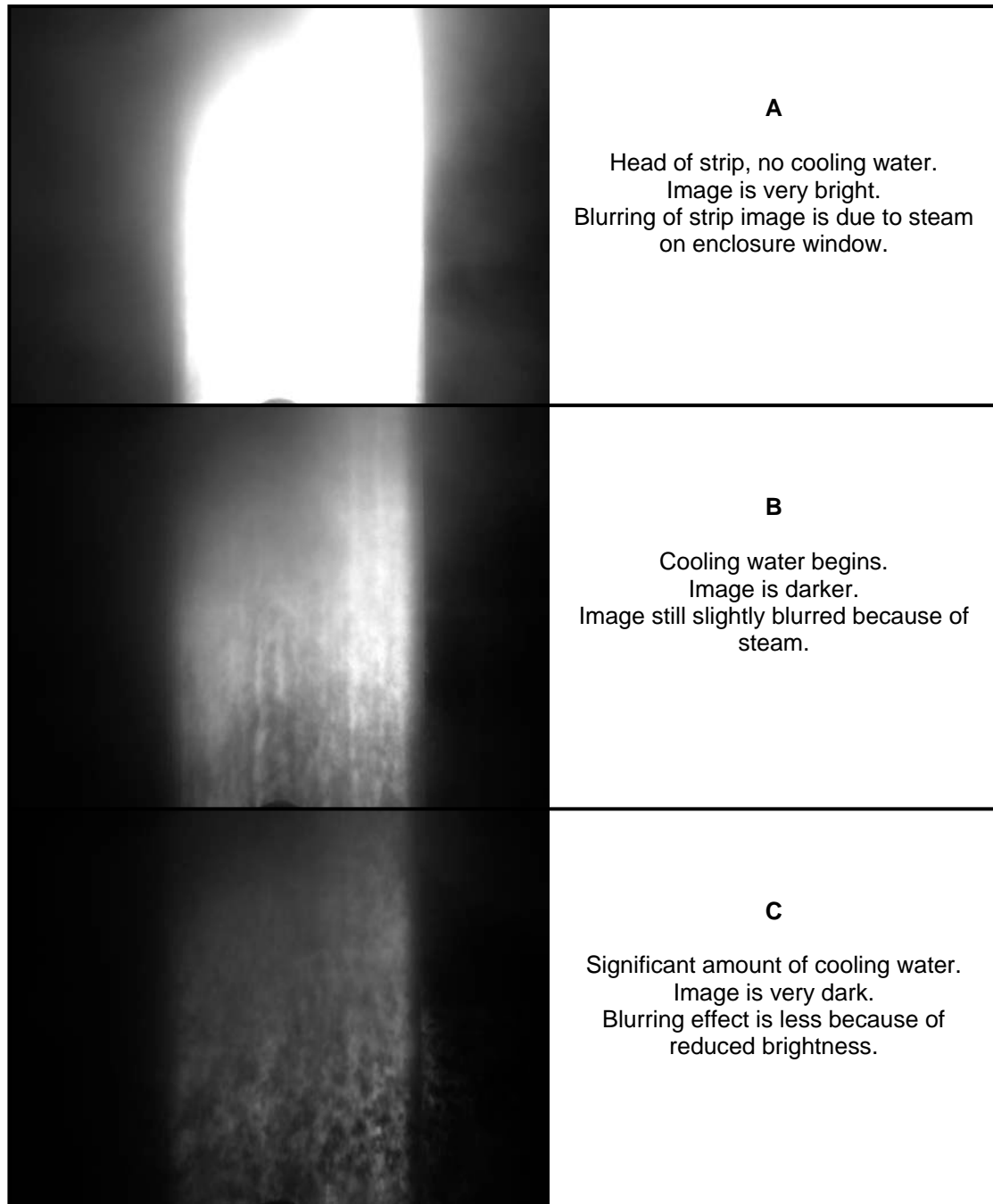
Figure 6.2: Images taken from Stand 1 camera

The recorded images show a few minor problems which hinder analysis but do not cause major problems.

The first issue is the variation in brightness which was not foreseen in the original trial images used to initially create the image analysis software because of the auto-iris used on the original trial camera. This brightness variation occurred when the cooling water increased in intensity, cooling and darkening the strip. This could be relatively easily be overcome by introducing a software component to adjust the camera exposure to maintain a relatively even brightness in all images. One thing to note is that in the original installation the fixed camera

iris was set too small so the image brightness could not be increased to sufficiently see the darkest strips. The camera iris had to be reset to a wider opening to allow more flexibility in the software exposure settings.

The second problem was a small amount of blurring on the images, apparently due to the build up of steam on the view screen. At this stage this had not caused a large problem but it did signify that the problem could worsen and cause further and more significant issues with the analysis. On top of this, the accumulation of debris on the screen could cause similar problems such as obscured and darkened patches on the image. It was thought that the darkening of the top-left corner of the images was due to debris accumulation. These two problems were essentially due to the same cause, that the air barrier on the view screen did not operate as effectively as originally thought. It was recommended that the cleaning of the screens on the enclosure become a part of standard maintenance and carried out whenever possible.

The final problem was the size of the viewable area itself. When the original system was specified a 12mm lens was chosen under the advice of an external supplier to gain the viewable area desired. However, after installation, upon inspection of the acquired images it became apparent that the visible strip width was slightly too narrow. For the wider strips, the strip almost entirely filled the image area. It was desired that some areas of the mill beyond the strip edges would be visible to use as points of reference. By replacing the lens with a wider lens, such as an 8mm lens, more area would come into view.

Besides the above mentioned points, the quality of the images was very good. With the required alterations made, especially to compensate for the brightness variation, it was expected that the resulting images would be of very good quality for the analysis software.

6.4   Operation of image analysis software

Full evaluation of the effectiveness of the analysis software could not be completed because of the problems identified above with the images. However, the functional analysis of the method had already previously been completed in an earlier study (Chapter 4) so only points relating to the specifics of this installation are of immediate concern.

The main problem preventing a full evaluation was the large variations in brightness of the images, particularly the very dark images. It was thought that once the camera iris set point had been widened, the software could then be updated to manage to exposure time to ensure the image brightness was suitable.

One aspect which was overlooked during the initial development of the software was the variation in width of the strip during rolling. The analysis software operated around a given set point as an estimate of where the strip would be. This method worked very well when strip width was relatively uniform, however with the large variations that were used in practice, the method was not as effective. A modification would be required to the software method which handled the overall position estimation in order to cope with all possible strip widths.

A significant but simple problem was found with the naming of cameras and saving of configuration files. The cameras would initialise successfully and create a configuration file with the correct name, but after changing configuration settings, the file was saved with a blank name, so when the system was re-started, the original configuration file was loaded into the camera and not the saved settings. This bug effectively prevented the saving of camera and analysis settings and was due to the method used for determining the camera name in software when saving the configuration file.

Additional to these points, a number of very minor possible improvements to the user interface were noted. These were mainly things such as button positions, labelling and general usability. These are not listed in detail because they did not represent significant problems.

The problems found with the analysis software were only minor and relatively simple to implement solutions. In general the software running on the PXI functioned very well. General system architecture and communication, such as logging data in the IBA logger over OPC and remote access to the system all operated as desired.

7 Final Measurement System Configuration

Following the evaluation of the system in Chapter 6, a number of improvements were implemented to both the hardware and software components of the system. These improvements in the "final" configuration of the system are detailed in this chapter.

7.1 Hardware

After the rapid destruction of the camera originally mounted on Stand 2, a priority was to improve the water proofing of the enclosures. Upon inspection, the cause of water entry became apparent as the cable glands in the back of the enclosure, sealing around the power and GigE cables for the camera. The original glands on the enclosure were for larger diameter cables than the ones installed, and therefore did not provide adequate sealing. New cable glands more suitable to the cables in use were sourced and the level of water protection hence found to be adequate.

The short cable connecting the cameras to the local termination box was replaced with a more suitable length, removing the tension in the cable and the iris of the camera adjusted to brighten the image.

The camera lens on stand 2 was left as a 12mm lens for some time after the majority of the other hardware modifications were made, but was eventually changed to an 8mm lens allowing a wider field of view to allow both strip edges to be clearly visible at all widths.

One undesired major change to the system was the removal of the Stand 1 camera due to maintenance issues at a major stop on the mill and subsequent rolling issues on Stand 1. This left the system with a single camera on Stand 2, which was suitable for evaluation of the image analysis method but limited other conclusions that could be drawn.

Note that throughout this chapter, logged data files and screenshots are frequently referred to and these often show a camera named "Stand6", which appears to contradict the hardware setup specified here. This camera name was used to reflect the naming of the stands in the finishing mill in Port Talbot, which are numbered F5 to F11 for historical reasons. The naming of the camera was hence used to comply with the local names of the stands to prevent confusion when used by staff in the steelworks.

7.2 Software

7.2.1 Computer configuration

The largest single change to the software configuration in the final measurement system design was from using a Hypervisor controlled split RT-XP system to a solely Windows XP system. This change was made because of a number of issues found with the Hypervisor system, particularly with communication between the XP and RT sides of the system which created a lot of instability and unreliability. This change also increased the transparency in the programming, simplifying data communication and allowing for a single piece of analysis, configuration and OPC communication software. The final system configuration is shown in Figure 7.1.
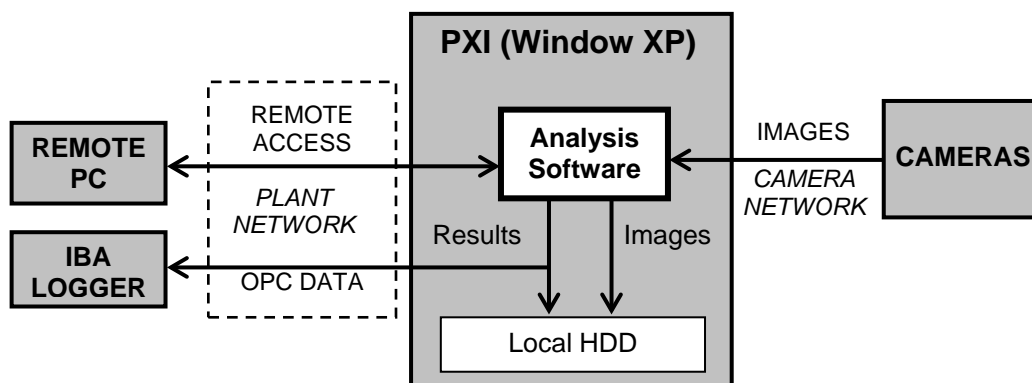
Figure 7.1: Final measurement system configuration

An added benefit to this configuration change was to allow the ability to view the camera image and analysis in process even when not in configuration mode, providing access to instant visual feedback on analysis performance.

Access to the system was normally achieved using remote desktop across the plant network, although was still possible at the PXI in the computer room using local peripherals.

A minor configuration change was also made to increase flexibility by removing the requirement for the cameras to be named in order of stand "Scout1" to "Scout 7". The new configuration allowed any camera name to be used and then each camera mapped to the correct OPC data items in software. This implementation is explained in more detail in section 7.2.2.

7.2.2 Programming

The functional side of the software was not modified significantly with the change to a fully XP system. The general flow of software operation remained significantly similar to the flow described in Chapter 5, but with the functionality of all previous software components (RT analysis software, XP user interface including configuration and XP OPC data manager) combined into a single piece of software. The major changes were:

- Amalgamation of software components
- Removal of strict camera naming requirements
- Addition of "Width Estimate" element to handle variable strip widths

The program retained the original state machine architecture but slightly modified. The final program flow is shown in Figure 7.2. Note that this diagram has been simplified for clarity; between each state it was possible to either enter error state if a software error had occurred or shutdown is a program shutdown request had occurred. This is shown in the separate sub-diagram for completeness.
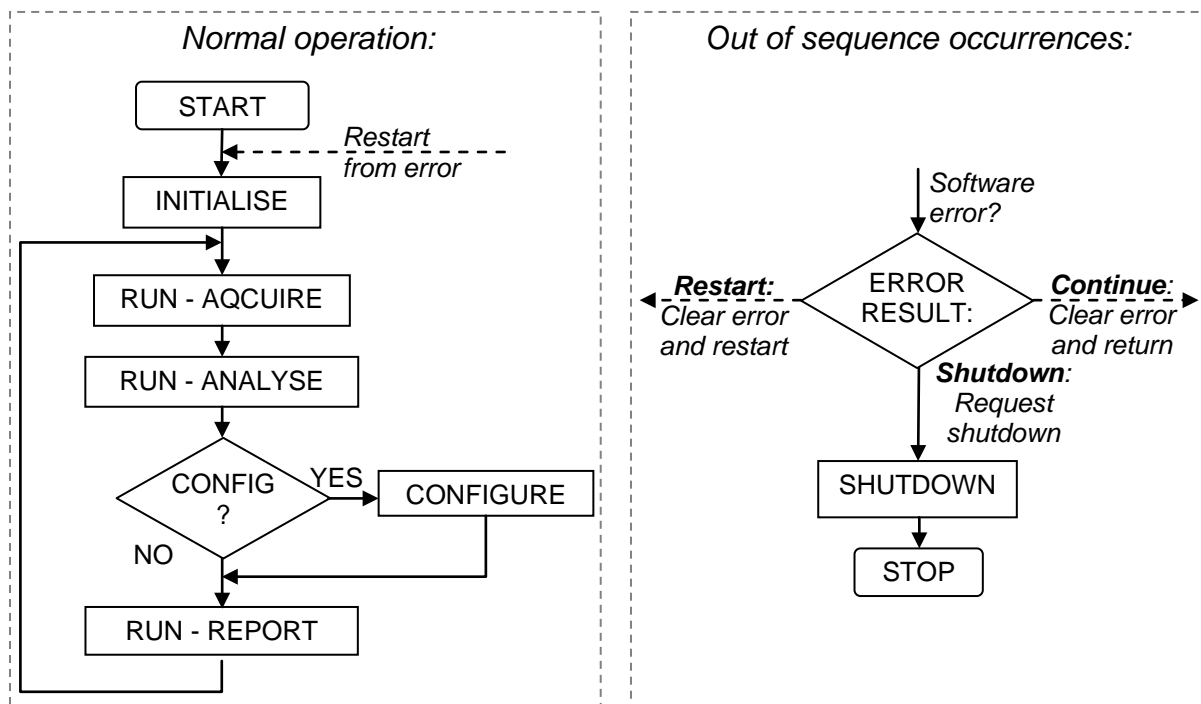
Figure 7.2: Program flow in final measurement system

The main change in normal program operation compared the original software structure (Figure 5.9) is that the "Configuration" mode, if requested, would enter between "Analyse" and "Report" instead of as a completely separate section. This allowed the program to continue to output results when the software was in configuration mode.

Figure 7.3 shows the LabVIEW code of the main program state machine. The left and right highlighted sections are the "Start" and "Stop" processes which operated outside normal program flow.
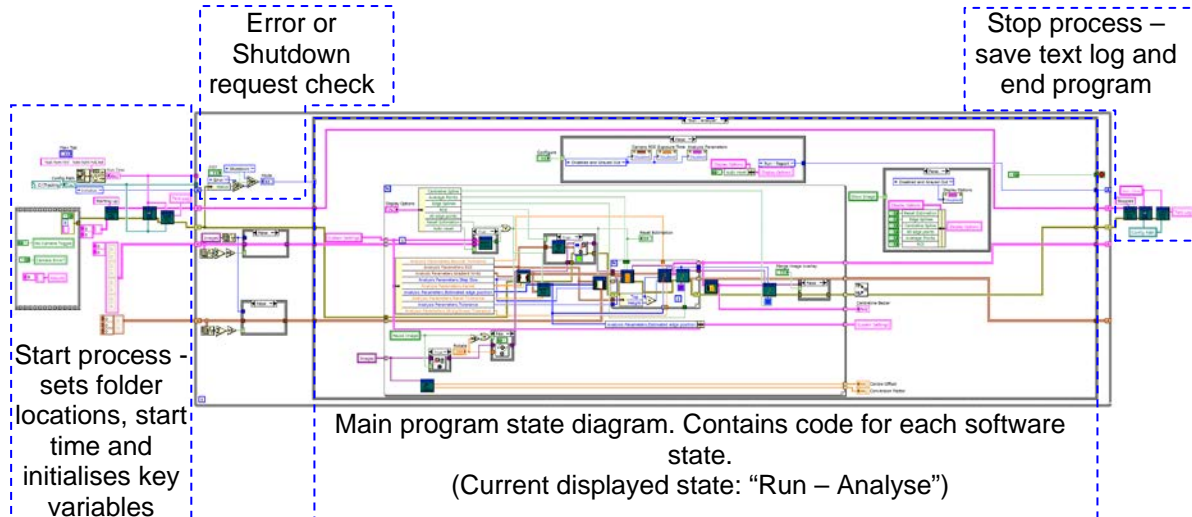
Figure 7.3: Main program code

The "Start" process (left) initialised some key variables, such as setting the starting time of the software and folder location for saved files and initiating the text log. The "Stop" process simply updated and saved the text log with a final "Stopped" message.

The text log was a stream of text which ran throughout the program, updating as key activities occurred, such as analysis configuration and error occurrences. The log entries would typically contain the time and date of entry and a short description of the occurrence. In the case of errors, the LabVIEW generated error along with a summary and response action was entered. The log was saved to a file on the local hard drive during operation and could be accessed using a text editor. The contents of the log for the current program operation were also periodically displayed to the user interface screen. An example text log is shown in the following:

```
15/06/2011 10:11:56    Starting up
15/06/2011 10:12:11    1 cameras found.
                       Initialising...
15/06/2011 10:12:41    Loading config file  C:\Tracking\Stand6.xml
15/06/2011 10:12:41    Error found
                       Initialisation failed.
15/06/2011 10:12:42    Error -1074360308 occurred at IMAQdx Open Camera.vi
                       Possible reason(s):
                       NI-IMAQdx: (Hex 0xBFF6900C) Camera has been removed.
```

```
15/06/2011 10:12:42    Camera missing.
                       Re-initialising
15/06/2011 10:12:50    No cameras found
                       Retrying...
15/06/2011 10:14:05    1 cameras found.
                       Initialising...
15/06/2011 10:20:52    Loading config file  C:\Tracking\Stand6.xml
15/06/2011 10:23:28    Initialisation successful.
                       Running
15/06/2011 10:43:14    Entering configuration mode...
15/06/2011 10:45:40    Exiting configuration mode...
                       Saving Settings
15/06/2011 10:45:40    Saving config file  C:\Tracking\Stand6.xml
15/06/2011 11:10:44    Shutting Down...
15/06/2011 11:10:44    Stopped
```

The text log above is a typical example of the program operation and the information that was saved and displayed. The log shows that the program was started at 10:11.56, and during initialisation one camera (named "Stand6") was found, however communication to the camera was lost before initialisation was completed, most likely due to a GigE network error. The software re-entered initialisation mode at 10:12.42 but could not find any cameras until 10:14.05, when Stand6 was found again. This time initialisation was successful and the program began running normally. At 10:43.14 a request from the user placed the software into configuration mode, until 10:45.40 when configuration mode was left, and the new camera settings saved. The software continued to run uninterrupted until 11:10.44 when the user requested the software to shutdown.

These text logs provided a valuable tool in analysing program operation particularly when developing the error handling process of the software by identifying which errors occurred and ensuring the software could adequately cope when they arose.

The following sub-sections detail the programming and software methods in the core software states.

Initialise

The initialisation state was used to prepare the system for running by evaluating all connected cameras on the system, loading or creating settings files and memory references for them and setting each camera into "Grab" acquisition mode, continuously acquiring images so one was available at all times if requested. Following successful initialisation, the software would then enter "Run" mode. If there were no connected cameras, then the state would indefinitely search until either a camera was found or a user intervened and stopped the program. The initialise process followed the process shown in Figure 7.4. As with the description flow chart

of the complete program, the error and shutdown checks are not included for clarity. In operation, these were checked after the initialisation cycle had been completed; either before entering Run mode or before re-checking for connected cameras. Figure 7.5 shows the main portion of the code for the initialisation.
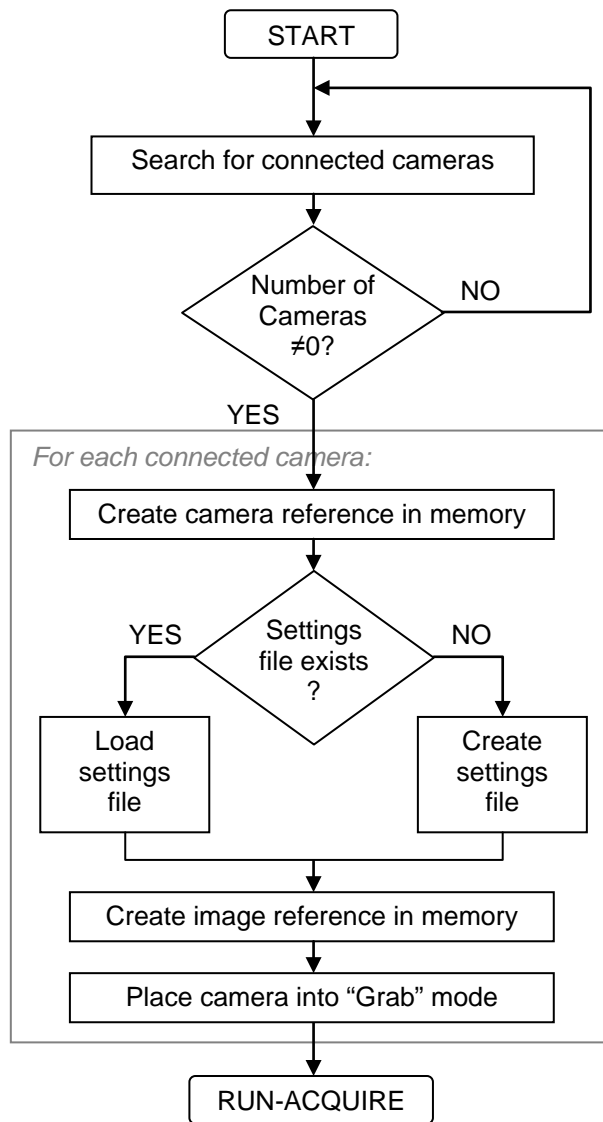
Figure 7.4: Initialise flow diagram
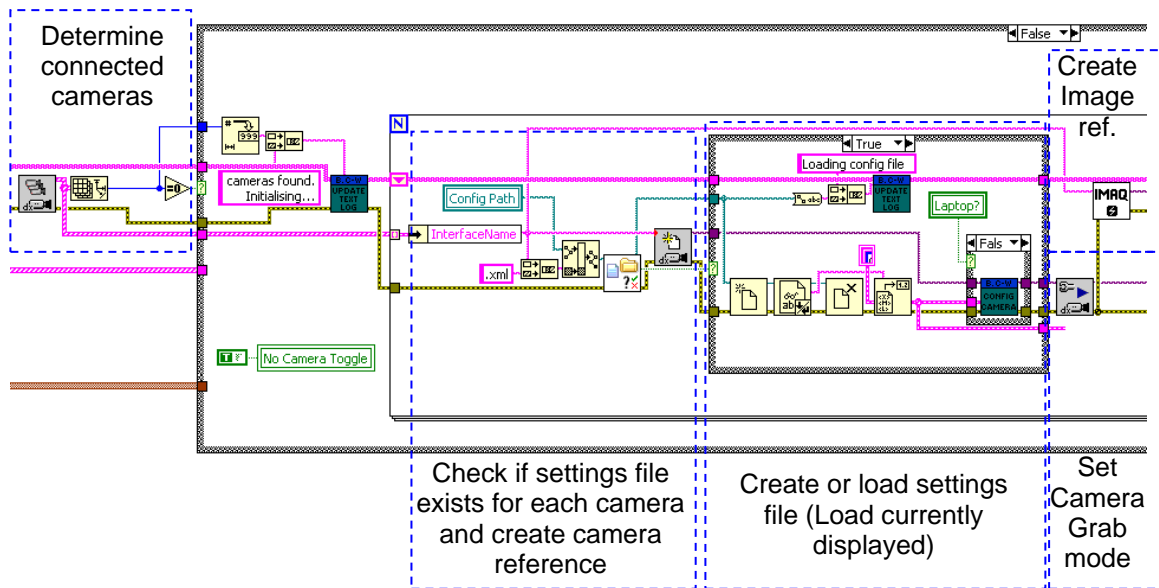
Figure 7.5: Initialisation code

Run – Acquire

The Acquire state had the sole task of grabbing an image from each camera and placing these into the preset memory locations assigned during initialisation. The images were then available at any point in the software by using the memory location references. Following grabbing the camera images, the program would move to the Analysis state. The flow for this state is shown in Figure 7.6 and the operational code in Figure 7.7.
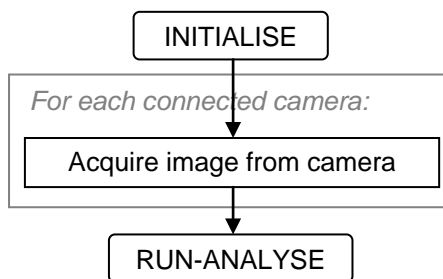
Figure 7.6: Acquire flow diagram
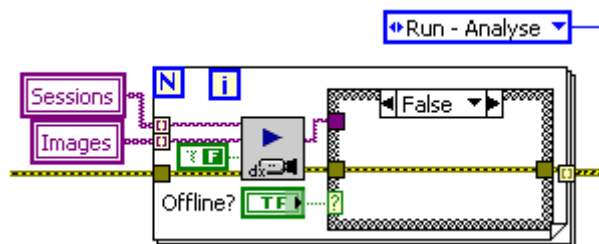
Figure 7.7: Acquire program code

124

Run – Analyse

The analysis state was the core part of the measurement system, performing the image analysis described in Chapter 4 to determine the strip centreline position. The diagram in Figure 7.8 shows the core functional flow of the state, and Figure 7.9 shows the analysis code at the top level.
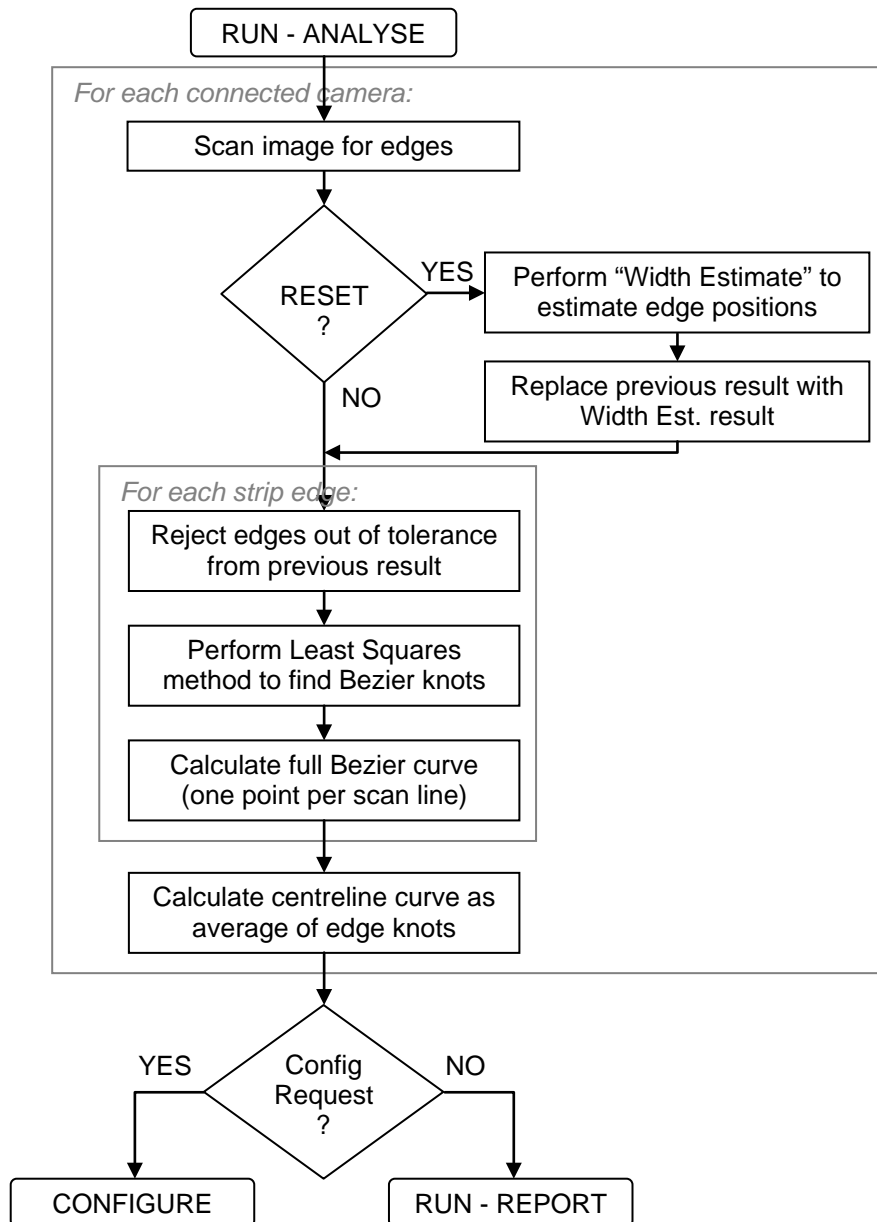
Figure 7.8: Analysis flow diagram

The first stage in the process was to scan the length of the image with a series of horizontal lines, at increments set in the Configuration process. Edges (significant transitions between light and dark) along each search line were then determined and a check performed to see if the estimate of edge position (used for the edge rejection process) should be reset. If a reset

125

was required then the Width Estimate method was performed to find an approximate location of each strip edge location. Next, for both of the strip edges, the edge points found were accepted or rejected if they were in or out of a certain distance from the previous result. The least squares method was then used on the accepted edge points to find the four Bezier knots. Using the knots, the full Bezier curve was evaluated and output as a set of points for each search line. This curve output was used as the result to reject or accept edges in the next measurement. Finally, the centreline Bezier curve knots were calculated as the average of the two strip edge curve knots.

The next state the program would enter would normally be Report, unless there was a configuration request from the user, in which case the program would step to Configure mode.
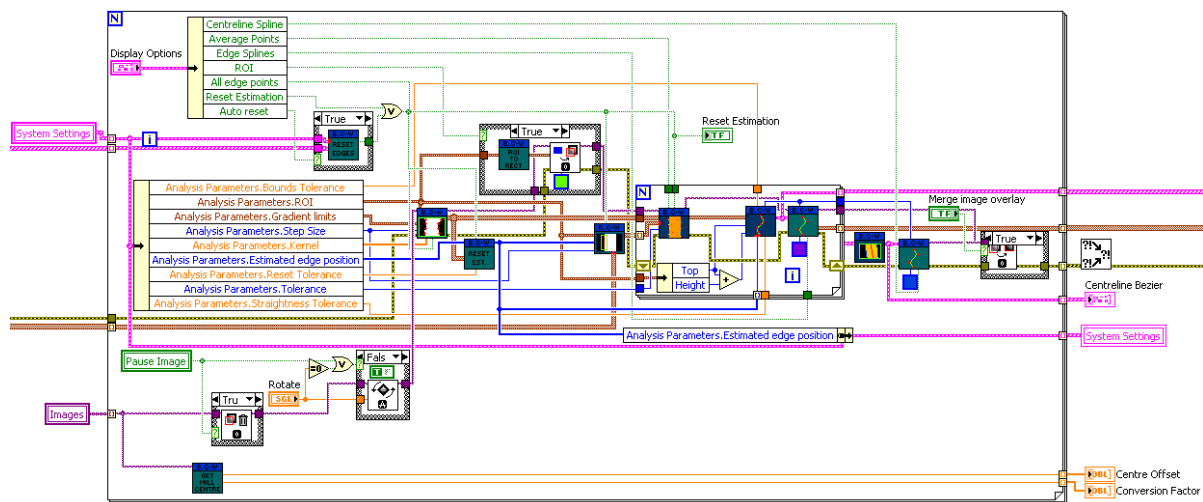
Figure 7.9: Analysis program code

The program flow as shown in Figure 7.8 and the description above cover the core functionality of the analysis state. The following subsections detail a few functional areas not previously explained and also a few minor sub functions not included in the core process flow.

Reset and width estimate

In certain circumstances, it was necessary to reset the strip edge position estimation that was used to determine whether a found edge point was to be rejected. This reset would be necessary if it was deemed that the current measurement of edge position was incorrect. During general operation, the reset could either occur automatically or from a user input. The user input reset would generally only be used during configuration and system setup. The automatic reset could optionally be disabled whilst in configuration mode.

The code for the automatic reset is shown in Figure 7.10 and the reset conditions that were programmed were:

- If a strip edge measurement was too close to the bounds tolerance.
- If the measured width was significantly larger than the existing width estimate.

The first case would typically enforce the bounds tolerance, which was used to define the range from the expected location that the strip could be in. This prevented steam and other noise outside the reasonable location of the strip from being seen as a measurement. The second case would occur if one or more strip edges were lost and the measured width became a lot narrower than the expected width. This reset condition was designed to occur between strips and provide a trigger to re-estimate the expected width and location of the strip, but could also occur if a large amount of noise obscured one edge of the strip and a measurement was instead made somewhere within the strip bounds.
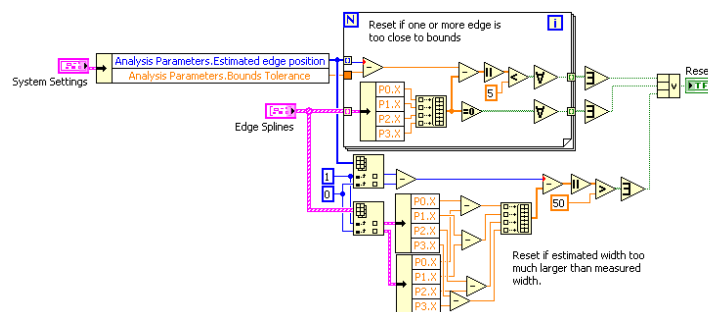
Figure 7.10: Automatic reset code

These two reset conditions proved to greatly increase the reliability and robustness of the measurement software, and also to provide an indicator when a measurement was not trusted.

Following a reset condition, three things would be triggered:
- The estimated location of strip edges was reset using the "Width Estimation" method described below.
- The previous measurement result was replaced by the new estimated strip location.
- The rejection tolerance was widened by a factor of five to account for the increased uncertainty in strip position.

The width estimation method was included following an inflexibility of the software to cope with changing strip widths identified in Chapter 6. The width estimation analysed all the edge points found in the image, then identified the maximum (rightmost) and minimum (leftmost) edges for each scan line. The modal averages of the sets of minimum and maximum edges were then calculated to find an approximation of the location of the strip edges The code for the width estimation is shown in Figure 7.11. These new edge estimates were then used for

127

the estimation of strip position and widths for bounding and for the immediate next measurement for edge rejection. The reasoning behind the method was that in general, the most common values for maximum and minimum edges for the entire strip would be the strip edges as the noise from steam and spray would be more randomly distributed.

This reset and edge estimation method also would be triggered at the beginning of analysis to provide the initial estimate of edge position for the predictive element of the image analysis method. This proved to be particularly effective simply because there would typically be little or no cooling water at the head of the strip so the more approximate method was sufficient.
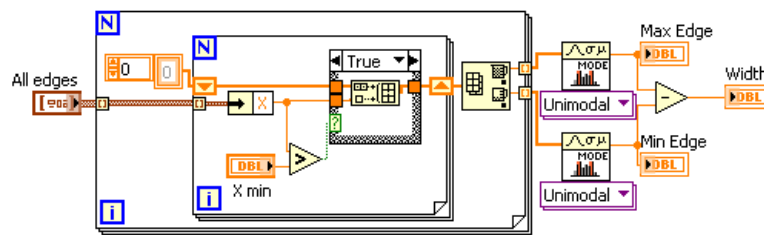
Figure 7.11: Width estimation code

Rotate

Following one maintenance stop where work was undertaken on the camera enclosure, the camera was reinstalled at an angle to the strip. To overcome this problem a "Rotate" option was included in the analysis software to rotate the incoming image be a fixed angle to allow analysis to take place. Due to time constraints on the development of the system, the rotate function was added in a very simple fashion and would rotate the images from all cameras by the same amount if multiple cameras were connected to the system. Additionally, the rotation angle was not included in the system settings saved to the PXI hard drive, therefore would not be loaded when the program was started up.

Mill centre reference

Included in the software was the ability to have a mill centreline reference as a zero point for the strip position. This functionality was included by adding the fixed offset to the results. Due to development time constraints the calculation of mill centreline was not completed, but instead a null function was used outputting a zero value for offset, therefore using raw pixel offset values for strip position measurements. The function remained in the software to support further development.

It was envisaged that a mill centre offset would be automatically periodically calculated using a further image analysis method to identify a fixed point on the mill. This would allow the

software to automatically compensate for any movements in camera position due to vibration or physical knocks.

Display functions

In addition to the core analysis tasks, the analyse state also performed some actions affecting the user interface. The optional image display and results overlays (ROI, Edge points, Bezier curves) were all performed in this state during the analysis. By disabling overlays and image displays when not required, the rate of analysis would be improved.

Other aesthetic functions performed here were disabling and greying out the configuration and image overlay control on the front panel when not in configuration mode and when the image was not being displayed. These tasks were not functional in the analysis and measurement task but did improve the interface and usability of the software.

Run – Report

The report state handled all aspects of outputting results and logs and saving files as well as the majority of user interface requests. The code for the report state is shown in Figure 7.12. Unlike the other states, the report state did not follow a logical flow so no flow diagram is presented here, instead program operations are detailed.
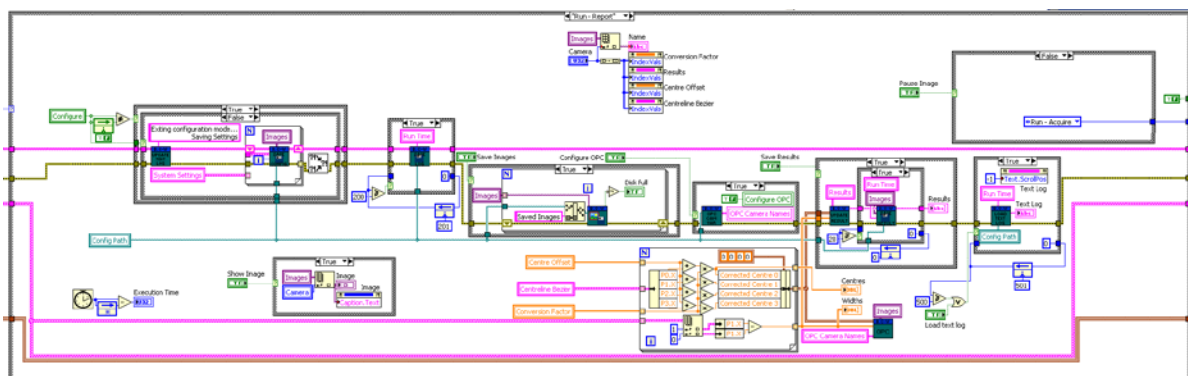
Figure 7.12: Report program code

Output OPC data

The main functional task of the report state was to manage the measurement results from the analysis process. The lateral (x-coordinate) component of the centreline Bezier curve knots was adjusted by the resolution factor and centreline offset amount to convert the results to a distance value relative to the mill centreline. Note that as discussed previously the conversion factor and centreline offset were not implemented, so null values for these were used instead, resulting in the software outputting raw pixel values relative to the image frame. The results were then sent to the OPC manager function, shown in Figure 7.13. The OPC manager would then match up the output data to the correct network variables as set in the OPC configuration

manager. The network variables were automatically published as OPC data by the NI Variable Engine so the results were then available to other systems on the network. In addition to publishing the results in the OPC variables, they were displayed on the user interface at this point.
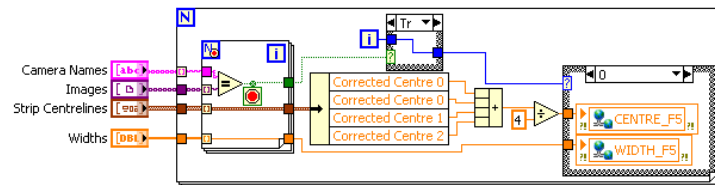
Figure 7.13: OPC Data management

The report section had a heavy interaction with the user interface, the actions which triggered certain events within the report state are discussed in more detail in section 7.2.3. The programming operation of the various actions are detailed in the following sub sections.

OPC management configuration tool

The OPC configuration manager was used to set which camera name was on which stand so the results could be matched to the correct OPC variable. The stand matching was made available to the software and also saved in a configuration file to the local hard drive so the same configuration would be loaded each time the program was run. The configuration tool loaded as a separate sub-program when requested by the user. More detail about the user interface for the tool is in section 7.2.3, and the code for the OPC configuration manager is shown in Figure 7.14.
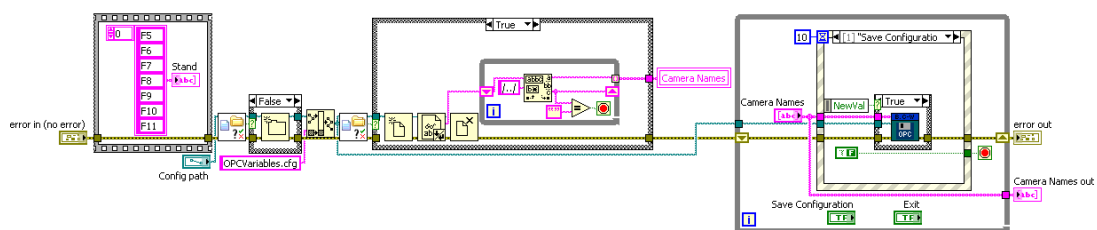
Figure 7.14: OPC Configuration manager code

Save images and save results

The images captured by the camera and the measurement results could both be optionally saved to the local hard drive. Saving of each of these was enabled using buttons on the user interface.

If image saving was enabled, the images would be saved to the local disk and sorted into a folder with the same name as the camera. Each image was named as the full date and time to one hundredth of a second, allowing direct comparison of images and results and saved in JPEG format. An extra optional feature allowed the enabled image analysis overlays to be merged saved on the image to allow the performance of the image analysis to be visually assessed at a later date. The save function performed a check on available drive space before saving images to ensure the software did not fill the hard drive.

The result saving option set the calculated and adjusted results to be saved to a file on the local hard drive located within a folder named the same as the camera. The results file was named as the time and date that the program was initially run and saved as a tab-delimited text file. To optimise program operation time by minimising file access, results were saved in batches of 20, stored in a string variable which was appended to the end of the existing results file and cleared each save iteration. The results file format is shown in Table 7.1. Results values were adjusted for centreline offset and resolution factor as with the OPC results.

Table 7.1: Results file output format

Date (dd/mm/yyyy hh:mm:ss.000)	Centreline Bezier knots				Width
	0	1	2	3	

Save configuration settings

The configurations settings save sub-diagram was triggered by a change in the value for the "Configuration" button on the user interface. When configuration mode was entered, the sub diagram appended to the text log the message "Entering configuration mode". When configuration mode was left, the message "Exiting configuration mode. / Saving settings..." was appended and the software would save the new configuration settings to the hard drive.

Show image

The image display on the user interface was not displayed by default in order to optimise the program running time. When the "Show Image" button on the user interface was pressed, this sub-diagram would pass the image data from the selected camera to the image display on the interface.

Pause image

The pause image function allowed the user to pause the image under analysis on the most recent one. When enabled, the software would bypass the "Acquire" state, and instead use the

current image held in memory. The pause button enable also adjusted how the image rotation was applied to prevent the same image being constantly rotated at each stage, which would have resulted in a spinning image, and also disabled the merge overlay option to ensure the image was clean at each analysis pass.

Save text log

The text log, in a similar manner to the results file, was saved in batches to reduce file access and reduce analysis time. Throughout the program the log would be updated into a string variable. The log variable was then appended to a saved file on the hard drive every 200 program iterations.

Manage text log display

Due to the nature of the text logging, the log had to be read from the saved file to display the full log in the user interface. If the text log string variable were displayed, this would have only displayed the most recent logged report, which was cleared every time the log was saved so would most often be empty. Loading and displaying of the log in the interface was triggered either by a user request from the interface, or every 500 program iterations. When the log was loaded, the display on the user interface would also automatically scroll to the most recent entry (the bottom of the log).

Configure

The configure state was used to change analysis and camera settings to tune the measurement performance of the system. The configure state would only be entered if requested by the user. Figure 7.15 shows the flow diagram for the state and Figure 7.16 shows the LabVIEW code.

The configure state was used to change analysis settings and camera settings. The analysis settings were automatically updated every program loop, whereas the camera settings were only updated if a change had been made. The camera settings were updated like this because before updating some settings (notably the camera ROI which specifies the area of image to be captured on the sensor) the camera had to be un-configured from grab mode, and then re-configured once the settings changes had been made. This process took a noticeable amount of time and if it occurred every program loop whilst in configure mode, usability would have been severely decreased.

When settings were changed, the entry limits of the configuration controls on the user interface were adjusted too. This enforced the values entered into the controls were within the limits of the camera to prevent errors occurring, and also ensured the analysis ROI was within the visible image frame.
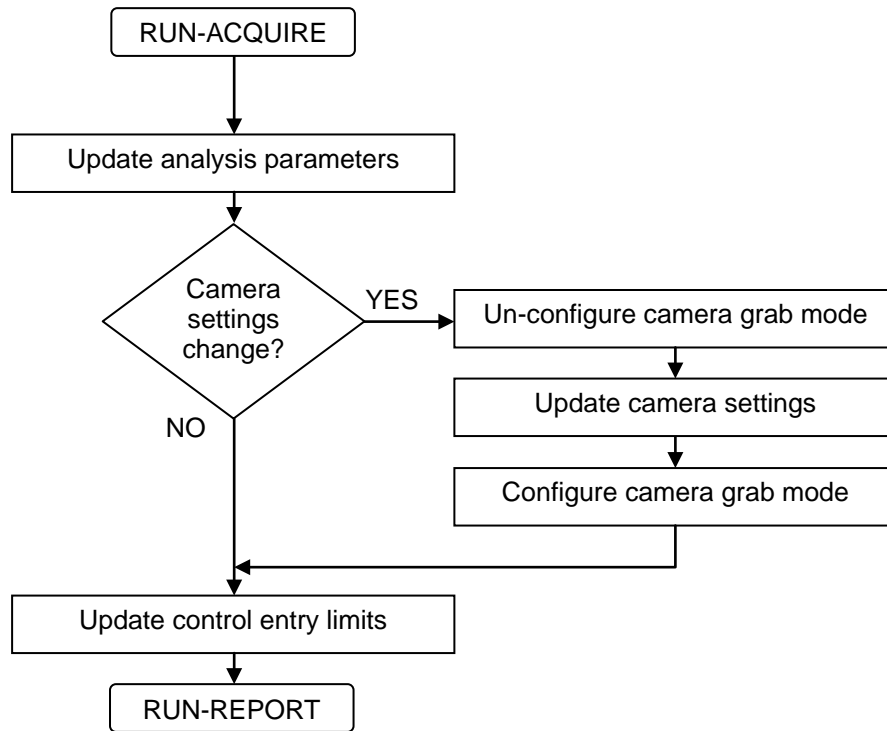
Figure 7.15: Configure program flow
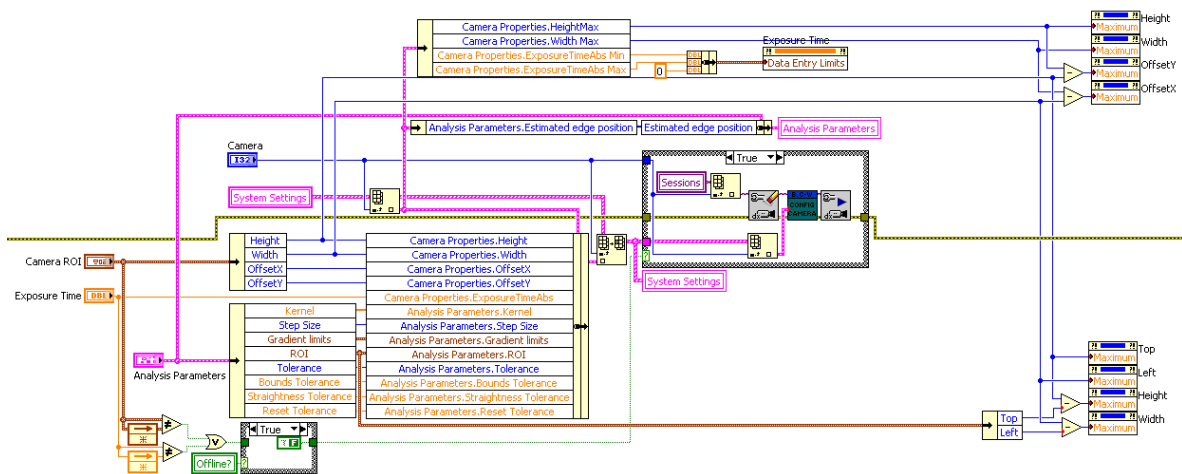
Figure 7.16: Configure program code

Error

The error state was only entered if an error had occurred during program operation. The program would attempt to handle the error and have one of three outcomes:

- Stop: shutdown program.
- Continue: Clear error and continue operation
- Restart: Restart program

The program flow for the error state is shown in Figure 7.17 and the code in Figure 7.18.

The stop action would only occur if the error was catastrophic and the program could not recover. The continue action would occur if the error was insignificant and the program could carry on. The restart action would occur when the program could recover when restarted from the initialise state.
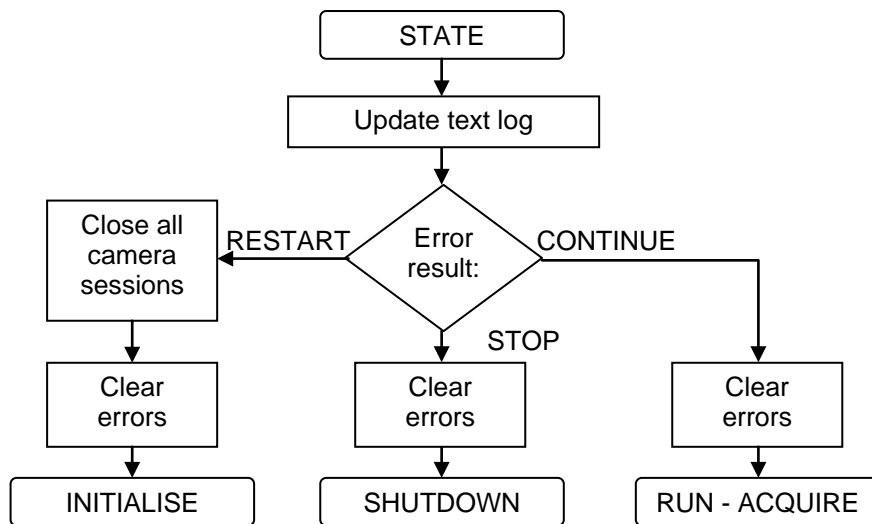
Figure 7.17: Error program flow

In practice, all encountered errors were fixed with a software restart. Any errors which were found during development that could be solved by continuing were seen as bugs and the root cause fixed in software. During development, no errors were found that required a shutdown. All errors which were frequently seen were hardware and network errors, typically the software losing connection to the cameras.
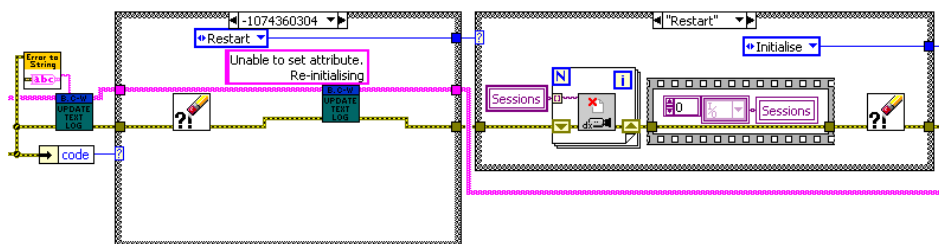
Figure 7.18: Error program code

Shutdown

The shutdown process was the final process before the program stopped. The state existed to ensure all memory references (camera and image) were correctly deleted when the program was terminated. The program flow is shown in Figure 7.19 and the code in Figure 7.20.
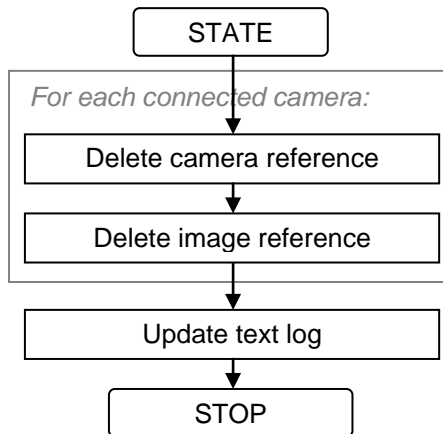
Figure 7.19: Shutdown program flow
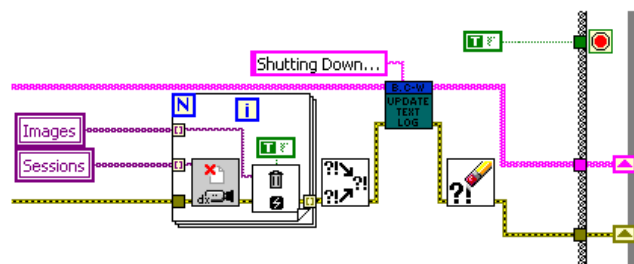
Figure 7.20: Shutdown program code

7.2.3 User interface

The user interface for the measurement system was designed to provide the user with the ability to set up the camera system, configure the image analysis and to monitor the operation of the system. During the installation of the compiled software on the measurement system PXI a shortcut was placed on the desktop to allow convenient access to the program. A shortcut was also placed in the "Startup" folder of the PXI to start the software running as soon as the system was booted up. The shortcut was grouped on the desktop with two other useful shortcuts, shown in Figure 7.21; a link to the "Hot Mill Web Mimic" and the configuration folder, containing the saved results and images, system logs and camera configuration files.
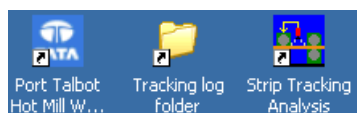
Figure 7.21: Program access icons on desktop

The hot mill web mimic is a tool used within the steel works at Port Talbot to monitor the operation of the hot strip mill in a web browser. An example screenshot of the mimic is displayed in Figure 7.22, which shows the strip undergoing deformation in all seven finishing stands and cooling on the run-out table. This was a useful tool and included in the group of

135

shortcuts because it allowed the user to see the current location of the strip and provide information of when a strip was next expected in the stand observed by the camera.
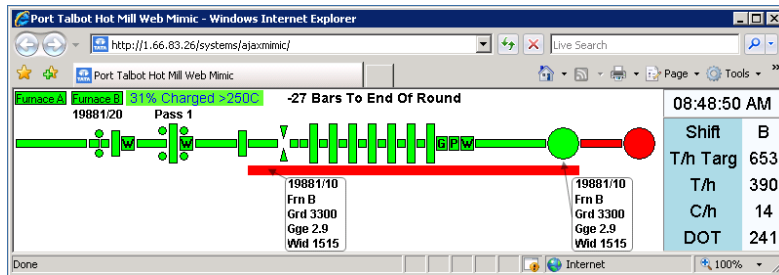
Figure 7.22: Hot mill web mimic

The structure of the interface in the final version of the software was designed in a similar manner to the original interface detailed in Chapter 5. The interface used a tabbed structure to access various data screens with different information. The four tab screens were:

- Main view
- Image view
- Detailed view
- Advanced

Also in the tab strip of the interface were indicators for execution time in milliseconds, software state (mode) and a stop button. The execution time indicated the time for a complete operation cycle to take place, and was useful to monitor the effects of changing various software parameters. The mode indicator displayed active software state and could be used to see what the software was doing at any given time. The stop button would enable a shutdown request in the software and stop the program running.

The individual tabs are described in the following sub-sections.

Main view

The main view, which is shown in Figure 7.23, provided controls and basic information about the system operation.
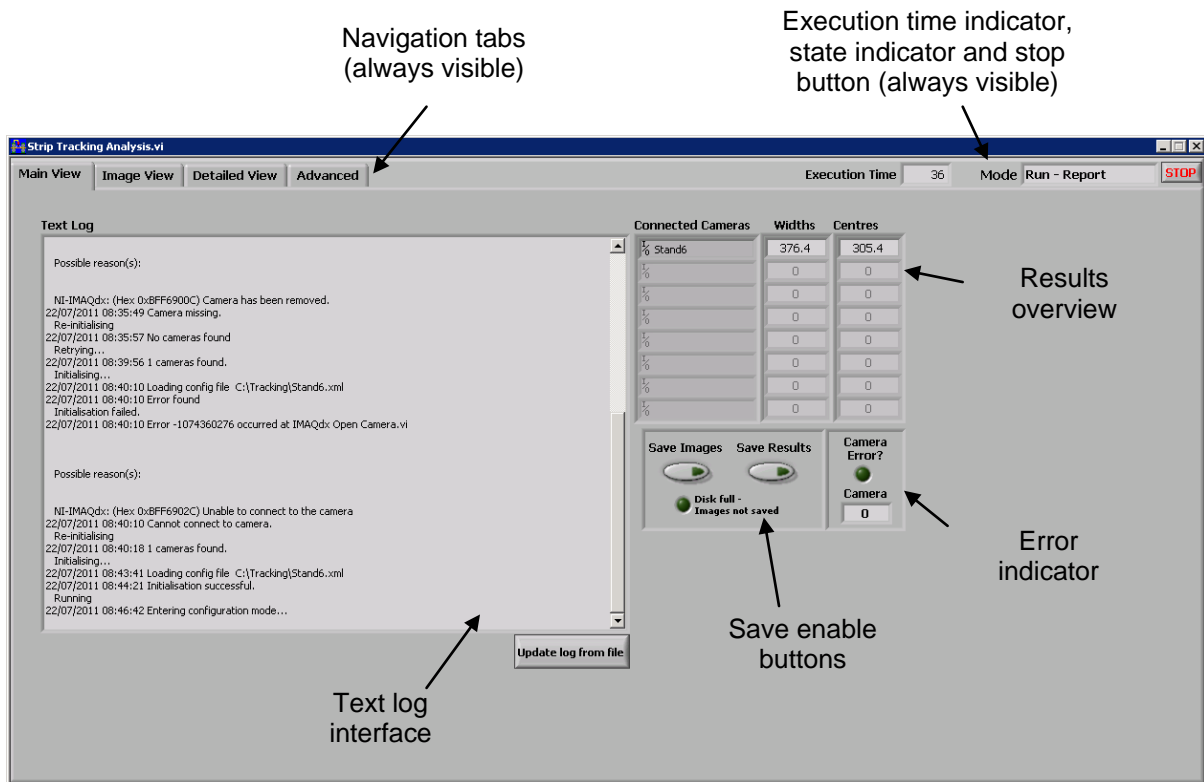
Figure 7.23: User interface main view tab

Text log interface

This indicator was used to display the most up to date loaded version of the text log, providing the user with information on the operation of the software. The information in the display would update automatically every 500 program cycles, or could be manually updated by the user pressing the "Update log from file" button.

Save enable buttons

These two buttons were used to enable the saving of captured images and results files. By default they were both disabled as enabling them would slow down program operation. If the disk was filled and image saving was disabled then the LED indicator would illuminate to alert the user.

Results overview

This set of indicators provided a simplified view of the results of the measurement process. "Connected cameras" listed all the cameras connected to the system. The camera name was aligned against the most recent results for centreline and width measurements from that camera.

Error indicator

The error indicator provided a simple alert to the user if a camera error had occurred during initialisation. The LED indicator would illuminate and the number of the camera (zero indexed of the "Connected Cameras" indicator array) would be displayed. This allowed the user to identify which camera was causing the problem.

Image view

The image view tab, which is shown in Figure 7.24, was the main interface for viewing the operation of the analysis process and to configure the system.
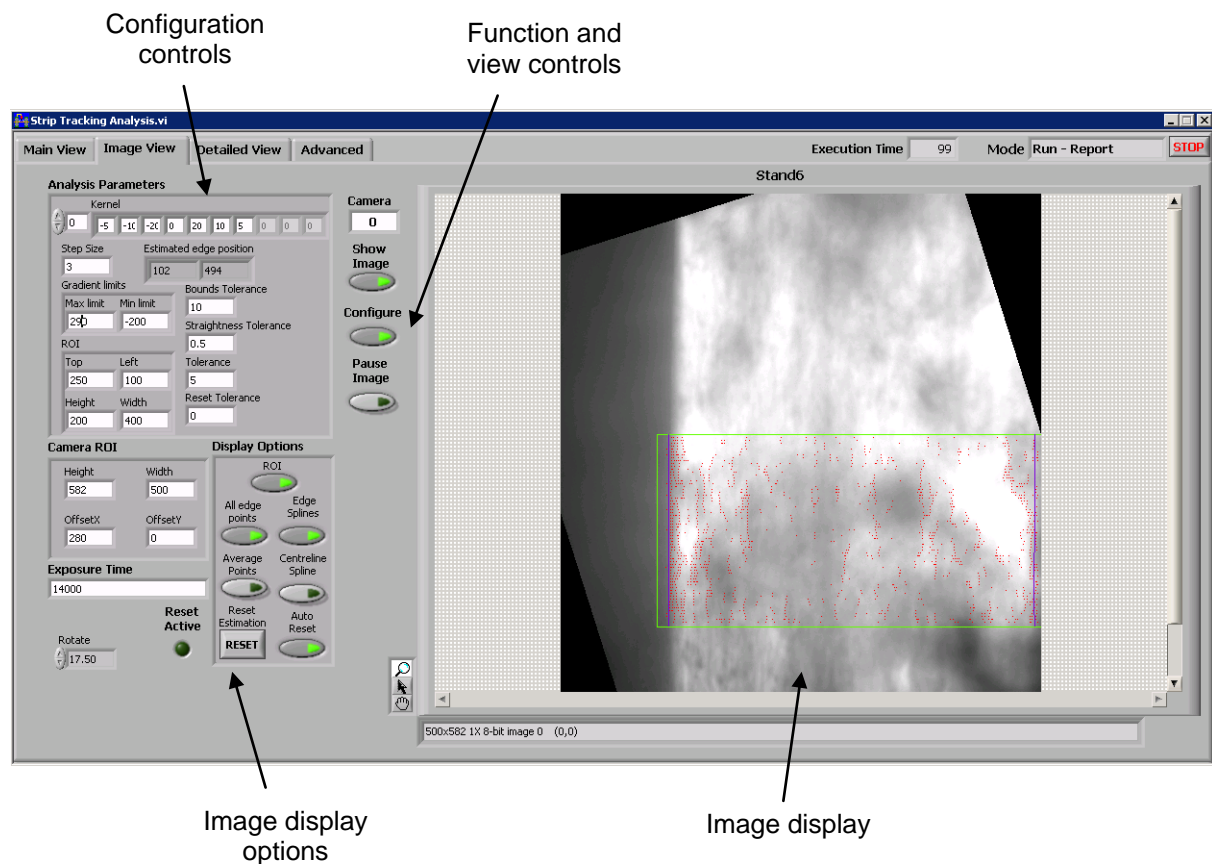
Figure 7.24: User interface image view tab

Image display

The image display was used to view the image captured by the camera. This image could also be overlayed with the results of the measurement operation to provide a visual assessment of the measurement performance.

Image display options

These controls were used to change which results were overlayed on the image view. "ROI" displayed the current region of interest as a green rectangle. "All edge points" would display

all edge points identified as red dots. "Average points" highlighted those points used in the least-squares curve fitting process (the non-rejected edges) as yellow dots. The full length strip edge Bezier curves could be displayed in blue using the "Edge splines" switch, and the "Centreline spline" switch displayed the resultant central Bezier curve as a purple line.

The "Reset" button was used to manually force a reset of the edge position estimation, and the "Auto reset" switch could be used to disable the automatic reset function. The "Auto reset" switch could not be used unless the software was in configuration mode. If the edge position was being reset then the "Reset active" LED indicator would illuminate. The "Rotate" control allowed the image to be rotated before analysis. This was only added as a quick fix to a problem which has been discussed in section 7.2.2.

Configuration controls

The configuration controls were used to configure the analysis parameters and camera settings. The "Camera ROI" altered the portion of the camera sensor used in the acquisition of images. Reducing the camera ROI to only the useful portion reduced the execution time of the software and increased the frame rate of the camera so was a useful method of easily improving software performance. The "Exposure time" control was used to set a fixed time for the camera exposure.

The "Analysis Parameters" controls adjusted the parameters of the image analysis method, which is described in Chapter 4. The "ROI" controls set the size and location of the ROI in which the analysis was performed. The vertical distance between each edge point search line was set with the "Step size" control. The "Kernel" control was used to set the filter weights of the differentiation process. "Gradient limits" adjusted the maximum and minimum limits of brightness gradients (the result of the kernel multiplication) for the initial edge point identification step. The "Edge point estimation" display was used to show the current estimated location of the edge location, used in the bounding and automatic reset process. In the original software, this was an input, but when the process was automated in the final version, this indicator was changed to a control for information purposes. "Bounds tolerance" set the distance the Bezier curve could be from the estimated edge position. The "Straightness tolerance" set a value of how straight the Bezier curve should be by limiting knot values by a set amount beyond the average point location. The value named "Tolerance" was the distance which an edge point could be from the result in the previous measurement. "Reset tolerance" was a minimum value of edge point x-location used in the reset process.

Function and view controls

This group was used to control program operation mode and the visible information in the tab. "Camera number" was used to select which camera was being displayed and configured. The "Show image" switch was used to enable the display of the captured image to the user. When this was off, the image display options were disabled and all overlays turned off to optimise measurement performance time. The "Configure" switch was used to toggle the software in and out of configuration mode. When switched off, all configuration controls were disabled. The "Pause image" button was used to pause the display and analysis on the current image.

Detailed view

The detailed view tab provided the user with more in depth information about the results of the measurement process. A screenshot of the tab is shown in Figure 7.25.
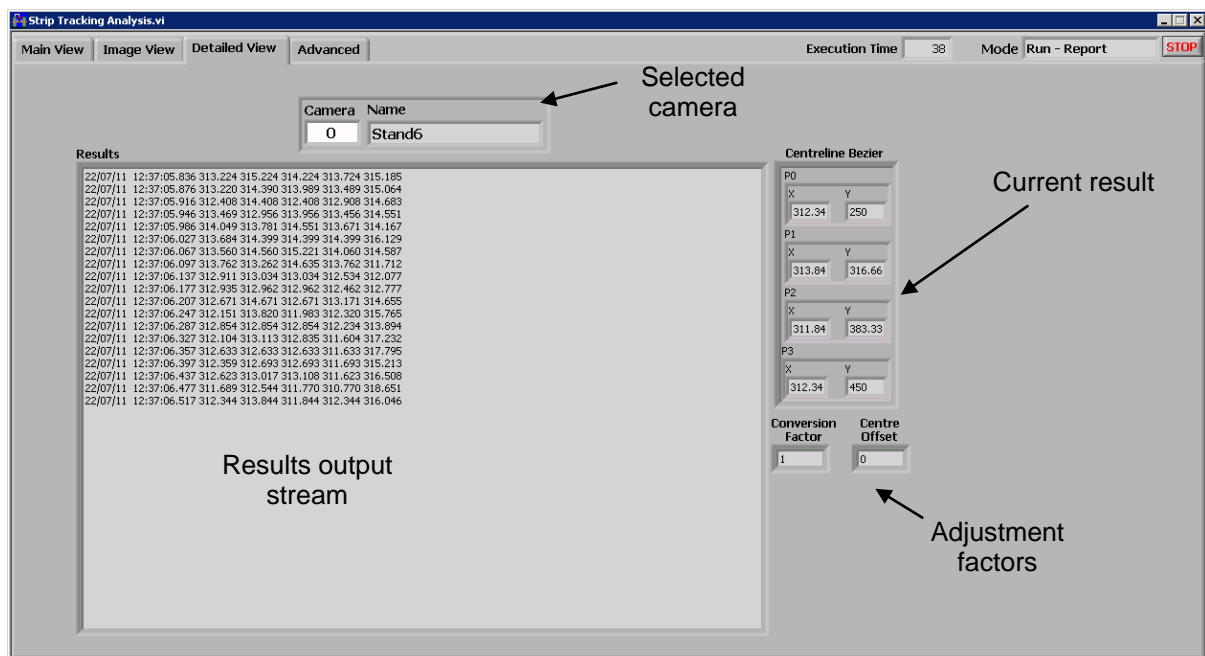
Figure 7.25: User interface detailed tab

Selected camera

The numerical "Camera" control was used to select which camera the results were displayed for. The name of the chosen camera was also displayed here for reference.

Results output stream

This text stream displayed the current output results before they were saved to the results file. The results were cleared every time they were saved to file, therefore this display only showed the most recent results. The results stream was only active when results saving was enabled from the main view tab.

Current result

This display was used to show the current measurement result in full detail. The result is the location of both x and y locations of all four knots of the centreline Bezier curve.

Adjustment factors

These indicators displayed the linear offset of the mill centreline and resolution factor used to calculate the final results.

Advanced

The advanced tab, shown in Figure 7.26, was used to control more advanced system features, not used in general operation.
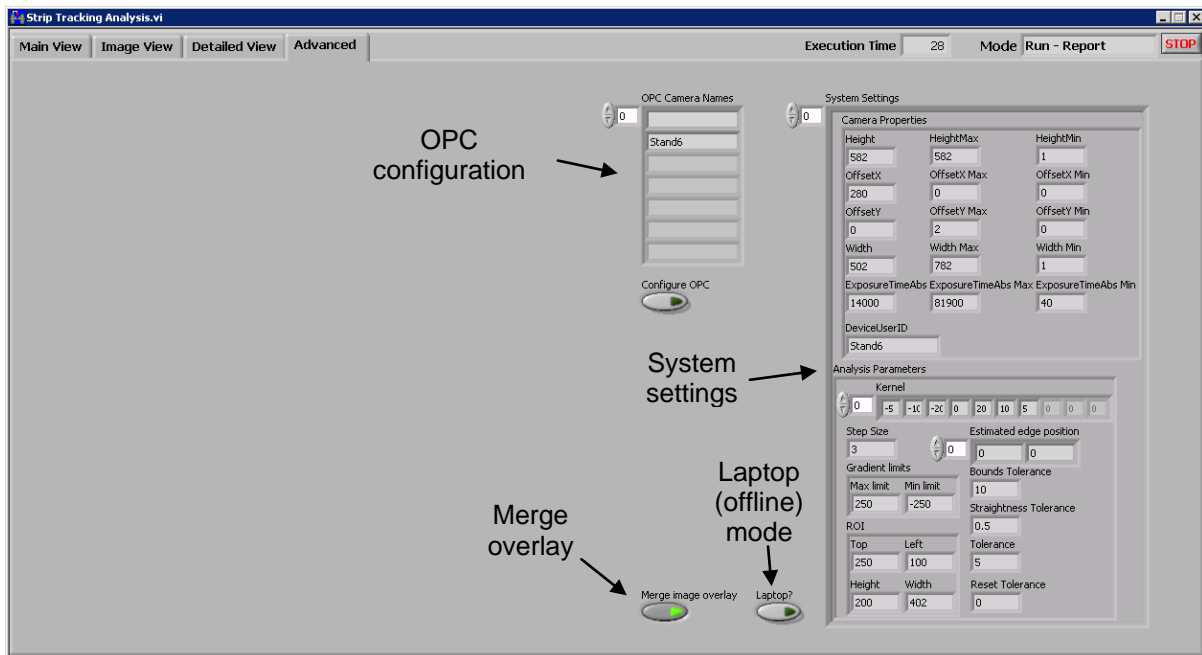
Figure 7.26: User interface advanced tab

System settings

This indicator displayed the full system settings currently in use, including cameras properties and analysis settings. The information contained in this display was the same as saved in the settings files.

Laptop (offline) mode

This switch would put the software into a development mode used only when testing the software. Some updates and testing of the image analysis process was performed on a computer with a USB camera attached. The software used standard settings names in the GigE protocol which were not supported by the USB camera, therefore would put the system in a state of error and not function. This switch was used to disable certain portions of the software during development.

Merge overlay

This switch would enable the merging of the results information selected in the image view tab with the image so when images were saved to the local hard drive, the overlays were also included.

OPC configuration

The OPC camera names indicator displayed the camera names ordered in stand number, used to match up the results with the correct OPC variable. The "Configure OPC" switch opened the configuration manager tool, shown in Figure 7.27. The configuration manager was used to match up the camera names with the stands. Note that the Port Talbot finishing mill stands were named F5 to F11.
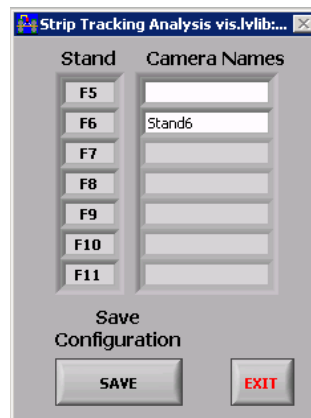
Figure 7.27: OPC Configuration manager

8 Measurement System Results and Findings

The strip tracking measurement system was developed from proof of concept tests using low-cost camera equipment up to a full stand alone online measurement system. The system underwent a long term evaluation and development process up to what is referred here as the final version.

The final version of the measurement system consisted of a single camera mounted to the second finishing stand in the Port Talbot hot strip mill, viewing the strip passing from the second to third stands from vertically above. The camera was connected using the GigE Vision protocol to a National Instruments PXI industrial computer running a piece of software created with a bespoke analysis method to identify the strip edge locations and hence derive the strip centreline.

The term "final" was used in reference to the logical end point of this project in terms of development and time constraints, however does not imply that the version presented here would not benefit from any further work and improvement. This chapter presents an evaluation of the final version both in terms of hardware and software performance and suggests further work which could improve the operation of the system. The system was designed as a measurement device to be used in an industrial control situation, therefore the evaluation process has covered the whole system and not just the core analysis methods.

8.1 Hardware performance

The hardware performance of the system was very important because a hardware error could put the entire measurement system offline; no matter how good the analysis method was; without a robust hardware platform the system would not function. Two areas of concern were identified during the evaluation process, the connection to the camera and the image quality returned by the camera. The concerns surrounding these two areas are detailed below.

8.1.1 Camera connection

A recurring problem with the system was frequent loss of connectivity to the camera. This problem presented itself by the analysis software losing partial or full communication with the camera and ultimately not being able to find the camera on the system during initialisation. When the connection was lost the system would not acquire any images so effectively be offline. By analysing a system text log from one software session of just over 8.6 days, statistics of the online and offline performance of the system could be found, and presented in Table 8.1. These statistics show that during that period the system was online

(connected to the camera and performing analysis) for only 84% of the time, and on average was only online for 37.3 minutes before losing connection again.

Table 8.1: Online/Offline stats for measurement system

Evaluation Period		12418	mins
Total	Online	84	%
	Offline	16	%
Max.	Online	857.1	mins
	Offline	85.4	mins
Min.	Online	0.3	mins
	Offline	0.8	mins
Avg.	Online	37.3	mins
	Offline	7.1	mins

The online analysis statistics show that system performance was not satisfactory and the cause of the loss of connection had to be found and rectified before the system would be reliable.

The precise nature of the error was not known, although suspected to be related to the configuration of the GigE network. Other possibilities are that it was caused by loss of power to the camera or an intermittent electrical fault caused by vibration of the mill. The fault persisted when the camera was replaced with a new camera, therefore was not thought to be a fault with the camera itself.

8.1.2 Camera view

The viewable area and images acquired by the camera affected the performance of the analysis software because obscured strip edges and some other issues could not be accounted for by the analysis software. An example of a typical image is shown in Figure 8.1 with some problem areas highlighted.

The first significant problem with the image quality was due to the alignment of the camera; the images were rotated to the mill centreline by approximately 20° and also the image centreline was significantly misaligned with the mill centreline. The linear misalignment was a problem because unless the strip was narrow (less than approximately 1000mm) then only one edge was visible. This meant that the measurement system did not perform correctly on the wider strips. The rotational misalignment has already been discussed in Chapter 7 where a quick solution was implemented in software to allow analysis to take place. The image rotation caused a problem because the nature of the analysis was essentially a 1D process,

relying on the strip to be travelling vertically in the image. Some more efficient software options are put forward in chapter 9, by using a more robust and faster method to rotate the analysis process, however the camera should be aligned correctly to the mill to maximise the useable image area and minimise of remove the requirement for an in-software rotation.

The second problem identified in Figure 8.1 is the dirt and smudges on the enclosure window, partially obscuring the strip edge. The prevention of dirt accumulation was accounted for in the system design by specifying enclosures with an air barrier, however this did not operate as effectively as originally conceived.
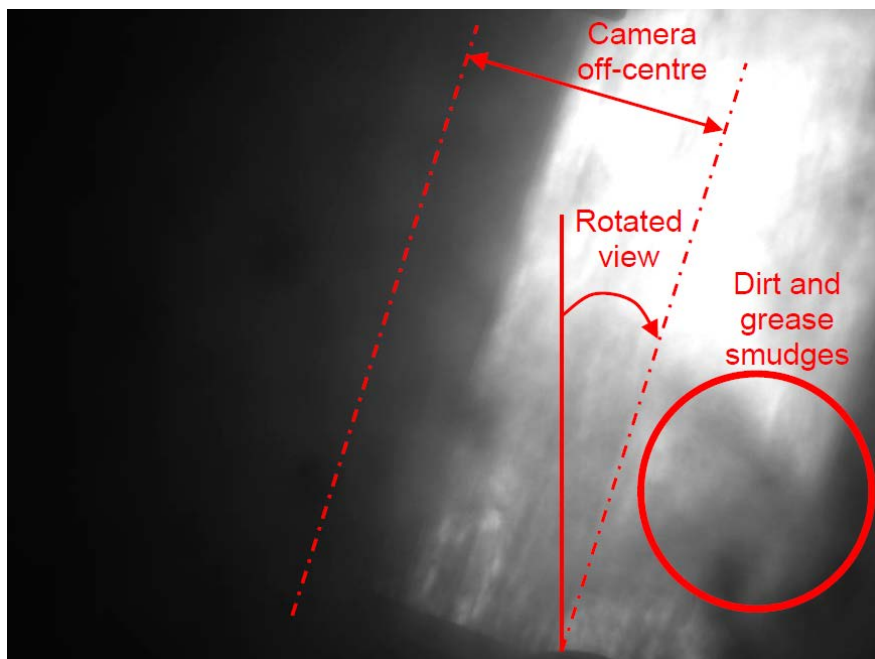
Figure 8.1: Quality of acquired images

8.2 Software performance

The system software was designed to perform the analysis of the images and measure strip position and also to make this measurement available to the mill systems. The evaluation of the software hence covers both the core analysis process and also other aspects of software performance.

8.2.1 System configuration and initialisation

The system configuration at initialisation was an important aspect to the system performance because it ensured that the system would return the to configured state should the software be restarted. Configuration files were created and saved locally for each connected camera, saving all aspects of camera and analysis settings. This allowed the cameras to automatically be reconfigured and the system return to a running state. In addition to cameras settings files

being locally saved, the configuration of the OPC manager was also saved to a configuration file to ensure measurements were output to the correct OPC variable.

The operation of the analysis and OPC configuration was confirmed to work correctly during the system evaluation process.

8.2.2 System outputs

OPC outputs

The OPC variables were the main system output, being the method of transfer of measured results from the measurement system to the mill computers. To confirm the correct output of OPC variables, OPC DataSpy [54] was used. Figure 8.2 shows a screenshot of OPC DataSpy monitoring the centreline variables, showing a measured result correctly assigned to the F6 (second stand) variable, with all other variables empty because no other cameras were present on the system.
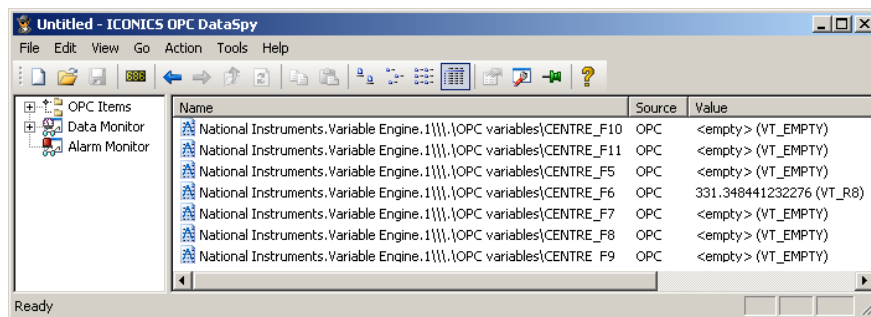
Figure 8.2: Using OPC Data Spy to confirm OPC data publication

Local file outputs

A minor system output were the local files, consisting of saved results, saved images, operation logs and configuration files. The local files were all saved in a dedicated folder on the hard drive, and the file structure is shown in Figure 8.3. During evaluation it was confirmed that all files were saved correctly in the correct folder structure and the software would create the structure if it was not already present on the system.
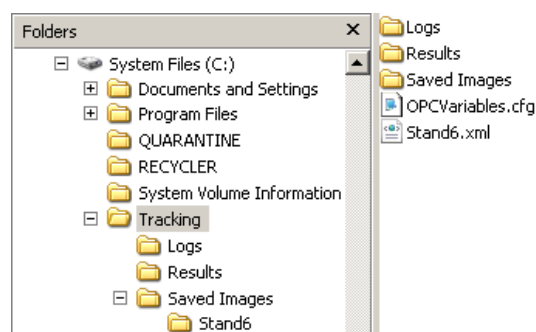
Figure 8.3: Output files folder structure

146

8.2.3 Measurement performance

The core of the system and main point of focus was the measurement of strip position and the image analysis methods developed for this task. The evaluation process consisted of varying some analysis parameters and observing the effects, and also testing the ability of the software to measure strip position.

Variation of edge detection parameters

The correct identification of strip edges was the core process of the measurement of strip position because without identifying edge points on the strip edges, it was impossible to fit the Bezier curve.

The parameters used in the edge detection process were the analysis kernel and the gradient limits. The effect of varying these two parameters was investigated by applying the edge detection method to the three images shown in Figure 8.4. These three images were taken from the same strip and cover the complete range of brightness seen during rolling due to varying levels of cooling water. The ideal values for kernel and gradient limits should provide a clear definition of edge for the range of possible images without introducing too much noise. Noise points identified inside the strip would be preferable to noise outside the strip because the width estimation method, used to provide an estimate of strip position used throughout the analysis, uses maximum and minimum modal edge point values.

Figure 8.4: Test images used in evaluation of edge detection parameters

In the analysis method, the kernel was applied to the images without taking into account the weightings of the kernels; the magnitude of the gradient of any given analysis point was proportional to the total magnitude of the kernel. The kernel was applied in this way in the measurement system to minimise the required steps and computations in the measurement process. To account for the method of kernel application, the gradient limits were adjusted

proportionally to the magnitude of the kernel in order to perform a representative comparison of different kernels and gradients limits, as in (117).

$$G_{Max} = G_{Norm} \frac{\sum |\mathbf{K}|}{2}$$

(117)

The image sample used in the study are a dark to light transition and the kernels used mean this was always a positive gradient, therefore the maximum gradient limit was the dominant limit for the study (all points with gradients above G_{Max} were accepted). However, for edges identified due to noise in the image the minimum limit (points with gradients below G_{Min} were accepted) was equally significant. To ensure the study remained representative of a full strip with, both maximum and minimum limits were used and the minimum limit was the negative to the maximum limit as in (118).

$$G_{Min} = -G_{Max}$$

(118)

Kernel

A variety of different kernels were investigated, varying in kernel size and relative weightings, and the result analysed to determine the effect on edge point determination. Throughout this study a value of $G_{Norm} = 16.7$ was used. Table 8.2 lists the test kernels and gradient limits used, and the results are shown in the images shown in Figure 8.5 to Figure 8.16.

Table 8.2: Tested kernels and normalised gradient limits

No.	Kernel											Gradient limit
K1	-	-	-	-	-1	0	1	-	-	-	-	16.7
K2	-	-	-	-1	-1	0	1	1	-	-	-	33.3
K3	-	-	-	-1	-2	0	2	1	-	-	-	50.0
K4	-	-1	-1	-1	-1	0	1	1	1	1	-	66.7
K5	-	-1	-1	-2	-2	0	2	2	1	1	-	100.0
K6	-	-1	-2	-3	-4	0	4	3	2	1	-	166.7
K7	-	-1	-2	-5	-10	0	10	5	2	1	-	300.0
K8	-	-1	-5	-10	-30	0	30	10	5	1	-	766.7
K9	-	-	-1	-2	-4	0	4	2	1	-	-	116.7
K10	-	-1	-2	-4	-8	0	8	4	2	1	-	250.0
K11	-1	-2	-4	-8	-16	0	16	8	4	2	1	516.7
K12	-	-1	-2	-5	-5	0	5	5	2	1	-	216.7
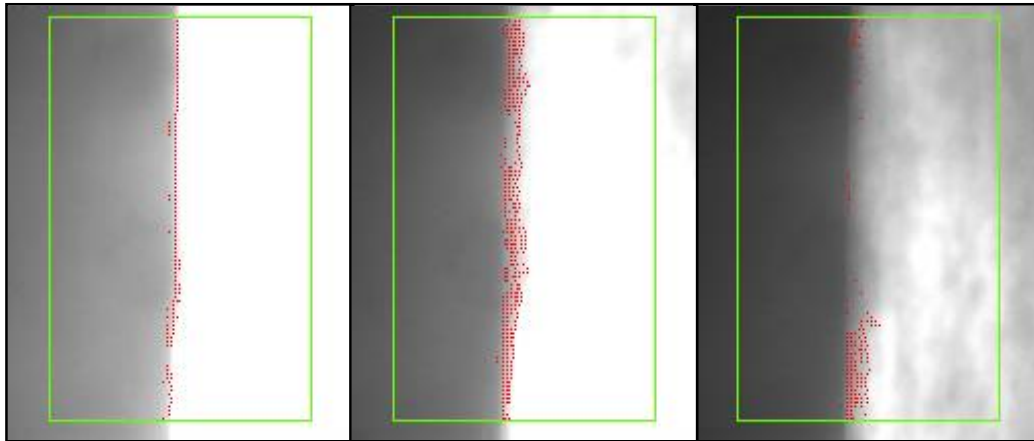
Figure 8.5: K1 Results

K1 was the most simple kernel used in the investigation and effectively performed a simple discrete differentiation on the image. The results, given in Figure 8.5, show reasonable edge definition in the brightest image, although showing some noise outside the strip location. The edge definition in the middle image is also reasonable, but in the dimmest image the edge was determined very poorly and has no definition along a significant portion of the length.
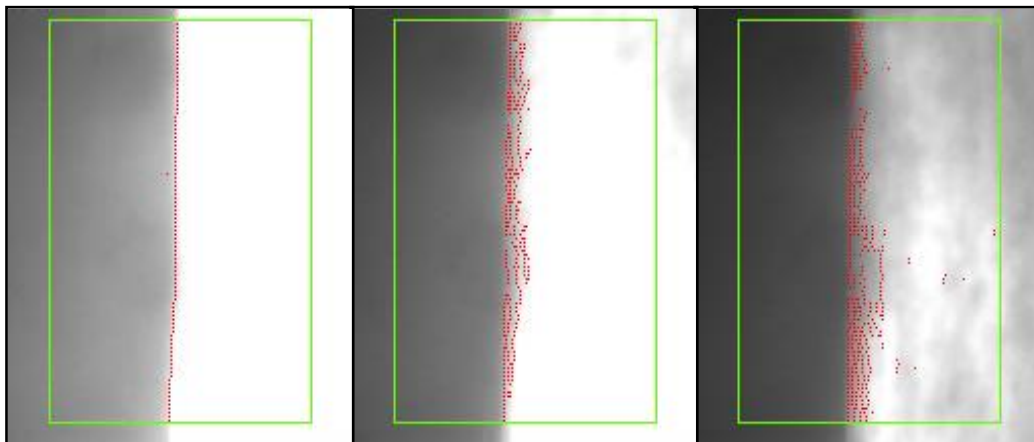
Figure 8.6: K2 Results

The kernel K2 is a simple extension beyond the K1 kernel, applying the differentiation process across one more pixel at each side, increasing the level of filtering in the analysis. Comparing the K2 results (Figure 8.6) to the K1 results, a very large improvement can be seen. The edge definition in the brightest image is still good along the entire length and additionally the noise that is seen from K1 is not present here. The mid brightness image is not significantly different to the K1 analysis. The largest improvement is seen in the dim image, in which the K1 analysis was ineffective, whereas the K2 analysis gave a good definition of the strip edge, although a large amount of noise within the strip area. The

difference between the K1 and K2 results highlights the effectiveness of using the kernel with a wider range than a simple discrete differentiation
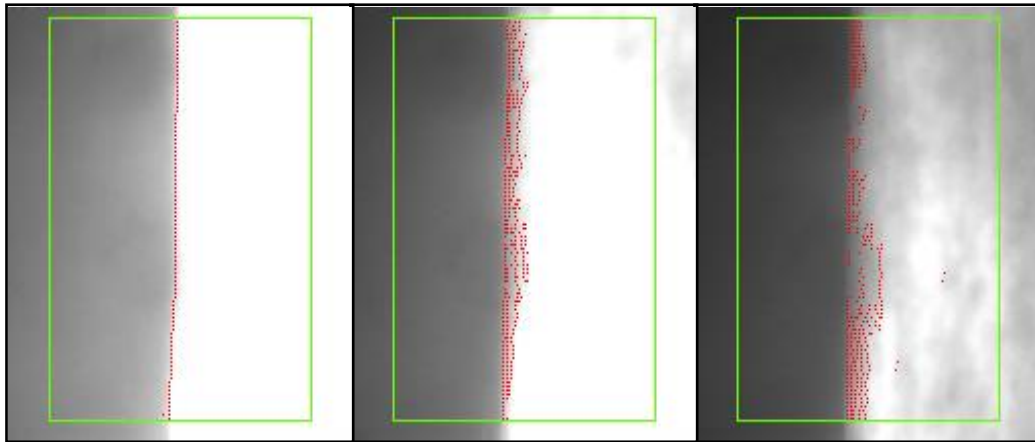
Figure 8.7: K3 Results

K3 introduced a weighting to the inner pixel pair, so the pixels closest to the pixel under analysis were more significant to the gradient result than the further pixels. Figure 8.7 shows the K3 results. Comparing K3 to K2, the bright and mid images are largely similar, however the edge definition in the dim image is poorer with K3.
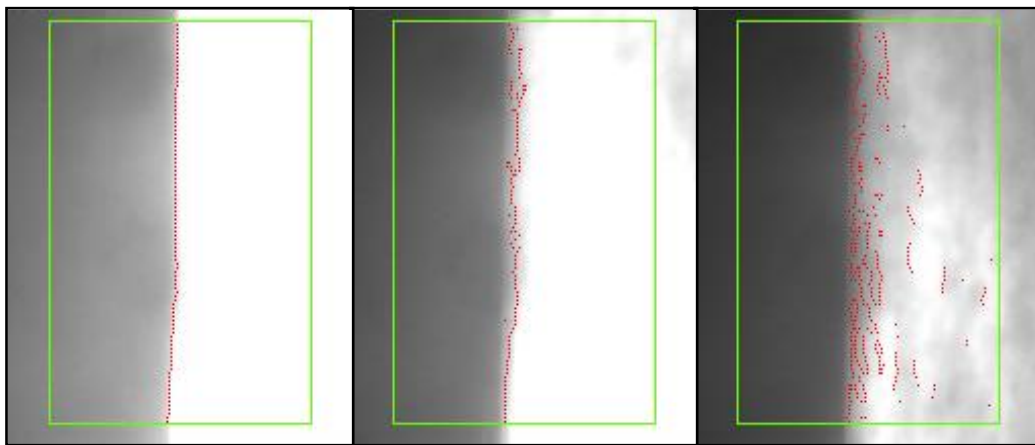
Figure 8.8: K4 Results

Figure 8.8 shows the K4 results, which is an extension to the K1 and K2 kernels with no extra weighting for any pixels. Again, the K4 results have given a good edge definition for the bright image with no noise points. However, the edges on the mid brightness image are mostly inside the strip area and not on the strip edge. The dimmest image also has a number of edges identified inside the strip area.
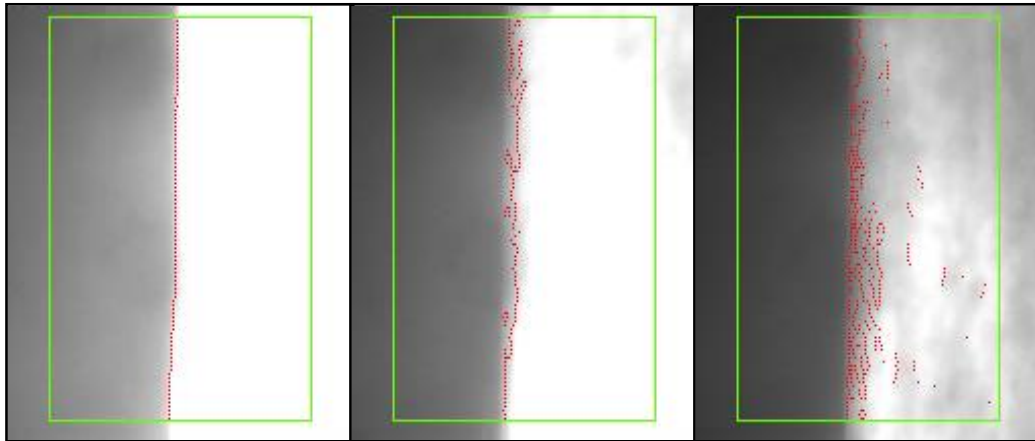
Figure 8.9: K5 Results

K5 has the same structure as K3 but twice the range of pixels included in the calculation. The results are shown in Figure 8.9. K5 defined the bright image edge very clearly and gave reasonable definition of the dim edge, improved compared to K3. However, the mid range edge definition is similar to the K4 result; off the strip edge within the strip area.
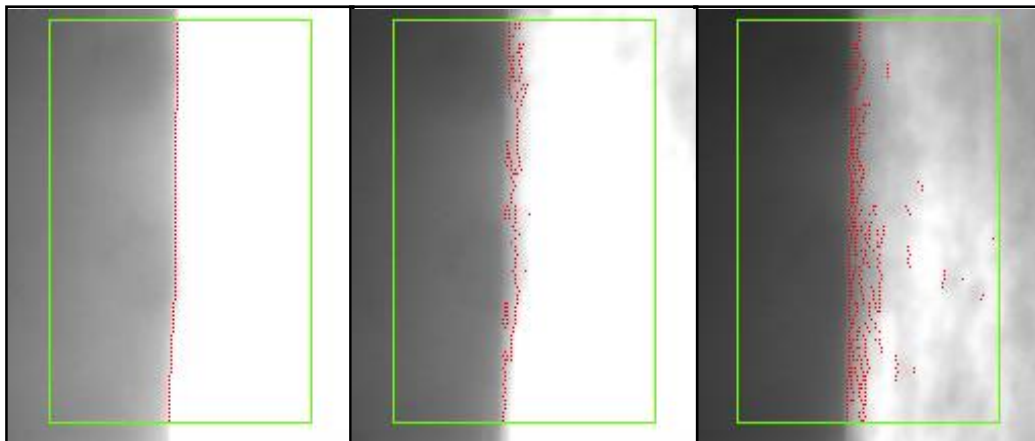
Figure 8.10: K6 Results

The kernel K6 has a linear weighting pattern across the entire kernel width, giving even more significance to the inner edge pairs than the outer than kernels K1 to K5. The results, shown in Figure 8.10, again are very good for the bright image with every edge point on the strip edge. Also, the dimmest image has a good definition of edge location, although with noise inside the strip area as with all the other kernels. The edge definition in the middle image however is very poor, although slightly improved over the less weighted kernels of the same size (K4 and K5).
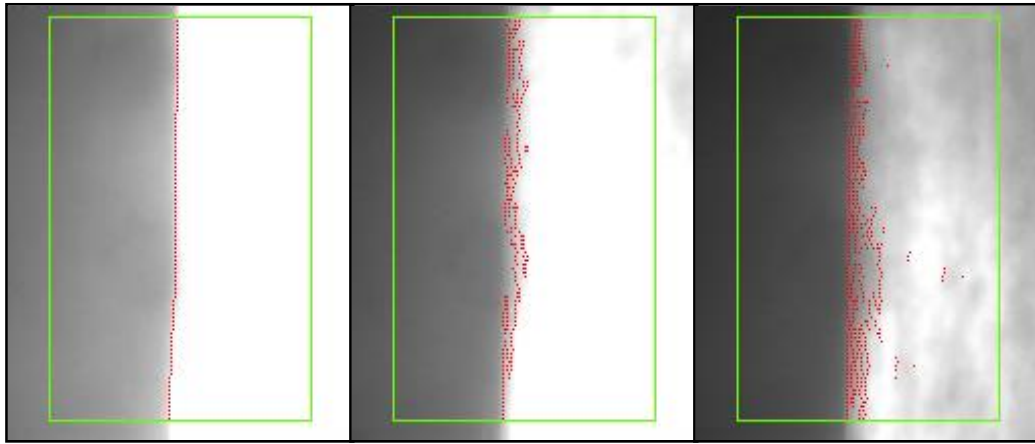
Figure 8.11: K7 Results

K7, results shown in Figure 8.11, increased the inner weightings from the linear pattern K6 to a further heavier weighting to the inner pixel pairs. The brightest and the dimmest images have a good definition of strip edge, although again a lot of noise in the dim image. The mid image edge is reasonably well defined, although with a few missing patches.
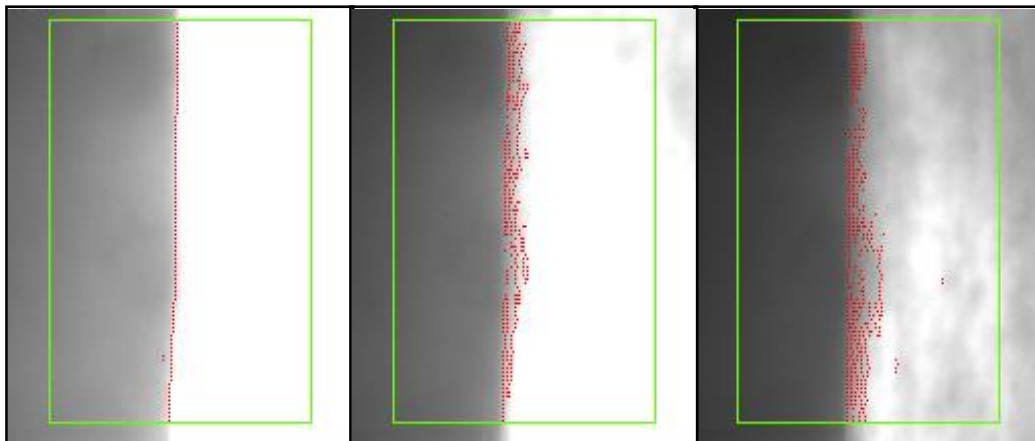
Figure 8.12: K8 Results

Figure 8.12 shows the results for K8, which has the largest range of weightings of all the test kernels. The bright image has a very good edge definition, although a couple of noise points are also present. The mid and dim images both have a reasonable edge definition, although with a few missing patches.
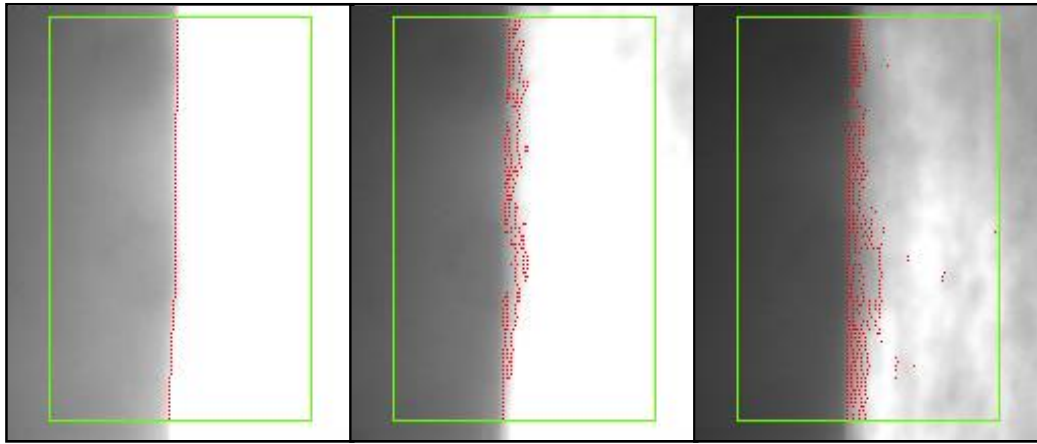
Figure 8.13: K9 results
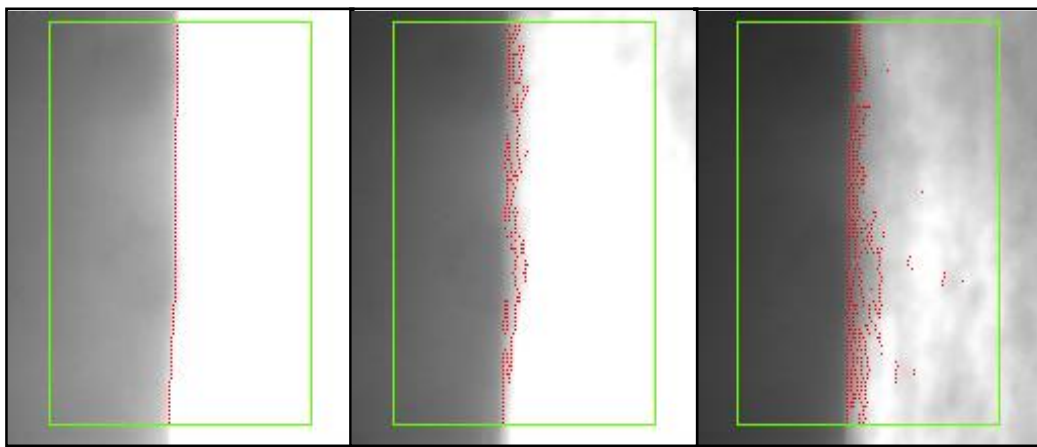
Figure 8.14: K10 Results
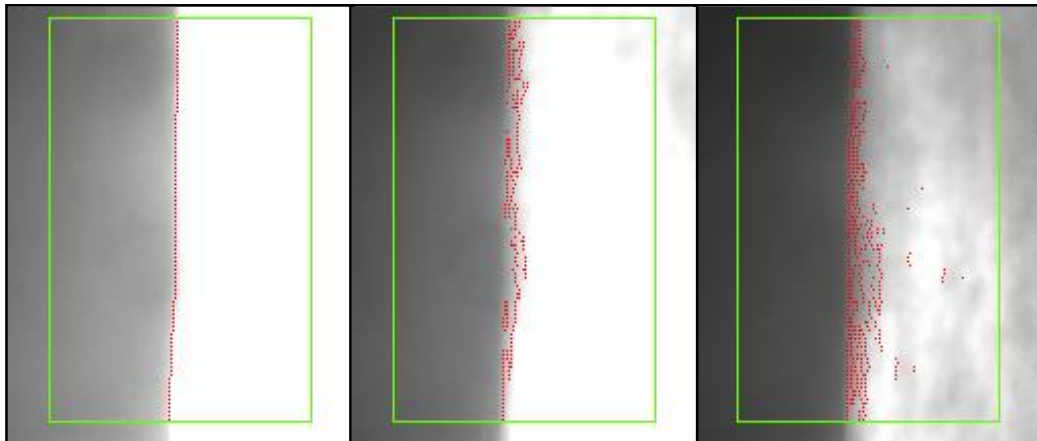
Figure 8.15: K11 Results

K9, K10 and K11 (Figure 8.13, Figure 8.14 and Figure 8.15 respectively) all have a binary weighting pattern with different kernel sizes. K3, which was discussed earlier, also follows the same binary pattern. The results from all four kernels are very similar, with a good definition of the bright image edge, and reasonable definition in the dim edge. The mid image

edge is also reasonable but patchy in places. The size of the kernel does not appear to significantly alter edge detection performance.
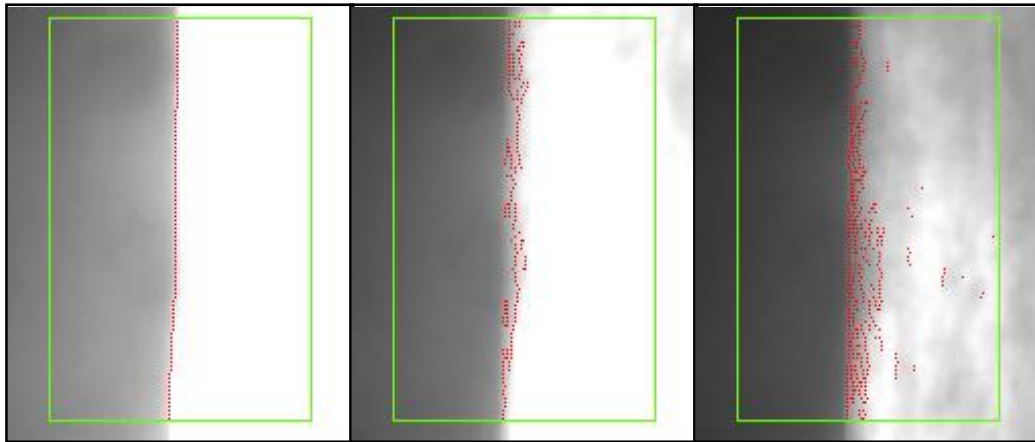
Figure 8.16: K12 Results

K12 has the same weighting for the inner two pixel pairs lower weightings for the outer pairs. Figure 8.16 shows the results from the K12 analysis. The bright image shows excellent edge definition, and the dimmest image has a good edge definition. The mid image has poor edge detection with most points identified inside the strip area and not on the strip edge.

Comparing all 12 kernel results, K1 showed the worst performance, with the most noise in the bright image and very poor edge detection in the dimmest image. Kernels K2 and K8, despite being of very different form, gave very similar results the overall best definition of the strip edge for the range of images.

Gradient limit

To demonstrate the effect of varying gradient limit on the edges detected, two distinct kernels from the kernel study which were both deemed to perform well (K2 and K8) were chosen and the gradient limits changed. The test gradient limits were normalised as before and the values used are shown in Table 8.3.

Table 8.3: Tested gradient limits

No.	Gradient limit Max		
	Norm.	K2	K8
G1	0	0	0
G2	10	20	460
G3	20	40	920
G4	30	60	1380
G5	40	80	1840
G6	50	100	2300

The results of the gradient limit study are shown in Figure 8.17 through to Figure 8.22.
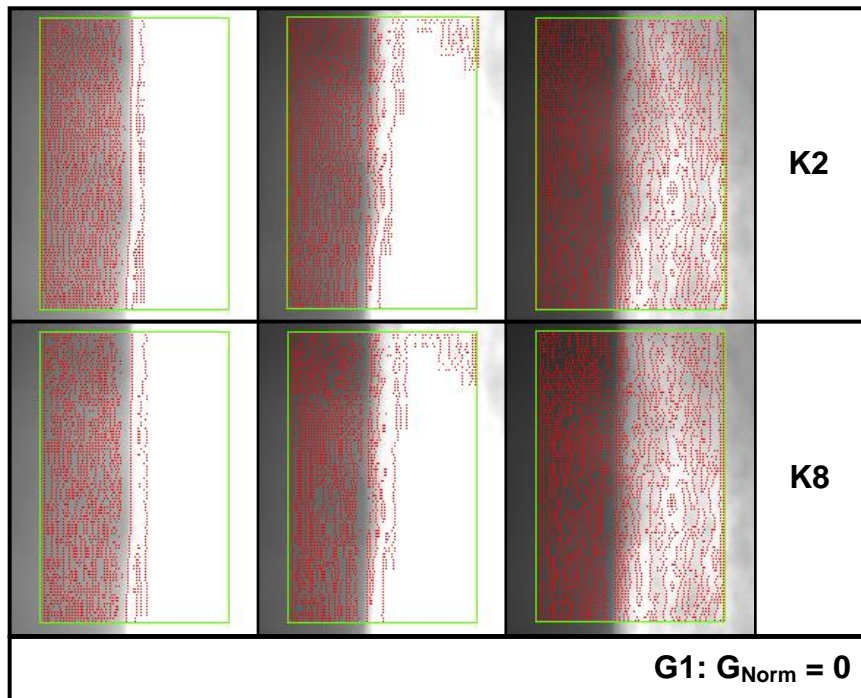
Figure 8.17: G1 Results

The G1 results, shown in Figure 8.17, have a gradient limit of 0, i.e. all turning points identified are accepted as edges. In all three images for both kernels there are many edge points and no clear identification of strip edge.
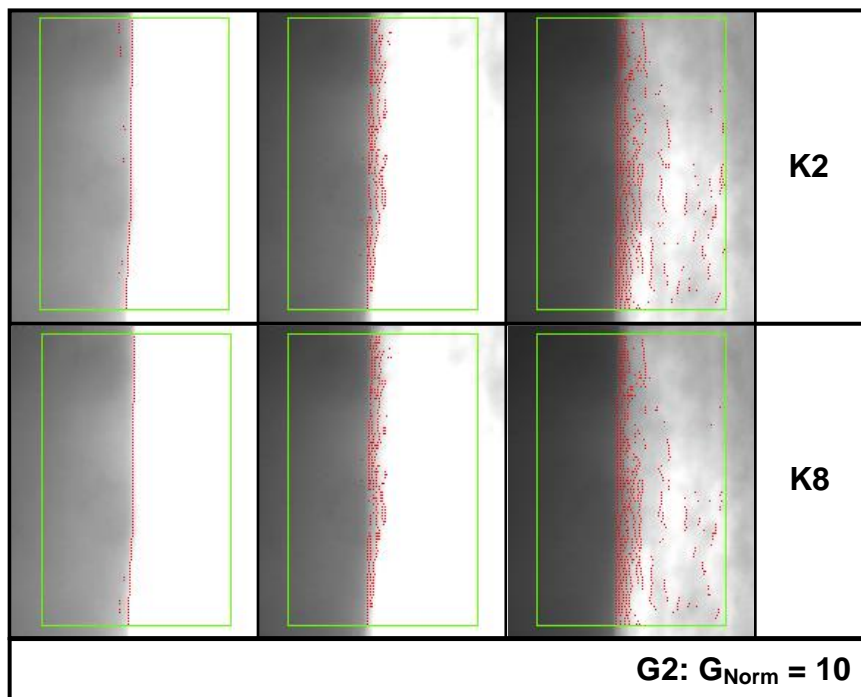
Figure 8.18: G2 Results
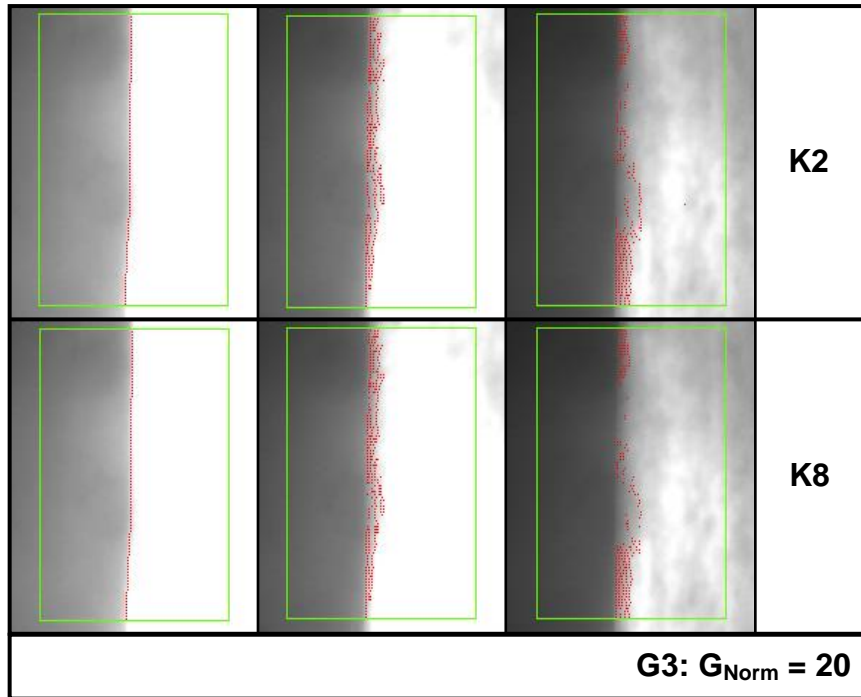
Figure 8.19: G3 Results

Figure 8.18 and Figure 8.19 show the results for G2 and G3. The G2 results show good definition of edge position, especially compared to the G1 results, however in the noisier dimmest image there is still a lot of noise found in the strip region. The G3 results still have a good edge definition but in the dimmest image the edge is missing for a large portion.
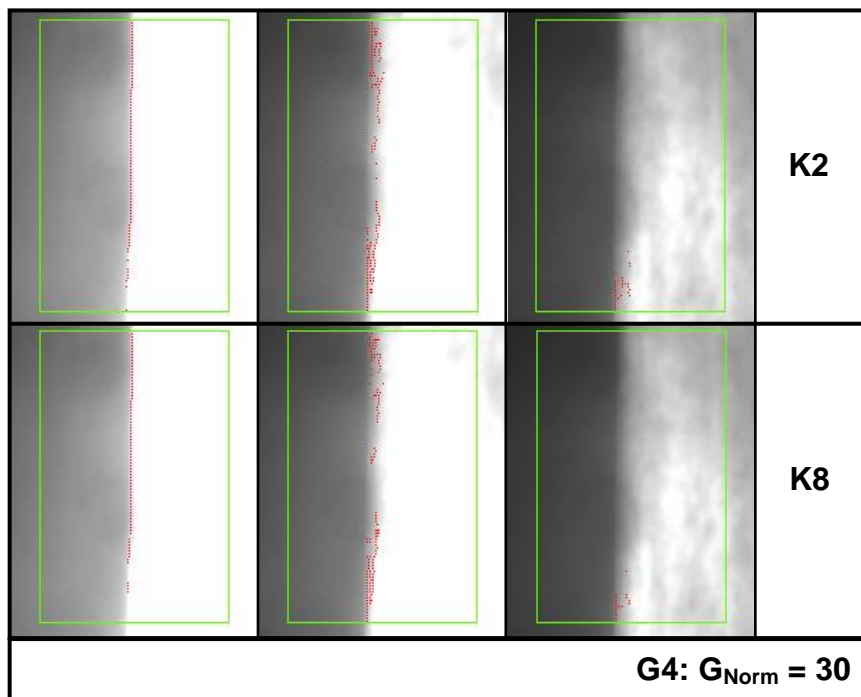
Figure 8.20: G4 Results

156

G4, shown in Figure 8.20, still found good definition of edge position in the brightest image, however the edge in the dimmest image is almost completely missing. The middle image still has some edge definition but not reliably on the strip edge.
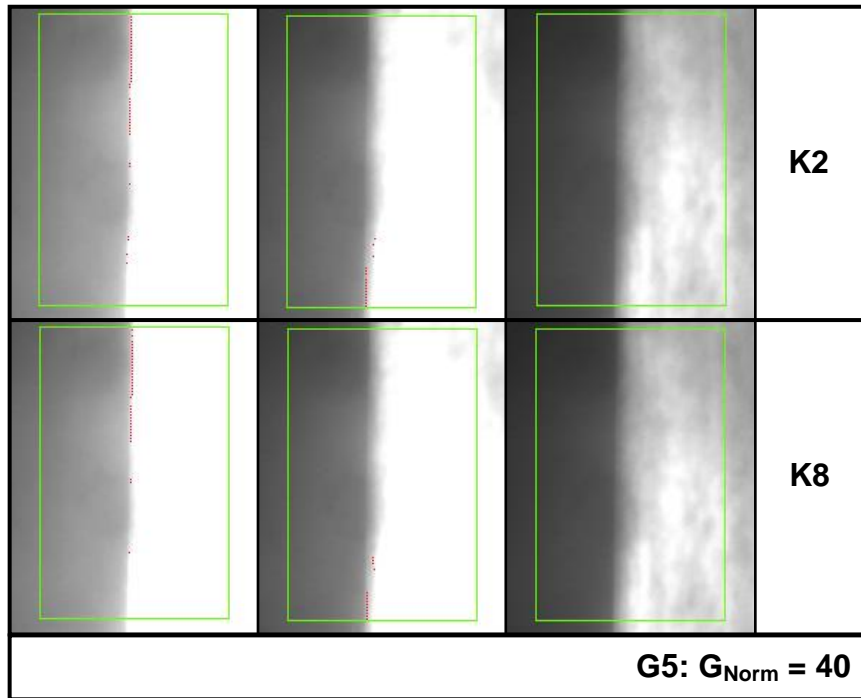
Figure 8.21: G5 Results
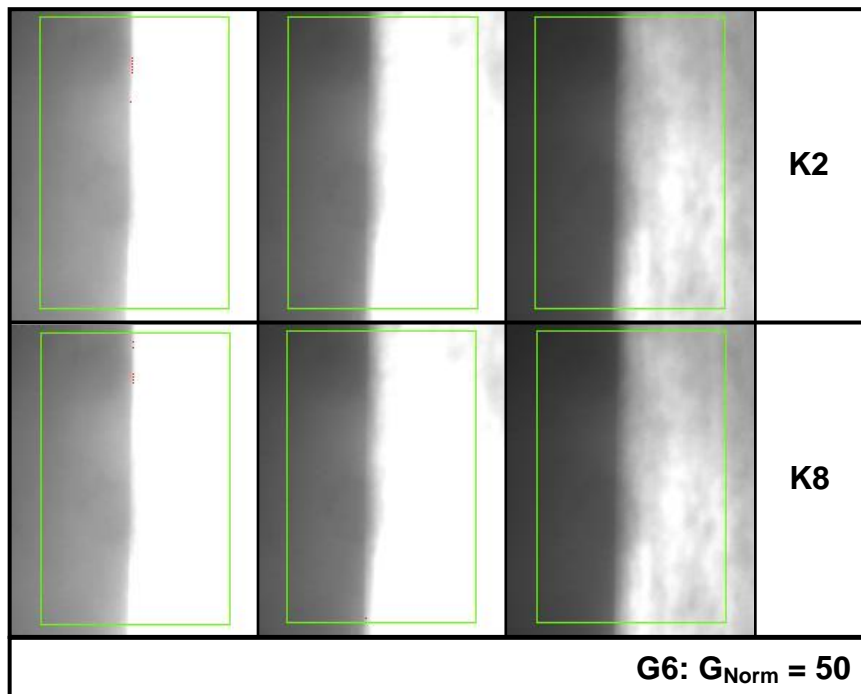
Figure 8.22: G6 Results

Figure 8.21 and Figure 8.22 show the results for the highest gradient limits, G5 and G6. The G5 results show edges all three images significantly missing, although some of the edges in

the brightest image were still identified. The G6 results show that only a few edge points were found in the brightest image and none in the other two images.

The results here demonstrate how the number of edge points found varied with the gradient limit. These results show that the optimal limit lies between G2 and G3, where a good population of edge points was identified on the strip edge without being obscured by noise. Note that the gradient limit used for the kernel test ($G_{Norm} = 16.7$) was between G2 and G3.

The results here also show that the brightest image was more flexible in terms of settings changes due to the large and clear change in brightness values. This highlights that the exposure and iris on the camera should be set as high as possible (without causing blooming and more edge distortion) to ensure the images are as bright as clearly defined as possible for the analysis.

Recovery between strips

One important aspect of the analysis software was the ability to restart measurement when the image view was lost. The best example of this was in between strips when the camera would have no previous reference for strip position and the width of the incoming strip could change. In these cases the software had to quickly evaluate an estimation of strip position and width for use in the image analysis method. Figure 8.23 shows four frames under analysis as a strip comes into view of the camera.
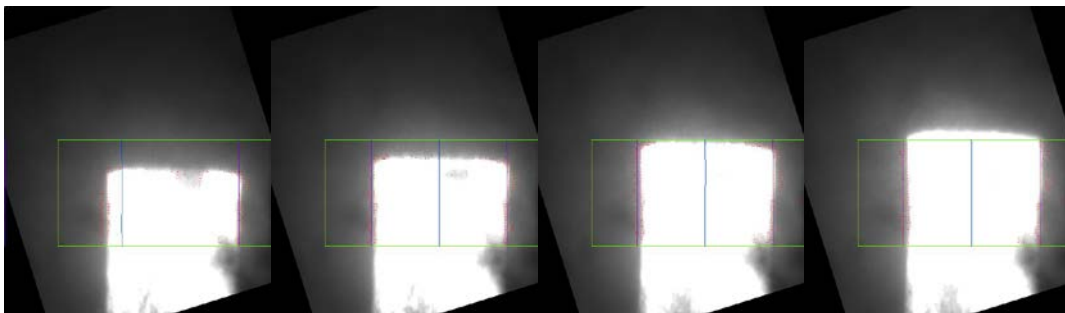
Figure 8.23: First estimation of strip width and position

In the first frame, the strip was not completely in view of the ROI (green rectangle) and the edges (blue lines) were not correctly defined. By the second frame the software had identified the strip edges correctly, and in the third and fourth frames the strip passed completely into view the software maintained a good measurement of strip position.

The process demonstrated in Figure 8.23 was a result of the reset process and width estimation method discussed in Chapter 7. As demonstrated here, this allowed the software to quickly restart measurement correctly when a new strip came into view.

Position measurement

The main task of the strip tracking system was to measure strip position. The method for determining mill centreline offset was never created in this version of the system so no absolute measurement of strip position was possible, however relative measurements could be found. Results presented in this section have been normalised to zero around average location and not mill centreline.

During the evaluation and development stages a pattern in strip movement was frequently observed, that the strip would undergo a large sudden change in position to the left shortly after threading into stand 3 (at the top of the image view area). It was determined that the movement was caused by the strip running up against the stand 3 entry side guides, which moved shortly after threading. During threading, the side guides would typically be held wide open to give the strip a large space to enter. After the strip threads, the side guides would be moved in to narrow the distance between them for rolling the strip.

The strip movement occurring due to side guide movement provided a good reference point to evaluate the software measuring strip movement. Figure 8.24 shows a graph of strip position data plotted with side guide reference position as an example of this. Data has been normalised in this example to allow for a direct comparison.
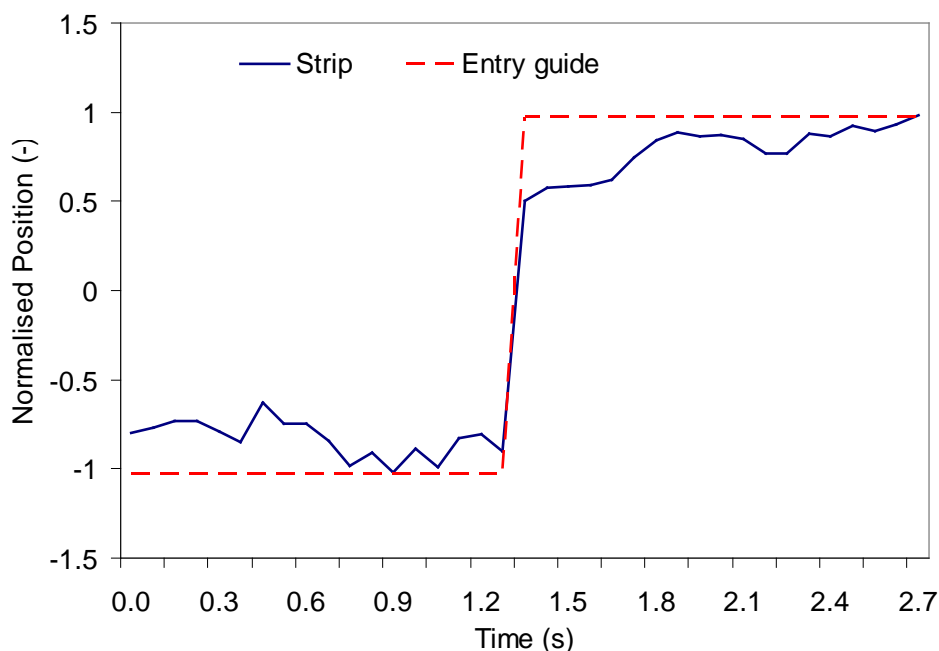
Figure 8.24: Normalised position of side guide and strip

The graph shown in Figure 8.24 demonstrates the measurement of position in the strip head, where the strip brightness was highest. Measurement along the entire length of the strip had to allow for the variation in images from the head to the tail as cooling water levels varied. A measurement of position along the length of a strip is shown in Figure 8.25, which is plotted with the measured width for that strip.
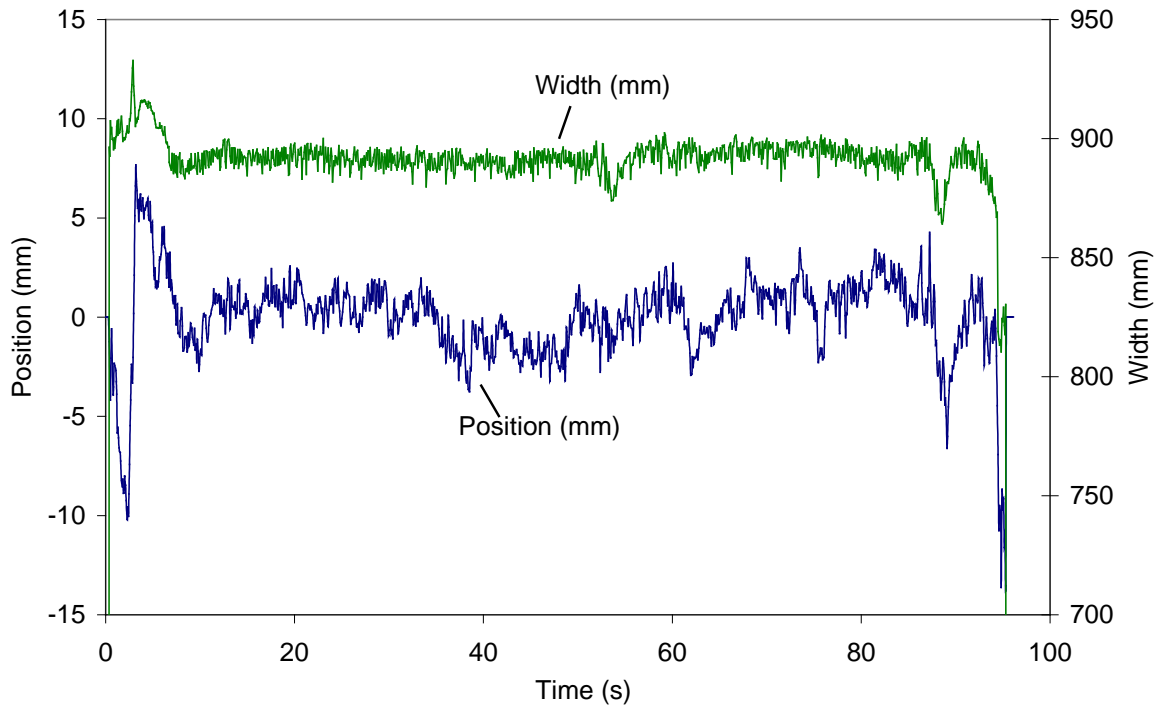
Figure 8.25: Position and width measurement

The position measurement shows some high frequency noise as well as more significant slower movements and appears to show a good measurement of strip position. However, looking at the width measurement, the early results are high before stabilising at about 10s, with a few more spikes later in the strip. The high measurement shown here was due to the strip edge being determined off the edge of the strip. Images from this strip are shown in Figure 8.26, where A is from the high measured region and B is after the width had stabilised.
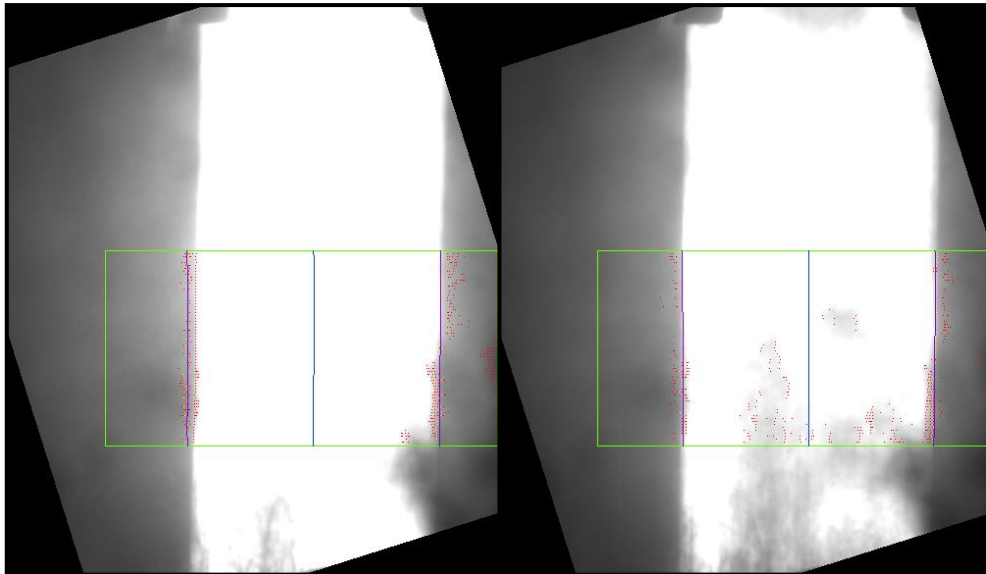
A: Width measured too wide   **B: Width measured correctly**

Figure 8.26: Width measurement

It can be seen that in A the left edge of the strip has been measured too far off the strip, whereas B was a correct measurement. It is likely that the image exposure was set slightly too high, causing some visible blooming in the image, and the gradient limit set too low therefore the blooming was determined as significant edges.

The software had not identified the incorrect measurement of width automatically because the original estimation of strip width and position was not based on production knowledge of the strip being rolled. Note that this strip is the same as in Figure 8.23 where the first estimation of strip width can be seen to be slightly to the left as in Figure 8.26(A).

Image variation

The effect of kernel and gradient limits has been demonstrated and it was noted that the best kernel and gradient limit would be one that found edge points clearly identifying strip edge for the entire range of images. Figure 8.27 shows a graph of strip position measurement, performed in an early analysis with a kernel and gradient limit not suited to the entire length of the strip. The data in this graph has been normalised to the mean.
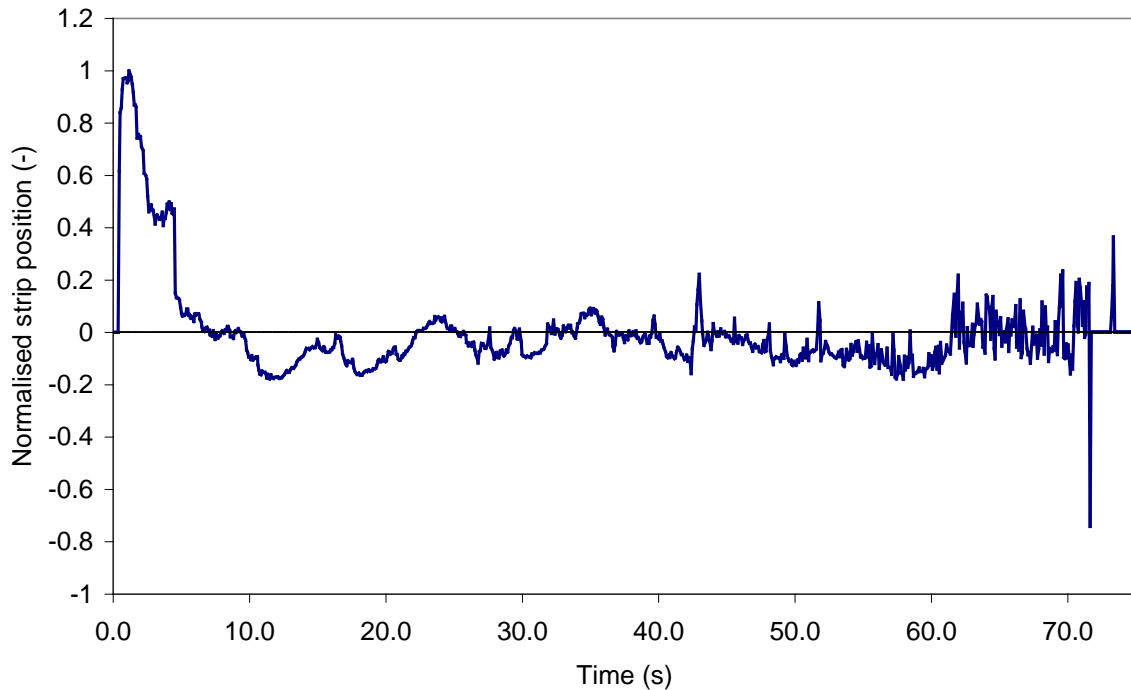
Figure 8.27: Strip position measurement for variable image

The early portion of the graph shows the characteristic step change in position as the stand 3 entry guide was moved into rolling position. Following this, there was a period of around 30 seconds where the system gave reasonably smooth measurements of position with little noise. The point the cooling water was turned on is clearly visible in the data where measurements were largely overcome with noise.

The data in this graph was taken before the 12mm lens was replaced with an 8mm lens and with the iris not open enough, hence the strip in the last section was too dim to determine the strip edge above the cooling water. Although the main causes of poor quality images were rectified for later measurements, this graph highlights the problem of image variation and the necessity for a good analysis configuration.

8.3 Evaluation

At the beginning of Chapter 5 a base specification of the measurement system was presented. To evaluate the performance of the measurement system, the final configuration was compared to this base specification

The key aim of the measurement system was to be able to run the analysis method described in Chapter 4. The analysis software was developed in National Instruments LabVIEW and compiled to an executable file included in an install package which was easily distributed to

the target computer. The developed software could be used to perform the analysis on any camera connected to the measurement system, although was designed to be used with GigE cameras. The computer chosen for the measurement system was a National Instruments PXI-8110 running the Microsoft Windows XP operating system in the final configuration. The computer was chosen to support the original system configuration, with the Hypervisor and XP/RT operating system setup, but provided a suitable platform for the XP configuration. In this aspect, the system has met the specifications.

The measurement system had to be robust; to suitably protect the hardware from the mill hazards and tolerant to the electrical noise on the mill.

The PXI itself was housed in the main computer room so was suitably protected from any hazards.

The enclosures performed well at protecting the camera from heat and water, once the improvements to sealing had been made. However, the air barrier on the window was not adequate. Dirt and grease continually accumulated on the enclosure window, causing a deterioration in image quality.

The connection to the camera was seen to be unreliable, and suspected to be a network related problem. The precise cause of the issue was not determined but it is possible it was due to electrical noise on the mill. If this was the source of the problem, then the system would not have met requirements for being noise tolerant.

In terms of robustness, the system did not meet the requirements. Although the cameras were suitably protected, the dirt accumulation and potential electrical noise problems seriously impaired system performance.

The computer system had to be stable to provide a reliable platform. The original Hypervisor configuration was seen to be unstable and unreliable, hence the system was converted to a Windows XP system. Following the change in configuration, the computer was proven to be stable and run for long periods of time without problem. The stability of the computer system in XP configuration satisfied the specification.

The specification stated that the system should be able to perform at least one measurement every 20ms with an error of less than 2mm.

System measurement speed was highly variable depending on the system settings. The analysis ROI, camera ROI and number of scan lines were most significant in variation of

analysis time, but also the number of edges identified in the image also was a factor. Additionally, the inclusion of the slow image rotation method increased analysis time. Due to all these factors, it was not possible to provide a precise measure of image analysis time, however with the system set up in operating mode and successfully measuring strip position, analysis was observed typically between 10ms to 15ms. This observation proves the ability of the system to perform analysis at the specified rate and it is anticipated that analysis speed could be further improved following some software and settings modifications.

The system accuracy was dependant on the effectiveness of the analysis method to determine the strip edge and also the area of image acquired by the camera. With the 8mm lens fitted in the final configuration, the camera had an accuracy of 3.5mm/pixel. Using the data from Figure 4.13, it is estimated that 60% of measurements were within 2mm. System accuracy could be improved by using a camera with a higher resolution and to use a more suitable lens which would view the full strip width, but without cutting off either edge.

The acquisition rate was satisfactory according to the specification, but the system accuracy was estimated to be slightly poorer than specified but could be improved.

To integrate with the mill systems, analogue voltages were specified for the Llanwern steel mill and OPC network variables for the Port Talbot mill. The provision to provide analogue outputs was provided with a card in the PXI, although the functionality was not programmed because the system was used in Port Talbot. The results were made available as OPC variables on the plant network so the specification was satisfied.

To be fully effective, the strip tracking measurement system had to be able to measure position on all seven stands. The work presented here was a small scale development system with a single camera used in the final configuration. The software was designed to allow for all seven stands, with OPC variables assigned for each stand. The system was also designed to be flexible by automatically determining the number of connected cameras on the system, and only requiring the analysis be configured and the camera name assigned to the OPC variable. The GigE camera communication protocol also supported this flexibility as new cameras could simply be plugged into the existing network, without requiring extra cabling and connections at the PXI, although new cabling at each stand would be required. The flexibility of the system and allowance for all seven stands means that this part of the specification was satisfied.

The evaluation has shown the system has not fully met the specifications. The core functionality of the system and analysis method were satisfactory, but implementation and installation problems with the hardware prevented the system operating to full capacity.

8.4 Conclusions

The strip tracking measurement system was critically evaluated and analysed to determine the effectiveness of the system as a whole and particularly the image analysis method and software created for this task.

The camera was the source of images for the measurement process and critical to the system operating correctly as the measurement was dependant on having images of the strip. The installed camera centreline was at an angle to the strip so limiting the effectiveness of the software. Additionally, the camera enclosure window was subject to accumulation of dirt, reducing the quality of the images.

The software in the system has been shown to operate correctly as part of the overall system, automatically configuring on system restart, saving results and images to the local hard drive and communicating results to the central plant computers.

The use of the kernel for edge detection was shown to be effective in noisy images, allowing the edge location to be identified and operating better than a simple discrete differentiation by introducing a weighted wide range differentiation. The choice of kernel was seen to be important to achieve correct performance, but had a large degree of flexibility. It was seen that the kernels with the highest range of weightings produced the best results. Edge detection was fundamentally easier on brighter, better defined images, where choice of kernel and gradient limit was less significant. For the example data set, a normalised gradient limit of $10 < G_{Norm} < 20$ was shown to produce the best results.

An initial position estimation method was used to gain an estimation of position when the strip first came into view. This provided the software with a value with which to compare the determined edge positions for the fitting of the Bezier curve to the strip edge.

The system was shown to measure strip position, but in some instances the edge was determined to be placed incorrectly. The incorrect edge determination was identified by

comparing position to the measured value of strip width. The actual strip width was not available to the software so could not be used proactively to identify an incorrect measurement.

The evaluation of the system against the initial specifications showed that the specification was partly met but not completely satisfactorily. The major points causing difficulties for the system were hardware related. The analysis method has proven to be effective in principle but highly influenced by the supporting hardware. Without a robust and reliable hardware configuration providing consistent good quality images to the software, the analysis system would struggle to function accurately.

9 Conclusions and Further Work

9.1 Conclusions

This thesis has been the description of work done in a project whilst pursuing an Engineering Doctorate (EngD). This project was conducted with Corus Strip Products UK, who were taken over and changed their name to Tata Steel Strip Products UK during the project. The work in this project was to investigate strip tracking in the hot strip mills; the lateral movement of the steel strip as it is being rolled.

The primary aim in the project was the development of a strip tracking measurement system, which was described in Chapters 3 to 8. This measurement system was a vision-based system, using cameras to acquire images of the strip as it was being rolled. The images were then analysed using a bespoke image analysis technique, using a novel combination of image analysis methods.

As a secondary aim of the project was the development of a computer simulation to model lateral strip movement during rolling, described in Chapter 2. This model was developed to further understand the dynamics of strip tracking and potentially as a base for the development and testing of an automated strip tracking control strategy. The model introduced the ability to simulate variable, non-linear rolling parameters across the strip width to assess the effects on tracking stability. The model was not completed to a point where satisfactory results could be gained but an evaluation of the model "as is" was provided in Appendix B. The modelling work was not considered a primary aim of the project, with the majority of work dedicated to the development of the measurement system. Therefore, shortcomings in the model were not considered to be failings in the project as a whole. The modelling theories and evaluation were included in this thesis to provide a reference point and framework for further study and to demonstrate an understanding of the root causes and dynamics involved in strip tracking.

The measurement system was critically evaluated in Chapter 8. The conclusions from that evaluation process are as follows:

- The camera was the source of images for the measurement process and critical to the system operating correctly as the measurement was dependant on having images of the strip. The installed camera centreline was at an angle to the strip so limiting the effectiveness of the software. Additionally, the camera enclosure window was subject to accumulation of dirt, reducing the quality of the images.

- The software in the system was shown to operate correctly as part of the overall system, automatically configuring on system restart, saving results and images to the local hard drive and communicating results to the central plant computers.

- The use of the kernel for edge detection was shown to be effective in noisy images, allowing the edge location to be identified and operating better than a simple discrete differentiation by introducing a weighted wide range differentiation. The choice of kernel was seen to be important to achieve correct performance, but had a large degree of flexibility. It was seen that the kernels with the highest range of weightings produced the best results. Edge detection was fundamentally easier on brighter, better defined images, where choice of kernel and gradient limit was less significant.

- An initial position estimation method was used to gain an estimation of position when the strip first came into view. This provided the software with a value with which to compare the determined edge positions for the fitting of the Bezier curve to the strip edge.

- The system was shown to measure strip position, but in some instances the edge was determined to be placed incorrectly. The incorrect edge determination was identified by comparing position to the measured value of strip width. The actual strip width was not available to the software so could not be used proactively to identify an incorrect measurement.

- The evaluation of the system against the initial specifications showed that the specification was partly met but not completely satisfactorily. The major points causing difficulties for the system were hardware related. In principle, the analysis method has proven to be effective in principle but highly influenced by the supporting hardware. Without a robust and reliable hardware configuration providing consistent good quality images to the software, the analysis system would struggle to function accurately.

9.2 Further work

The work undertaken for this project has been shown to have some limitations and improvements the measurement system have been proposed in Chapter 8. The computer modelling work has the scope for further development and included for reference purposes. The implementation and evaluation of the model was given in Appendix B, including further work to improve the model.

The suggested improvements from both the measurement system and the model are summarised in the following. Also, some additional suggestions for further work in the field are made which have not otherwise been covered.

9.3 Measurement system further work

The measurement system comprised of hardware and software components. The suggested improvements are presented in the following.

9.3.1 Hardware

The hardware performance of the measurement system was the most significant contributor to poor performance. Although designed to be robust, the image analysis software required a certain quality of images from the camera to operate satisfactorily. The misalignment of the cameras did significantly limit the performance of the system by requiring a software component to rotate the images and also only allow full evaluation on narrow strips. However, the misalignment was seen as an installation problem and not a fundamental system design problem, but it should be ensured that the camera be installed correctly.

The ineffective air barrier on the camera enclosures was detrimental to image analysis, although did not completely prevent the ability to perform measurements. To prevent the accumulation of dirt on the screen a more effective method would be required. Figure 9.1 shows a camera enclosure which was used in the hot mill in the Tata IJmuiden steelworks[55].
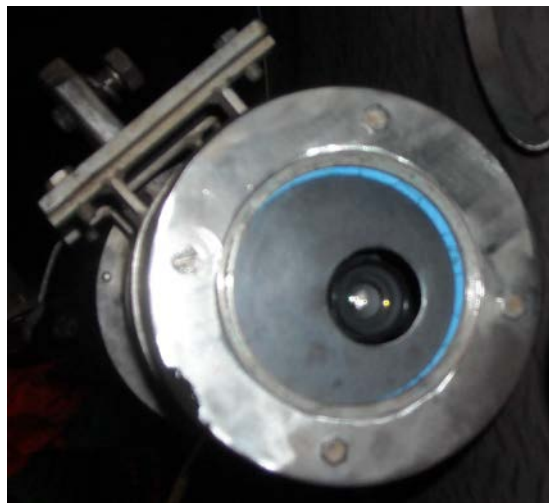
Figure 9.1: Camera enclosure in IJmuiden

The enclosure shown here had a single small hole in the front for the camera to view through. Pressurised air was blown into the enclosure and out of the view hole, providing a more concentrated stream of air to blow away debris directly around the camera. A similar solution could prove effective for the system described here, although it is thought that the camera would be vulnerable with no glass protecting against heat and other hazards.

9.3.2 Software

The software method described has been shown to be effective at measuring strip position, although could be improved to be more robust.

The measurements presented in this thesis have been relative measurements with reference to the image frame. This was because a method to create a reference to a point on the mill was not completed. In order for the system to provide a signal suitable for a control application, this step must be completed. It is suggested that the reference be to a static point on the mill, or to use the entry side-guides of the downstream stand.

Variable control of image exposure could be used to help compensate for the variation in brightness due to cooling water. The evaluation of the analysis technique has shown that the brighter images tended to have more defined strip edges, allowing more flexibility for the analysis settings and hence a wider tolerance for effective settings. There are a number of concerns with automatic exposure control however. Implemented incorrectly, image exposure would not adapt quickly enough to variation in brightness and could result in blooming from over exposure as the strip first enters the view. The other concern is that image analysis time would increase due to additional complexity and the time taken to change camera settings.

The example given of position measurement in section 8.2.2 showed the width measurement of the strip varying, and this variation was a useful sign that the measurement may not be accurate because the strip edge was determined to be in the wrong place. By using knowledge of the strip width being rolled, the measurement system would be able to have a further check on the results being generated, and hence be able to decide whether they could be trusted or whether the measurement should be reset.

The addition of the rotate image option to overcome the problem of camera misalignment was done quickly due to time constraints. The rotation of the image was a relatively slow process so when enabled would slow the entire image analysis process down. The following options could be used to improve system performance:

- Ensure the camera is aligned to the strip rolling direction correctly. This is the most simple solution but also the most inflexible because it would not allow for any camera misalignment.

- Remove the rotate image function and instead rotate the analysis. This option should be relatively fast compared to rotating the image

- Perform the analysis in 2D rather than 1D. This option would be most flexible as the amount of rotation would be automatically be accounted for in the image analysis method.

The second or third methods would be the preferred recommendations as these maintain flexibility in the software to handle rotated images. Depending on the impact on analysis speed, the third option would be most suitable. The analysis was originally designed as a 1D method intentionally to simplify and optimise the performance, given that the target would always be moving in a single direction. Given a perfect installation and maintenance of the system, ensuring the camera alignment is correct would be the most simple and effective solution, however in an industrial environment such as this that is not always realistic.

The reset process in the analysis process was used when the software determined (using a number of set measures) that the measurement was not correct and should be reset. This signal could be of use when using the results, particularly if used to control strip position, to know when the measurement could not be trusted. The Boolean reset value could be included in the set of output variables to make this data available.

The evaluation of the measurement system given here was performed using a hardware setup which was not ideal. A full and longer term evaluation would be required with the correct hardware setup and following the recommended alterations. The measurement system was designed to be used to control strip tracking and ultimately the measurements should be used in a control system to adjust the mill tilts if the measurement system is proven to be suitably robust over a long term trial. Before implementing in a full automatic control system, a suggested trial procedure is to present the live measurement of position to the operators and allow them to use their judgement and skill to determine what corrections to make. Following this, automatic control should be slowly introduced with a semi-manual monitored system, allowing the operator to take control if necessary.

The image analysis process could potentially be improved by the addition of dynamic filters pre and post image analysis. Investigation into the development and implementation of such filters would be a useful further study to improve the analysis method as a whole. Any such investigation must take into account the effect the filters would have on the analysis time and any subsequent effects on the final output data.

A pre-analysis dynamic image filter would compare the current image with previous images, using a function of the change in individual pixel values. This could help identify core image components that are relatively consistent over time, such as the strip, and isolate intermittent image components, such as cooling water. If successfully implemented, then the performance of the image analysis process could be greatly improved.

A post-analysis data processing filter was considered in Chapter 3 following the initial proof of concept studies in Llanwern. The filter used in this case was a simple first-order low-pass filter. This filter suffered from being susceptible to large amplitude high frequency noise. Investigation into the choice of a higher order low-pass filter could provide better noise rejection and improve the quality of the final output data.

9.4   Computer simulation further work

The computer model described in Chapter 2 and evaluated in Appendix B has been shown to have significant limitations. The work presented is thought to be a good base point for a tracking simulation but requires significant development in order to provide useful results.

The largest limiting factor of the model is the tracking component, which describes the lateral movement of the strip. The strip tracking model is very complex and there is a lot of interaction between different parameters. The theories used in the model require further development and refining.

A large interaction of strip movement between all the stands has been demonstrated. By expanding the model up to a full seven stands, the level of interactions and degree of upstream and downstream effects could be investigated

The control strategy demonstrated here was only a simple example of strip tracking control to show the principle of steering the strip using mill tilts with a proportional control system using single stand position feedback. To support the development of the strip tracking measurement system described in chapters 3 to 8 a robust control strategy should be developed. It is anticipated that an effective control strategy would use multiple stand position feedback for each controlled stand to allow for the interactions and dynamics of the strip throughout the whole mill.

9.5   Other further work

The simulation work undertaken by de Roo [5] noted that wider, harder, thinner, flatter strips were more laterally unstable. This was hypothesised to be due to the increased significance of

the flattening between the work roll and backup roll. A suggestion from his work which was considered but not undertaken in this project was to use FE modelling of a roll stand to verify this hypothesis and also to improve the accuracy of future and existing strip tracking models.

In the computer simulation section of this project, the principle of volume constancy was used to calculate the output shape of a strip being rolled, and was frequently used under the assumption of there being no lateral flow. This assumption can be used effectively for the modelling of the formation of camber and wedge but is not always valid, particularly during the early stages of rolling with thicker strip and under lateral constraint [6]. However, the assumption always has some level of validity and it thus follows that the camber and wedge at any point in the strip production is related to camber and wedge in previous and subsequent production stages. Hence, strip tracking cannot be considered purely as a finishing mill problem; the causes of a strip moving sideways can be from upstream processes such as the roughing mill, furnaces and caster and also actions taken in the finishing mill will effect strip tracking in the cold mill and all other downstream processes. This is a known effect, and particularly highlighted when rolling "slit slabs". These are slabs which are cast double the desired final output width, then cut down the centreline to form two slabs for rolling. During casting, a natural crown forms in the slab, with the strip centre being thicker than the edges. This is not a problem for conventional slabs and actually aids tracking stability, but when slit this thicker centre becomes an edge, and hence the slab is wedged going into the rolling mill. This wedge is either carried through the mill, or induces the formation of camber when rolled. It is recommended that a whole-process analysis of strip tracking, from caster to final product, be undertaken to determine the significance of introducing camber and wedge at all stages in the process. Such a study should also consider the validity the "no lateral spread" assumption at each stage, and hence the ability to remove wedge without inducing camber and visa-versa could be quantitatively assessed.

10 Appendices

A References

[1] Corus Strip Products UK, "*Making a difference: Llanwern and Port Talbot Works*", Corus UK Ltd., 2002

[2] Samarasekera, I.V., "*Hot Rolling*", Encyclopaedia of Materials: Science and Technology, Elsevier, 2001, pp 3836 – 3843

[3] Peal, B., "*Rolling mill metal shape*", Pfeiffer Engineering, [Date unknown: retrieved 2008]

[4] Ashley, D., Personal communication, Corus, Llanwern, 2008

[5] de Roo, J., "*Theoretical background of strip tracking and simulations with a strip tracking model*" Corus, IJmuiden, 2008

[6] Shiraishi, T., Ibata, H., Mizuta, A., Nomura, S., Yoneda, E., Hirata, K., "*Relation between camber and wedge in flat rolling under restrictions of lateral movement*", ISIJ international, Vol. 31, No. 6, ISIJ, 1991, pp. 583-587

[7] Suzuki, A. "*Recent progress in the rolling mills – Part 1*", Transactions ISIJ, Vol. 24, 1984, pp. 228-249

[8] Randall, A., "*Rolling mill control: architecture and applications*", IEE Colloquium on Industrial Automation and Control: Distributed Control for Automation, IEE, 2002, pp. 1-5

[9] Takahashi, R. "*State of the art in hot rolling process control*", Control Engineering Practice, Vol. 9, Elsevier, 2001, pp. 987-993

[10] Bush, A. et al, "*Improved quality of hot rolled coil by means of advanced control methods*", Corus, 2002

[11] Kajiwara, T., "*System and apparatus for effecting a correction of deflection of strip steel from its normal path of travel in a tandem rolling mill*", US Patents Office, Patent 3491562, 1970

[12] McCarthy, J. A., "*Method and apparatus for steering strip material through rolling mills*", US Patents Office, Patent 3587263, 1971

[13] Marushita, Y., Ikeda, H., Yano, K., Tsukiyama, M., "*Method and apparatus of stably controlling rolling mill*", US Patents Office, Patent 6082161, 2000

[14] Kimura, T., Tagawa, M., "*Automatic steering control of strip rolling mills*", The Hitachi Review, Vol. 65 No. 2, Hitachi, 1983, pp. 25-30

[15] Okamura, Y., Hoshino, I., "*State feedback control of the strip steering for aluminium hot rolling mills*", Control Engineering Practice, Vol. 5, No. 8, Elsevier 1997, pp. 1035-1042

[16] Kiyota, T., Matsumoto, H., Adachi, Y., Kondo, E., Tsuji, Y., Aso, S., "*Tail crash control in hot strip mill by LQR*", Proc. American Control Conference, IEEE, 2003, pp. 3049-3054

[17] Okada, M., Murayama, K., Anabuki, Y., Hayashi, Y., "*VSS control of strip steering for hot rolling mills*", Proc. 16th IFAC World Congress, IFAC, 2005

[18] Malloci, I., Daafouz, J., Iung, C., Bonidal, R., Szczepanski, P., "*Switched system modelling and robust steering control of the tail end phase in a hot strip mill*", Nonlinear Analysis: Hybrid Systems, Vol. 3, Elsevier, 2009, pp. 239-250

[19] Naumann, N., Moretto, C., Iung, C., Koschack, U., "*Steering control at Arcelor Eko Stahl finishing HSM*", Steel Times International, Quartz Business material Ltd., 2007, pp. 38-42

[20] Malloci, I., Daafouz, J., Iung, C., Bonidal, R., Szczepanski, P., "*Robust steering control of hot strip mill*", IEEE Transaction on Control Systems Technology, Vol. 18, Issue 4, IEEE, 2010, pp. 908-917

[21] De Roo, J., "*Simulation of automatic tilt control in a seven stand finish mill: Control by using a limited amount of CCD cameras*", Corus, IJmuiden, 2009

[22] Kikuma, T., Matsumoto, H., Tagawa, M., Kajiwara, T., Kimura, T., Iida, Y., Yoshimoto, K., "*Method and apparatus for controlling snake motion in rolling mills*" US Patents Office, Patent 4700312, 1987

[23] Tibbs, M., Ziegelaar, J.A., "*Strip steering*", US Patents Office, Patent 61291236, 2000

[24] Brown, K.J., "*A study of strip tracking in the finishing train of a wide hot strip mill*", British Steel Corporation, London, 1991

[25] Oliver, K., Steeper, M., "*Hot flat rolling mill stand and control method and apparatus therefore*", World Intellectual Property Organization, Patent WO 99/12670, 1999

[26] Oliver, K., Steeper, M., "*Hot flat rolling mill stand and control method and apparatus therefore*", US Patents Office, Patent 5996384, 1999

[27] Oliver, K., Steeper, M., "*Automatic strip steering and control system for a rolling mill*", UK Patent Office, Patent 3239264, 2000

[28] Gonzalez, R.C., Valdes, R., Cancelas, J.A., "*Vision based measurement system to quantify straightness defect in steel sheets*", Proceedings 9th Intl. CAIP, 2001, pp. 427-434

[29] Montague, R.J., Watton, J., Brown, K.J., "*A machine vision measurement of slab camber in hot strip rolling*", Journal of Materials Processing Technology, Vol. 168, Elsevier, 2005, pp. 172-180

[30] Morris, A.J., "*Port Talbot Hot Mill camber cameras: first measurements*", Tata Steel RD+T, Port Talbot, 2010

[31] Ferreira, A.B.S., "*Adaptive fuzzy logic steering controller for a Steckel mill*", https://ujdigispace.uj.ac.za/bitstream/handle/10210/2164/909220186.pdf, University of Johannesburg, 2005, cited 09/02/2010

[32] O'Leary, P. "*Machine vision for feedback control in a steel rolling mill*", Computers in Industry vol. 56, Elsevier, 2005, pp. 997-1004

[33] National Instruments, "*NI Vision concepts manual*", National Instruments, 2007

[34] Basler Vision Technologies, "*The elements of GigE Vision*", Basler, 2010

[35] Litwiller, D., "*CCD vs. CMOS: Facts and fiction*", Photonics Spectra, Laurin Publishing, 2001

[36] Ginzburg, V.B., "*Steel-rolling technology: Theory and practice*", CRC Press, New York, 1989

[37] Schurmans, J., "*Control Audit Hot Strip Mill Llanwern*", Corus, Llanwern, 2004

[38] Jones, K. Personal Communication, Corus, Port Talbot, 2009

[39] Benson, R.C., "*Lateral dynamics of a moving web with geometrical imperfection*", Journal of Dynamic Systems, Measurement and Control, Vol. 124, ASME, 2002, pp. 25-34

[40] Tarnopolskaya, T., Gates, D.J., de Hoog, F.R., Yuen, W.Y.D., "*Instability in lateral dynamics of a metal strip in cold rolling*", Australian and New Zealand Industrial and Applied Mathematics Journal, Vol. 46, Australian Mathematical Soc., 2005, pp. C987-C1000

[41] Tarnopolskaya, T., Yuen, W.Y.D., "*Analysis of the effect of tension at the entry of cold rolling mill on the stability of strip tracking*", ISIJ International, Vol. 45, No. 9, ISIJ, 2005, pp. 1316-1321

[42] Tarnopolskaya, T., Gates, D.J., "*Analysis of the effect of strip buckling on stability of strip lateral motion with application to cold rolling of steel*", Journal of Dynamic Systems, Measurement and Control, Vol. 130, ASME, 2008, pp. 1-7

[43] Tarnopolskaya, T., Gates, D.J., "*Linear theory for lateral displacements of a metal strip in tandem cold-rolling mill with asymmetries*", Journal of Mechanical Engineering Science, Vol. 222, IMechE, 2008, pp.1131-1148

[44] De Roo, J., "*Theoretische beschijving van het bandloopmodel*", Corus, IJmuiden, 2008

[45] De Roo, J., Personal communication, Corus, IJmuiden, 2008

[46] http://www.keyence.co.uk/products/vision/machine/cv3000/cv3000.php, cited 19/5/2011

[47] Carruthers-Watt, B.N., Xue, Y., Morris, A.J., "*A vision based system for strip tracking measurement in the finishing train of a hot strip mill*", Proceedings of the International Conference on Mechatronics and Automation, Xian, IEEE, 4th-7th Aug 2010, pp.1115-1120

[48] Cohen, E. et al., "*Geometric modelling with splines*", A.K. Peters, Natick, 2001

[49] Kreyszig, E., "*Advanced engineering mathematics*", Wiley, New York, 1999

[50] Basler Vision Technologies, "*Basler Scout*", Basler, 2009

[51] VideoTec, "*NXW Special stainless steel liquid-cooed enclosure*", VideoTec, 2009

[52] OPC Task Force, "*OPC Overview*", The OPC Foundation, 1998

[53] National Instruments, "*Running a LabVIEW Application as a Windows NT/2000/XP User-Defined Service*", http://tinyurl.com/3yeas4g, Accessed 01/07/2010

[54] http://www.iconics.com/ cited 27/7/2011

[55] Kampmeijer, L. Personal Communication, Tata, IJmuiden, 2011

[56] Gere, J.M., Goodno, B.J., "*Mechanics of Materials*", Cengage Learning, Stamford, 2009

B Evaluation of Strip Tracking Simulation

B.1 Model description

A strip tracking computer model was created using the theories described in Chapter 2. The model was created using The MathWorks Matlab and Simulink.

The model was created as a 3-stand model with the general dimensions shown in Appendix Figure 1.
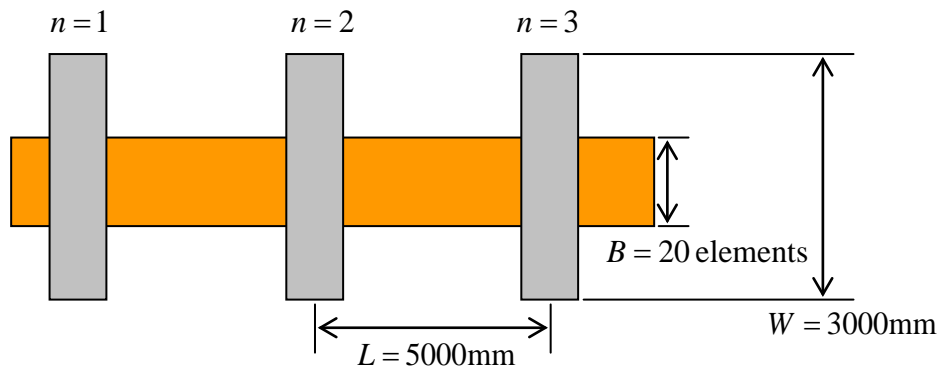
Appendix Figure 1: Implemented model layout

The general structure of the model was a separate section for each of the roll stand models and a single tracking section. This structure was adopted because the roll stand calculations and outputs were independent to one another so could be used in a modular fashion whereas the tracking model was fundamentally linked between all stands.

The simulation was used in two ways; the whole model was used to investigate tracking behaviour for parameter significance analysis and for a demonstration of tracking control, and also a single stand model was used to investigate the variation of differential force. An evaluation of the model was also performed to highlight some limitations found with the simulation.

B.2 Evaluation

The simulation was evaluated in the two component sections; roll stand model and tracking model.

B.2.1 Roll stand model

The roll stand model was built using well proven equations and theories used within the steel mill for mill setup and control. The main output of the model was the roll force, which was validated by comparison to logged mill data. Appendix Figure 2 is a histogram showing error distribution between measured force values and modelled force values for the full range of mill operation, using input and output thicknesses, strip width and rolling temperature from

the data and the other parameters set as in Appendix Table 1. The other parameters were unknown during validation but chosen to be representative of normal rolling parameters, however because of this some variation was expected between the model and the plant data. The validation results histogram shows a reasonably wide distribution of errors, however significantly centred around 0%. The results provided confidence in the roll stand model.
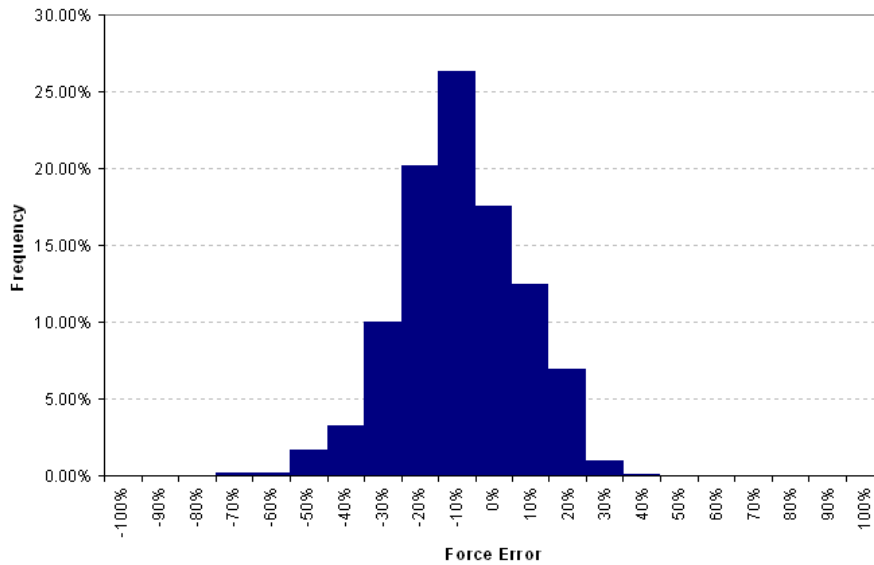
Appendix Figure 2: Distribution of errors between rolling data and model for roll force calculations

Appendix Table 1: Modelling parameters

Parameter	Value
R	350mm
Y_0	900MPa
T_m	1410°C
s_1	10MPa
s_2	10MPa

B.2.2 Tracking model

The theories used in the strip tracking model were built around various sources and relatively new research compared to the roll stand model. The inputs to the model, particularly the variation of parameters across the strip width were significantly unknown during the rolling process and not recorded in the plant data loggers, therefore it was impossible to validate the model against plant data as had been done with the roll stand model.

The tracking model could be validated in part by comparing the output results to existing tracking data and qualitative information about how the strip moves. It was expected to have up to approximately 50mm of movement side to side, with relatively slow movements of up to 20mm/s in the strip body [55][24].

During model development, tracking behaviour was seen to be very unstable and sensitive to small changes in the parameters. It was found that if the strip position exceeded approximately 1.5mm then the strip would rapidly track outside the bounds of the stand given by the model. This behaviour was identified early in the model development and much effort was put into solving the instability, however no solution could be found. It was thought that a fundamental theory of tracking behaviour was not correct, most likely the strip rotation. The instability of the model meant that the behaviour of strip movement could not be accurately described and the conclusions gained from the model were severely limited.

B.3 Results

The limitation of the strip tracking model have been highlighted in section B.2, which noted that only limited studies could be performed using the model. Three studies were undertaken;

- A small-scale tracking parameter investigation
- An example of strip tracking control
- An investigation of differential force variation

B.3.1 Tracking parameter significance

Despite the limitations, it was thought that the general behaviour described by the model was representative in part of true tracking behaviour. Therefore a small study was performed with the model by identifying a relatively stable operating region and varying a few parameters within a small stable region. This study allowed some limited relative conclusions to be drawn.

A set of standard parameters was used, chosen because they produced relatively stable results from the model. These parameters are shown in Appendix Table 2.

The value "Crown" used in the model was a percentage difference in height between the strip edges and centre with a parabolic profile and was set by varying roll radius, maintaining an average set value across the width of the strip about the roll centreline. The standard inputs set out in the table were used for all simulation runs, unless a value is stated to have been varied.

Additionally, a standard disturbance to normal rolling conditions was used of +0.001mm in the OS screw at 20s for a period of 5s. The standard disturbance was used for all simulations unless stated otherwise.

Appendix Table 2: Standard input parameters

Parameter	Stand		
	1	**2**	**3**
b (mm)	800	800	800
h1 (mm)	40	25.5	17.7
h2 (mm)	25.5	17.7	13.0
M (mm/T)	500	500	500
R (mm)	350	350	350
s_1 (MPa)	0	10	10
s_2 (MPa)	10	10	10
T (°C)	1100	1050	1010
T_m (°C)	1410	1410	1410
Y_0 (MPa)	900	900	900
Crown (%) @ b=800mm, h = 25mm	0.6	0.6	0.6

The standard input parameters were used to find a set of standard results. These results are shown in the graph in Appendix Figure 3, which shows strip position against time for all three stands.
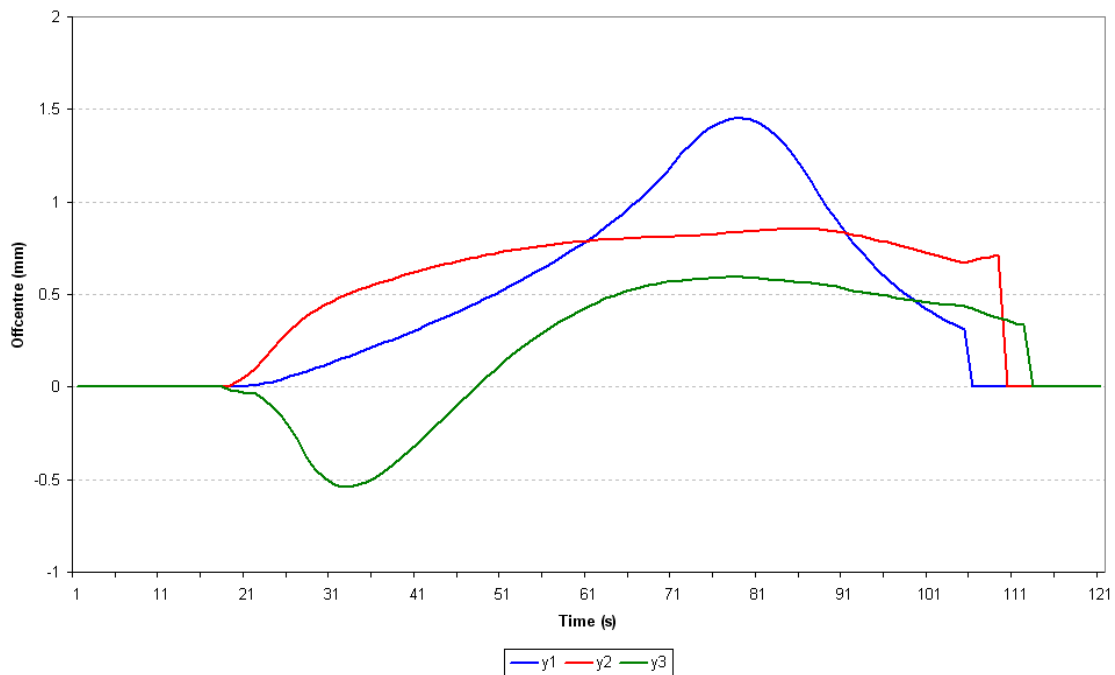
Appendix Figure 3: Graph of position vs. time for standard model inputs

From the graph, it can be seen that the strip tracked centrally (0mm) up until the disturbance at 20s, when the Stand 2 position began to move towards the OS, as would be expected because the OS gap was increased. Strand 1 followed Stand 2 in moving to OS due to the lateral forces pulling the strip sideways. Stand 3 moved towards the DS at first as a result of the rotation of the strip in Stand 2, but then gradually moved to follow the location in the other two stands.

Crown

Strip crown is the relative measure of thickness across the strip width and in practice is one of the controls available to inherently stabilise strip tracking during rolling. A positively crowned roll profile would aid strip tracking by increasing the level of deformation on the strip edges as the strip moved away from the mill centreline.

Various simulation were performed by varying the strip crown and the results for strip position in Stand 2 are shown in Appendix Figure 4. The measure of strip crown is percentage thickness difference for a strip 800mm wide and on 25mm thick on average across the width. The average value of roll radius was maintained as the value set in the standard inputs for values across the strip width from the centre of the roll.
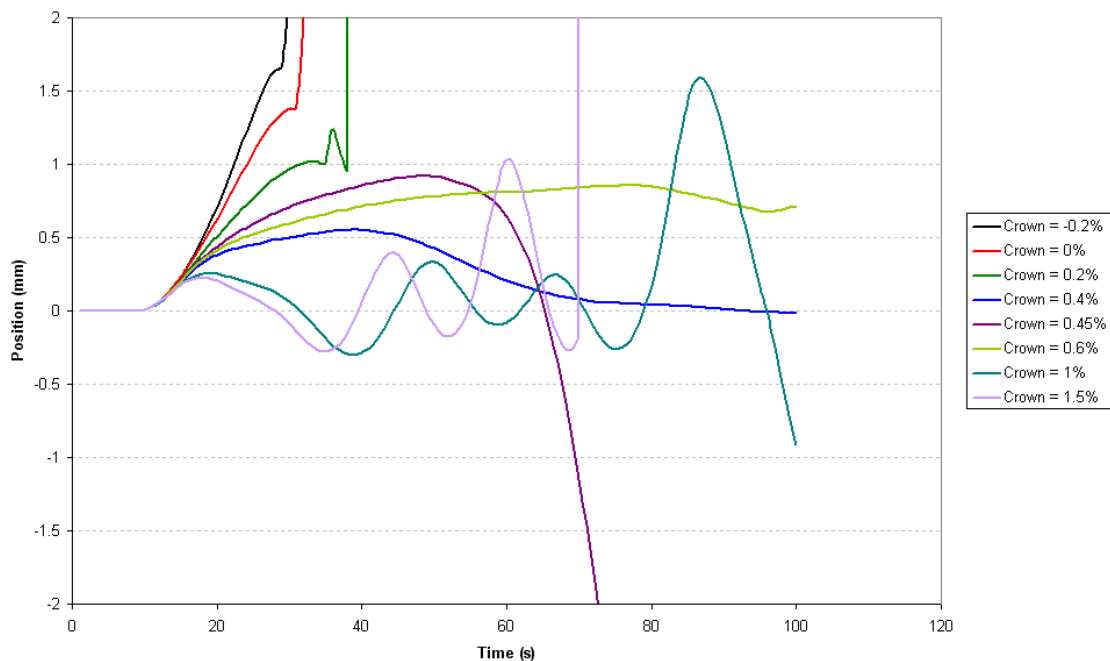
Appendix Figure 4: Graph of stand 2 position vs. time for varying levels of crown

The results from strip crown are partially as expected. The inherent stability and natural tracking control was seen to increase with strip crowning, and can be seen by comparing the results to the 0% (flat rolls) line. The only negative crown included caused the strip to rapidly move away from the centreline. As crowning increased, the strip speed was seen to decrease. At 0.4% crown, the strip moved the least and eventually returned to 0mm. The standard input of 0.6% was also seen to stabilise, although not return to 0mm. The 0.45% result is interesting because it was expected to be between the 0.4% and 0.6% curves, however the initial movement was larger than the 0.4% curve and then it rapidly moved in the opposite

direction and out of the stand. Other results in this region (not included) demonstrated similar behaviour and this was one of the signs on instability in the model.

The results for crown above 0.6% again follow the trend of increasing levels of tracking correction and a slower initial movement, however they appear to over compensate for strip off-centre and produced unstable oscillating results, again highlighting the instability of the model.

It has been noted that the 0.4% crown produced the most stable result for Stand 2 position, however the standard crown was set at 0.6%. The choice of 0.6% over 0.4% was because the position for all three stands, shown in Appendix Figure 5, was not as stable, particularly in Stand 3.
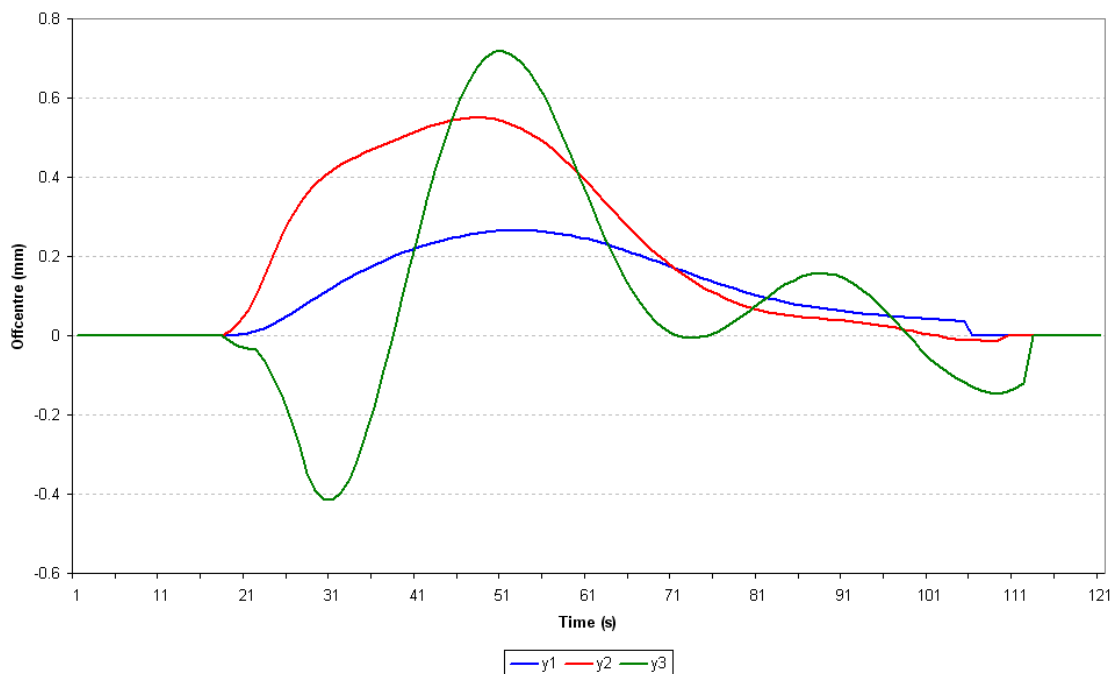
Appendix Figure 5: Graph of position vs. time for 0.4% Crown

The simulations of varying crown suggest that tracking performance is improved with increased crown, although the results are too unstable to provide more detailed conclusions.

Temperature profile

Different temperature profiles were used across the strip to investigate the effect on tracking from temperature variation. The temperature profiles used were linear "wedge" profiles across the strip width and measured as a percentage of nominal strip temperature. A positive wedge profile was the OS hotter than DS. Note that the profiles were scaled with temperature in each stand to maintain the same relative temperature profile. Also, the wedge profile was created around the strip centreline to maintain the average temperature across the width.

The disturbance used in the temperature effect simulations was not the standard screw disturbance, but instead the specified 5s temperature wedge occurred at 20s. The results are shown in Appendix Figure 6 as a graph of strip position in Stand 2 for a range of temperature wedges.
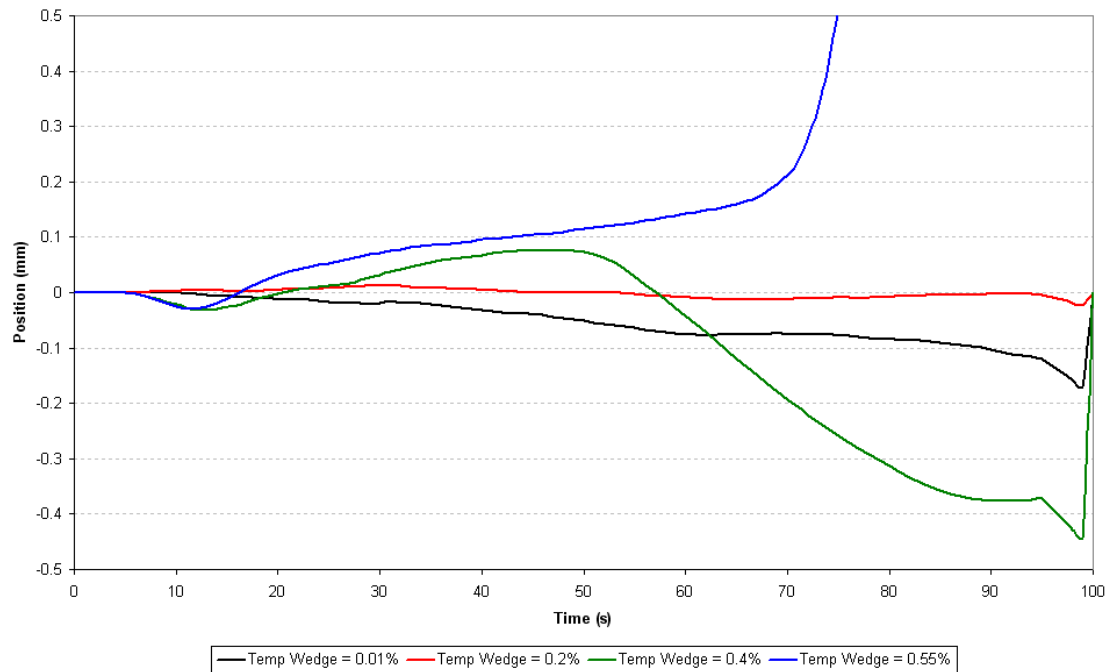
Appendix Figure 6: Graph of stand 2 position vs. time for varying temperature wedge

The temperature profile results shown a range of different behaviour. In general the amount of tracking instability appears to increase as temperature wedge increased, first deviating towards the cooler DS as the hotter and softer OS underwent more deformation. As the wedge profile magnitude increased, the strip would begin to track back towards the OS as a result of interactions with adjacent stands. At 0.2% a balance point appears to have been reached between the natural tracking characteristics of the model and the lateral deviation.

Tilt disturbance

The nature of the tilt (screw position) disturbance was investigated in three ways:

- Which stand the disturbance occurred in
- The size of the disturbance
- The total time of the disturbance

For each of these areas, the standard disturbance was modified in one area at a time to investigate the effects of each one.

Disturbed stand

The stand the disturbance occurred in was varied and the results are given in Appendix Figure 7, which shows strip position in all three stands for each disturbance location.
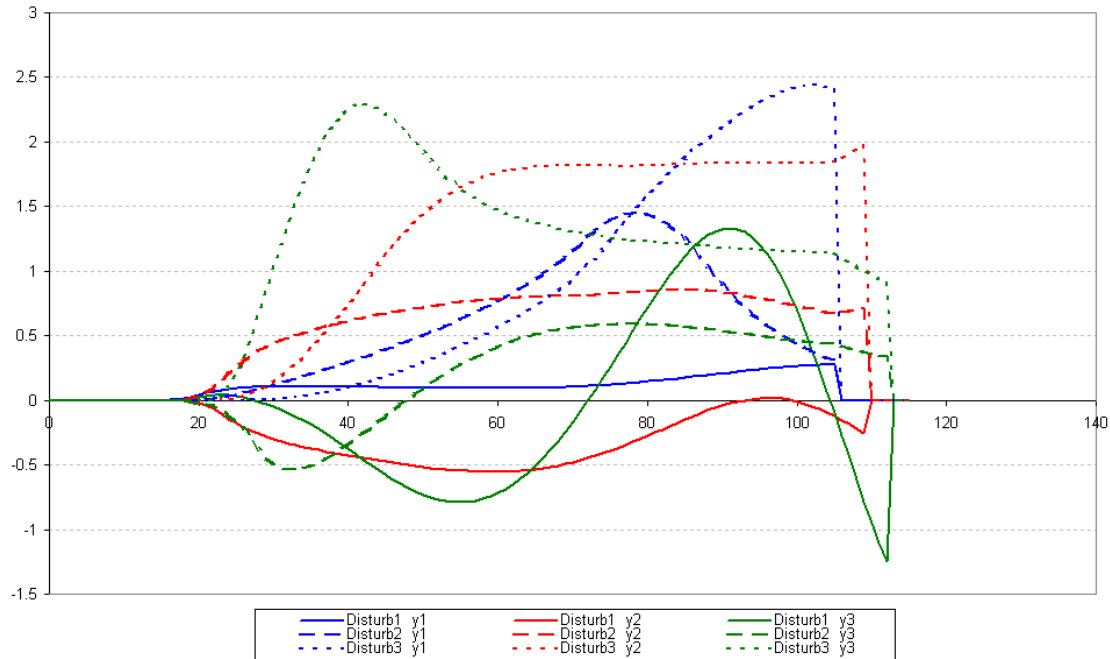
Appendix Figure 7: Graph of position vs. time for varying stand disturbance occurred in

It can be seen from the graph that in general, the maximum magnitude of strip position for each simulation was roughly the same, although when the disturbance was in the third stand the maximum position was greatest in all three stands.

The general behaviour of the strip appears to follow the same pattern that in the stand the disturbance occurred in and the preceding stand, the strip tended to move in the same direction, but for the following stands the strip would initially move in the opposite direction before moving back in line with the other stands.

Disturbance size

The magnitude of the screw disturbance was changed and the results shown in Appendix Figure 8 as a graph of strip position in Stand 2.

The results show that as the magnitude of screw disturbance increases, the initial rate and final value of strip position increase. In this simulation, the screw disturbance magnitude was limited to a value of under 0.00125mm before the model became unstable.
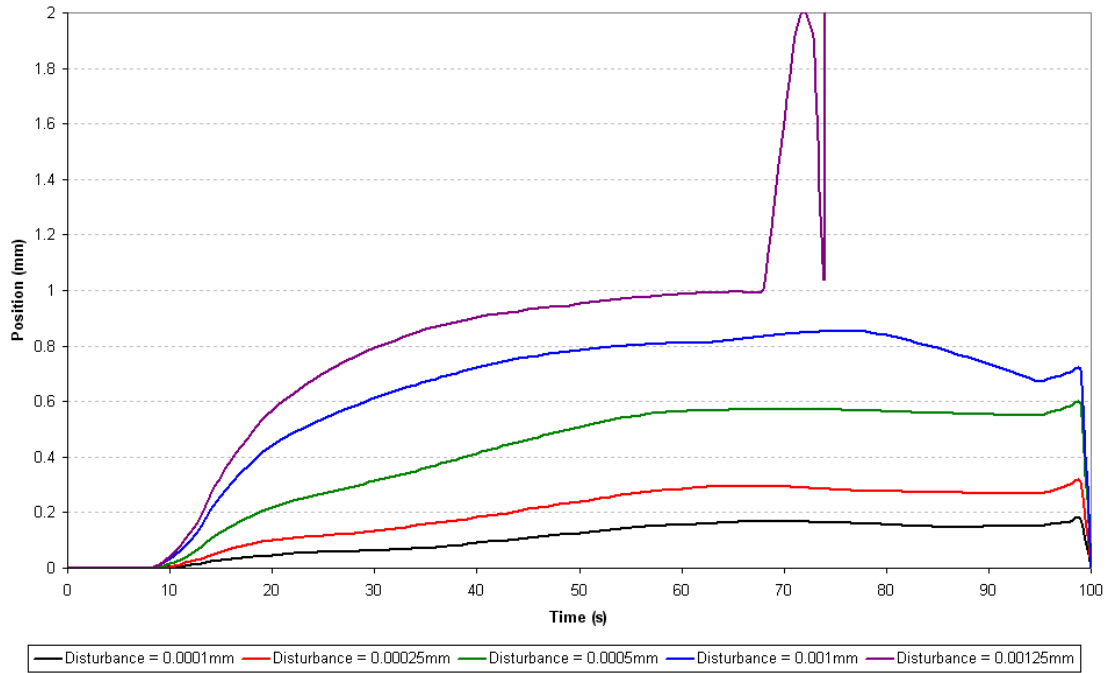
Appendix Figure 8: Graph of stand 2 position vs. time for varying levels of disturbance

Disturbance period

The disturbance period was varied and the results shown in Appendix Figure 9, which shows a graph of strip position in Stand 2. The results shown that as disturbance time increases, both initial rate of movement and final position increase. The model was limited to a disturbance time of 5s, above which the results became unstable.
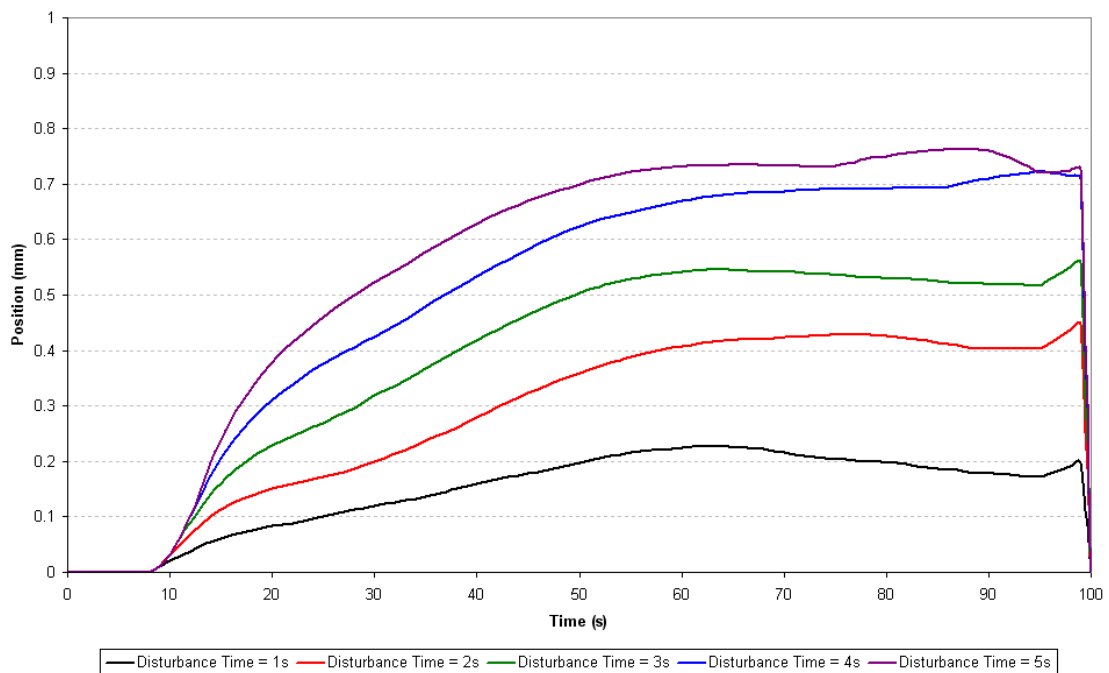
Appendix Figure 9: Graph of stand 2 position vs. time for varying disturbance periods

B.3.2 Tracking control demonstration

To demonstrate the principle of strip tracking control, a simple proportional control system was implemented. The model has been shown to be unstable and not provide an accurate measure of strip tracking behaviour, therefore only a simple control strategy was investigated for demonstration purposes as any thorough development of a control strategy would not have been relevant to the real rolling mill.

The control system adjusted the DS and OS screw positions by opposite amounts, depending on strip position in that stand. A graph showing strip position with and without control in all three stands is shown in Appendix Figure 10. The control demonstration used the standard simulation inputs and a proportional gain of 0.00001. The gain was chosen through trial and error to identify a stable control point.
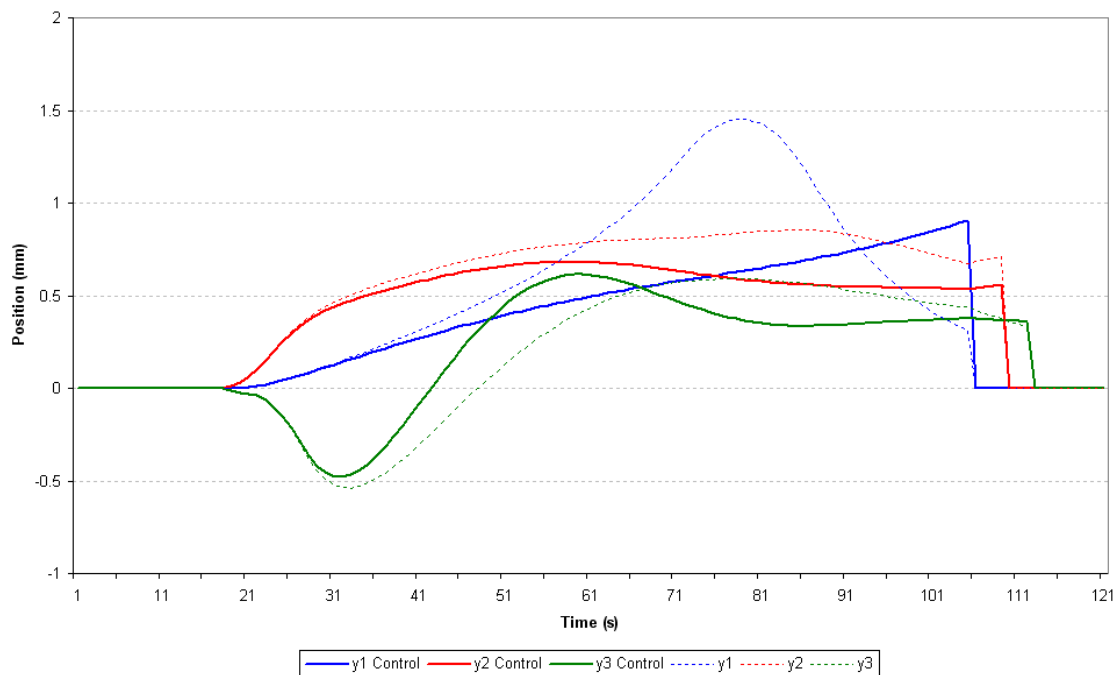
Appendix Figure 10: Graph of position vs. time with low-gain proportional tracking control enabled

In the graph, the dotted lines show the uncontrolled simulation and the solid lines show the simulation with the proportional control in place. The position in all three stands was improved with the simple control strategy in place. Stand 2 was controlled most effectively with the entire movement profile less than the uncontrolled version. Stand 3 was quickly corrected although slightly overcompensated, but the position stabilised. The Stand 1 results show a smaller total movement than the uncontrolled results, although in the simulation period there was no sign of position stabilising.

This simple control strategy was simulated to demonstrate the theory of strip tracking control by adjusting stand screws. Although the accuracy of the results is very limited, the general trend demonstrated that the principle of this control method is feasible. The results from this simple demonstration and the other strip tracking investigations suggest that a more complex strategy should be used to effectively control position. In this example, position feedback from only the controlled stand was used, however it has been shown that strip movement is dependent on the position in the neighbouring stands. It is therefore suggested that any further work in developing a control strategy use position feedback from the directly adjacent stands at a minimum, and potentially other stands in the mill as well.

B.3.3 Variation of differential force

A number of simulations were performed using only a single roll stand model to investigate the variation in differential force with unsymmetrical variation in position, temperature and input thickness. The measure of differential force can be used to control strip tracking but is dependant on factors other than position. This set of simulations was designed to highlight the effect on differential force that these other parameters have and find their significance if a differential force tracking control strategy were developed.

For the temperature and thickness deviations, a linear wedge was applied across the strip width measured as a percentage of the total edge to edge deviation of the nominal value. Positive wedge measurements were for DS values higher then nominal values. All results are presented as relative forces of DS-OS difference in force as a ratio of total roll force.

Unless stated otherwise, the input parameters for the simulations were as in Appendix Table 3

Appendix Table 3: Input parameters for differential force analysis

Parameter	Stand 1
b (mm)	1000
h1 (mm)	25
h2 (mm)	17
M (mm/T)	500
R (mm)	350
s_1 (MPa)	10
s_2 (MPa)	10
T (°C)	1100
T_m (°C)	1410
Y_0 (MPa)	900
Crown (%)	0

Position

The position of the strip was varied and the resulting differential force measured. Simulations were performed for a range of input thicknesses, measuring the reduction as the change in thickness as a ratio of total thickness. Output thickness was not changed from the value in Appendix Table 3. The results for the position variation are shown in Appendix Figure 11.
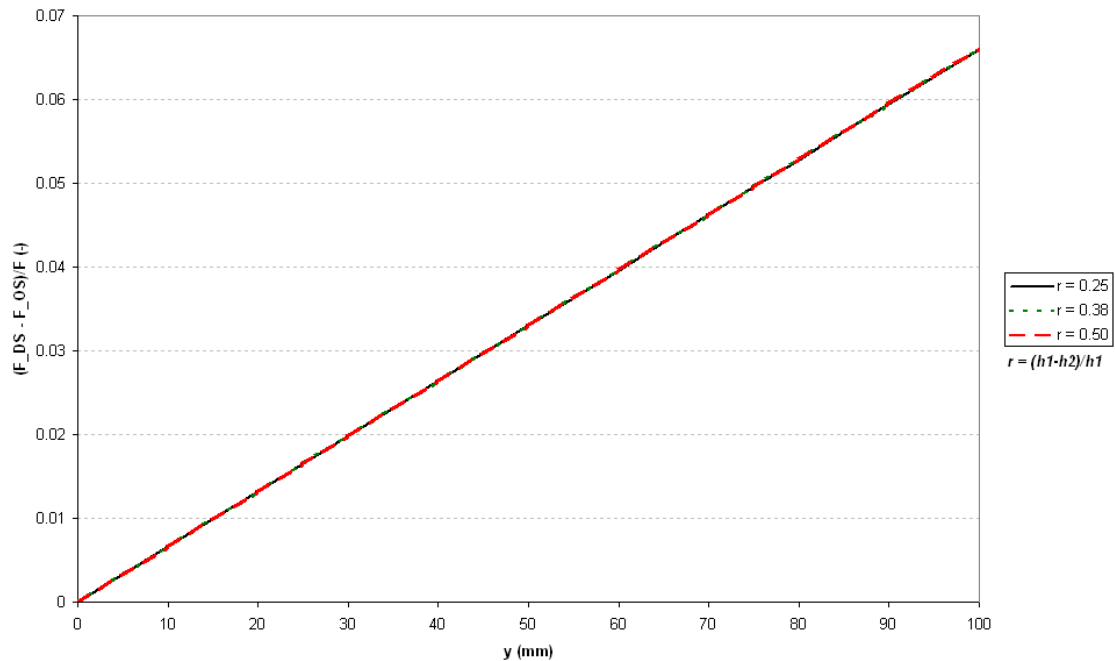
Appendix Figure 11: Graph of relative differential force vs. position for varying reduction

The graph shows a linear relationship between position and differential force, and that the relationship between the two was not affected by the amount of reduction. The differential force increased towards the side that the strip was moving. For these input parameters, 0.06% of differential force was found per millimetre of strip off-centre.

Temperature wedge

A range of linear temperature wedges were used at different strip positions. The results graph is shown in Appendix Figure 12. The results show a linear relationship between temperature wedge and differential force and that the position of the strip in the stand as independent of the relationship between temperature wedge and differential force. The graph shows a negative gradient of the lines, which shows that the force decreased on the hotter, softer edge of the strip. For these input parameters, a relationship of -0.31(% differential force)/(% temperature wedge) was seen. A temperature wedge of -0.22% is equivalent to +1mm of strip off-centre.
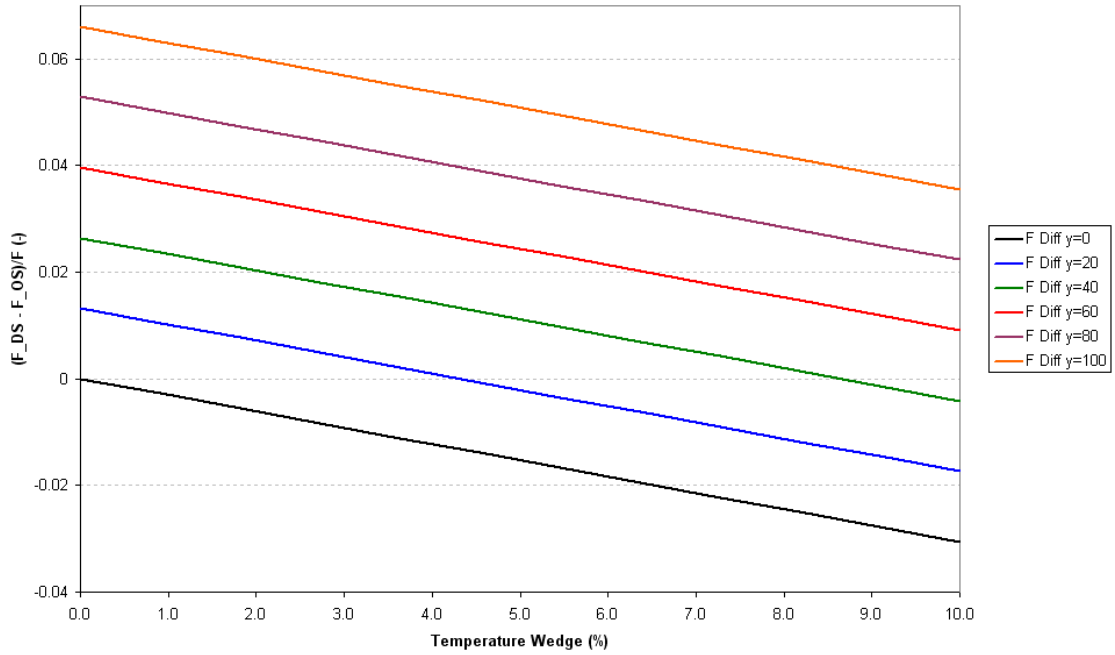
Appendix Figure 12: Graph of relative differential force vs. temperature wedge for varying strip positions

Thickness wedge

The input thickness wedge was varied and simulations performed with a range of strip positions. The results are shown in Appendix Figure 13.
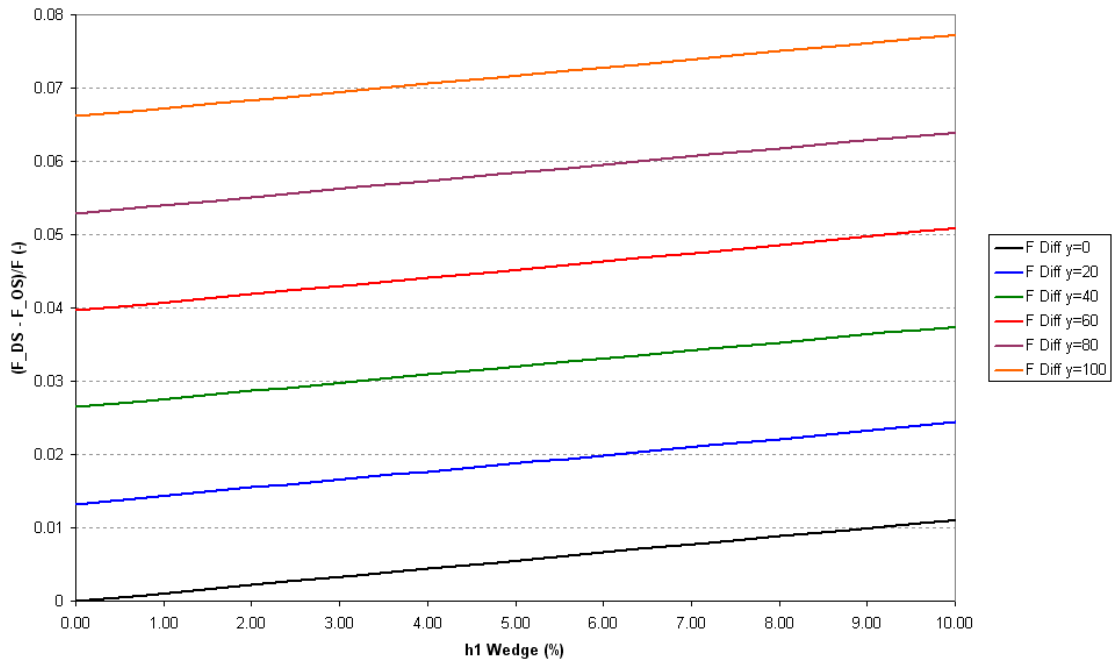
Appendix Figure 13: Graph of relative differential force vs. input thickness wedge for varying strip positions

The graph shows a linear relationship between thickness wedge and differential force, and that the relationship is independent of strip position. The force increased towards the DS as the wedge increased because the DS edge of the strip was thicker and hence required more force to deform. For these input parameters, a 0.11% differential force was seen for every 1% wedge. A 0.6% wedge is equivalent to 1mm of strip off-centre.

B.4 Conclusions

The evaluation of the model found that the tracking component was very unstable and as such results were not an accurate representation of strip tracking behaviour. The conclusions that were drawn from this section of the model were only general descriptions of tracking behaviour. The development of the computer model was a secondary project aim, with precedence going to the development of the tracking measurement system, therefore failing in the model were not seen as failings in meeting the project aims.

Strip crown was found to be very influential in stabilising tracking. In general, an increased strip crown was see to increase the inherent tendency of the strip to move towards the centreline. The results from the model show that beyond a critical limit the crown has an overcompensating effect and introduces oscillations and instability, but this is thought to be a dynamic of the model and not a true reflection of tracking behaviour.

A temperature wedge was seen to cause tracking instability but a quantitative relationship could not be confidently determined.

By varying the stand in which the disturbance occurred, it was demonstrated that a strip movement would affect position in neighbouring stands and other upstream and downstream stands.

The time period and magnitude of a screw disturbance had a direct effect on strip position, as either was increased both the initial rate of movement and final stable location increased.

A simple proportional control strategy was demonstrated using position feedback from only the controlled stand to adjust the mill screws. The control results showed that strip position was improved using this method. Only a simple method of control was implemented because the limitations with the model meant any detailed control strategy would not be relevant to an actual rolling mill. The control demonstration and the other tracking work highlighted the interdependency of position in all rolling stands, therefore it is thought that a control strategy would be most effective if it incorporated position feedback from all stands.

The simulations performed using only a single roll stand highlighted the effect of parameters other than strip position on differential force. The roll stand model was well validated, therefore there is some confidence in the validity of these results.

Strip position was found to have a linear relationship with differential force. The input parameters tested here showed a ratio of 0.06 (% differential force)/(mm strip off-centre). This relationship was independent of reduction.

A linear temperature wedge across the strip was found to have a linear relationship with differential force. The temperature effect was seen to be -0.31 (% differential force)/(% temperature wedge) with the input parameters tested. This relationship was found to be independent of strip position.

A linear input thickness wedge across the strip was found to have a linear relationship with differential force. The temperature effect was seen to be 0.11 (% differential force)/(% input thickness wedge) with the input parameters tested. This relationship was found to be independent of strip position.

The relationships given were used to find equivalent strip off-centres. In terms of differential force, 1mm of strip off-centre was equivalent to a -0.22% temperature wedge or a 0.60% input thickness wedge. These equivalencies demonstrate that if differential force was used as feedback for a tracking control system, both temperature and input thickness profile would have to be accounted for to ensure the cause of the differential force was strip position an no other factor.

B.5   Further work

The computer model described and evaluated in Chapter 2 and Appendix B has been shown to have significant limitations. The work presented is thought to be a good base point for a tracking simulation but requires significant development in order to provide useful results.

The largest limiting factor of the model is the tracking component, which describes the lateral movement of the strip. The strip tracking model is very complex and there is a lot of interaction between different parameters. The theories used in the model require further development and refining.

A large interaction of strip movement between all the stands has been demonstrated. By expanding the model up to a full seven stands, the level of interactions and degree of upstream and downstream effects could be investigated

The control strategy demonstrated here was only a simple example of strip tracking control to show the principle of steering the strip using mill tilts with a proportional control system using single stand position feedback. To support the development of the strip tracking measurement system a robust control strategy should be developed. It is anticipated that an effective control strategy would use multiple stand position feedback for each controlled stand to allow for the interactions and dynamics of the strip throughout the whole mill.

C Measurement System Code

The complete source code for the measurement system (programmed in National Instruments LabVIEW) is available on the CD attached with the thesis.

D Measurement System Risk Assessments

Safe Working Procedure	Document No.:	
	Revision:	
Status: Draft- 26/05/2011	Owner:	Ben Carruthers-Watt/UK/Corus

Title:		Strip tracking camera maintenance

Cell	Engineering	Section:	Area
Subsection	Finishing	Detail:	

Document

Is this activity related to COMAH?
If you are unsure please contact your COMAH support engineer, shift support engineer or process co-ordinator.

A risk assessment is to be completed prior to the writing of a SWP and also as a final stage in the process on completion of the SWP to ensure that the requirements of the SWP are appropriate and ensure that risks are within acceptable limits.

To complete this Risk Assessment form please fill in the grey boxes

Assessor(s):	Ben Carruthers-Watt	Date:	01/08/2011
Task:	Strip tracking camera maintenance		
Location:	F6		
Task Summary:	Inspect and perform maintenance on strip tracking camera and enclosure		

1. Identify Hazard Categories

- **Dust**
- **Fall of person from height**
- **Fall of person from same level**
- **Hand tools**
- **Manual Handling**
- **Noise**
- **Water**

2. Evaluation of Risk

The Risk needs to be evaluated for each hazard category identified in Section 1. Risks are rated from 1 (Low) to 25 (High) using the Risk Matrix process, where the overall risk is defined by the equation

Probability x Likely Severity = Hazard Rating

The Task Hazard Rating will be the highest risk identified

Probability		Severity				
		Minor Injury	Lost Time Injury	Lost Time Injury	Major Injury	Fatality
		No Lost Time Injury	<= 3 Days	> 3 Days		
	Risk Score	1	2	3	4	5
Improbable	1	1	2	3	4	5
Remote	2	2	4	6	8	10
Possible	3	3	6	9	12	15
Probably	4	4	8	12	16	20
Likely	5	5	10	15	20	25

RISK	HAZARD RATING NUMBER	ACTION
Low Risk	1 - 7	Follow Recommended review frequency (1 to 3 = 5 Years, 4 to 7 = 3 Years)
Moderate Risk	8 - 15	Follow Recommended review frequency (8-10 = 2 Years, 11 to 13 = 1 Years, 14 to 15 = 6 months)
High Risk	16 - 25	Stop - Take Action - Review need for Task

Initial Risk Assessment
To be completed before writing the Safe Working Procedure for the Job and without any controls in place

Hazard Category	Detail of Hazard	Who might be harmed	Prob.	Sev.	Hazard Rating
Dust	Dust in atmosphere	All personnel	2	2	4
Fall of Person from height	Open gaps when top screw down walk way is removed.	All personnel	4	5	20
Fall of Person same level	Uneven surfaces, oil and grease in area.	All personnel	4	5	20
Hand Tools	Improper use, poorly maintained hand tools	Working Party	3	2	6
Manual Handling	Back injuries, strains, sprains from incorrect lifting practice	Working Party	3	4	12
Noise	Noise from operating machinery and tooling	All personnel	4	2	8
Water	Enclosure cooling water supply	Working Party	4	3	12

The Task Hazard Rating is the highest Hazard identified	Initial Hazard Rating	20	High Risk

On reviewing the Risk Assessment, the HSE Principles of the Hierarchy of risk should be noted:
1. Can we eliminate the hazard
2. Can we reduce the hazard at source
3. Can we remove person from hazard
4. Can we contain the hazard
5. Can we reduce exposure
6. Can we control hazard with system of work
7. Can we control hazard with PPE

Second Risk Assessment

To be completed after identifying controls for each Hazard

Hazard Category	Detail of Hazard	Who might be harmed	Controls	Prob.	Sev.	Hazard Rating
Dust	Dust in atmosphere	All personnel	Safety Glasses to be worn at all times	2	1	2
Fall of Person from height	Open gaps when top screw down walk way is removed. Open gaps when looper table is removed	All personnel	Scaffold barriers to be erected across all open gaps	1	1	1
Fall of Person same level	Uneven surfaces, oil and grease in area.	All personnel	Clean area before starting work, carry out housekeeping checks through outwork and ensure adequate lighting	2	3	6
Hand Tools	Inproper use, poorly maintained hand tools	Working Party	Tooling to be kept clean and in good working order. All tools to be inspected before use. Correct PPE to be worn. Correct tool to be used for the correct application.	1	2	2
Manual Handling	Back injuries, strains, sprains from incorrect lifting practice	Working Party	Mechanical lifting to be used at all times where practicable to do so. Team lifting may be carried out where the former is not possible, assessment of the lift to be made before lifting carried out.	1	4	4
Noise	Noise from operating machinery and tooling	All personnel	Ensure correct ear defenders to be worn	1	2	2
Water	Enclosure cooling water supply	Working Party	Water to be isolated and water status card issued and signed	1	2	2
The Task Hazard Rating is the highest Hazard identified				Hazard Rating	5	Low Risk

RISK	HAZARD RATING NUMBER	ACTION
Low Risk	1 - 7	Follow Recommended review frequency (1 to 3 = 5 Years, 4 to 7 = 3 Years)
Moderate Risk	8 - 15	Follow Recommended review frequency (8-10 = 2 Years, 11 to 13 = 1 Years, 14 to 15 = 6 months)
High Risk	16 - 25	Stop - Take Action - Review need for Task

Recommended Further Controls

Hazard Category	Recommended Further Controls	Status	Status Comments
Dust			
Fall of Person from height			
Fall of Person same level			
Hand Tools			
Manual Handling			
Noise			
Overhead Cranes			
Water			

Ensure that you have fully read and understood this Safe Working Procedure before attempting to carry out this task

Task: Strip tracking camera maintenance
Location: F6
Task Summary: Inspect and perform maintenance on strip tracking camera and enclosure

1. Risk Assessment

Hazard Category	Detail of Hazard	Who might be harmed	Controls	Prob.	Sev.	Hazard Rating
Dust	Dust in atmosphere	All personnel	Safety Glasses to be worn at all times	2	1	2
Fall of Person from height	Open gaps when top screw down walk way is removed. Open gaps when looper table is removed	All personnel	Scaffold barriers to be erected across all open gaps	1	1	1
Fall of Person same level	Uneven surfaces, oil and grease in area.	All personnel	Clean area before starting work, carry out housekeeping checks through outwork and ensure adequate lighting	2	3	6
Hand Tools	Inproper use, poorly maintained hand tools	Working Party	Tooling to be kept clean and in good working order. All tools to be inspected before use. Correct PPE to be worn. Correct tool to be used for the correct application.	1	2	2
Manual Handling	Back injuries, strains, sprains from incorrect lifting practice	Working Party	Mechanical lifting to be used at all times where practicable to do so. Team lifting may be carried out where the former is not possible, assessment of the lift to be made before lifting carried out.	1	4	4
Noise	Noise from operating machinery and tooling	All personnel	Ensure correct ear defenders to be worn	1	2	2
Water	Enclosure cooling water supply	Working Party	Water to be isolated and water status card issued and signed	1	2	2

The Task Hazard Rating is the highest Hazard identified	Hazard Rating	5	Low Risk

2. People

Minimum Number of Personnel:	2 Technicians
Minimum Training, Knowledge or Experience:	Competent in task

3. Safety Equipment

PPE Requirements:

- PSG07 - GLOVE C/CHROME K/W
- PSB059 - SPECTACLES SAFETY
- PSJ014 - PROBAN TROUSERS

- As Supplied PROBAN JACKET
- PSC003 - EAR-MUFF PELTOR H7P3
- SBSF 001 - SAFETY BOOT

- PSA017 - HELMET PLASTIC HARD
-
-

Additional Safety Equipment:
- None

4. Tools to Complete the Task

Specific Tools Required:

Allen keys
10mm Spanner or socket
Cleaning rag

5. Specific Permits Isolations

1		
2		
3		
4		
5		
6		
7		
8		
9		
10		

If an ATW/PBS is normally required it is in addition to the above permits

6. Access & Egress into Task Area

Safe Access is via: Enter Hot Mill via main pedestrian entrance opposite the main Hot Mill office block. Proceed via the designated walkways to the Finishing Mill area and access mill from Mill Floor doorway. To gain access to the back of the Mill, proceed along walkway to the stairs just after F11 and follow walkway to the rear of the Finishing Mill

Safe Egress is via: Same as access

7. Plant Status

List specific items of plant and their required positions to safely complete the task.   List in order of sequence

No.	Plant Positioning	Status

8. Procedure

Must be listed in chronological order and should include the following as applicable: Commissioning, Isolations and permits when required, functional testing, specific PPE requirements when required during the task, spares required, guarding requirements, slinging & lifting requirements, any checks & test, other affected during task activity.

1.1 Undo four Allen bolts on rear of enclosure
1.2 Remove rear of enclosure and camera rail assembly
1.3 Use rag to clean enclosure window. View through enclosure from rear to ensure clear view
1.4 Visually assess camera condition
1.5 If camera requires replacing then follow 2
1.6 Refit enclosure rear and camera rail assembly
1.7 Fasten enclosure Allen bolts
2.1 Undo two bolts securing camera mount to enclosure rail
2.2 Unscrew four Allen bolts securing camera to mount
2.3 Attach new camera to mount using four Allen bolts
2.4 Re-attach camera mount to rail using two bolts

The Task Hazard Rating is the highest Hazard identified	Hazard Rating	5	Low Risk

9. Emergency Issues

Emergency Assembly Point Location:	Hot Sheet Finishing Car Park or main canteen car park
Link to Local Emergency Plan:	
Link to Local Environmental Emergency Issues:	
Applicable Contact Numbers:	Port Talbot
Civil:	4191
Environmental:	4291
Transport:	2509
Energy:	4272
Emergency Telephone Number :	3333/4444

Reference Documents

Cross References

Document Distribution

Paper

Document Review

Originator		Reviewers
Ben Carruthers-Watt/UK/Corus	⇨	

Document Approval

Approver Name(s)   Approver Signature(s)   Date

Modifications

Cleaning rag	N/A

12. Personal Protective Equipment To be used:

a. Type:	b. Make & Model:	c. To protect against:
Safety gloves	-	General protection
Safety boots	-	General protection
Helmets	-	General protection
Safety Glasses	-	Metal splinters / airborne dust
Ear defenders	Peltor	Noise

13. Hazardous Substances to be Used:

a. Hazardous Substance:	b. Risk to health?	c. Controls required:
N/A	N/A	N/A

14. Subcontractors to be used:	All must be Tata approved and have their own Job Method, PBS and ATW.
N/A	

15. Technical Content of the Job:

- Checking alignment of camera enclosure and adjusting as necessary
- Checking and cleaning enclosure window
- Replacing camera
- Replacing or performing maintenance on enclosure

16. Safety Risk Assessment of the work to be done. What / Who are the:-

a. Hazards?	b. Risk to people?	c. Controls to be used?
Carrying equipment	Working party members	Careful use of stairs when carrying
Accessing Mill floor during down time	Working party members	Inform Pulpit, sign pulpit register

Triangle Ref: Valid from 01/08/2011

TATA STEEL

Cleaning rag	N/A

12. Personal Protective Equipment To be used:		
a. Type:	b. Make & Model:	c. To protect against:
Safety gloves	-	General protection
Safety boots	-	General protection
Helmets	-	General protection
Safety Glasses	-	Metal splinters / airborne dust
Ear defenders	Peltor	Noise

13. Hazardous Substances to be Used:		
a. Hazardous Substance:	b. Risk to health?	c. Controls required:
N/A	N/A	N/A

14. Subcontractors to be used:	All must be Tata approved and have their own Job Method, PBS and ATW.
N/A	

15. Technical Content of the Job:

- Checking alignment of camera enclosure and adjusting as necessary
- Checking and cleaning enclosure window
- Replacing camera
- Replacing or performing maintenance on enclosure

16. Safety Risk Assessment of the work to be done. What / Who are the:-		
a. Hazards?	b. Risk to people?	c. Controls to be used?
Carrying equipment	Working party members	Careful use of stairs when carrying
Accessing Mill floor during down time	Working party members	Inform Pulpit, sign pulpit register

Triangle Ref: Valid from 01/08/2011

TATA STEEL

Working at height	Working party members	Work within fenced gantry area at all times

17. Safety Content of the Job:	Using ALL the controls listed above in 8,11,12,13,14,15 & 16, describe clearly how you are going to complete the work:

- All persons to sign on and off mill register and ATW each day (mill office)
- Never inspect part of the mill during down time without the pulpit knowing where we are.
- Work must never be done unless the mill is down

Check the camera and enclosure for damage and perform maintenance and cleaning.
The window of the enclosure should be cleaned with a rag from the underneath to ensure it is clear. The rear of the enclosure should be removed by unscrewing the four Allen bolts which attach it to the body. The rear, along with the camera, can then be removed from the enclosure. The camera should be checked to ensure it is securely mounted and undamaged and both power and GigE cables firmly connected. All damage should be assessed and rectified.
To remove the camera, first the two bolts securing the camera mount to the enclosure rail must be undone. The camera can then be removed from the mount by undoing the four Allen bolts. Replacing is the reversal of removal.
The camera is a sensitive electronic device and must be handled with care. Whenever the camera is removed from the enclosure, a lens cover must be fitted to ensure the lens remains clean.

***NOTE *** ENSURE ANY LENS COVERS ARE REMOVED WHEN THE CAMERA IS REPLACED ***

18. Environmental Risk Assessment of the work to be done. What are the:		
a. Hazards	**b. Risk to the Environment**	**c. Controls to be used?**
N/A	N/A	N/A

19. Contractor Signature	Contractor **MUST print name , sign** and **Date** the Job Method Statement
	Ben Carruthers-Watt 7 September 2011

Triangle Ref: Valid from 01/08/2011

xxxiii